Global Mineral Resource Assessment

Porphyry Copper Assessment of Eastern Australia

Prepared in cooperation with Geological Survey of New South Wales and Geoscience Australia

Scientific Investigations Report 2010–5090–L

U.S. Department of the Interior
U.S. Geological Survey

This page left intentionally blank.

Global Mineral Resource Assessment

Michael L. Zientek, Jane M. Hammarstrom, and Kathleen M. Johnson, editors

Porphyry Copper Assessment of Eastern Australia

By Arthur A. Bookstrom, Richard A. Glen, Jane M. Hammarstrom,
Gilpin R. Robinson, Jr., Michael L. Zientek, Benjamin J. Drenth, Subhash Jaireth,
Pamela M. Cossette, and John C. Wallis

Prepared in cooperation with Geological Survey of New South Wales and
Geoscience Australia

Scientific Investigations Report 2010–5090–L

U.S. Department of the Interior
U.S. Geological Survey

U.S. Department of the Interior
SALLY JEWELL, Secretary

U.S. Geological Survey
Suzette M. Kimball, Acting Director

U.S. Geological Survey, Reston, Virginia: 2014

For more information on the USGS—the Federal source for science about the Earth,
its natural and living resources, natural hazards, and the environment:
World Wide Web: http://www.usgs.gov, Telephone: 1-888-ASK-USGS

For an overview of USGS information products, including maps, and publications,
visit http://www.usgs.gov/pubprod

Suggested citation:
Bookstrom, A.A., Glen, R.A., Hammarstrom, J.M., Robinson, G.R., Jr., Zientek, M.L., Drenth, B.J., Jaireth, S., Cossette, P.M., and Wallis, J.C., 2014, Porphyry copper assessment of eastern Australia: U.S. Geological Survey Scientific Investigations Report 2010–5090–L, 160 p. and GIS data, *http://dx.doi.org/10.3133/sir20105090L*.

ISSN 2328-0328 (online)

Contents

Figures

Tables

Acronyms and Abbreviations Used

ANOVA	analysis of variance
GIS	geographic information system
g/t	grams per metric ton
kt	thousand metric tons
Ma	millions of years before the present
Mt	million metric tons
PGE	platinum-group elements
REE	rare-earth elements
SHRIMP	sensitive high resolution ion microprobe
SSIB	small-scale digital international boundaries
t	metric ton (tonne) or megagram (Mg)
USGS	United States Geological Survey

Conversion Factors

Inch/Pound to SI

	Multiply by	To obtain
Length		
foot (ft)	0.3048	meter (m)
mile (mi)	1.609	kilometer (km)
yard (yd)	0.9144	meter (m)
Area		
acre	0.4047	hectare (ha)
acre	0.004047	square kilometer (km^2)
square mile (mi^2)	259.0	hectare (ha)
square mile (mi^2)	2.590	square kilometer (km^2)
Mass		
ounce, troy (troy oz)	31.103	gram (g)
ounce, troy (troy oz)	0.0000311	megagram (Mg)
ton, short (T) (2,000 lb)	0.9072	megagram (Mg)

SI to Inch/Pound

	Multiply by	To obtain
Length		
meter (m)	3.281	foot (ft)
kilometer (km)	0.6214	mile (mi)
meter (m)	1.094	yard (yd)
Area		
hectare (ha)	2.471	acre
square kilometer (km^2)	247.1	acre
hectare (ha)	0.003861	square mile (mi^2)
square kilometer (km^2)	0.3861	square mile (mi^2)
Mass		
gram (g)	0.03215	ounce, troy (troy oz)
megagram (Mg)	1.102	ton, short (2,000 lb)
megagram (Mg)	0.9842	ton, long (2,240 lb)
Other conversions used in this report		
metric ton (t)	1	megagram (Mg)
troy ounce per short ton	34.2857	gram per metric ton (g/t)
percent	10,000	parts per million (ppm) or grams per metric ton (g/t)
percent metal	0.01 × metal grade (in percent) × ore tonnage (in metric tons)	metric tons of metal

Porphyry Copper Assessment of Eastern Australia

By Arthur A. Bookstrom[1], Richard A. Glen[2], Jane M. Hammarstrom[3], Gilpin R. Robinson, Jr.[3], Michael L. Zientek[1], Benjamin J. Drenth[4], Subhash Jaireth[5], Pamela M. Cossette[1], and John C. Wallis[1]

Abstract

The U.S. Geological Survey (USGS) conducts national and global assessments of resources (mineral, energy, water, and biologic) to provide science in support of decision making. Mineral resource assessments provide syntheses of available information about where mineral deposits are known and suspected to occur in the Earth's crust and which commodities may be present, together with estimates of amounts of resources that may be present in undiscovered deposits. The USGS collaborated with geologists of the Geological Survey of New South Wales and Geoscience Australia (formerly the Australian Geological Survey Organisation) on an assessment of Phanerozoic-age porphyry copper resources in Australia. Porphyry copper deposits contain about 11 percent of the identified copper resources in Australia. This study addresses resources of known porphyry copper deposits and expected resources of undiscovered porphyry copper deposits in eastern Australia.

A three-part form of assessment was used for estimation of undiscovered resources. Using this method, four tracts were delineated that are permissive for porphyry copper deposits. A probabilistic estimate of the expected number of deposits in each tract was prepared on the basis of existing information about geology, geochemistry, geophysics, exploration history, and mineral occurrences. Monte Carlo simulation was used to combine the estimated number of deposits with an appropriate model of grade and tonnage for porphyry copper deposits to provide a probabilistic estimate of metal content and total tonnage for undiscovered deposits.

The Delamerian permissive tract comprises igneous rocks of Cambrian age in the Delamerian Orogen, which borders the western margin of the Tasmanides. The Delamerian tract contains no known porphyry copper deposits, but the Adelaide sub-tract, one of three sub-tracts that compose the Delamerian tract, contains four porphyry copper prospects. The Adelaide sub-tract is estimated to contain 2.5±2.2 undiscovered deposits in an area of about 50,700 km^2 (square kilometers).

The Macquarie permissive tract comprises volcanic, volcaniclastic, and minor exposed intrusive igneous rocks of the Macquarie Arc. The nine known deposits in this tract are now estimated to contain a total of about 13.5 million metric tons of copper and 1,700 metric tons of gold. This tract is estimated to contain 6.9±3.5 undiscovered deposits for a total of about 16 deposits in an area of about 41,500 km^2.

The Yeoval permissive tract includes subequal areas of permissive volcanic and intrusive rocks of Silurian to Devonian age exposed in and around the Cowra-Buchan Rift System, which overlaps the previously accreted Macquarie Arc. The Yeoval tract contains one porphyry copper deposit and several porphyry copper prospects. This tract is estimated to contain 1.3±0.75 undiscovered porphyry copper deposits, for a total of about 2 expected deposits in an area of about 53,200 km^2.

The East Tasmanide permissive tract includes a semi-continuous belt of plutonic and subordinate volcanic rocks along the eastern margins of Queensland and northeastern New South Wales. The East Tasmanide tract contains 14 known porphyry copper deposits and many porphyry copper prospects, which are all in the Central sub-tract. This sub-tract is expected to contain 4.8±3.3 undiscovered porphyry copper deposits, for a total of about 19 deposits in an area of about 291,000 km^2.

This assessment estimates that 15 undiscovered deposits contain an arithmetic mean of ~21 million metric tons or more of copper in four tracts, in addition to the 24 known porphyry copper deposits that contain identified resources of ~16 million metric tons of copper. In addition to copper, the mean expected amount of undiscovered byproduct gold predicted by the simulation is ~1,500 metric tons. The probability associated with these arithmetic means is on the order of 30 percent. Median expected amounts of metals predicted by the simulations may be ~50 percent lower than mean estimates.

[1]U.S. Geological Survey, Spokane, Washington, United States.

[2]Geological Survey of New South Wales, Hunter Region Mail Centre, New South Wales, Australia.

[3]U.S. Geological Survey, Reston, Virginia, United States.

[4]U.S. Geological Survey, Denver, Colorado, United States.

[5]Geoscience Australia, Canberra, Australian Capital Territory, Australia.

Introduction

Global Mineral Resource Assessment

This assessment of known and undiscovered mineral resources associated with porphyry copper deposits in Australia is part of a U.S. Geological Survey (USGS)-led global mineral resource assessment. The global assessment aims to provide a consistent, comprehensive level of current information and analysis of global, nonfuel mineral resources of platinum-group elements, copper in porphyry and sediment-hosted deposits, and potash in selected types of deposits (Briskey and others, 2001). These commodities and deposit types were chosen partly for their economic importance, and partly as prototypes for estimation of resources in orthomagmatic, magmatic-hydrothermal, sediment-hosted hydrothermal, and evaporitic deposit types.

Results of this assessment are provided at a scale of 1:1,000,000 and could be used to:

- Evaluate known and undiscovered copper resources;
- Design and evaluate new mineral exploration programs;
- Anticipate economic, environmental, and social impacts of mineral development; and
- Provide information for aiding in land-use decisions where competing or mutually exclusive uses or environmental issues may coincide.

This study was done by the USGS in collaboration with geologists from the Geological Survey of New South Wales and Geoscience Australia (GA, formerly Australian Geological Survey Organisation).

Report Format

This report begins with a review of Australian copper production and resources. A summary of mineral resource assessment methods is followed by a description of how those methods were applied to this assessment of porphyry copper resources in Australia, including the use of descriptive models, compilation of information about known porphyry copper deposits, prospects, and occurrences, application of the 2-kilometer (km) rule for aggregation of spatially grouped deposits, and a summary of results for each permissive tract (see Terminology section below).

Appendix A contains a description of how grade-tonnage models were chosen, tested, and developed, as required to represent grade-tonnage characteristics of known porphyry Cu (copper) and porphyry Cu-Au (copper-gold) deposits in eastern Australia. Appendixes B through E present assessment data and results for tracts permissive for porphyry copper deposits in eastern Australia. Appendix F contains a spreadsheet listing attributes of known porphyry copper deposits, prospects and occurrences, and attributes of other types of deposits that either contain copper or may be directly or indirectly associated with porphyry copper deposits. Appendix G contains geographic information system (GIS) files for permissive-tract boundaries, including an attribute table for significant deposits and prospects. Appendix H provides biographical information about members of the assessment team.

Australian Copper Production and Resources

According to Edelstein (2011), in 2009 Australia produced about 854 thousand metric tons (kt) of mined copper (Cu), while world production was 15.9 megatons (Mt) copper. Thus, Australian production was about 5 percent of world copper production. Consequently, Australia is the world's 6th largest producer of mined copper (after Chile with about 5.4 Mt, Peru with about 1.3 Mt, United States with about 1.2 Mt, Indonesia with about 996 kt, and China with about 995 kt).

According to Jaques and others (2002), however, porphyry copper deposits contain only about 11 percent of Australia's total copper resources, whereas 47 percent is in iron-oxide copper-gold (IOCG) deposits, 30 percent is in Mount Isa metamorphosed sedimentary exhalative (SEDEX) copper deposits, 7 percent is in volcanic-hosted massive sulfide deposits, and the remaining 5 percent is in other deposit types.

Most of the known economic copper resources in Australia are in Precambrian cratons, which are exposed in the western two-thirds of the country (fig. 1). The giant Olympic Dam IOCG deposit is beneath Neoproterozoic strata of the Stuart Shelf, where it is hosted in Mesoproterozoic granite of the Archean Gawler Craton. The giant Mount Isa SEDEX copper deposit and the Ernest-Henry IOCG deposit are in Proterozoic rocks of the McArthur Basin. In Western Australia, the giant Boddington porphyry Au-Cu deposit is in the Archean Yilgarn Craton, and the large but low-grade Coppin Gap porphyry Mo-Cu deposit is in the Archean Pilbara Craton. No assessment was made of undiscovered porphyry copper resources in these Archean cratons.

Most of the known porphyry copper deposits in Australia are in the Phanerozoic Tasmanide orogens, which occupy the eastern third of Australia (fig. 1). Inasmuch as porphyry copper deposits generally are related to igneous intrusions in magmatic arc to back-arc settings, this study is focused on belts of igneous rocks in the Tasmanide orogens.

Mineral Resource Assessment Terminology

The terminology used in this study follows definitions used in the 1998 assessment of undiscovered deposits of gold, silver, copper, lead, and zinc in the United States (Cox and Singer, 1986; U.S. Geological Survey National Mineral Resource Assessment Team, 2000; U.S. Bureau of Mines and U.S. Geological Survey, 1980; Bates and Jackson, 1997; American

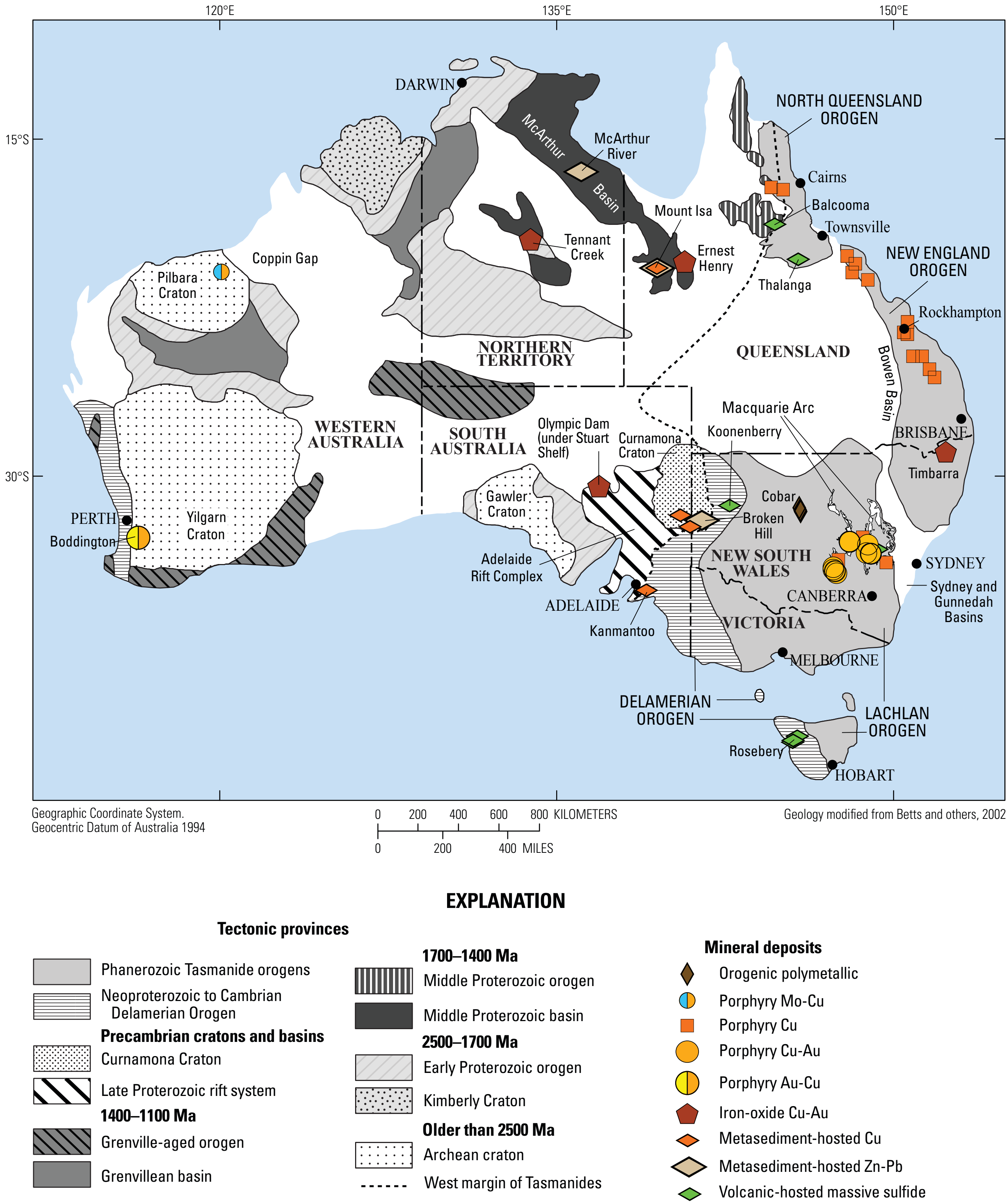

Figure 1. Terrane map of Australia showing major Archean and Proterozoic terranes, major Phanerozoic Tasmanide orogens, and locations of selected types of copper-bearing deposits, including porphyry copper, and selected iron-oxide copper-gold (IOCG) and metamorphosed sedimentary-exhalative (SEDEX) copper deposits. Site locations of deposits are from Geoscience Australia (2010). Ma, millions of years before present.

Geological Institute, 1997). The usage (listed below) is intended to represent standard definitions and general usage by the minerals industry and the resource-assessment community.

Some countries recently have adopted more rigorous definitions of terms for estimating mineral resources and mineral reserves and for reporting exploration information to comply with legal mandates. The Australasian Code for Reporting of Mineral Resources and Ore Reserves (JORC) (Australasian Joint Ore Reserves Committee, 2004), and the reporting template of the U.S. Securities and Exchange Commission (CRIRSCO) (U.S. Securities and Exchange Commission Committee for Mineral Reserves International Reporting Standards, 2006) include such definitions.

mineral deposit A mineral concentration of sufficient size and grade that it might, under the most favorable of circumstances, be considered to have potential for economic development.

mineral prospect An area that is a potential site of mineral deposits, based on preliminary exploration results. For purposes of this study, a significant prospect for porphyry copper is one for which exploration results indicate characteristics consistent with those of porphyry copper deposits, as summarized in porphyry copper mineral deposit models. A mineral deposit of one type (skarn, for example) may be a prospect for a related type (porphyry copper).

mineral occurrence A concentration of minerals or rocks (usually, but not necessarily, considered in terms of some commodity, such as copper or gold) that is considered valuable.

undiscovered mineral deposit A mineral deposit expected to exist 1 km or less below the surface of the ground, or an incompletely explored mineral occurrence or prospect that could have sufficient size and grade to be classified as a deposit.

descriptive mineral deposit model A set of data in a convenient, standardized form that describes a group of mineral deposits having similar characteristics.

grade and tonnage model Frequency distributions of the grades and sizes of thoroughly explored, or completely mined out, individual mineral deposits that fit a descriptive mineral deposit model.

permissive tract A geographic area representing the surface projection of a volume of rock in which the geology permits the existence of a mineral deposit of a specified type. The probability of deposits of the type being studied occurring outside the boundary is negligible.

resource A mineral concentration of sufficient size and grade and in such form and amount that economic extraction of a commodity from the concentration is currently or potentially feasible.

identified resources Resources whose location, grade, quality, and quantity are known or can be estimated from specific geologic evidence. For this study, identified resources are the deposits included in the grade and tonnage models used in the assessment. In addition, deposits that are not included in the models used for the assessment may be considered as identified resources if they are characterized well enough by deposit type, grade, and tonnage to meet reporting guidelines of JORC or CRIRSCO.

undiscovered resources Resources in undiscovered mineral deposits whose existence is postulated on the basis of indirect geologic evidence. These include undiscovered resources in known types of mineral deposits postulated to exist in favorable geologic settings where other deposits of the same types have been mined, or where mineral discoveries have not been made. Undiscovered resources may include active mines if the resource is delineated incompletely. For example, a deposit that is explored only partially and reported as “open to the west or open at depth” could be counted as an undiscovered resource. Undiscovered resources in extensions to identified resources are not addressed explicitly in the assessment process.

Assessment Methods

This assessment of undiscovered porphyry copper deposits in eastern Australia was done using the three-part form of mineral resource assessment based on mineral deposit models (Singer, 1993, 2007a, b). This form of mineral resource assessment provides internally consistent estimates of undiscovered resources that can be evaluated using economic filters and other tools for economic, environmental, and policy analysis.

In the three-part form of mineral resource assessment: (1) permissive tracts are delineated according to the types of deposits permitted by the geology, (2) the amount of metal in typical deposits is estimated by using grade and tonnage models, and (3) the number of undiscovered deposits of each type is estimated by using a variety of subjective methods (Singer, 2007a). For more detailed descriptions of the three-part form of mineral resource assessment, see Singer (1993, 2007a, b), Singer and Berger (2007), and Singer and Menzie (2010).

Permissive Tracts

Permissive tracts delineate the geologic setting that is characteristic for the occurrence of the specified deposit type. Descriptive models, which are available for a wide range of types of mineral deposits, highlight geological characteristics of the deposit type that can be recognized on geologic maps. Examples include lists of rock types that commonly host, or are genetically associated with, deposits of the specified type and geological environments in which such deposits are known to occur.

Geologic maps, geologic literature, and mineral-occurrence databases are used to plot the spatial distribution of permissive rock types and known deposits and prospects of the specified deposit type. Areas that include permissive geology, as well as known deposits or prospects of the specified deposit type, are identified as permissive tracts for the specified deposit type.

A permissive tract for porphyry copper deposits is delineated as an area that includes intrusive and volcanic rocks of specified ranges of composition and age and may include porphyry copper deposits and prospects of the specified age range. In general, such an area coincides with a magmatic belt that is directly or indirectly related to a convergent plate margin boundary zone.

The permissive tract generally is bounded by the outline of the magmatic belt, as depicted at the scale of the maps available for tract delineation. Spatially overlapping magmatic arcs that were active during different time intervals may be split into separate permissive tracts, or may be considered to represent a composite magmatic belt. A permissive tract may also include areas where younger or structurally overlying materials are thought to be underlain by permissive rocks at depths of less than 1 km.

Descriptive Models

The general descriptive model for porphyry copper deposits by Cox (1986a) does not distinguish between various subtypes, all of which contain chalcopyrite in stockwork veinlets in hydrothermally altered tonalitic to monzogranitic or syenitic porphyries and adjacent country rocks. Permissive tectonic settings are described as areas of island-arc or continental-arc magmatism in convergent plate boundary zones. Amounts of uplift and levels of erosion should be sufficient to expose subvolcanic intrusions but not so deep as to destroy high-level porphyries and associated porphyry copper systems. Ore-related porphyries generally contain phenocrysts in a microaplitic quartz-feldspar groundmass. Such porphyries generally occur in high-level intrusive stocks, or cupolas of batholiths, with abundant contemporaneous dikes, breccia pipes, and faults.

The descriptive model for porphyry Cu-Mo deposits by Cox (1986b) is similar to the general model for porphyry copper deposits, the only distinction being that in porphyry Cu-Mo deposits the ratio of gold (in parts per million, or ppm) to molybdenum (in percent) is less than three. According to Blevin and others (1996), molybdenum increases relative to gold with increasing fractionation, as indicated by increasing Rb/Sr in associated granitoid rocks.

The descriptive model for porphyry Cu-Au deposits by Cox (1986c) defines these as porphyry copper deposits in which the ratio of gold (ppm) to molybdenum (percent) is 30 or more in the ore zone. These deposits tend to form late in a magmatic episode, in association with subvolcanic porphyry plugs, dikes, and breccias in coeval volcanic rocks, emplaced at relatively shallow depths (1–2 km). Two suites of permissive rocks are listed in the model by Cox: an alkaline suite of monzonite to syenite, or coeval high-K, low-Ti volcanic rocks (shoshonites); and a calc-alkaline suite of tonalite to monzogranite, or andesite to dacite. Descriptive models for porphyry Cu-Au deposits by Panteleyev (1995b, 2005b), Cooke and others (1998), and Jaireth and Miezitis (2004) provide additional information about the character of porphyry Cu-Au deposits and their associated rock types.

The descriptive model for porphyry Cu, skarn-related deposits by Cox (1986d) describes such deposits as having chalcopyrite in stockwork veinlets in hydrothermally altered intrusive rocks and in skarn with extensive retrograde alteration. Permissive rocks listed in this model include tonalite to monzogranite, emplaced into carbonate or calcareous clastic rocks.

A wealth of useful information about the geological characteristics of porphyry copper deposits also is available in recent overview publications. Examples, cited in chronological order, are those by Tosdal and Richards (2001), Richards (2003), Seedorf and others (2005), John and others (2010), and Sillitoe (2010).

Grade-Tonnage Models

Assessment of undiscovered mineral resources is based on analogy with known deposits. It is assumed that undiscovered deposits will be like those that already have been discovered. It is therefore necessary to inventory the identified resources of known deposits in the study area before undiscovered resources are assessed. Estimated tonnages and grades of the known deposits are then tested against frequency distributions of premining tonnages and average grades of thoroughly explored deposits, which serve as models for grades and tonnages of undiscovered deposits (Singer, 1993).

The grade-tonnage model for porphyry copper deposits of the world by Singer and others (2008) includes frequency distribution diagrams for tonnage, copper grade, molybdenum grade, gold grade, and silver grade. The model for porphyry copper deposits (undivided by subtype) is based on grade-tonnage data for 422 known deposits. A subset of porphyry Cu-Au deposits, for which the ratio of gold (ppm) to molybdenum (percent) is greater than 30, includes data for 115 deposits. A subset for porphyry Cu-Mo deposits, for which the ratio of gold (ppm) to molybdenum (percent) is less than 3, includes data for 51 deposits. A subset for porphyry copper deposits that are not of either the Cu-Au or Cu-Mo subtype includes data for 256 deposits.

If the tonnages and grades of deposits in the study area match those of an available grade-tonnage model for the deposit type, that model is applied to estimation of resources of undiscovered deposits in the study area. However, if tonnages and grades of deposits in the study area differ significantly from those represented by an available grade-tonnage model, then a grade-tonnage model for the population of the study area should be found and applied, or a custom regional model should be constructed and applied.

Undiscovered Deposits

Numbers of undiscovered deposits are estimated at various levels of subjective probability (or degrees of belief) by members of an assessment team of well-informed experts. A variety of strategies may be used to arrive at such estimates. Examples include counting the number of significant prospects, ranking the favorability of prospects, and comparing the spatial density of known and postulated undiscovered deposits to that of known deposits in similar, well-explored regions (Singer, 2007b). Results are reported as the mean number of undiscovered deposits based on the team's consensus estimates for each permissive tract, along with the associated standard deviation and variance.

Undiscovered Resources

Undiscovered resources for each quantitatively assessed permissive tract were estimated by combining consensus estimates for numbers of undiscovered porphyry copper deposits with an appropriate porphyry copper grade and tonnage model (appendix A) using the EMINERS program (Root and others, 1992; Duval, 2012; Bawiec and Spanski, 2012). Cumulative probability graphs and associated data tables show predicted amounts of the commodities.

Assessment of Undiscovered Porphyry Copper Resources of Eastern Australia

A probabilistic assessment of undiscovered resources associated with porphyry copper deposits in Australia was conducted as part of a global mineral resource assessment. Available geologic maps, geophysical data, and databases of known deposits and prospects were used to outline areas permissive for the occurrence of porphyry copper deposits, and grade-tonnage models were prepared to serve as the basis for estimation of undiscovered resources.

Principal Sources of Information

Digital Geologic Maps

Digital geologic maps compiled at 1:1,000,000 scale were used to identify areas of permissive rocks for porphyry copper in Australia. Permissive map units were identified on the basis of map unit descriptions presented in tables of map unit attributes for the digital geologic source maps for each of the following eastern Australian provinces: Queensland (Whitaker and others, 2007), New South Wales (Raymond, Liu, Kilgour, Retter, Stewart, and Stewart, 2007), South Australia (Whitaker and others, 2008), Victoria (Raymond, Liu, Kilgour, Retter, and Connolly, 2007), and Tasmania (Raymond, Liu, and Kilgour, 2007).

The attribute tables that accompany Australian provincial geologic maps generally contain excellent descriptions of igneous rocks represented by map units. Visibly crystalline igneous rocks are classified and named according to proportions of key minerals, and microcrystalline to glassy igneous rocks are classified and named according to chemical composition. In addition, some granitoid rocks are classified as I-type, S-type, or A-type, and some can be so classified on the basis of characteristics mentioned in descriptions of rock types in map-unit descriptions in these databases.

I-type granitoids are inferred to be derived from meta-igneous sources. They are the most common granitoid rocks in subduction-related magmatic belts, and they normally have calcium and sodium contents that are high enough for hornblende to occur (White, 1979). Porphyry copper deposits typically are associated with I-type igneous rocks of tonalitic to monzogranitic composition or of dioritic to syenitic composition. Therefore, most I-type igneous rocks are considered permissive for the occurrence of porphyry copper deposits.

S-type granitoids are peraluminous in composition and are derived from metasedimentary sources (White, 1979). S-type granitoids typically contain biotite + primary muscovite ± cordierite ± garnet ± metasedimentary inclusions (Chappell and White, 1974, 2001). Deposits of tin, rather than copper, are typically associated with S-type granites. Therefore, S-type igneous rocks are not considered permissive for porphyry copper deposits.

A-type granitoids are generally late orogenic to postorogenic in age, and they form in relatively atectonic settings. They probably are generated by partial melting of residues from a previous partial-melting event. These rocks have alkaline affinities and may be associated with coeval mafic-alkalic intrusions. They typically contain fluorine-bearing minerals and may contain sodic amphibole. A-type granitoids are characterized by high concentrations of incompatible trace elements, such as Zr, Nb, Ga, Zn, Y, and rare earth elements (REE), except for Eu (Loiselle and Wones, 1979; White, 1979). Deposits of molybdenum, rather than copper, are typically associated with A-type granitoid intrusions. Therefore, A-type igneous rocks are not considered permissive for porphyry copper deposits.

Although geologic maps are used to delineate distributions of permissive igneous rocks, most general-purpose geologic maps do not show locations of ore deposits or hydrothermally altered rocks. Furthermore, geologic maps at 1:1,000,000 scale may not display relatively small stocks, plugs, dikes, and breccias, such as those that are typically associated with porphyry copper systems. Nevertheless, such small intrusions generally occur in or near areas of larger intrusions or associated volcanic fields, which are shown at 1:1,000,000 scale.

Geophysical Databases and Maps

Australian aeromagnetic databases (Geoscience Australia, 2004) were used to make maps that show magnetic anomaly patterns. Aeromagnetic grids of the area in and around the Adelaide sub-tract of the Delamerian permissive tract, and the area in and around the Macquarie permissive tract were used. These magnetic grids were reduced to the magnetic pole and were interpreted to indicate locations of relatively magnetic igneous rocks or magnetite-bearing hydrothermal systems in the subsurface.

Australian gravimetric databases (Geoscience Australia, 2009) were processed using a high-pass filter with a cutoff wavelength of 150 km. The resulting gravity-anomaly maps were interpreted to indicate hidden bodies of rock with anomalously high density (such as gabbro) or low density (such as granite or unconsolidated basin-fill sediments).

In sparsely vegetated areas, color anomalies visible on satellite imagery can be helpful in identification of hydrothermally altered and limonite-stained areas. Global satellite imagery also was examined to locate disturbed areas related to mines and prospects for which geographic coordinates were not otherwise available. More advanced methods of spectral imaging and analysis were not applied in this study.

Known Porphyry Copper Deposits and Prospects

It is important to map the locations of known porphyry copper deposits and prospects, each of which should be included in a permissive tract. The online Australian Atlas of Mines and Mineral Deposits (Geoscience Australia, 2010) is an important source for names and locations of mines and mineral deposits. Estimated tonnages and grades of identified resources are tabulated, but no descriptive geological information is included, and mineral deposits are not classified by deposit type in this database. Nevertheless, most known porphyry copper deposits and some prospects are described in published geological literature. In addition, descriptions of many porphyry copper prospects are available on internet sites of mining and minerals-exploration companies.

Appendix F describes a list of known porphyry copper sites and other relevant types of deposits. Some of these are of types that may occur within or near porphyry copper systems, but may also occur independent of porphyry copper systems. Examples of other types are included because they are important sources of copper or they are characteristic of a geologic setting that is directly or indirectly relevant to this study. Sources of information for each known deposit and prospect are cited in appendix F and full citations are given in the reference list for the appendix.

The 2-km Rule for Grouping of Porphyry Copper Sites

Singer and others (2005) promulgated the 2-km rule for aggregation of spatially grouped porphyry copper ore zones or deposits. This rule provides a consistent strategy for grouping of porphyry copper deposits or prospects within a single or composite porphyry copper system. Resources of spatially grouped deposits are aggregated to represent the total resources of the composite porphyry copper system. Such grouping and aggregation is required for construction of internally consistent grade-tonnage models, for comparison of known deposits in a study area with those included in a grade-tonnage model, and for consistent calculation of spatial densities of porphyry copper deposits in permissive tracts.

The 2-km rule for aggregation of porphyry copper resources states that “deposits that have mineralization or alteration separated by less than an arbitrary but consistent distance—2 km for porphyry copper deposits—are combined into one” (Singer and others, 2005, p. 491). To rigorously apply the 2-km rule, the length, width, and orientation of every deposit in every cluster of porphyry copper sites would have to be known. However, we do not know the axial dimensions or orientations of zones of mineralized or altered rocks associated with most porphyry copper deposits in eastern Australia.

The axial dimensions of mapped zones of mineralized or altered rocks associated with ten Australian porphyry copper deposits, as compiled by Singer and others (2008), are listed in table 1. Five porphyry Cu-Au sites are relatively elongate, with a mean axial ratio of about 3:1, whereas five porphyry copper sites have a mean axial ratio of about 2:1. However, the orientations of their long axes are unknown. We therefore assume that such zones are approximately circular, with a diameter approximated by the 2.3-km mean of the lengths of the long axes of the ten examples listed by Singer and others (2008). Rotation of this 2.3-km axis through 360 degrees about its midpoint describes a circle with a diameter of 2.3 km, and a radius of 1.15 km. This provides a mean-based approximation of the area within which mineralized or altered rocks associated with an Australian porphyry copper or porphyry Cu-Au site are likely to occur.

Figure 2 shows examples of how deposits and prospects of the Temora Central and Temora South groups of deposits are grouped according to this strategy. Each point location is surrounded by a circular buffer zone with a radius of 1.15 km. Sites are grouped if their buffer zones are less than 2 km apart or their point locations are less than 4.3 km apart, since (2 radii + 2) km = 4.3 km.

Aggregation of Estimated Resources of Spatially Grouped Deposits

Estimated resources of grouped deposits are aggregated to yield the total tonnage and average grade of the group. Estimated tonnages and grades of the individual deposits and of deposit groups are given in a table of known deposits for each permissive tract, as well as in appendix F. A prospect that is spatially grouped with a known deposit is regarded as an indication of a possible extension to the known deposit, and any resources subsequently discovered at a prospect within the group are aggregated with those of the known deposit or deposits of the group. Thus, a prospect that is grouped with a known deposit is not considered to represent a possible undiscovered deposit.

Ranking and Rating of Prospects

Ranking and rating of prospects provides a way to arrange prospects in order of quality, based on known

Table 1. Axial lengths of areas of mineralized or altered rocks around 10 porphyry copper sites in eastern Australia.

[km, kilometer. Axial lengths from Singer and others (2008). Coordinates and descriptions for these sites are presented in appendix F; locations are shown on figures B1, C1, D1, and E1. -, not applicable]

Site name	Site status	Tectonic setting	Deposit type	Zone of mineralized or altered rocks	
				Long axis (km)	Short axis (km)
Allendale	Prospect	Island arc	Porphyry Cu-Au	2.5	1.5
Bowan Park	Prospect	Island arc	Porphyry Cu-Au	3.7	0.3
Copper Hill	Deposit	Island arc	Porphyry Cu-Au	2.7	1
Dairy Hill	Prospect	Island arc	Porphyry Cu-Au	0.55	0.15
Endeavour E-48	Deposit	Island arc	Porphyry Cu-Au	1	0.5
Anabama Hill	Prospect	Continental arc	Porphyry Cu	0.98	0.5
Coalstoun	Deposit	Continental arc	Porphyry Cu	1.1	0.8
Dogwood	Prospect	Continental arc	Porphyry Cu	4	2
Frogmore	Prospect	Continental arc	Porphyry Cu	0.8	0.4
Moonmera	Prospect	Continental arc	Porphyry Cu	5.9	2.5
Means of axes of zones of mineralized or altered rocks				2.3	1.0
Add 2 kilometers between zones of mineralized or altered rocks				2.0	-
Maximum distance between grouped sites				4.3	-

exploration results to date. In this study, prospects were ranked and rated according to criteria listed in table 2. Ranks are numbered in ascending order from most- to least-favorable, so that the best prospects are listed first. Conversely, ratings are numbered in descending order from most- to least-favorable, so that the sum of the ratings in a tract gives an overall indication of the exploration potential of the tract, based on the number and quality of prospects, as indicated by known exploration results. It should be borne in mind, however, that some relatively untested prospects may have more potential than those that have been more thoroughly tested. Thus, results-based rankings and ratings must be considered in the context of relevant geology and exploration history.

Grade-Tonnage Models

Tonnages and average grades of copper and gold in Australian porphyry Cu-Au deposits do not differ significantly from those of the global grade-tonnage model for deposits of the porphyry Cu-Au subtype (by Singer and others, 2008). However, tonnages and average grades of 15 Australian porphyry copper deposits are significantly lower than those of the global porphyry copper, porphyry Cu-Au, or porphyry Cu-Mo grade-tonnage models by Singer and others (2008). A custom grade-tonnage model was therefore developed to represent undiscovered porphyry copper deposits in some areas of eastern Australian (appendix A).

Delineation of Porphyry Copper Permissive Tracts in Eastern Australia

Permissive tracts for porphyry copper were delineated on the basis of spatial and temporal distributions of known porphyry copper and porphyry Cu-Au deposits and prospects, and of igneous rocks of permissive composition in geologic settings considered permissive for the occurrence of porphyry copper deposits.

Spatial Distributions of Known Porphyry Copper Sites

Every known deposit and significant prospect of a specified type in a study area should be included in a permissive tract for that deposit type. In well-explored study areas, such as eastern Australia, locations of most exposed porphyry copper deposits and prospects probably are known, and some hidden ones also are known. Thus, a map showing the spatial distribution of known porphyry copper deposits and prospects provides a minimum representation of areas that must be included in permissive tracts for porphyry copper.

Permissive Rock Types

A list of permissive rock types, compiled from descriptive models for porphyry copper (Cox, 1986a), porphyry Cu-Mo (Cox, 1986b), skarn-related porphyry copper (Cox, 1986d),

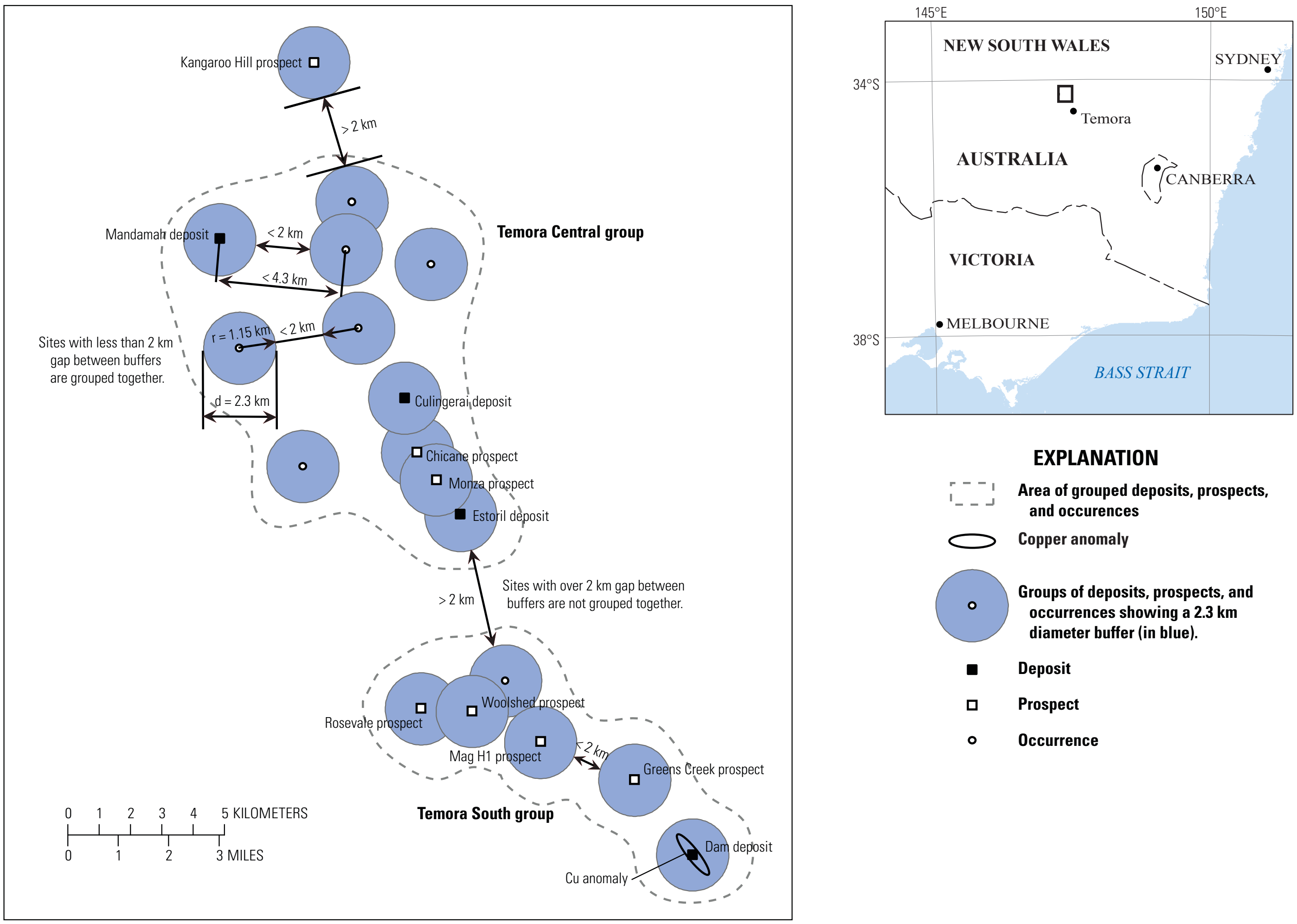

Figure 2. Map of porphyry copper deposits and prospects in the southern and central parts of Temora area, eastern Australia, as grouped according to the 2-kilometer (km) rule of Singer and others (2005). Diameter of the blue site-centered buffer is 2.3 km. This is the mean length of the long axes of zones of mineralization or alteration associated with five porphyry copper and five porphyry Cu-Au sites in eastern Australia (table 2). Where the distance between such buffers is less than 2 km (or the distance between point-locations of sites is less than 4.3 km) the sites are grouped according to the 2-km rule, and their resources are aggregated. r, radius; d, diameter.

Table 2. Criteria for ranking and rating of porphyry copper deposits, prospects, and related sites in eastern Australia.

[%, percent; m, meter]

Rank	Criteria	Rating points
1	Porphyry copper deposit containing at least 20,000 metric tons Cu at average grade of at least 0.15% Cu	9
2	Porphyry copper deposit or prospect with an estimated resource, and known to be open in one or more directions	8
3	Porphyry copper prospect with a best intercept of 20 m or more at an average grade of at least 0.15% Cu	7
4	Porphyry copper prospect with a best intercept of less than 20 m, or an average grade of less than about 0.15% Cu	6
5	Site that may be part of, or directly associated with, a porphyry copper system (for example, a porphyry-related, copper-bearing site either near a porphyry copper deposit or with copper as a byproduct; or a copper-bearing skarn, breccia, or vein swarm; or a high-sulfidation epithermal gold system)	5
6	Porphyry copper prospect with little or no assay data, but with prospective geological, geochemical, or geophysical characteristics	4
7	Copper occurrence, geochemical, or geophysical anomaly with weak indications of geological, geochemical, or geophysical characteristics deemed prospective for a porphyry copper deposit	3
8	Site that may be indirectly associated with a porphyry copper system (for example, base-metal skarn, vein or replacement, low-fluorine porphyry Mo, distal disseminated Au-Ag, or low-sulfidation epithermal Au-Ag system)	2
9	Copper occurrence or geochemical anomaly, with or without Mo or Au, with little or no evidence of a porphyry-related hydrothermal system	1
10	Copper-bearing deposit, prospect, or occurrence not classified as porphyry copper, and unlikely to be related to a porphyry copper system (for example, volcanic-hosted massive sulfide, sedimentary-exhalative, epigenetic sediment-hosted copper, iron-oxide copper-gold, or orogenic gold deposits)	0

and porphyry Cu ± Mo ± Au deposits (Panteleyev, 1995a, 2005a), includes the following visibly crystalline (plutonic) rock types of calc-alkaline affinity: gabbro, diorite, quartz diorite, quartz monzonite, and I-type granitoids, such as tonalite, monzogranite, and granite (of calc-alkaline affinity). Aphanitic to porphyro-aphanitic equivalents of calc-alkaline affinity include basalt or diabase to basaltic andesite, andesite, quartz andesite, quartz latite, and I-type dacite, rhyodacite, and rhyolite.

A list of permissive rock types, compiled from descriptive models for porphyry Cu-Au deposits by Cox (1986c) and Panteleyev (1995b, 2005b), includes the following visibly crystalline (plutonic) rock types of alkaline affinity: gabbro, diorite, monzodiorite, monzonite, quartz monzonite, syenite, quartz syenite, and foidal syenite. Aphanitic to porphyro-aphanitic equivalents of alkaline affinity include basalt, andesite, trachyandesite, shoshonite (potassic basalt to potassic trachyandesite), latite, quartz latite, trachyte, quartz trachyte, and foidal trachyte.

From geologic map-unit descriptions, permissive rock types were identified and classified as intrusive, volcanic, or volcanic-sedimentary. Map units representing lithologic assemblages that include permissive rock types were classified as permissive intrusive, volcanic, or volcanic-sedimentary. Volcanic and intrusive rock types considered permissive for porphyry copper in eastern Australia were included in permissive tracts and sub-tracts (table 3).

Spatial Distribution and Age Constraints for Permissive Rocks in Relation to Orogens

Maps showing the spatial distribution of compositionally permissive volcanic and intrusive units were derived from source geologic maps. Permissive tracts and known porphyry copper sites occur in the Delamerian, Lachlan, New England, and North Queensland Orogens (fig. 1 and table 3).

These orogens provide a geologic framework for definition and delineation of permissive tracts. The Delamerian permissive tract is co-spatial with the partly exposed southern part of the Delamerian Orogen. The Macquarie tract is co-spatial with the accreted Macquarie island-arc complex in the eastern part of the Lachlan Orogen. The Yeoval tract is in and around the post-Macquarie Cowra-Buchan Rift System, in the eastern part of the Lachlan Orogen. The East Tasmanide tract is in the New England and North Queensland Orogens (figs. 1 and 4, and table 4).

A first attempt at classification of permissive tracts by age was based on the sequence of successive tectonic cycles. According to Glen (2005) and Champion and others (2009), the following sequence of tectonic cycles occurred in the Tasmanides of eastern Australia:

1. Delamerian cycle—Late Neoproterozoic to Late Cambrian (600–490 million years before present, Ma),

2. Benambran cycle—Late Cambrian to Earliest Silurian (490–430 Ma),

3. Tabberabberan cycle—Middle Silurian to Late Devonian (430–380 Ma),

Table 3. Volcanic and intrusive rocks in porphyry copper permissive tracts of eastern Australia.

[Igneous rock terminology recommended by the International Union of Geological Sciences, according to Le Maitre (2002); volcanic/intrusive areal ratio, area of mapped volcanic rocks (v) compared to area of mapped igenous rocks (i) in the permissive tract. >>, much greater than; <<, much less than]

Permissive tract or sub-tract	Coded_ID	Permissive volcanic rocks	Permissive intrusive rocks	Volcanic/ intrusive areal ratio (v/i)
Delamerian tract	009pCu8001			
Adelaide sub-tract	009pCu8001a	basalt to andesite	minor diorite to I-type granite	v >> i
Adelaide sub-tract	009pCu8001a	magnetic volcanics in subsurface	I-type granitoid plutons	v << i
Adelaide sub-tract	009pCu8001a	andesite	dacitic plugs and dikes	v > i
Victoria sub-tract	009pCu8001b	basalt to boninite; andesite to dacite	minor metagabbro	v >> i
Tasmania sub-tract	009pCu8001c	shoshonitic basalt, andesite, felsite	minor I-type granitoid intrusions	v >> i
Macquarie tract	009pCu8002	shoshonitic basaltoid to andesitoid and trachytoid volcanics; minor dacitoid volcanics	small gabbroic to dioritic and monzonitic to quartz monzonitic intrusions; minor tonalitic to dacitic intrusions	79v / 1i
Yeoval tract	009pCu8003	rhyolitic ignimbrites, and later andesite to dacite	diorite to dacite porphyry, and later granite	1v / 1.1i
East Tasmanide tract	009pCu8004			
Island-arc sub-tract	009pCu8004a	basalt to andesite	I-type trondhjemite	v >> i
Central sub-tract	009pCu8004b	basalt, andesite, dacite, rhyolite flows, tuffs	I-type granitoid, syenitoid, dioritoid, and gabbroid plutons; minor pegmatites, aplites, mafic to felsic dikes and intrusive breccias	1v / 2i
South sub-tract	009pCu8004c	basalt, andesite, dacite, rhyolite flows, tuffs	I-type granitoid and minor dioritoid to syenitoid plutons	1v / 9.9i
North sub-tract	009pCu8004d	andesite, dacite, rhyolite flows, tuffs	I-type granitoid and minor dioritoid plutons; rare felsitic intrusions	1v / 2.7i

4. Kanimblan cycle—Late Devonian to Early Carboniferous (380–350 Ma), and
5. Hunter Bowen cycle—Early Carboniferous (Mississippian) to Middle Triassic (350–230 Ma).

In order for age-ranges of map units to be sorted and classified in terms of tectonic cycles, age-ranges of map units, listed in terms of geologic-age units, had to be converted to numerical age-ranges in millions of years. These conversions were made using a table by Rohde (2005), which indicates internationally accepted numerical age limits for each Period and Epoch, as well as for each Australian biostratigraphic stage. After age ranges of map units were bracketed by maximum and minimum numerical age limits, a mid-range age was calculated for each.

Permissive units were then sorted by mid-range age, classified by tectonic cycle, and plotted as a function of age, from 540 to 10 Ma, in 10-million-year increments (fig. 3*A*). This worked well for map units representing rocks formed during relatively short and well-constrained time intervals, but was less satisfactory for units representing rocks formed during long, poorly constrained time intervals. Furthermore, figure 3*A* does not distinguish between map units formed in different tectonic environments, such as volcanic island arcs, continental magmatic arcs, or postorogenic rifts.

A parallel approach to definition of age constraints for permissive tracts was based on a comparison of rates of magmatism and porphyry copper formation through time (fig. 3*B*). Comparison of figures 3*A* and 3*B* indicates the following episodes of relatively high rates of magmatism and porphyry-related mineralization in eastern Australia:

1. Late Cambrian,
2. Late Ordovician to Early Silurian,
3. Late Silurian to Devonian,
4. Carboniferous to Middle Permian,
5. Late Permian to Triassic, and
6. Early Cretaceous.

For each of these intervals of geologic time, locations of permissive map units and known porphyry copper deposits and prospects were plotted to define a refined set of permissive tracts on the basis of both spatial and temporal constraints.

Permissive units and known porphyry copper prospects of Late Cambrian age define the area of the Delamerian tract in the Delamerian Orogen. Similarly, permissive units and known porphyry Cu-Au and porphyry copper sites of

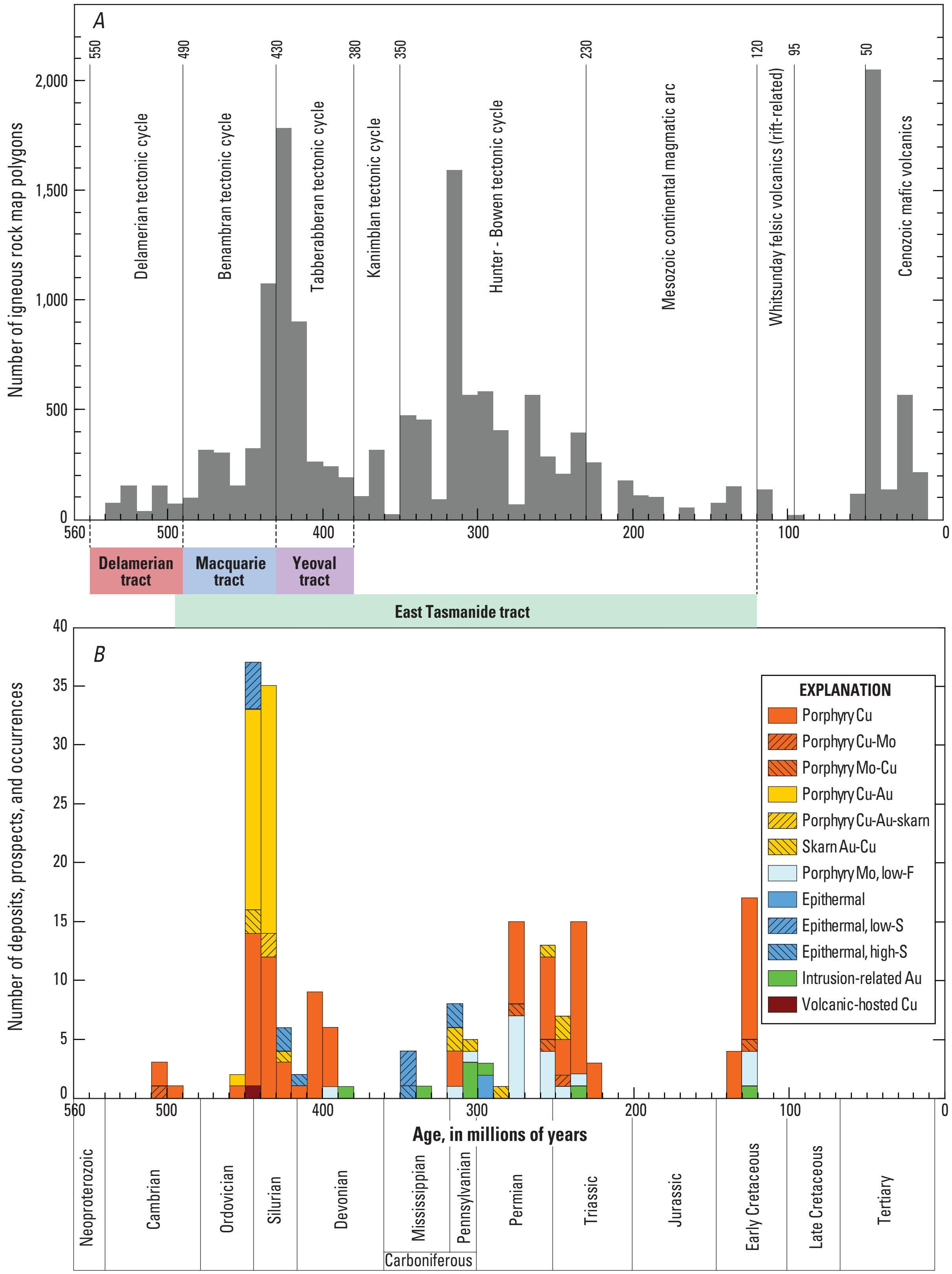

Figure 3. Frequency diagrams of geologic-map polygons that represent eastern Australian igneous rocks (*A*) and porphyry and porphyry-related mineral deposits (*B*) plotted against age, in millions of years (Ma). Mid-range ages of igneous-rock map units are from attribute tables accompanying 1:1,000,000-scale geologic maps (Raymond, Liu, and Kilgour, 2007; Raymond, Liu, Kilgour, Retter, and Connolly, 2007; Raymond, Liu, Kilgour, Retter, Stewart, and Stewart, 2007; Whitaker and others, 2007, 2008). Mid-range ages of mineral deposits are based on isotopic age determinations or relative age relations, as tabulated in appendix F.

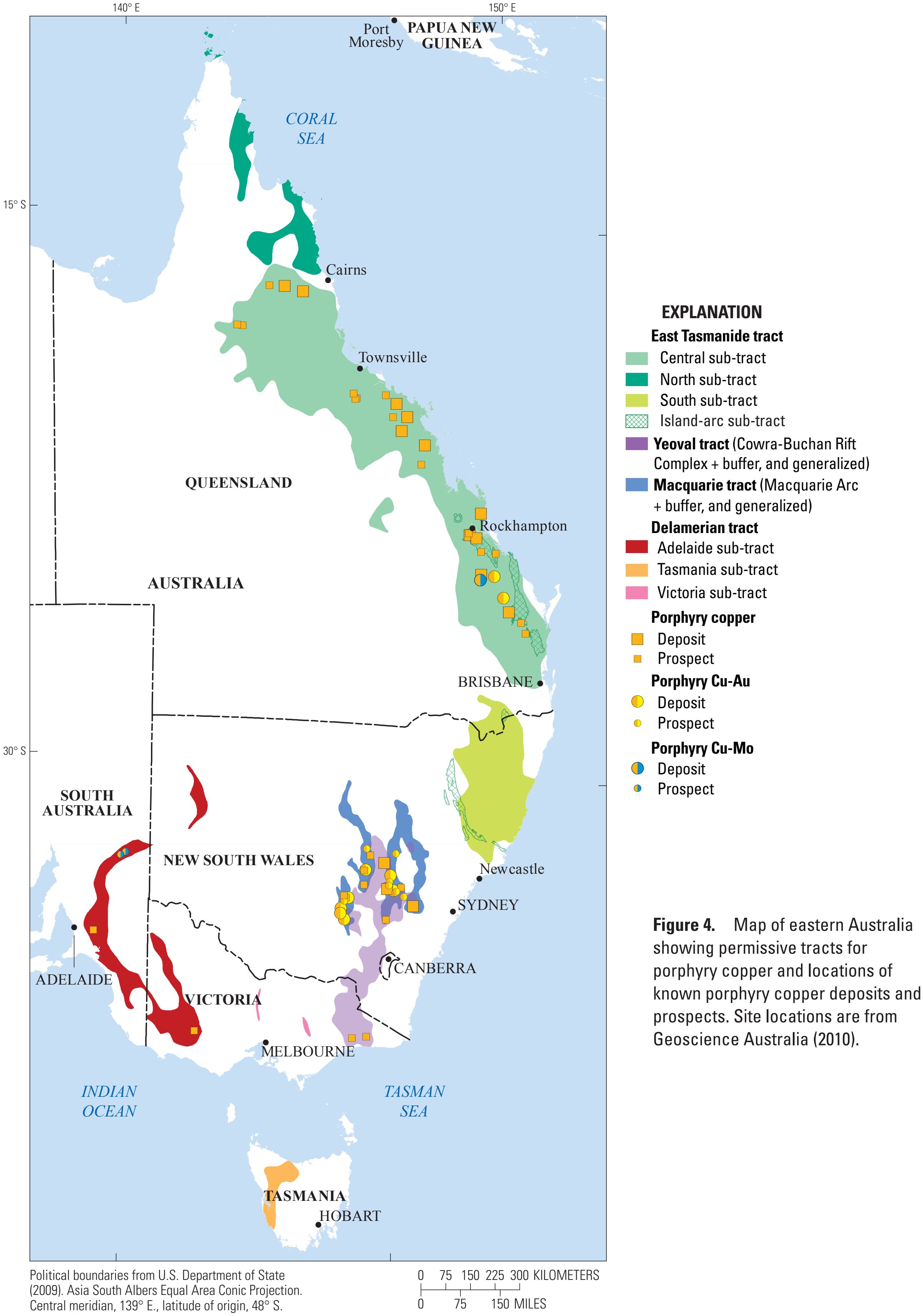

Figure 4. Map of eastern Australia showing permissive tracts for porphyry copper and locations of known porphyry copper deposits and prospects. Site locations are from Geoscience Australia (2010).

Table 4. Ages and inferred tectonic settings of permissive rocks and porphyry copper sites in eastern Australia.

[Ma, million years; units of geologic time and their numerical age boundaries in millions of years before the present (Ma) are in accordance with geologic time scales by the International Commission on Stratigraphy (2010) and the U.S. Geological Survey Geologic Names Committee (2007) for internationally recognized Periods and Epochs, and by Rohde (2005) for Australian biozone Stages; no pCu, no known porphyry copper sites]

Permissive tract or sub-tract	Coded_ID	Tectonic setting	Porphyry copper age (Ma)	Geologic age range of permissive units in tract or sub-tract	Permissive-unit age (Ma)
Delamerian tract	**009pCu8001**	Delamerian Orogen	503–490	Late Neoproterozoic to Cambrian	630–488
Adelaide sub-tract	009pCu8001a	island arc, continental arc, and postorogenic backarc rift	503–490	Cambrian	542–488
Victoria sub-tract	009pCu8001b	incipient island arc and back-arc-rift fragments	no pCu	Cambrian	542–488
Tasmania sub-tract	009pCu8001c	postorogenic back-arc rift	no pCu	Middle to Late Cambrian	513–488
Macquarie tract	**009pCu8002**	accreted island arc in Lachlan Orogen	447–433	Late Ordovician to Early Silurian	488–428
Yeoval tract	**009pCu8003**	postorogenic back-arc rift in Lachlan Orogen	422–407	Late Silurian to Early Devonian	423–397
East Tasmanide tract	**009pCu8004**	New England Orogen and North Queensland Orogen	395–119	Cambrian to Early Cretaceous	542–100
Island-arc sub-tract	009pCu8004a	island-arc fragments	no pCu	Silurian to Permian	444–251
Central sub-tract	009pCu8004b	continental magmatic arcs	395–119	Cambrian to Early Cretaceous	542–100
South sub-tract	009pCu8004c	continental magmatic arcs	no pCu	Carboniferous to Triassic	359–200
North sub-tract	009pCu8004d	continental magmatic arcs	no pCu	Carboniferous to Permian	359–251

Late Ordovician to Early Silurian age define the Macquarie tract in the Macquarie Arc, and permissive units and known porphyry copper sites of Late Silurian to Devonian age define the Yeoval tract in and around the Cowra-Buchan Rift System (figs. 1 and 4, and table 4).

In the East Tasmanide tract, however, the New England and North Queensland Orogens contain closely spaced and contiguous to interspersed permissive units and porphyry-related deposits and prospects that range in age from Late Cambrian to Early Cretaceous (figs. 1 and 4, and table 4). Regardless of their ages, however, porphyry-related deposits and prospects of the eastern Tasmanide region are generally similar in terms of their geological character (appendix E), and their grade-tonnage characteristics (appendix A). The East Tasmanide tract is therefore delineated on the basis of spatial distributions of permissive units and porphyry-related deposits and prospects, regardless of differences in age and tectonic setting (fig. 4 and table 4). East Tasmanide sub-tracts are defined on the basis of tectonic setting, and presence or absence of known porphyry copper sites.

Buffering Outcrop Patterns and Smoothing Tract Shapes

After selecting permissive map units, we added buffers around them to expand the area of the permissive tract and to fill spaces between known bodies of permissive rocks. We added a 10-km buffer zone around mapped igneous intrusions and a 2-km buffer zone around bodies of volcanic rocks. We did not buffer polygons representing units of interlayered volcanic and sedimentary strata. Such buffering expanded the area of the permissive tract to include all significant porphyry copper prospects. The buffers allow for possible downward expansion of intrusions below their surface expressions (subsurface satellite cupolas of intrusions and unmapped parts of plutons), and also provide extensions of intrusive and extrusive units beneath overlapping cover materials, such as younger basalt flows, glacial till, colluvium, alluvium, or basin-fill sediments less than 1 km thick. The rationale for buffering, and in particular 10-km and 2-km buffers, includes a number of factors:

- Intrusion contacts commonly slope outwards, and porphyry copper deposits, which can form peripherally to intrusive bodies, can have dimensions as large as 10 km;
- Bodies of permissive volcanic rocks may have relatively thin edges, which might be discontinuous, covered, or otherwise not mapped at the scale of the source geologic maps used for the assessment;
- Proximity analysis of volcanic rock-hosted gold and silver deposits in Nevada, United States, indicates that the majority of significant occurrences lie within

10 km of a plutonic body, as mapped at 1:500,000 scale (Mihalasky, 2001, p. 75–76);

- Ten kilometers is a subjective, expert-based estimate representing the nominal extent of a mining lease, which may or may not include peripheral claims, prospects, or other exploration areas;
- A radius of 10 km around a pluton may be a fair approximation for the extent of (or at least encompasses) the potentially mineralizing system (that is, the extent of district or local-scale hydrothermal circulation (see Nesbitt and Muehlenbachs, 1989; Sillitoe and Bonham, 1990));
- A radius of 2 km around volcanic map units represents an expert-based judgment that related or concealed intrusions in those map units are likely to be much smaller and limited in extent; and
- Accepted precedent for the use of buffers around igneous map units to delineate permissive tracts in previous USGS mineral resource assessments, including Singer (1996) and Wallace and others (2004).

Although these buffers may not be appropriate in all instances—10 km may be an overestimate with regard to small igneous bodies or an underestimate for extensive, long-lived bodies—for all practical purposes, they are considered reasonable for including permissive areas of interest within the tectonic environment being assessed (for more detailed discussion, see Wallace and others, 2004, p. 105, 125–126, 131).

Geophysical Detection of Permissive Rocks in the Subsurface

Clark (1999) noted that porphyry copper deposits generally are associated with oxidized, I-type, mafic to felsic igneous rocks, which he characterized as ferromagnetic rocks of the magnetite series. Where such ferromagnetic rocks are surrounded by less ferromagnetic rocks, they can be detected by magnetic and aeromagnetic surveys. We therefore interpreted positive reduced-to-pole magnetic anomalies to indicate ferromagnetic rocks in the subsurface.

After buffering exposures of permissive rocks, we adjusted tract boundaries to include aeromagnetic anomalies interpreted to represent subsurface intrusions related to the tract, but extending beyond its buffered margins. Next, we used a spatial modeling algorithm to connect permissive areas less than 20 km apart and to smooth the boundaries of the permissive tracts. See the metadata included with appendix G for additional details. We trimmed the buffered and smoothed tracts so as not to extend across major strike-slip faults and terrane boundaries, except as necessary to include permissive rocks to a depth of 1 km. We also excluded areas of plutons that are younger than the time span of the magmatic arc represented by the permissive tract.

Porphyry Copper Tracts in Eastern Australia

Porphyry copper tracts in eastern Australia include permissive volcanic and intrusive igneous rocks of the Delamerian tract in the Delamerian Orogen, the Macquarie tract in the Macquarie Arc of the Lachlan Orogen, the Yeoval tract in the Cowra-Buchan Rift System of the Lachlan Orogen, and the East Tasmanide tract in the New England and North Queensland Orogens (figs. 1 and 4, and tables 3, 4, and 5).

Mildly alkaline assemblages of igneous rocks are considered permissive for porphyry Cu-Au deposits in the Macquarie Arc, whereas calc-alkaline assemblages of igneous rocks are considered permissive for porphyry copper deposits in the Delamerian, Yeoval, and East Tasmanide tracts (table 3). Inferred tectonic settings of igneous rocks in permissive map units include subduction-related oceanic island arcs, continental magmatic arcs, and postorogenic back-arc rifts, possibly related to subduction rollback (table 4).

Porphyry copper deposits generally are associated with high-level intrusions, such as porphyry stocks, plugs, dike swarms, and associated breccias. However, such small features are not likely to be shown on regional geologic source maps at 1:1,000,000 scale. Nevertheless, such maps do show the distribution of volcanic and intrusive rocks, and depth of exposure can be inferred from a combination of igneous textures, intrusion sizes, and ratios of areas of related volcanic and intrusive rocks (Staude and Barton, 2001).

The ratio of volcanic rocks to small porphyry intrusions is very high (79v/1i) in the Macquarie tract (table 3). This indicates a very high level of exposure where porphyry Cu-Au deposits are likely to have formed, and to have been preserved, but may be hidden beneath volcanic cover. Small to moderate-sized intrusions of porphyritic to phaneritic rocks and a ratio of nearly 1v/1i in the Yeoval tract indicates favorable levels of exposure, where porphyry copper deposits may have formed and may be partially to fully preserved and exposed. Large, phaneritic intrusions and a very low ratio of 1v/10i in the South sub-tract of the East Tasmanide tract indicate deep levels of exposure, too deep for either generation or preservation of porphyry copper deposits.

As shown in table 5, quantitative assessments were completed for the resources expected in undiscovered deposits of the Delamerian Adelaide sub-tract, the Macquarie tract, the Yeoval tract, and the East Tasmanide Central sub-tract. The global grade-tonnage model for porphyry Cu-Au deposits by Singer and others (2008) was used for estimation of resources in undiscovered deposits of the Macquarie tract. A custom Australian grade-tonnage model, however, was used for estimation of resources in undiscovered deposits of the Delamerian, Yeoval, and East Tasmanide tracts.

Table 5. Selected characteristics of permissive tracts for porphyry copper deposits in eastern Australia.

[km², square kilometers; Australian, Australian grade-tonnage model (appendix A); Global, global grade-tonnage model (Singer and others, 2008)]

Permissive tract or sub-tract	Coded_ID	Assessment type	Porphyry copper			Tract area (km²)
			Known deposits	Significant prospects	Grade-tonnage model	
Delamerian tract	**009pCu8001**		0	4		
Adelaide sub-tract	009pCu8001a	quantitative	0	4	Australian	50,700
Victoria sub-tract	009pCu8001b	qualitative	0	0		
Tasmania sub-tract	009pCu8001c	qualitative	0	0		
Macquarie tract	**009pCu8002**	quantitative	9	10	Global	41,500
Yeoval tract	**009pCu8003**	quantitative	1	8	Australian	53,200
East Tasmanide tract	**009pCu8004**		14	15		
Island-arc sub-tract	009pCu8004a	qualitative	0	0		
Central sub-tract	009pCu8004b	quantitative	14	15	Australian	291,000
South sub-tract	009pCu8004c	qualitative	0	0		
North sub-tract	009pCu8004d	qualitative	0	0		

Permissive Tract Descriptions

Permissive tract descriptions are given in appendixes B through E. Each of these tract descriptions contains tract maps showing locations of known deposits and prospects, tables of identified resources in known deposits, and descriptions of the known deposits. Also included are maps and tables of significant prospects, and summaries of recent exploration activities. Rationales for tract delineation and estimation of numbers of undiscovered deposits are explained. Results of probabilistic estimation of tonnages of mineralized rock and contained copper, molybdenum, gold, and silver that are expected to occur in undiscovered deposits are graphed across a range of subjective probabilities. Summary descriptions of porphyry copper permissive tracts in eastern Australia follow below.

Delamerian Tract (009pCu8001[6])

The Delamerian permissive tract is defined by the distribution of permissive rocks in parts of the Delamerian Orogen, as exposed or indicated by magnetic anomalies in bedrock under less than 1 km of cover. The Delamerian Orogen overlaps the eastern margin of cratonic Australia and is transitional with the Neoproterozoic Adelaide Rift Complex to the southwest. Because much of the Delamerian Orogen is covered, the Delamerian tract is geographically divided into three sub-tracts (fig. 4).

[6]Each tract and sub-tract has been assigned a unique identifier for the global assessment geographic information system. This identifier includes a three-digit code for the United Nations geographical region (UNdata, 2009), such as 009 for Oceania, a deposit type abbreviation (pCu for porphyry copper), a four-digit number for the permissive tract (8001–8004 for this assessment), and a letter code, if necessary, to indicate a sub-tract.

Adelaide Sub-Tract (009pCu8001a)

The Adelaide sub-tract extends southward from northwestern New South Wales into South Australia and continues southeastward into Victoria. At the north end of the Adelaide sub-tract, permissive volcanic and subordinate intrusive rocks are interpreted as products of island-arc magmatism, related to west-dipping subduction (Greenfield and others, 2011). In the west-central part of the Adelaide sub-tract, tightly folded turbidites, interlayered with subordinate volcanic rocks, are intruded by permissive granitoid plutons, which are interpreted as products of a continental magmatic arc, related to west-dipping subduction beneath the eastern continental margin during the Delamerian Orogeny (Foden and others, 2006). In the southeastern part of the Adelaide sub-tract, permissive volcanic rocks and subordinate intrusions are interpreted as products of postorogenic magmatism and extensional tectonism, related to rollback of subduction following the Delamerian Orogeny.

Although the Adelaide sub-tract contains no known porphyry copper deposits, it does contain four porphyry copper prospects—three in synorogenic granitoid plutons in the west-central part of the sub-tract, and one in postorogenic volcanic and subvolcanic rocks in the southeastern part of the sub-tract. A five-member assessment panel considered the geology of the Adelaide sub-tract, the known prospects, the apparently deep level of exposure of granitoid plutons, the relatively shallow level of exposure of postorogenic intrusions, the extent of cover, and the history of exploration for porphyry copper deposits in this permissive tract. On the basis of this information, the panel estimates 2.5±2.2 undiscovered porphyry Cu-Au deposits (table 6).

Victoria Sub-Tract (009pCu8001b)

The Victoria sub-tract includes pre-orogenic metavolcanic rocks of a boninite-andesite-tholeiite assemblage in fault-bounded greenstone belts in central Victoria and calc-alkaline volcanic and volcaniclastic rocks in the fault-bounded volcanic belts in east-central Victoria. Although these rocks are considered permissive for porphyry copper resources, they contain no known porphyry copper deposits or prospects, so this sub-tract was qualitatively judged to have low potential for porphyry copper deposits.

Tasmania Sub-Tract (009pCu8001c)

The Tasmania sub-tract is in western Tasmania. It includes volcanic rocks of calc-alkaline affinity, which erupted into half-grabens during post-Delamerian extension. It also includes minor post-volcanic granitoid intrusions (Foster and others, 2005). Volcanic rocks in this sub-tract contain significant volcanic-hosted massive sulfide deposits, some of which show evidence of later epithermal mineralization. However, there are no known porphyry copper deposits or prospects in this sub-tract, so it was qualitatively judged to have low potential for undiscovered porphyry copper deposits.

Macquarie Tract (009pCu8002)

The Macquarie tract includes permissive rocks for porphyry copper and porphyry Cu-Au deposits in the Macquarie Arc. This arc is an accreted oceanic island-arc complex of Ordovician to Early Silurian age (about 490–430 Ma) in the east-central part of the Lachlan Orogen (compare figs. 1 and 4). The Macquarie Arc consists mostly of volcanic to volcaniclastic rocks with subordinate sedimentary interlayers, and minor subvolcanic intrusions. Permissive intrusions are mapped in only about 1.3 percent of the surface area of the Macquarie permissive tract.

The Macquarie Arc, west of the Sydney Basin in eastern New South Wales (fig. 1), comprises volcanic, volcaniclastic, and intrusive rocks exposed in north-trending, fault-bounded volcanic belts. Glen and others (2007) interpreted mapped exposures, drill intercepts, and magnetic anomaly patterns to indicate surface and subsurface expressions of the volcanic belts within this arc.

The Macquarie permissive tract contains nine known porphyry copper deposits, seven of which are of the porphyry Cu-Au subtype (fig. 1). Most of the known porphyry Cu-Au deposits are associated with mildly potassic (shoshonitic) suites of monzonitic to quartz monzonitic intrusions (Blevin, 2002). These deposits and their associated intrusions range in age from Late Ordovician to Early Silurian (about 447–433 Ma, as documented in appendix F). This tract also contains two porphyry copper deposits that are related to calc-alkaline suites of tonalitic to dacitic intrusions.

The Macquarie tract contains more than 20 significant porphyry Cu-Au prospects, about half of which are spatially grouped with known deposits. Most of the spatially independent prospects have best intercepts of 20 m or more at an average copper grade of at least 0.15 percent Cu. This tract also contains Cu-Au skarn and epithermal deposits, some of which are known to be spatially associated with porphyry copper systems.

A five-member assessment panel considered the geology of the Macquarie permissive tract, the high level of exposure of intrusions, the high proportion of cover, the known mineral deposits and prospects, and the history of exploration for porphyry Cu-Au deposits. On the basis of this information, the panel estimates 6.9±3.5 undiscovered porphyry Cu-Au deposits in the Macquarie permissive tract (table 6). Adding this to the 9 known deposits in the Macquarie permissive tract indicates that this tract is expected to contain 15.9±3.5 porphyry Cu-Au deposits within 1 km of the surface.

Yeoval Tract (009pCu8003)

The Yeoval permissive tract (fig. 4) is defined by a belt of permissive volcanic and intrusive igneous rocks of Late Silurian to Devonian age in and around the Cowra-Buchan Rift Complex. Sedimentary and felsic volcanic and volcaniclastic debris filled subsiding grabens and troughs of this rift system in Silurian time. Andesitic volcanic rocks, plutons of dioritic to granodioritic composition, and small intrusions of dacite porphyry were emplaced after rift-fill sedimentary and volcanic strata were folded during the Bindian Orogeny (420–410 Ma, according to Champion and others, 2009).

The Yeoval porphyry copper deposit is hosted by small dacite intrusions of the Yeoval Complex (previously known as the Yeoval Diorite Complex, dated 411±2 Ma; Gulson and Bofinger, 1972). According to Gulson and Bofinger (1972) this intrusive complex consists of a calc-alkaline suite of igneous rocks with compositions similar to those of subduction-related, circum-Pacific magmatic arcs.

Igneous intrusions within or near the Cowra-Buchan Rift System are of permissive composition and of Late Silurian to Devonian age. These intrusions may have been emplaced in response to subduction or subduction rollback associated with the Late Silurian-Early Devonian Bindian Orogeny or the Late Devonian Tabberabberan Orogeny, or both.

Plutons of permissive composition and age are mapped to the east and west of the Yeoval permissive tract. However, these plutons are not considered permissive for porphyry copper, because of their relatively low volcanic-plutonic ratios, large sizes, phaneritic textures, and lack of known porphyry copper deposits or prospects.

A five-member assessment panel considered the geology of the Yeoval permissive tract, the known deposit and prospects, the moderate levels of exposure of intrusions in and around the Cowra-Buchan Rift System, the extent of cover, and the history of exploration for porphyry copper deposits. On the basis of this information, the panel estimates 1.3±0.75 undiscovered porphyry copper deposits expected in the Yeoval permissive tract (table 6). Adding this to the 1 known deposit indicates an expected 2.3±0.75 porphyry copper deposits within 1 km of the surface in the Yeoval permissive tract.

Table 6. Undiscovered deposit estimates, deposit numbers, tract areas, and deposit density for permissive tracts of eastern Australia.

[N_{XX}, estimated number of deposits associated with the xxth percentile; N_{und}, expected number of undiscovered deposits; *s*, standard deviation; C_v%, coefficient of variance; N_{known}, number of known deposits in the tract that are included in the grade and tonnage model; N_{total}, total of expected number of deposits plus known deposits; Tract area, area of permissive tract in square kilometers (km²); Deposit density, total number of deposits per 100,000 km². N_{und}, *s*, and C_v% are calculated using a regression equation (Singer and Menzie, 2005)]

Permissive tract (sub-tract)	Consensus undiscovered deposit estimates					Summary statistics					Tract area (km²)	Deposit density (N_{total}/100,000 km²)
	N_{90}	N_{50}	N_{10}	N_{05}	N_{01}	N_{und}	*s*	C_v%	N_{known}	N_{total}		
Delamerian (Adelaide)	0	2	5	7	7	2.5	2.2	91	0	2.5	50,747	4.9
Macquarie	2	7	12	12	12	6.9	3.5	52	9	15.9	41,463	39
Yeoval	1	1	2	3	3	1.3	0.75	57	1	2.3	53,157	4.3
East Tasmanide (Central)	1	4	10	10	10	4.8	3.3	68	14	18.8	290,646	6.5

East Tasmanide Tract (009pCu8004)

The East Tasmanide permissive tract extends along the eastern margin of Australia, from northeastern Queensland to northeastern New South Wales (fig. 4). This tract includes permissive igneous rocks of the New England and North Queensland Orogens (fig.1). Permissive rocks included in the East Tasmanide tract occur in several closely spaced to interspersed subduction-related magmatic belts. The East Tasmanide permissive tract is divided into four sub-tracts (fig. 4), as follows.

Island-arc Sub-tract (009pCu8004a)

The Island-arc sub-tract includes permissive igneous rocks in accreted fragments of volcanic island-arcs of Silurian-Devonian and Permian ages in the southern part of the New England Orogen (figs. 4, E2). One Silurian-Devonian island-arc fragment contains a significant pre-accretionary Cu-Au deposit, which appears to be a unique hybrid of volcanic-hosted massive-sulfide, intrusion-related replacement, and stockwork-veinlet deposit types. However, the Island-arc sub-tract contains no pre-accretionary porphyry copper deposits or significant prospects, so it was qualitatively judged to have low potential for undiscovered resources in undiscovered porphyry copper deposits.

Central Sub-Tract (009pCu8004b)

The Central sub-tract extent is based on the distribution of permissive igneous rocks of continental magmatic belts along the eastern continental margin (fig. 4). This sub-tract contains 14 known porphyry copper deposits and at least 15 significant porphyry copper prospects. Known deposits in this sub-tract are related to intrusions in four magmatic belts of different ages. Nevertheless, permissive rocks in these belts are mutually similar, and known porphyry copper deposits and prospects also are similar to each other. These deposits also are consistent with a single grade-tonnage model, developed for assessment of undiscovered porphyry copper resources in eastern Australia. For purposes of estimation of resources in undiscovered deposits, it is therefore appropriate to include these four magmatic belts and their associated porphyry copper sites in one permissive sub-tract.

A five-member assessment panel considered the geology of the Central sub-tract, the known deposit and prospects, the levels of exposure of intrusions, the extent of cover, and the history of exploration. On the basis of this information, the panel estimates 4.8±3.3 undiscovered porphyry copper deposits (table 6). Adding this to 14 known deposits indicates that 18.8±3.3 porphyry copper deposits are expected within 1 km of the surface in the Central sub-tract.

South Sub-Tract (009pCu8004c)

The South sub-tract is defined by the distribution of igneous rocks of permissive composition at the southern end of the New England Orogen, in northeastern New South Wales (fig. 4). There are no known porphyry copper deposits or significant prospects in this sub-tract. Furthermore, the presence of large, phaneritic intrusions with very little associated volcanic rock indicates that levels of exposure of intrusions in this sub-tract are too deep for generation or preservation of porphyry copper deposits. This sub-tract was therefore qualitatively judged to have low potential for undiscovered porphyry copper deposits.

North Sub-Tract (009pCu8004d)

The North sub-tract is defined by the distribution of igneous rocks of permissive composition in northeastern Queensland (fig. 4). Such rocks are sparsely scattered along the eastern margin of the Cape York Peninsula. This sub-tract, which contains no known porphyry copper deposits or prospects, was qualitatively judged to have low potential for undiscovered porphyry copper deposits.

Identified Resources of Porphyry Copper Deposits in Eastern Australia

Identified resources of known porphyry copper deposits in each of four permissive tracts are summarized in table 7. The Australian Mines Atlas (Geoscience Australia, 2010) is an important source of tonnage and grade information for identified resources of known copper deposits in Australia. These data should comply with classification standards of the JORC Code (Australasian Joint Ore Reserves Committee, 2004). However, mineral deposits are not described or classified by deposit-type in this database, so identification of porphyry copper deposits in this database requires information from other sources.

Other sources of information about Australian porphyry copper deposits and prospects include Australian national and provincial governmental reports and databases, published articles in the geologic literature, and internet sites of mining and mineral-exploration companies. Internet sites of Canadian companies may also include Canadian NI 43–101 reports, as required by Canadian stock exchanges (CIM Standing Committee on Reserve Definitions, 2004; British Columbia Securities Commission, 2005). NI 43–101 reports also are available at http://www.sedar.com/.

Ideally, a consistent cutoff grade should be used for compilation of estimated resources of multiple deposits. To be inclusive, workers on this project have been instructed to use the largest resource estimates available, based on the lowest available cutoff grades, and including not only identified, but also inferred resources. However, cutoff grades are not always mentioned in published resource estimates.

Identified resources of known mineral deposits are subject to change. An apparent increase in estimated resources can occur if metal prices rise faster than mining costs, and lower-grade mineralized rock is reclassified as ore. Conversely, an apparent decrease in estimated resources can result from the economic need to apply a higher cutoff grade. Negative changes in estimated resources also can occur if further testing indicates that a previous estimation was unrealistically optimistic. Production also decreases remaining resources, and it is not always clear whether a reported resource represents a total resource or a remaining resource.

Identified resources of a known deposit also may increase by discovery of previously unknown extensions to a known deposit or group of deposits. In this regard, it is important to note that by far the largest recent increase in Australian porphyry copper resources has resulted from discoveries of extensions to the known Cadia group of porphyry Cu-Au deposits. The total estimated resource at Cadia increased from 3.87 Mt copper in 1,210 Mt of ore (Singer and others, 2008) to 9.55 Mt copper in 3,450 Mt of ore (Geoscience Australia, 2010).

Probabilistic Assessment of Undiscovered Resources

Quantitative assessments of undiscovered resources rely on use of grade and tonnage data from well explored deposits as the basis for estimation of amounts of metal contained in undiscovered deposits. Two models were required for this assessment of Australian copper porphyry copper deposits.

Appropriate Grade-Tonnage Models

Tonnages and grades of known porphyry Cu-Au deposits in the Macquarie permissive tract are generally higher than those of known porphyry Cu deposits in the East Tasmanide and Yeoval permissive tracts. This indicates that the grade-tonnage model for porphyry Cu-Au deposits of the Macquarie permissive tract would be inappropriate for porphyry copper deposits in other permissive tracts in eastern Australia.

The 9 deposits in the Macquarie Arc were found to be statistically indistinguishable (in terms of tonnages of ore, and average grades of copper and gold) from the population of 112 other porphyry Cu-Au deposits represented in the global grade-tonnage model (appendix A).

Tonnages and average grades of 15 Australian porphyry copper deposits in the East Tasmanide and Yeoval tracts are significantly lower than those of the population of porphyry copper deposits represented in the global grade-tonnage model for porphyry copper deposits by Singer and others (2008). On the basis of grades and tonnages of these 15 known porphyry copper deposits, all from the East Tasmanide and Yeoval permissive tracts, a regional grade-tonnage model was developed for estimation of undiscovered porphyry copper resources of the East Tasmanide, Yeoval, and Delamerian permissive tracts (appendix A).

Estimation of Undiscovered Resources

A workshop was held in September 2010 to estimate numbers of undiscovered porphyry copper deposits in eastern Australia. USGS members of the estimation panel were geologists Arthur A. Bookstrom, Jane M. Hammarstrom, Gilpin R. Robinson, Jr., and Michael L. Zientek. The panel also included Richard A. Glen, of the Geological Survey of New South Wales, who provided helpful guidance and valuable suggestions based on his long experience and thorough knowledge of the geology and mineral resources of eastern Australia.

Before the estimation workshop, preliminary maps of four permissive tracts were made and a preliminary table of known porphyry copper deposits and prospects was compiled. Deposits and prospects were tentatively assigned to permissive tracts, and preliminary statistical testing was done

Table 7. Identified resources of known porphyry copper deposits and estimated resources in undiscovered deposits in permissive tracts of eastern Australia.

[Cu, copper, and Au, gold, in metric tons (t); Rock, in million metric tons (Mt)]

Permissive tract (sub-tract)	Material	Identified resouces	Undiscovered resources							
			Probability of at least the indicated amount						Probability of	
			0.95	0.9	0.5	0.1	0.05	Mean	Mean or greater	None
Delamerian (Adelaide)	Cu (t)	0	0	0	52,000	410,000	560,000	140,000	0.34	0.27
	Rock (Mt)	0	0	0	36	150	180	56	0.40	0.21
Macquarie	Cu (t)	13,500,000	350,000	1,500,000	13,000,000	52,000,000	72,000,000	21,000,000	0.34	0.04
	Au (t)	1,710	38	140	1,100	3,500	4,500	1,500	0.36	0.04
	Rock (Mt)	4,180	89	340	2,900	11,000	13,000	4,300	0.36	0.04
Yeoval	Cu (t)	49,700	0	0	25,000	210,000	310,000	71,000	0.30	0.24
	Rock (Mt)	12.9	0	0	20	80	91	30	0.34	0.07
East Tasmanide (Central)	Cu (t)	2,300,000	0	0	190,000	690,000	860,000	280,000	0.39	0.09
	Rock (Mt)	1,120	0	3	94	250	290	110	0.43	0.06

to compare tonnages and grades of Australian deposits to those of the global grade-tonnage models for porphyry copper and porphyry Cu-Au deposits by Singer and others (2008).

At the workshop, the geology of each permissive tract and the list of porphyry copper deposits and prospects assigned to that tract were reviewed and discussed. After discussion of each tract and its deposits and prospects, panel members were asked to estimate numbers of undiscovered deposits expected at three levels of subjective probability (for example, at 90, 50, and 10 percent; at 50, 10, and 5 percent; or at 10, 5, and 1 percent). At each level of probability, the high and low estimators were asked to justify their estimates. The validity of their reasons and the firmness of their opinions were considered by the other panel members, and individual estimates were adjusted accordingly.

During this process, the team calculated results of the Monte Carlo simulation based on alternative versions of preliminary consensus estimates. For each permissive tract, this process was repeated until consensus was reached. After a set of estimates was agreed upon for every tract, the estimate for each tract was compared with estimates for other tracts to ensure that the consensus estimates conformed to the team's overall perceptions of the relative merits of the tracts.

The team also considered numbers of deposits predicted by deposit density models for porphyry copper deposits (Singer and others, 2005; Singer and Menzie, 2010) for comparison with their estimates made by expert judgment. Deposit density models are based on counts of total numbers of deposits per unit area in well-explored control areas. These models can provide guidelines for estimates of numbers of undiscovered deposits but are not recommended for arriving at final estimates unless no other information is available (Singer and Menzie, 2010). The deposit density model for porphyry copper deposits described by Singer and Menzie (2010), an update of the original model published by Singer and others in 2005, is plotted in figure 5, along with the observed tract areas and consensus estimates for each of the tracts or sub-tracts in eastern Australia that were assessed quantitatively. The figure shows the regression lines for the 50-percent model estimate, along with the lower prediction limit for the 90-percent estimate of numbers of deposits and the upper prediction limit for the 10-percent estimate. The graph can be used to estimate total numbers of deposits (known plus undiscovered) by projecting the permissive area from the x-axis to the 80-percent prediction interval and reading the total number of deposits off the y-axis (Singer and Menzie, 2010).

Summary of Probabilistic Assessment Results

The Macquarie tract is expected to have the highest density of known and undiscovered deposits (39 deposits per 100,000 km^2), followed by the Central sub-tract of the East Tasmanide tract (6.5 deposits per 100,000 km^2), the Adelaide sub-tract of the Delamerian tract (4.9 deposits per 100,000 km^2), and the Yeoval tract (4.3 deposits per 100,000 km^2) (table 6). In comparison with the range of numbers of porphyry copper deposits predicted by the deposit density model, the consensus estimates for the Macquarie tract and the Central sub-tract of the East Tasmanide tract lie within the 80 percent prediction interval. The Yeoval tract and the Adelaide sub-tract of the

Delamerian tract are estimated to contain fewer deposits than predicted by the deposit density model. Exposed permissive rocks represent more than 50 percent of the Central sub-tract of the East Tasmanide tract. Exposed permissive rocks represent less than 50 percent of the Macquarie tract and Adelaide sub-tract of the Delamerian tract; these areas are largely defined by subsurface projections from geologic maps and aeromagnetic anomaly patterns.

The Macquarie tract has by far the largest total resources of copper and gold in known porphyry copper deposits, and is expected to contain the largest total of undiscovered resources of copper and gold in undiscovered porphyry copper deposits in eastern Australia. In terms of known and expected undiscovered resources of copper, the Central sub-tract of the East Tasmanide tract is a distant second. The Yeoval tract is a more distant third, and the Adelaide sub-tract of the Delamerian tract is an even more distant fourth.

Considerations for Users of this Assessment

This report presents a synthesis of current, readily available information. Ideally, assessments are done on a recurring basis, at a variety of scales, because available data change over time. This assessment is based on the descriptive and grade-tonnage data contained in published mineral deposit models. Data in the models represent average grades for each commodity of possible economic interest and tonnages based on the total of production, reserves, and resources at the lowest cutoff grade for which data were available when the model was constructed. The present-day economic viability of the deposits used to construct the models varies widely, so care must be exercised when using the results of this assessment to answer questions that involve economics. Furthermore, these estimates are of numbers of deposits that are likely to exist, not necessarily those likely to be discovered (Singer, 2007a, b). In some cases, the assessment team was aware of prospects, revealed by past or current exploration efforts, that are believed to be significant deposits, but that do not yet have a citable grade and tonnage. These probable deposits are treated here as undiscovered deposits, albeit deposits with a high degree of certainty of existence.

The mineral industry explores the area around known deposits for extensions of identified resources, as well as for new projects in emerging exploration areas. Extensions to identified resources are not estimated in this assessment, although they are a substantial part of newly discovered copper resources each year. This assessment considers the potential for concealed deposits within 1 km of the surface.

Boundaries of permissive tracts are based on geology, irrespective of political boundaries. Therefore, permissive tracts may include lands that already have been developed for other uses, or withdrawn from mineral development as protected areas. In the GIS files that accompany this report, permissive tracts are mapped at a scale of 1:1,000,000 and are not intended for use at larger scales. For additional information about appropriate use of the tracts, see the completeness and accuracy statements in the metadata of the accompanying GIS files (appendix G).

Acknowledgments

We thank Jenny Tait, who arranged for Web conference capabilities for our assessment workshop, which was held jointly in Edinburgh, Scotland; and in Reston, Virginia and Spokane, Washington, in the United States. Thanks also are extended to technical reviewers N.K. Foley, R.A. Koski, and Vladimir Lisitsin for constructive criticism and suggestions.

We acknowledge Geoscience Australia for providing excellent digital geologic maps, databases of mineral deposits and prospects, and annual summaries of exploration activities. We also acknowledge the many geologists who have contributed to annual Mines and Wines Symposia on mineral exploration in eastern Australia, and the organizations that support these symposia and publish their proceedings online. These are a valuable source of current information. Supporting organizations include the Sydney Mineral Exploration Discussion Group (SMEDG), the Australian Institute of Geoscientists (AIG), the New South Wales Department of Minerals and Energy (NSW DME), the New South Wales Department of Mineral Resources (NSW DMR), and the mining and exploration companies that sponsored presentations on their projects.

Special thanks are due to Kathleen M. Johnson for a thorough series edit, and to Heather L. Parks, Shane Kostka, and Michael E. Landkammer who checked text, tables, and figures for consistent usage of geographic and geologic nomenclature, created supplementary illustrations, and fine-tuned figures to USGS editorial standards.

References Cited

American Geological Institute, 1997, Dictionary of Mining, Mineral, and Related Terms, second edition: American Geological Institute in cooperation with the Society for Mining, Metallurgy, and Exploration, Inc., 646 p.

Australasian Joint Ore Reserves Committee (JORC), 2004, Australasian code for reporting of exploration results, mineral resources and ore reserves—The JORC Code: Australian Institute of Mining and Metallurgy, Australian Institute of Geosciences, and Minerals Council of Australia, 32 p., accessed March 5, 2012, at http://www.jorc.org/pdf/jorc2004web_v2.pdf.

Bates, R.L., and Jackson, J.A., eds., 1997, Glossary of Geology, fourth edition: Alexandria, Virginia, American Geological Institute, 769 p.

Bawiec, W.J., and Spanski, G.T., 2012, Quick-start guide for version 3.0 of EMINERS—Economic Mineral Resource Simulator: U.S. Geological Survey Open-File Report 2009–1057, 26 p., available at http://pubs.usgs.gov/of/2009/1057/. (This report supplements USGS OFR 2004–1344.)

Betts, P.G., Giles, D., Lister, G.S., and Frick, L.R., 2002, Evolution of the Australian lithosphere: Australian Journal of Earth Sciences, v. 49, no. 4, p. 661–695.

Blevin, P.L., 2002, The petrographic and compositional character of variably K-enriched magmatic suites associated with Ordovician porphyry Cu-Au mineralization in the Lachlan fold belt, Australia: Mineralium Deposita, v. 37, p. 87–99.

Blevin, P.L., Chappell, B.W., and Allen, C.M., 1996, Intrusive metallogenic provinces in eastern Australia based on granite source and composition: Transactions of the Royal Society of Edinburgh—Earth Sciences, v. 87, p. 281–290.

Briskey, J.A., Schulz, K.J., Mosesso, J.P., Horwitz, L.R., and Cunningham, C.G., 2001, It's time to know the planet's mineral resources: Geotimes, v. 46, no. 3, p. 14–19. (Also available at http://www.geotimes.org/mar01/.)

British Columbia Securities Commission, 2005, National Instrument 43–101 (NI 43–101) Standards for Disclosure for Mineral Projects: 17 p., accessed December 2009, at http://www.bcsc.bc.ca/uploadedFiles/NI43–101(1).pdf.

Champion, D.C., Kositcin, N., Huston, D.L., Mathews, E., and Brown, C., 2009, Geodynamic synthesis of the Phanerozoic of eastern Australia and implications for metallogeny: Geoscience Australia, Record 2009/18, GeoCat#68866, 222 p., digital, accessed October 4, 2010, at http://www.ga.gov.au/products/.

Chappell, B.W., and White, J.R., 1974, Two contrasting granite types: Pacific Geology, v. 8, p. 173–174.

Chappell, B.W., and White, J.R., 2001, Two contrasting granite types—25 years later: Australian Journal of Earth Sciences, v. 48, no. 4, p. 489–499.

CIM Standing Committee on Reserve Definitions, 2004, CIM definition standards—On mineral resources and mineral reserves: Canadian Institute of Mining, Metallurgy and Petroleum, 10 p.

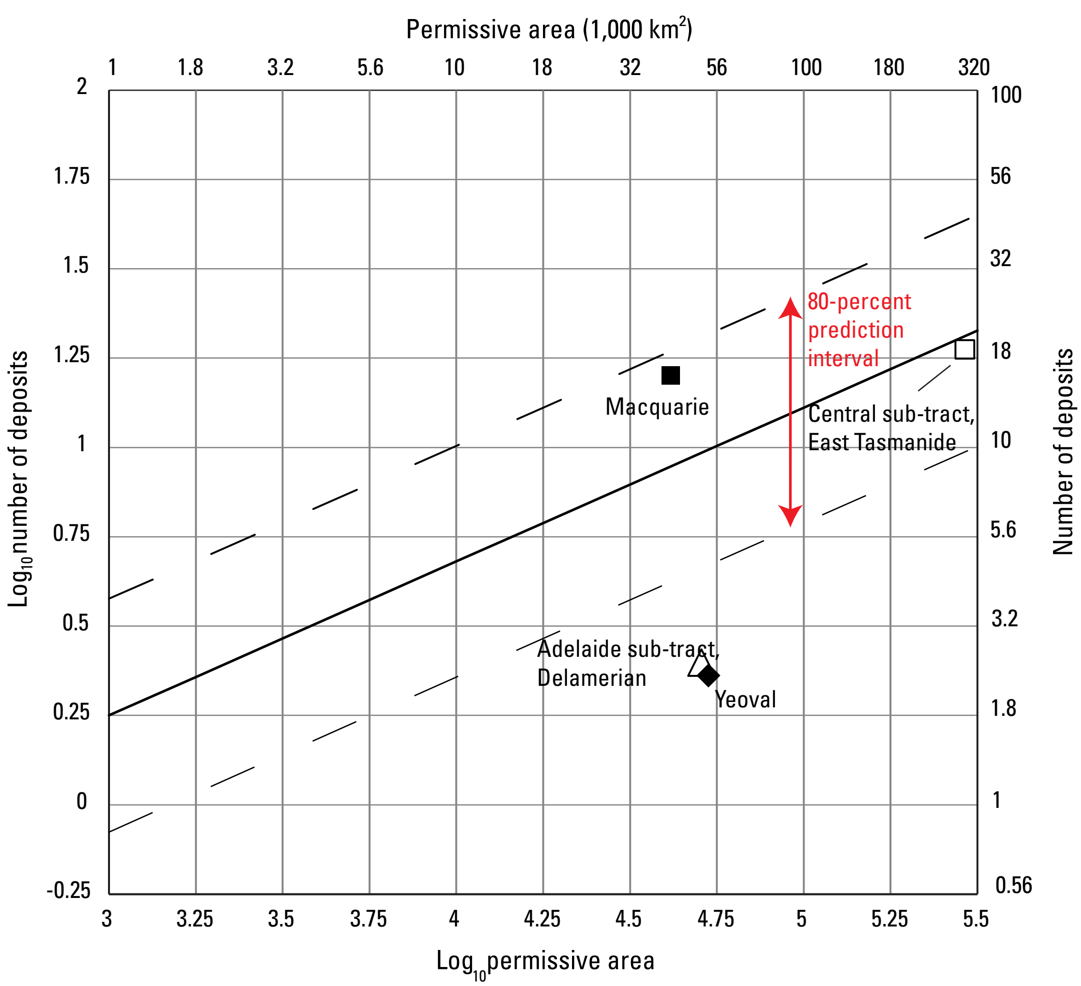

Figure 5. Graph of log of total numbers of porphyry copper deposits as a function of log of permissive area. The 50-percent regression line (solid line) and the 90- and 10-percent prediction limits (dashed lines) are based on figure 4.4 of Singer and Menzie (2010). Observed permissive tract areas and estimates of total numbers of deposits (known plus consensus mean estimate of undiscovered) are plotted for the two tracts and two sub-tracts in eastern Australia that were assessed quantitatively. km^2, square kilometers.

Clark, D.A., 1999, Magnetic petrology of igneous intrusions—Implications for exploration and magnetic interpretation: Exploration Geophysics, v. 30, p. 5–26.

Cooke, D.R., Heithersay, P.S., Wolfe, Rohan, and Losada Calderon, Alex, 1998, Australian and western Pacific porphyry Cu-Au deposits—Exploration model: AGSO Journal of Australian Geology and Geophysics, v. 17, no. 4, p. 97–104.

Cox, D.P., 1986a, Descriptive model of porphyry Cu (model 17), *in* Cox, D.P., and Singer, D.A., eds., Mineral deposit models: U.S. Geological Survey Bulletin 1693, p. 76.

Cox, D.P., 1986b, Descriptive model of porphyry Cu-Mo (model 21a), *in* Cox, D.P., and Singer, D.A., eds., Mineral deposit models: U.S. Geological Survey Bulletin 1693, p. 115–120.

Cox, D.P., 1986c, Descriptive model of porphyry Cu-Au (model 20b), *in* Cox, D.P., and Singer, D.A., eds., Mineral deposit models: U.S. Geological Survey Bulletin 1693, p. 110–111.

Cox, D.P., 1986d, Descriptive model of porphyry Cu, skarn-related deposits (model 18a), *in* Cox, D.P., and Singer, D.A., eds., Mineral deposit models: U.S. Geological Survey Bulletin 1693, p. 82.

Duval, J.S., 2012, Version 3.0 of EMINERS—Economic Mineral Resource Simulator: U.S. Geological Survey Open-File Report 2004–1344, available at http://pubs.usgs.gov/of/2004/1344/.

Edelstein, D.L., 2011, Copper *in* Metals and minerals—Volume I: U.S. Geological Survey 2009 Minerals Yearbook, p. 20.1–20.29, accessed June 2012, at http://minerals.usgs.gov/minerals/pubs/commodity/copper/myb1-2009-coppe.pdf.

Foden, J.D., Elburg, M.A., Dougherty-Page, Jon, and Burtt, Andrew, 2006, The timing and duration of the Delamerian Orogeny—Correlation with the Ross Orogen and implications for Gondwana assembly: The Journal of Geology, v. 114, p. 189–210.

Foster, D.A., Gray, D.R., and Spaggiari, C., 2005, Timing of subduction and exhumation along the Cambrian east Gondwana margin, and the formation of Paleozoic backarc basins: Geological Society of America Bulletin, v. 117, p. 105–116.

Geoscience Australia, 2004, Fourth edition total magnetic anomaly (TMI) grids of Australia: Canberra, Geoscience Australia, accessed May 19, 2010, at http://www.geoscience.gov.au/.

Geoscience Australia, 2009, Australian national gravity database 0.5 minute offshore-onshore gravity grid: Canberra, Geoscience Australia, accessed May 19, 2010, at http://www.geoscience.gov.au/.

Geoscience Australia, 2010, Australian atlas of mines and mineral deposits: Canberra, Geoscience Australia, accessed October 20, 2010, to December 27, 2010, at http://www.australianminesatlas.gov.au/.

Glen, R.A., 2005, The Tasmanides of eastern Australia, *in* Vaughan, A.P.M., Leat, P.T., and Pankhurst, R.J., eds., Terrane processes at the margins of Gondwana: Geological Society, London, Special Publications, 246, p. 23–96.

Glen, R.A., Dawson, M.W., and Colquhoun, G.P., 2007, Eastern Lachlan Orogen Geoscience Database, Version 2: Geological Survey of New South Wales, Department of Primary Industries—Mineral Resources, Maitland, New South Wales, DVD.

Greenfield, J.E., Musgrave, R.J., Bruce, M.C., Gilmore, P.J., and Mills, K.J., 2011, The Mount Wright arc—A Cambrian subduction system developed on the continental margin of east Gondwana, Koonenberry belt, eastern Australia: Gondwana Research, v. 19, p. 650–669.

Gulson, B.L.,and Bofinger, V.M., 1972, Time differences within a calc-alkaline association: Contributions to Mineralogy and Petrology, v. 36, p. 19–26.

International Commission on Stratigraphy (ICS), 2010, International Stratigraphic Chart: International Union of Geological Sciences (IUGS), 1 p., accessed July 3, 2012, at http://www.stratigraphy.org/.

Jaireth, S., and Miezitis, Y., 2004, OZPOT Geoprovince-scale assessment of mineral potential [1:2,500,000 scale GIS]: Canberra, Geoscience Australia, accessed June 21, 2010, to December 27, 2010, at http://www.australianminesatlas.gov.au/build/common/minpot.html.

Jaques, A.L., Jaireth, S., and Walshe, J.L., 2002, Mineral systems of Australia—An overview of resources, settings and processes: Australian Journal of Earth Sciences, v. 49, no. 4, p. 623–660.

John, D.A., Ayuso, R.A., Barton, M.D., Blakely, R.J., Bodnar, R.J., Dilles, J.H., Gray, Floyd, Graybeal, F.T., Mars, J.C., McPhee, D.K., Seal, R.R., Taylor, R.D., and Vikre, P.G., 2010, Porphyry copper deposit model, chapter B *of* Mineral deposit models for resource assessment: U.S. Geological Survey Scientific Investigations Report 2010–5070–B, 169 p., available at http://pubs.usgs.gov/sir/2010/5070/b/.

Lemaitre, R.W., ed., 2002, Igneous Rocks—A classification and glossary of terms, Recommendations of the International Union of Geological Sciences Subcommission on the Systematics of Igneous Rocks, 2nd edition: Cambridge, UK, Cambridge University Press, 236 p.

Loiselle, M.C., and Wones, D.R., 1979, Characteristics and origin of anorogenic granites [abs.]: Geological Society of America Abstracts with Programs, v. 11, no. 7, p. 468.

Mihalasky, M.J., 2001, Mineral potential modeling of gold and silver mineralization in the Nevada Great Basin—A GIS-based analysis using weights of evidence: U.S. Geological

Survey Open File Report 01–291, 448 p., available at http://pubs.usgs.gov/of/2001/of01-291/.

Nesbitt, B.E., and Muehlenbachs, K., 1989, Origins of movement of fluids during deformation and metamorphism in the Canadian Cordillera: Science, v. 245, p. 733–736.

Panteleyev, A., 1995a, Porphyry Cu±Mo±Au (model L04), *in* Lefebure, D.V., and Ray, G.E., eds., Selected British Columbia mineral deposit profiles, vol. 1—Metallics and coal: British Columbia Ministry of Energy and Mines, Division of Mines and Mineral Resources Open File 1995–20, p. 87–92, accessed April 5, 2012, at http://www.empr.gov.bc.ca/Mining/Geoscience/MineralDepositProfiles/.

Panteleyev, A., 1995b, Porphyry Cu-Au—Alkalic (model L03), *in* Lefebure, D.V., and Ray, G.E., eds., Selected British Columbia mineral deposit profiles, vol. 1—Metallics and coal: British Columbia Ministry of Energy and Mines, Division of Mines and Mineral Resources Open File 1995–20, p. 83–86, accessed April 5, 2012, at http://www.empr.gov.bc.ca/Mining/Geoscience/MineralDepositProfiles/.

Panteleyev, A., 2005a, Porphyry Cu±Mo±Au L04., *in* Fonseca, A., and Bradshaw, G., compilers, Yukon Mineral Deposits Profiles: Yukon Geological Survey Open File 2005–5, 175 p., accessed July 28, 2009, at http://www.geology.gov.yk.ca/mineral_deposit_profiles.html; http://ygsftp.gov.yk.ca/publications/openfile/2005/of2005_5.pdf; http://www.geology.gov.yk.ca/pdf/l04_porphyry_cu_mo_au.pdf.

Panteleyev, A., 2005b, Porphyry Cu-Au—Alkalic L03., *in* Fonseca, A., and Bradshaw, G., compilers, Yukon Mineral Deposits Profiles: Yukon Geological Survey Open File 2005–5, 175 p., accessed July 28, 2009, at http://www.geology.gov.yk.ca/mineral_deposit_profiles.html; http://ygsftp.gov.yk.ca/publications/openfile/2005/of2005_5.pdf; http://www.geology.gov.yk.ca/pdf/l03_alkalic_porphyry_cu_au.pdf.

Raymond, O.L., Liu, S.F., and Kilgour, P., 2007, Surface geology of Australia, 1:1,000,000 scale, Tasmania, 3rd edition [Digital Dataset]: Canberra, Geoscience Australia, accessed May 9, 2010, at http://ga.gov.au/.

Raymond, O.L., Liu, S.F., Kilgour, P., Retter, A.J., and Connolly, D.P., 2007, Surface geology of Australia, 1:1,000,000 scale, Victoria, 3rd edition [Digital Dataset]: Canberra, Geoscience Australia, accessed May 9, 2010, at http://ga.gov.au/.

Raymond, O.L., Liu, S.F., Kilgour, P., Retter, A.J., Stewart, A.J., and Stewart, G., 2007, Surface geology of Australia, 1:1,000,000 scale, New South Wales, 2nd edition [Digital Dataset]: Canberra, The Commonwealth of Australia, Geoscience Australia, accessed June 7, 2010, at http://ga.gov.au/.

Richards, J.P., 2003, Tectono-magmatic precursors for porphyry Cu-(Mo-Au) deposit formation: Economic Geology, v. 98, p. 1515–1533.

Rohde, R.A., 2005, GeoWhen database—Alphabetical list of geologic stages: Purdue University Web site, accessed June 8, 2010, at https://engineering.purdue.edu/Stratigraphy/resources/geowhen/region_Australia.html.

Root, D.H., Menzie, W.D., and Scott, W.A., 1992, Computer Monte Carlo simulation in quantitative resource estimation: Natural Resources Research, v. 1, no. 2, p. 125–138.

Seedorf, E., Dilles, J.H., Proffett, J.M., Jr., Einaudi, M.T., Zurcher, Lukas, Stavast, W.J.A., Johnson, D.A., and Barton, M.D., 2005, Porphyry deposits—Characteristics and origin of hypogene features, *in* Hedenquist, J.W., Thompson, J.F.W., Goldfarb, R.J., and Richards, J.P., eds., One hundredth anniversary volume 1905–2005: Littleton, Colo., Society of Economic Geologists, p. 251–298.

Sillitoe, R.H., 2010, Porphyry copper systems: Economic Geology, v. 105, p. 3–41.

Sillitoe, R.H., and Bonham, H.F., Jr., 1990, Sediment-hosted gold deposits—Distal products of magmatic-hydrothermal systems: Geology, v. 18, p. 157–161.

Singer, D.A., 1993, Basic concepts in three-part quantitative assessments of undiscovered mineral resources: Nonrenewable Resources, v. 2, no. 2, p. 69–81.

Singer, D.A., ed., 1996, An analysis of Nevada's metal-bearing mineral resources: Nevada Bureau of Mines and Geology Open-File Report 96–2, accessed April 2010, at http://www.nbmg.unr.edu/dox/ofr962/.

Singer, D.A., 2007a, Short course introduction to quantitative mineral resource assessments: U.S. Geological Survey Open-File Report 2007–1434, at http://pubs.usgs.gov/of/2007/1434/.

Singer, D.A., 2007b, Estimating amounts of undiscovered resources, *in* Briskey, J.A., and Schulz, K.J., eds., Proceedings for a workshop on deposit modeling, mineral resource assessment, and their role in sustainable development, 31st International Geological Congress, Rio de Janeiro, Brazil, August 18–19, 2000: U.S. Geological Survey Circular 1294, p. 79–84. (Also available at http://pubs.usgs.gov/circ/2007/1294/.)

Singer, D.A., and Berger, V.I., 2007, Deposit models and their application in mineral resource assessments, *in* Briskey, J.A., and Schulz, K.J., eds., Proceedings for a workshop on deposit modeling, mineral resource assessment, and their role in sustainable development, 31st International Geological Congress, Rio de Janeiro, Brazil, August 18–19, 2000: U.S. Geological Survey Circular 1294, p. 71–78. (Also available at http://pubs.usgs.gov/circ/2007/1294/.)

Singer, D.A., Berger, V.I., Menzie, W.D., and Berger, B.R., 2005, Porphyry copper density: Economic Geology, v. 100, no. 3, p. 491–514.

Singer, D.A., Berger, V.I., and Moring, B.C., 2008, Porphyry copper deposits of the world—Database and grade and tonnage models, 2008: U.S. Geological Survey Open-File Report 2008–1155, 45 p., available at http://pubs.usgs.gov/of/2008/1155/.

Singer, D.A., and Menzie, W.D., 2005, Statistical guides to estimating the number of undiscovered mineral deposits—An example with porphyry copper deposits, *in* Cheng, Qiuming, and Bonham-Carter, Graeme, eds., Proceedings of IAMG—The annual conference of the International Association for Mathematical Geology: Toronto, Canada, York University Geomatics Research Laboratory, p. 1028–1033.

Singer, D.A., and Menzie, W.D., 2010, Quantitative mineral resource assessments—An integrated approach: New York, Oxford University Press, 219 p.

Staude, J.G., and Barton, M.D., 2001, Jurassic to Holocene tectonics, magmatism, and metallogeny of northwestern Mexico: Geological Society of America Bulletin, v. 113, no. 10, p. 1357–1374.

Tosdal, R.M., and Richards, J.P., 2001, Magmatic and structural controls on the development of porphyry Cu/Mo/Au deposits, *in* Richards, J.P., and Tosdal, R.M., Structural controls on ore genesis: Reviews in Economic Geology, v. 14, p. 157–181.

UNdata, 2009, Countries or areas, codes and abbreviations: United Nations Statistics Division, accessed December, 2009, at http://unstats.un.org/unsd/methods/m49/m49alpha.htm.

U.S. Bureau of Mines and U.S. Geological Survey, 1980, Mineral reserves, resources, resource potential and certainty: U.S. Geological Survey Circular 831, 5 p.

U.S. Department of State, 2009, Small-scale digital international land boundaries (SSIB)—Lines, edition 10, and polygons, beta edition 1, *in* Boundaries and sovereignty encyclopedia (B.A.S.E.): U.S. Department of State, Office of the Geographer and Global Issues.

U.S. Geological Survey Geologic Names Committee, 2007, Divisions of geologic time—Major chronostratigraphic and geochronologic units: U.S. Geological Survey Fact Sheet 2007–3015, 2 p., available at http://pubs.usgs.gov/fs/2007/3015/.

U.S. Geological Survey National Mineral Resource Assessment Team, 2000, 1998 assessment of deposits of gold, silver, copper, lead, and zinc in the United States: U.S. Geological Survey Circular 1178, 21 p., available at http://pubs.usgs.gov/circ/1178/.

U.S. Securities and Exchange Commission Committee for Mineral Reserves International Reporting Standards, 2006, International reporting template for the public reporting of exploration results and mineral reserves (CRIRSCO): U.S. Securities and Exchange Commission, 33 p., accessed June 2010, at http://www.crirsco.com/template.asp.

Wallace, A.R., Ludington, S., Mihalasky, M.J., Peters, S.G., Theodore, T.G., Ponce, D.A., John, D.A., and Berger, B.R., 2004, Assessment of metallic mineral resources in the Humboldt River Basin, northern Nevada, *with a section on* PGE potential of the Humboldt mafic complex by M.L. Zientek, G.B. Sidder, and R.A. Zierenberg: U.S. Geological Survey Bulletin 2218, 1 CD-ROM. (Also available at http://pubs.usgs.gov/bul/b2218/.)

White, A.J.R., 1979, Sources of granite magmas [abs.]: Geological Society of America, Abstracts with Programs, v. 11, no. 7, p. 539.

Whitaker, A.J., Champion, D.C., Sweet, I.P., Kilgour, P., and Connolly, D.P., 2007, Surface geology of Australia 1:1,000,000 scale, Queensland [Digital Dataset]: Canberra, Geoscience Australia, accessed May 9, 2010, at http://www.ga.gov.au/.

Whitaker, A.J., Glanville, H.D., English, P.M., Stewart, A.J., Retter, A.J., Connolly, D.P., Stewart, G.A., and Fisher, C.L., 2008, Surface geology of Australia 1:1,000,000 scale, South Australia [Digital Dataset]: Canberra, Geoscience Australia, accessed May 9, 2010, at http://www.ga.gov.au/.

This page left intentionally blank.

Appendixes A–H

Appendix A. Grade and Tonnage Model for Porphyry Copper Deposits of East Tasmanide and Yeoval Tracts, Eastern Australia

By Jane M. Hammarstrom[1] and Arthur A. Bookstrom[2]

Introduction

Statistical tests are made to compare tonnages and commodity grades of known deposits within a permissive tract with tonnage and grade data in the global porphyry copper models of Singer and others (2008) to determine the appropriate model for the simulation of undiscovered resources. The 14 known deposits in the East Tasmanide tract and the single known deposit in the Yeoval tract (table A1) form a distinct population of deposits with relatively low tonnages and low copper grades compared to deposits in global models. The nine known deposits in the Macquarie tract are comparable to global models in tonnage and grade. A custom model was built using the data for the 15 known deposits in the East Tasmanide and Yeoval tracts to provide an appropriate model for simulations of undiscovered resources.

Statistical Tests

Tonnages and average grades for copper, molybdenum, and gold for nine known porphyry copper deposits in the Macquarie tract are statistically indistinguishable from global models of Singer and others (2008), as indicated by *p*-values >0.01 (table A2). The *t*-test using the global model that includes 422 porphyry copper deposits fails in terms of contained copper, whereas the test using the Cu-Au subtype model (115 deposits that contain average gold grades of 0.2 grams per metric ton (g/t) or more) does not. Five of the nine known deposits in the Macquarie tract meet these criteria for classification as Cu-Au subtype deposits. In addition, most of the porphyry Cu-Au deposits in the Macquarie tract formed in association with shoshonitic (alkaline, potassic) intrusions of intermediate composition that are typical of Cu-Au porphyry settings. Therefore, the Cu-Au subtype model was adopted for the assessment of the Macquarie tract.

By contrast, the 14 known porphyry copper deposits in the East Tasmanide permissive tract and 1 known deposit in the Yeoval tract (table A1) do not fit existing global models. Despite differences in age (Cambrian through Cretaceous), all these deposits formed in continental magmatic-arc to back-arc settings, and they generally are associated with intrusions of calc-alkaline affinity. There are no known porphyry copper deposits in the Delamerian tract, and porphyry copper prospects in the Delamerian tract have generally low-grade copper intercepts. These copper grades are more like the average copper grades in deposits of the East Tasmanide and Yeoval tracts than the grades of porphyry copper deposits included in the global grade-tonnage model for porphyry copper deposits of the world by Singer and others (2008).

Data for tonnages and copper grades of the 15 deposits were log-transformed and compared with the global grade and tonnage model of Singer and others (2008) using box and whisker plots, histograms, and a *t*-test with a significance (α) level of 0.01 (figs. A1*A* and A1*B*). Inspection of the data shows that tonnages and copper grades for the 15 known deposits in the East Tasmanide and Yeoval tracts are low relative to those of deposits included in the global grade-tonnage model for porphyry copper by Singer and others (2008).

The global porphyry Cu-Au model is appropriate for the assessment of the Macquarie tract. However, none of the global porphyry copper models is appropriate for the assessment of the other eastern Australia tracts. Similar preliminary testing also showed that tonnages and average grades of these deposits are lower than those of deposits included in a regional grade-tonnage model for calc-alkalic porphyry Cu ± Mo ± Au deposits of the Canadian Cordillera by Mihalasky and others (2011).

Custom Grade-Tonnage Model

A custom grade-tonnage model was made for porphyry copper deposits of the East Tasmanide, Yeoval, and Delamerian tracts in eastern Australia, which are significantly smaller and have significantly lower average copper grades than indicated by the global grade-tonnage model of Singer and others (2008).

Tonnage and copper grade data for the 15 deposits listed in table A1 provide the basis for the custom grade-tonnage model. To construct the model, the data are log-transformed and plotted as normal quantile plots for tonnage and grade (fig. A2). The quantile plots indicate that there are no outliers in the data. Accompanying frequency plots and box and whisker diagrams provide alternative representations of the distributions of data on which the model is based. Selected quantiles that describe the data are listed in table A3.

[1]U.S. Geological Survey, Reston, Virginia, United States.

[2]U.S Geological Survey, Spokane, Washington, United States.

Table A1. Deposits included in the grade and tonnage model for the East Tasmanide and Yeoval tracts, Australia.

[Ma, million years; Mt, million metric tons; %, percent; t, metric tons; g/t, grams per ton; -, no data]

Name	Latitude	Longitude	Age (Ma)	Tonnage (Mt)	Copper (%)	Molybdenum (%)	Gold (g/t)	Silver (g/t)	Contained copper (t)	References
Yeoval	-32.728	148.643	388	12.9	0.38	0.01	0.14	2.20	49,000	Ewers and others (2002), Geoscience Australia (2010)
Ben Mohr	-21.266	148.868	123	20	0.20	-	-	-	40,000	Horton (1978), Ewers and others (2002), Geoscience Australia (2010)
Chinaman Creek	-25.230	151.617	250	200	0.20	-	0.33	-	400,000	Horton (1978), Ewers and others (2002), Geoscience Australia (2010)
Coalstoun	-25.617	151.830	235	80	0.30	-	-	-	240,000	Geoscience Australia (2010)
Dimbulah	-17.097	144.100	275	20	0.25	-	-	-	50,000	Horton (1978), Ewers and others (2002), Geoscience Australia (2010)
Julivon Creek	-20.539	148.299	132	35	0.16	0.01			54,600	Geological Survey of Queensland (2010)
Kiwi Carpet	-24.664	150.877	225	200	0.15	0.01	-	-	300,000	Horton (1978), Ewers and others (2002)
Limonite Hill	-23.687	150.630	246	100	0.30	-	-	-	300,000	Ewers and others (2002), Geoscience Australia (2010)
Mount Abbot	-20.197	147.950	119	200	0.15	-	-	-	300,000	Ewers and others (2002), Geoscience Australia (2010)
Mount Cannindah	-24.671	151.276	235	17.5	0.65	-	0.16	6.75	120,000	Geoscience Australia (2010)
Mount Leslie	-20.937	148.160	124	20	0.20	-	-	-	41,500	Ewers and others (2002), Geoscience Australia (2010)
Ruddygore	-17.129	144.549	275	10	0.4	-	-	-	40,000	Horton (1978), Ewers and others (2002), Geoscience Australia (2010)
Struck Oil	-23.605	150.462	244	100	0.20	-	-	-	200,000	Ewers and others (2002), Geoscience Australia (2010)
Whitewash	-24.807	150.875	237	71.5	0.10	0.04	-	1.19	71,000	Geoscience Australia (2010)
Yeppoon	-22.998	150.694	220	50	0.30	0.01	-	-	150,000	Ewers and others (2002), Geoscience Australia (2010)
Total									2,356,000	
Total, rounded									2,400,000	

Table A2. Results of Student's *t*-test comparisons of tonnage and grade of deposits in the Macquarie and East Tasmanide and Yeoval tracts with deposits in global models.

[Pooled *t*-test results assuming equal variances; $p>0.01$ indicates that the deposits in the tract are not significantly different from those in the global models of Singer and others, 2008) in terms of tonnage and commodity grades at the 1-percent level; $p<0.01$ indicates that the deposits in the tract are significantly different from those in the model at the 1-percent level and, therefore, the tract fails the selected test (as indicated by the *) and the model is inappropriate for the assessment. See table A1 for data used in tests for the East Tasmanide and Yeoval tracts; see table C3 for data used in the tests for the Macquarie tract. N_{known}, number of known deposits in the tract; -, no data; Cu, copper; Mo, molybdenum; Ag, silver; Au, gold; g/t, grams per metric ton]

Tract name	Coded _ID	N_{known}	Global porphyry Cu-Au-Mo model (*p* values)						Global porphyry Cu-Au subtype model (*p* values)						Model selected	Basis for selection
			Tonnage	Cu	Mo	Au	Ag	Contained Cu	Tonnage	Cu	Mo	Au	Ag	Contained Cu		
Macquarie	009pCu8002	9	0.14	0.12	0.04	0.09	-	0.006*	0.24	0.12	0.87	0.14	-	0.14	Cu-Au	Five of the nine deposits are classified as Cu-Au deposits based on gold grades of 0.2 g/t or more. Two of the nine deposits report Mo; none report Ag. The general model fails on contained copper.
East Tasmanide and Yeoval	009pCu8003 and 009pCu8004	15	<0.001*	0.0002*	0.79	0.48	0.67	<0.001*	<0.001*	0.000	0.0043*	0.11	0.86	<0.001*	Custom model	The 15 deposits fail both models on tonnage and Cu grade. This indicates that these models are inappropriate for the simulation of undiscovered resources in these tracts.

Table A3. Comparison of East Tasmanide and Yeoval deposit tonnages and grades with global models of Singer and others (2008).

[Cu, copper; Mo, molybdenum; Ag, silver; Au, gold]

Model	East Tasmanide and Yeoval	Global Cu-Au-Mo	Global Cu-Au	Global Cu-Mo	Global Cu
Tonnage, in million metric tons					
90th percentile of deposits	200	1,500	1,200	4,800	1,400
50th percentile of deposits	50	240	200	280	250
10th percentile of deposits	12	33	34	48	30
Copper, in percent					
90th percentile of deposits	0.50	0.75	0.79	0.83	0.74
50th percentile of deposits	0.20	0.44	0.44	0.48	0.44
10th percentile of deposits	0.13	0.24	0.23	0.19	
Number of deposits	15	422	115	51	256

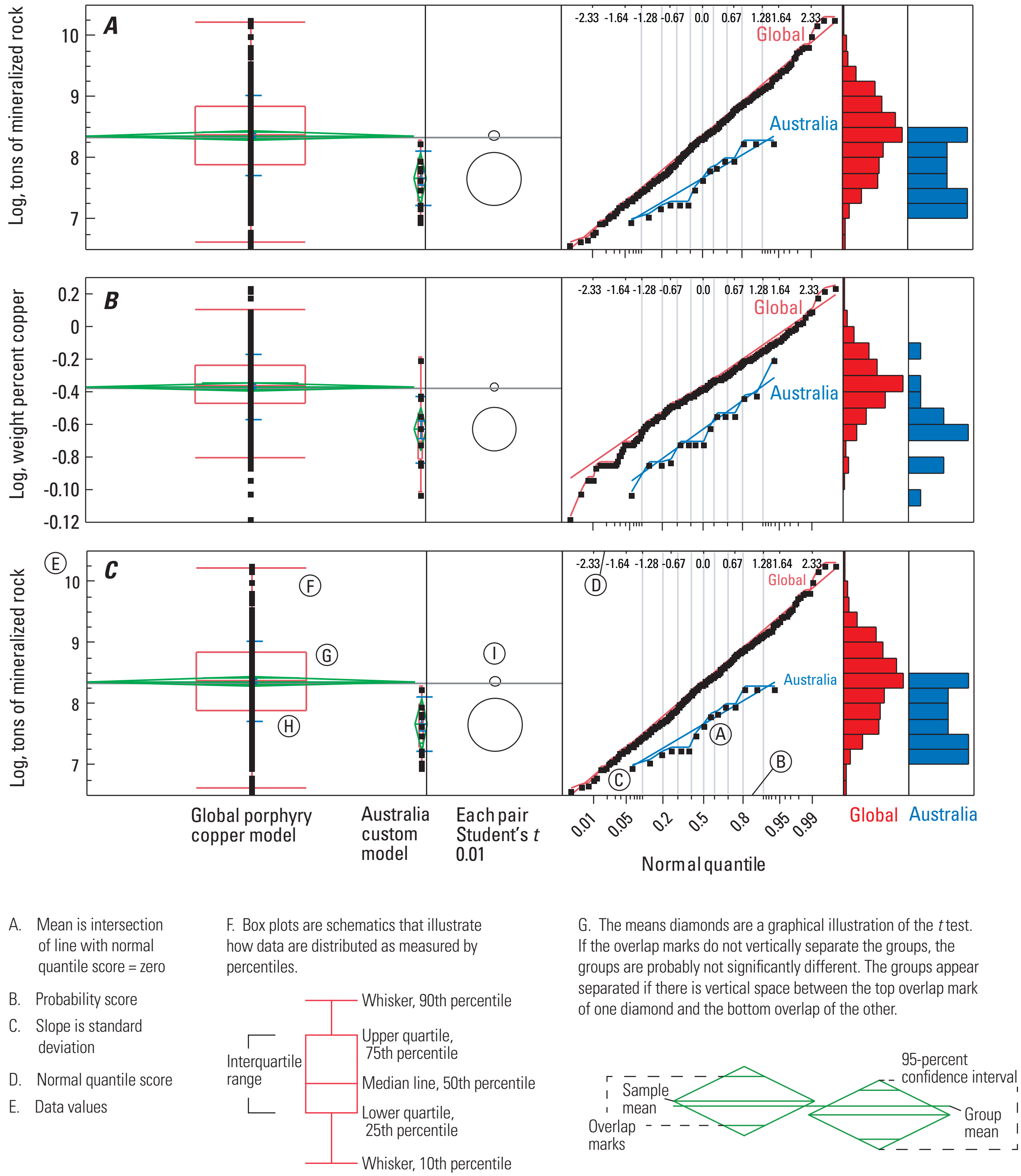

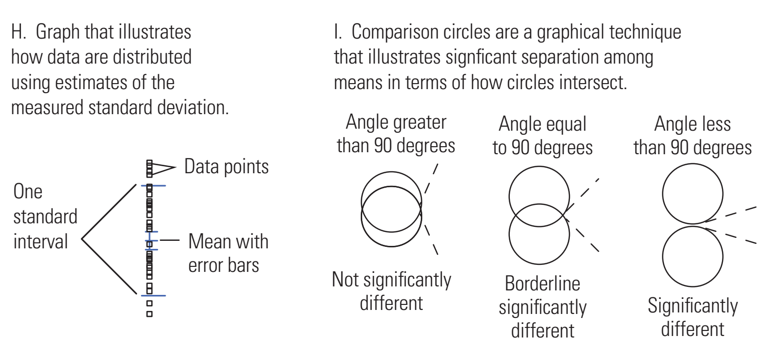

Figure A1. Statistical comparisons between tonnages and copper grades of 15 Australian porphyry copper deposits (table A1) and the general global porphyry copper model of Singer and others (2008). *A*, Box and whisker plot, *t* test, probability plot, and histograms comparing log-transformed tonnages. *B*, Box and whisker plot, *t*-test, probability plot, and histograms comparing log-transformed copper grades (in weight percent). *C*, Explanation of plots in *A* and *B*.

Examination of the references used to construct table A1 shows that although at least one of the deposits is known to be open, the data are recent, based on drilling, and include deposits with measured resources or production. Although further characterization may result in larger tonnages, we conclude, on the basis of available information and the assessors' assumption that undiscovered deposits in the East Tasmanide, Yeoval, and Delamerian permissive tracts are likely to be similar to those that have been discovered, that use of this regional model is warranted.

Models are likely to be stable if the following criteria are met (Singer and Menzie, 2010): (1) tonnages and grades are not significantly different from a lognormal distribution, (2) at least 20 deposits are used, (3) standard deviations for tonnages are less than 1.0, and (4) there are no significant correlations between tonnage and grade. Tests of various distributions for the log-transformed data from Australian deposits indicate that a normal distribution describes the data (fig. A2). The goodness of fit test, a formal test for normality, confirms that the assumption of a normal distribution is acceptable. The standard deviation for tonnage (0.45) also is acceptable. However, the number of deposits in the model (15) is less than ideal, and tonnage and grade are weakly correlated (fig. A3). Nevertheless, this custom model is much more appropriate than the global grade-tonnage model for estimation of resources in expected undiscovered deposits of the East Tasmanide, Yeoval, and Delamerian permissive tracts in eastern Australia.

Discussion

The relatively low concentrations of copper found in these 15 deposits probably have discouraged complete definition of their spatial limits in 3 dimensions. Parts of these deposits probably have higher average grades than indicated by the average grade for the total known tonnage. In most cases, however, additional drilling to increase tonnage probably would decrease average grade. The total contained copper estimated in these deposits is 2.34 Mt (table A1). By comparison, approximately one-third of the individual deposits in the global model each contain 2.4 Mt copper or more.

As stated by Richards (2003, p. 1515) porphyry copper deposits are "relatively rare but reproducible products of subduction-related magmatism. No unique processes appear to be required for their formation, although additive combinations of common tectono-magmatic process, or optimization of these processes, can affect the grade and size as well as the location of the resulting deposits." Possible reasons for the relatively small sizes and low grades of porphyry copper deposits in the East Tasmanide, Yeoval, and Delamerian tracts, as compared to those that constitute the global grade-tonnage model for porphyry copper deposits by Singer and others (2008), include the following (in probable order of decreasing importance):

1. Levels of erosion and exposure are too deep to have preserved high-grade porphyry copper systems, which tend to form at relatively shallow depths, in association with relatively small, porphyro-aphanitic intrusions (with visible crystals in a microcrystalline to glassy matrix). Plutons associated with these deposits generally have phaneritic (visibly crystalline) textures, and relatively small proportions of associated volcanics.
2. Levels of igneous emplacement of exposed intrusions were too deep to allow magmatic hydrothermal pressure to exceed confining pressure sufficiently that explosive release of hydrothermal fluid would produce intense and extensive stockwork fracturing and copper mineralization, typical of high-grade porphyry copper deposits.

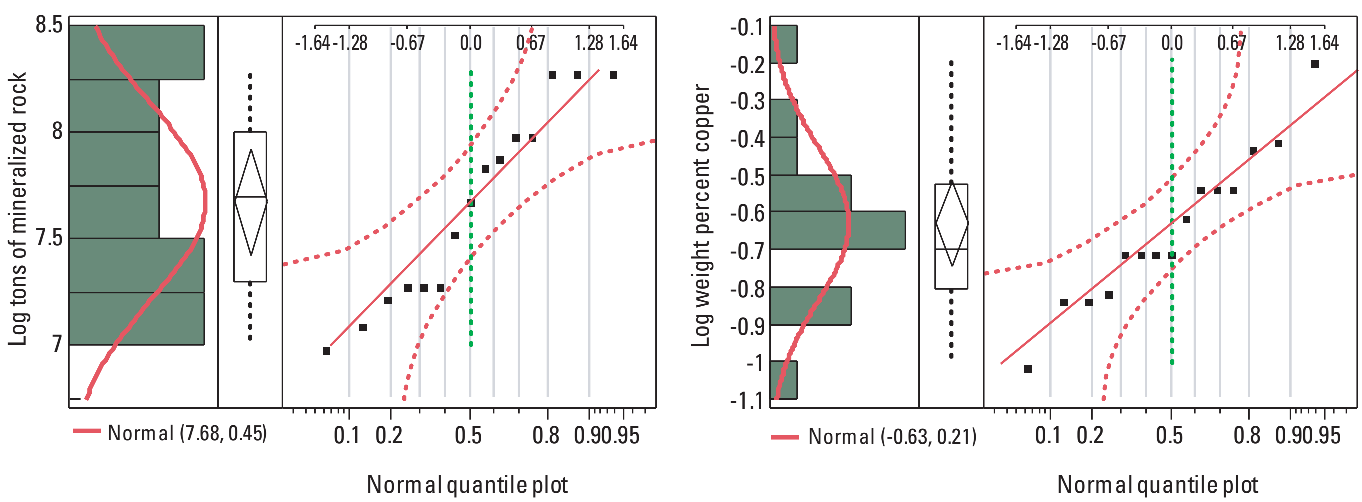

Figure A2. Custom log tonnage and log copper grade model for 15 Australian porphyry copper deposits (listed in table A1, and not in the Macquarie tract). Red curve on histogram shows a normal distribution. Dotted red lines are confidence bounds for a normal distribution. Box and whisker plots and normal quantile plots show that there are no outliers in the data. Dashed green line shows the median (50 percent) value of the custom model for Australian porphyry copper deposits. Numbers in parentheses represent the mean and standard deviation of the log values. See figure A1*C* for an explanation of the plot.

3. Igneous rocks of permissive composition in these tracts may be too fractionated for optimum concentration of copper and gold versus molybdenum, as indicated by the common occurrence of porphyry molybdenum ± copper deposits in these tracts. This is in accordance with experimental evidence presented by Blevin and others (1996) that increasing fractionation results in increasing concentration of molybdenum, relative to copper and gold.
4. The magmas that crystallized to produce permissive igneous rocks in these tracts may have interacted with carbonaceous metasedimentary country rocks and acquired oxidation states that were too low for optimum concentration of copper and gold. This also would be consistent with experimental evidence presented by Blevin and others (1996) that high magmatic oxidation states favor concentration of copper and gold, whereas lower magmatic oxidation states favor concentration of tin and tungsten.
5. Supergene enriched zones are generally not well developed in these deposits. This may result from low concentrations of pyrite, which weathers to produce the acid required to leach copper from primary ore in the vadose zone, and transport it to the saturated zone, where it may be redeposited to form a blanket of supergene-enriched copper ore.

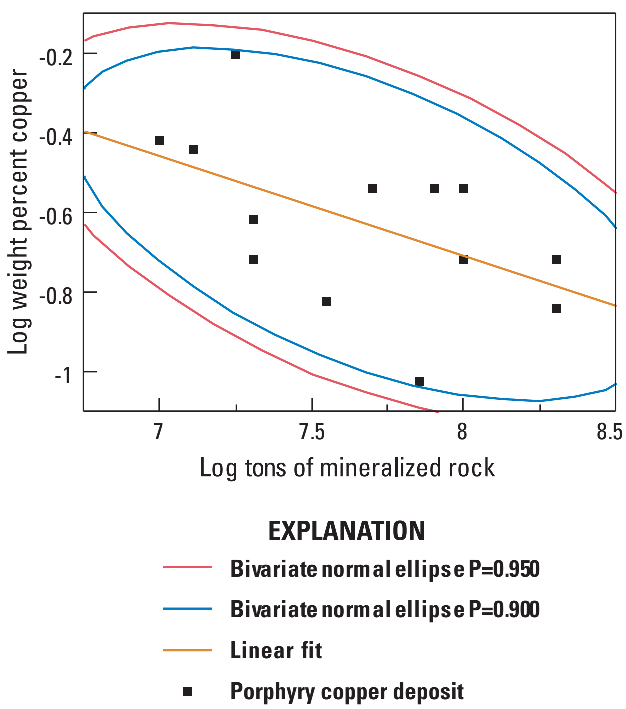

Figure A3. Plot of the log of copper grade versus the log of tonnage for 15 Australian porphyry copper deposits (listed in table A1, and not in the Macquarie tract). The red and blue density ellipses enclose 95 and 90 percent of the data, respectively. The analysis of variance indicates that the variation in copper grade explains some of the variation in tonnage; therefore, there is some degree of negative correlation between the two parameters as indicated by the slope of the linear fit. P, probability.

References Cited

Blevin, P.L., Chappell, B.W., and Allen, C.M., 1996, Intrusive metallogenic provinces in eastern Australia based on granite source and composition: Transactions of the Royal Society of Edinburgh, Earth Sciences, v. 87, p. 281–290.

Ewers, G.R., Evans, N., and Hazell, M., (Kilgour, B., compiler), 2002, OZMIN Mineral Deposit Database: Canberra, Geoscience Australia, digital dataset on CD ROM. (Also available at http://www.ga.gov.au/meta/ANZCW0703003393.html.)

Geological Survey of Queensland, 2010, Mineral occurrence and geology observations: Queensland Government, Department of Employment, Economic Development and Innovation (digital dataset on DVD).

Geoscience Australia, 2010, Australian atlas of mines and mineral deposits: Australian Geological Survey Organization, accessed December 27, 2010, at http://www.australianminesatlas.gov.au/.

Horton, D.J., 1978, Porphyry-type copper-molybdenum mineralization belts in eastern Queensland, Australia: Economic Geology, v. 73, p. 904–921.

Mihalasky, M.J., Bookstrom, A.A., Frost, T.P., and Ludington, S., 2011, Porphyry copper assessment of British Columbia and Yukon Territory, Canada: U.S. Geological Survey Scientific Investigations Report 2010–5090–C, 29 p. and spatial data, accessed November 15, 2012, available at http://pubs.usgs.gov/sir/2010/5090/c/.

Richards, J.P., 2003, Tectono-magmatic precursors for porphyry Cu-(Mo-Au) deposit formation: Economic Geology, v. 98, p. 1515–1533.

Singer, D.A., Berger, V.I., and Moring, B.C., 2008, Porphyry copper deposits of the world—Database and grade and tonnage models, 2008: U.S. Geological Survey Open-File Report 2008–1155, 45 p., available at http://pubs.usgs.gov/of/2008/1155/.

Singer, D.A., and Menzie, W.D., 2010, Quantitative mineral resource assessments—An integrated approach: New York, Oxford University Press, New York, 219 p.

Appendix B. Porphyry Copper Assessment for Tract 009pCu8001, Delamerian, Australia

By Arthur A. Bookstrom[1], Richard A. Glen[2], Jane M. Hammarstrom[3], Gilpin R. Robinson, Jr.[3], and Michael L. Zientek[1]

Deposit Type Assessed

Deposit type: Porphyry copper

Descriptive models: Porphyry copper, Cu-Au, and Cu-Mo (Cox, 1986a, b, c); porphyry Cu ± Mo ± Au (Panteleyev, 1995a, 2005a), porphyry Cu-Au (Panteleyev, 1995b, 2005b; Cooke and others, 1998, Jaireth and Miezitis, 2004a); porphyry copper (John and others, 2010)

Grade and tonnage model: Eastern Australian porphyry copper (appendix A)

Table B1 summarizes selected assessment results.

Table B1. Summary of selected resource assessment results for the Adelaide sub-tract (009pCu8001a), Delamerian tract, New South Wales, South Australia, and Victoria, Australia.

[km, kilometers; km^2, square kilometers; t, metric tons]

Date of assessment	Assessment depth (km)	Tract area (km^2)	Known copper resources (t)	Mean estimate of undiscovered copper resources (t)	Median estimate of undiscovered copper resources (t)
September 2010	1	50,747	0	140,000	52,000

Location

The Delamerian permissive tract is in the eastern Australia states of South Australia, New South Wales, Victoria, and Tasmania (fig. B1). The Adelaide sub-tract (009pCu8001a) extends from northwestern New South Wales to southeastern South Australia and western Victoria. The Victoria sub-tract (009pCu 8001b) is in central Victoria. The Tasmania sub-tract (009pCu8001c) is in western Tasmania.

Geologic Feature Assessed

I-type igneous rocks of Cambrian to Early Ordovician age in the Delamerian Orogen of southeastern Australia.

[1]U.S. Geological Survey, Spokane, Washington, United States.

[2]Geological Survey of New South Wales, Hunter Region Mail Centre, New South Wales, Australia.

[3]U.S. Geological Survey, Reston, Virginia, United States.

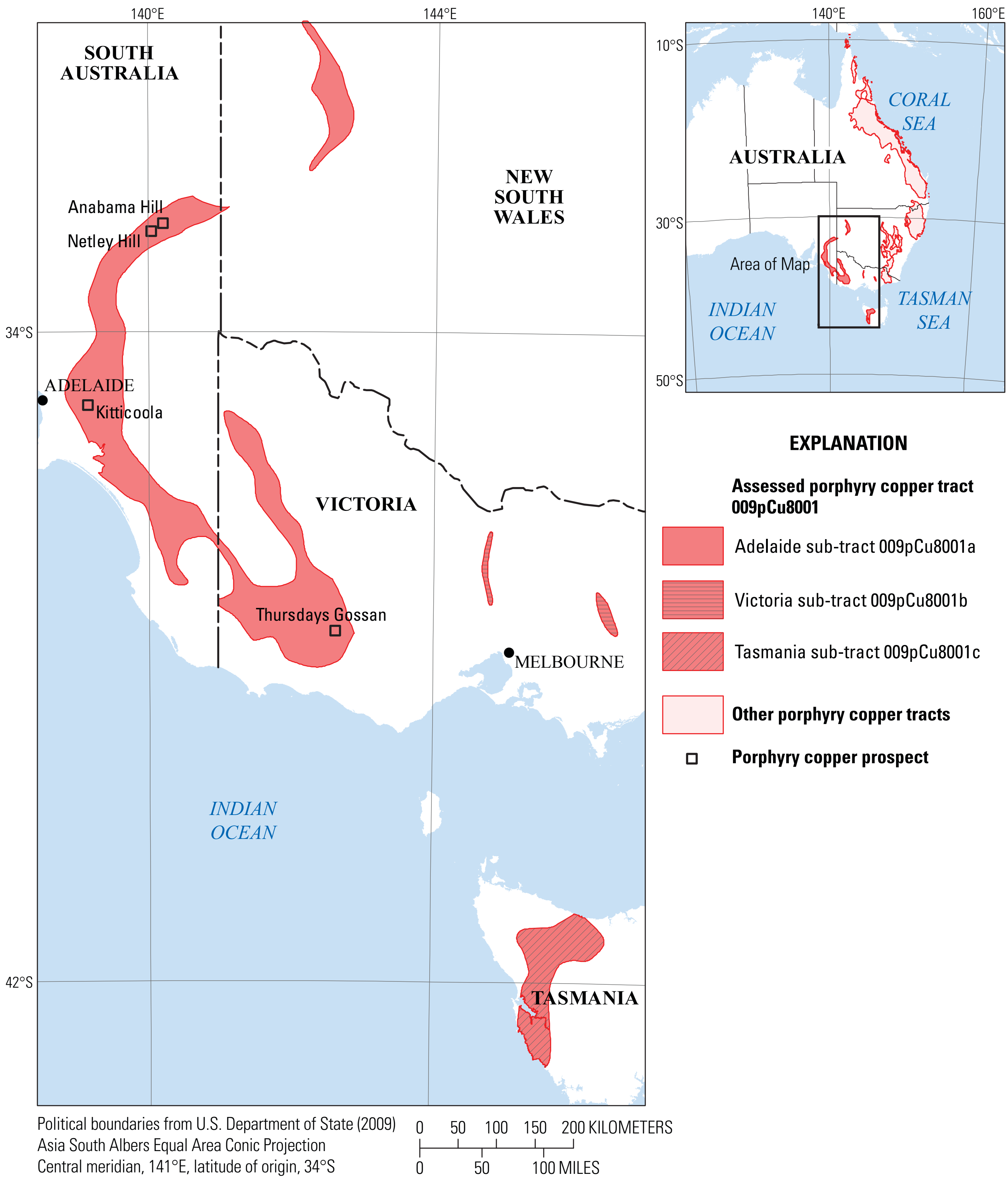

Figure B1. Map showing tract location, sub-tracts, and porphyry copper prospects, Delamerian tract (009pCu8001), New South Wales, South Australia, Tasmania, and Victoria, Australia.

Delineation of the Permissive Tract

The fundamental geologic units that define the Delamerian permissive tract are belts of I-type igneous rocks of Cambrian age in the Delamerian Orogen. Whether all of these belts of igneous rocks are related to subduction and, if so, in what subduction-related settings they formed, are topics of ongoing research and debate. Much of the area of the Delamerian Orogen is covered by at least 1 km of younger material. This tract is therefore divided into three separate sub-tracts, within which permissive rocks are either exposed or thought to be present less than 1 km below the surface.

Delamerian Orogen

The Delamerian Orogen encompasses Neoproterozoic and Cambrian rocks in eastern Australia that underwent deformation, metamorphism, and subduction-related magmatism during the Delamerian Orogeny in Middle to Late Cambrian time (about 514–490 Ma) (Foden and others, 2006). The Delamerian Orogen overlaps the eastern margin of a vast collage of Precambrian continental cratons, west of the Tasmanides, and is transitional with the Neoproterozoic Adelaide Rift Complex to the southwest.

According to Greenfield and others (2011, p. 650), "The Neoproterozoic East Gondwana margin in southeastern Australia represents a passive margin" that developed during and after the breakup of Rodinia. Extensional breakup of Rodinia began with rifting, mafic volcanism, and sedimentation in the Adelaide Geosyncline or rift system from about 830 to 600 Ma (Preiss, 2000; Betts and others, 2002). Renewed extension along this passive margin in Ediacaran time was accompanied by mafic-alkalic volcanism at about 586±7 Ma and by deposition of predominantly siliciclastic turbidites in the Kanmantoo Trough (fig. B2). Widening of this trough led to formation of the Panthalassic (or Paleo-Pacific) Ocean basin (Crawford and others, 1997; Scotese, 2002).

The Koonenberry Belt of volcanic and sedimentary rocks lies east of the Curnamona Craton, in northwestern New South Wales (fig. B2). The Mount Arrowsmith Volcanics are basaltic rocks associated with Neoproterozoic rifting. The Early to Middle Cambrian Mount Wright Volcanics include tholeiitic basalt, basaltic andesite, and an arc-like calc-alkaline basalt-andesite-dacite-rhyolite suite. Such rocks range in age from about 525 Ma (Crawford and others, 1997) to about 510 Ma (Greenfield and others, 2011).

Greenfield and others (2011) interpreted the Mount Wright Volcanics as a volcanic-arc assemblage. To the east are coeval ocean-floor sediments and mafic intrusions of the Ponto Group, which they interpreted as a fore-arc assemblage. Farther east are coeval turbidites of the Teltawongee Group, which they interpreted as an accretionary prism. Geophysical anomalies beneath the Bancannia Trough (fig. B2), west of the Mount Wright Volcanics, may represent a back-arc assemblage. From this arrangement of tectonic elements, Greenfield and others (2011) inferred that the Mount Wright Volcanics formed in response to west-dipping subduction. Rocks of these early subduction-related assemblages were later folded, metamorphosed, and oroclinally bent around the eastern edge of the Curnamona Craton during the Middle to Late Cambrian Delamerian Orogeny. Although the Mount Wright Volcanics contain no known porphyry copper deposits or prospects, they are included in the Adelaide permissive sub-tract.

Aeromagnetic anomalies, which extend northward and southward from the Koonenberry Belt, indicate that rocks similar to those of the Koonenberry Belt continue beneath cover to the north and southwest.

In the Mount Lofty Ranges, east of Adelaide (fig. B2), metasedimentary rocks of Neoproterozoic to Early Cambrian age are pervasively folded and metamorphosed in the Adelaide fold and thrust belt. These folded rocks are intruded by granitoid plutons of Middle to Late Cambrian age, which also are exposed in the Mount Lofty Ranges. Foden and others (2006) concluded that west-vergent folding and thrusting and synorogenic magmatism resulted from west-dipping subduction during the Delamerian Orogeny, which began at about 514±3 Ma and ended at about 490±3 Ma in the Adelaide fold and thrust belt. Although this pattern is consistent with postulated west-dipping subduction, there is no clear evidence of an east-to-west arrangement of fore-arc to arc to back-arc settings in the Adelaide belt. This may indicate that the Adelaide fold and thrust belt could have resulted from collision of continental lithospheric blocks, rather than from subduction of an oceanic plate beneath a continental margin.

In southeastern South Australia and western Victoria, the southeast-trending pattern of permissive igneous rocks and associated aeromagnetic anomalies appears to bend sharply to the north-northwest (fig. B3). According to Crawford and others (2003), this pattern may represent three belts of igneous rocks of Neoproterozoic to Late Cambrian age which converge southward. These three belts are (1) a western belt of basalts of Late Neoproterozoic age, related to the Kanmantoo Rift (which includes and extends north of the Kanmantoo Trough), (2) an eastern belt of tholeiite-boninite-ultramafic assemblage of Early to early Middle Cambrian age, interpreted to indicate ocean-floor to boninitic forearc settings related to an incipient intra-oceanic volcanic arc, and (3) the Mount Stavely Volcanic Complex, which consists of calc-alkaline volcanic and intrusive rocks of Late Cambrian age (about 500 Ma).

Foster and others (2005) interpreted rocks of the Mount Stavely Volcanic Complex as products of postorogenic magmatism, related to rollback of west-dipping subduction after the Delamerian orogeny. Rocks of the Mount Stavely Volcanic Complex are classified as permissive for porphyry copper, and they contain one porphyry copper prospect (figs. B1, B2).

In northwestern Tasmania, post-Delamerian extensional tectonism began at 508.1±2.6 Ma, as indicated by rapid uplift and cooling of the Forth Metamorphic Complex (Foster and

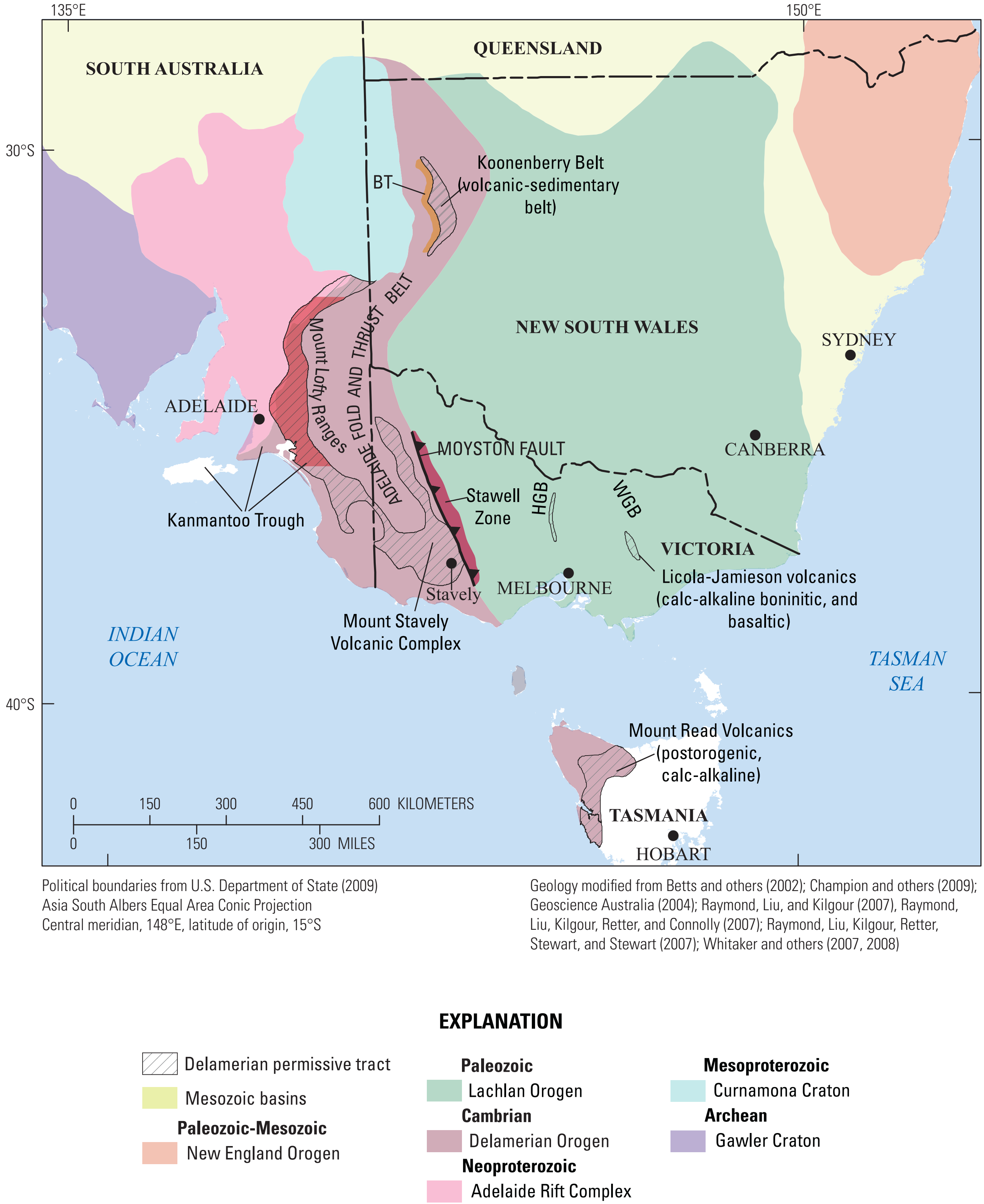

Figure B2. Map showing geologic setting for the Delamerian tract (009pCu8001), New South Wales, South Australia, Tasmania, and Victoria, Australia. Also shown are Precambrian cratons and Phanerozoic orogens. BT, Bancannia Trough; HGB, Heathcoate Greenstone Belt; WGB, Wellington Greenstone Belt.

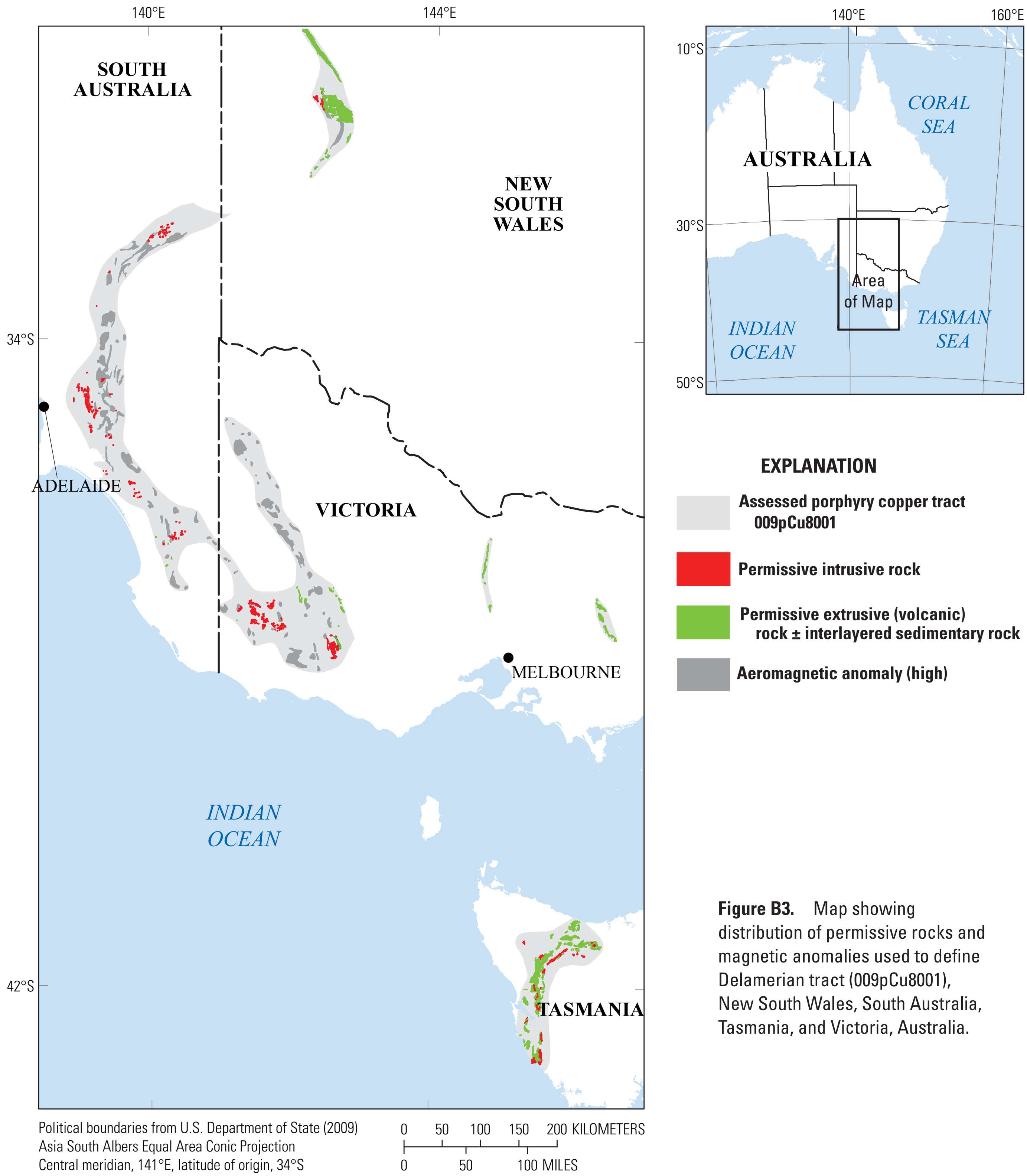

Figure B3. Map showing distribution of permissive rocks and magnetic anomalies used to define Delamerian tract (009pCu8001), New South Wales, South Australia, Tasmania, and Victoria, Australia.

others, 2005). This was closely followed by postorogenic rifting and eruption of the predominantly andesitic Mount Read Volcanics (fig. B2), which are of Middle to Late Cambrian age (about 505–497 Ma). Crawford and others (2003) characterized the Mount Read Volcanics as a calc-alkaline suite of volcanic and volcaniclastic rocks with medium- to high-K affinities. These rocks erupted into postorogenic half-grabens related to rollback of subduction after the Delamerian Orogeny (Foster and others, 2005)

According to Crawford and others (2003), Cambrian calc-alkaline volcanic and volcaniclastic rocks with medium- to high-K affinities also occur in thrust slices in the Licola and Jamieson and areas, in east-central Victoria (about 150 km east-northeast of Melbourne, as shown in fig. B2). These Licola-Jamieson Volcanics, calc-alkaline volcanic and volcaniclastic rocks, like those of the Mount Stavely Volcanic Complex and the Mount Read Volcanics, are interpreted as postorogenic in age, and related to rollback of subduction after the Delamerian Orogeny.

Rock Types Permissive for Porphyry Copper

Descriptive models by Cox (1986a, b, c), Panteleyev (1995a, b and 2005a, b), Cooke and others (1998), and Jaireth and Miezitis (2004a) indicate that alkaline suites of I-type igneous rocks are permissive for porphyry Cu-Au deposits, and calc-alkaline suites of I-type igneous rocks are permissive for porphyry copper deposits. Permissive alkaline suites may include gabbro, diorite, monzodiorite, monzonite, syenite, and foidal syenite or their microcrystalline to porphyro-aphanitic equivalents, including basalt, andesite, trachyandesite, latite, trachyte, and foidal trachyte. Permissive calc-alkaline suites may include diorite, quartz diorite, tonalite, granodiorite, quartz monzonite, monzogranite, and granite of calc-alkaline affinity. Porphyro-aphanitic equivalents include andesite, quartz andesite, dacite, rhyodacite, quartz latite, and rhyolite porphyries of calc-alkaline affinity.

Porphyry copper deposits generally are associated with porphyritic intrusions characterized by phenocrysts in a microcrystalline to aplitic groundmass. However, such rocks commonly intrude both volcanic and plutonic rocks of similar age and composition. Therefore, rocks of appropriate composition and age are considered permissive, whether or not they are intrusive porphyries. However, gabbro and basalt are considered permissive only where they occur with other permissive rock types in a setting interpreted to represent subduction-related magmatism.

Permissive Geologic-Map Units

Geologic map units that define this permissive tract represent lithologic assemblages within the Delamerian Orogen, are of Cambrian age, and contain any of the permissive rock types described above. Geologic map units included in Delamerian permissive tract 009pCu8001 are listed in table B2.

Extension of Permissive Tract Boundaries to 1-km Depth

Map units representing permissive rock types are the basic building blocks of permissive tracts. However, to extend permissive units to a depth of 1 km below the geologically mapped surface, we added a 10-km buffer to mapped bodies of igneous intrusive rocks and a 2-km buffer to mapped bodies of permissive volcanic rocks. The rationale for use of such buffers is explained in the main body of this report. A spatial modeling algorithm was applied to connect permissive areas and smooth the permissive tract boundaries. [See the metadata associated with the tracts in the GIS (appendix G) for additional details.]

Permissive I-type igneous rocks of the magnetite series generally are ferromagnetic and can be detected by magnetic surveys (Clark, 1999). Aeromagnetic evidence of such rocks within 1 km of the surface is considered permissive for porphyry copper. For this reason, permissive tract boundaries were extended beyond their buffered surface expressions where indicated by magnetic anomalies in covered areas. In general, positive aeromagnetic anomaly patterns with relatively short wavelengths were interpreted to indicate subsurface extensions of mafic to intermediate igneous rocks within about 1 km of the surface. Relatively large, long wave-length magnetic anomalies were interpreted to indicate deeper ferromagnetic bodies at depths below 1 km.

Delamerian Sub-tracts

The Delamerian permissive tract (009pCu8001) includes three geographically separate sub-tracts, separated by areas that are covered by younger materials that probably are greater than 1 km thick.

Adelaide Sub-tract (009pCu8001a)

The Adelaide sub-tract is in the southwestern part of the Delamerian Orogen, where Cambrian rocks overlap the eastern margin of the Neoproterozoic Adelaide Rift Complex (fig. B2). Figure B3 shows areas of permissive volcanic and intrusive igneous rocks, and areas of positive aeromagnetic anomalies. Such anomalies are interpreted to indicate relatively magnetic igneous rocks in the subsurface. Inasmuch as they may represent covered permissive igneous rocks, they are included in the Adelaide sub-tract.

In northwestern New South Wales, the Koonenberry Belt contains volcanic and intrusive units of the Mount Wright Magmatic Arc/Back-Arc Complex of Early Cambrian age (about 525–510 Ma).

In the Mount Lofty Ranges of southeastern South Australia, permissive synorogenic I-type granitoid plutons of Middle to Late Cambrian age intrude metasedimentary and subordinate I-type metavolcanic rocks of Neoproterozoic to Early Cambrian age. The Netley Hill, Anabama Hill, and Kitticoola porphyry copper prospects are hosted in synorogenic I-type granitoid intrusions in the Mount Lofty Ranges (figs. B1, B2, B3). Several stratabound sediment-hosted copper deposits also occur in the metasedimentary rocks of the Adelaide fold and thrust belt. These copper deposits are stratabound, however, and they do appear not to be related to porphyry copper systems.

In the Mount Stavely Volcanic Complex, western Victoria (fig. B2), I-type calc-alkaline igneous rocks of intermediate to felsic composition, medium- to high-K affinity, and Late Cambrian age are exposed near the southern end of the belt. Aeromagnetic anomalies indicate that the Mount Stavely Volcanic Complex extends under cover to the north-northwest.

The Thursdays Gossan porphyry copper prospect is near the southern end of the Mount Stavely Volcanic Complex (figs. B1, B2). It is hosted in postorogenic volcanic and subvolcanic intrusive rocks of andesitic to dacitic composition and of Middle Cambrian age (Rajagopalan, 1999).

The eastern margin of the Mount Stavely Volcanic Complex is bounded by the north-northwest-striking Moyston Fault, which also bounds the Adelaide sub-tract. East of the Moyston Fault, orogenic gold deposits of the Stawell Zone are hosted in Early Paleozoic turbidites and minor fault-bounded slivers of Cambrian metavolcanic rocks (Noble and others, 1980).

Victoria Sub-tract (009pCu8001b)

The Victoria sub-tract is in central Victoria (fig B1). Permissive igneous rocks occur in the fault-bounded Heathcote Greenstone Belt (HGB), the Wellington Greenstone Belt (WGB), and in the fault-bounded Licola-Jamieson Volcanics (fig. B2).

Rocks of the Heathcote and Wellington Greenstone Belts make up a meta-tholeiite-boninite-andesite assemblage of Early to Middle Cambrian age (table B2).These rocks are interpreted to represent metamorphosed rocks of an incipient oceanic volcanic-arc-forearc complex (Crawford, Cameron, and Keays, 1984; Crawford, Meffre, and Symonds, 2003). Although these rocks are considered marginally permissive for porphyry Cu-Au deposits, they are more likely to contain synorogenic volcanic-hosted Cu-Ni deposits (as described by Page, 1986).

The Jamieson Volcanic Group and Licola Volcanics comprise calc-alkaline volcanic and volcaniclastic rocks of Middle to Late Cambrian age. These permissive rocks, which are exposed in the Licola-Jamieson Volcanics (fig. B2), are medium- to high-K andesite, dacite, and rhyolite lavas and breccias, interlayered with volcaniclastic conglomerate, sandstone, and shale (table B2). They resemble volcanic and volcaniclastic rocks of the Mount Stavely Volcanic Complex, and they are interpreted as postorogenic, relative to the Delamerian Orogeny (Foster and others, 2005).

Although volcanic and volcaniclastic rocks of the Jamieson Volcanic Group and the Licola Volcanics are considered marginally permissive for porphyry copper, they contain no known porphyry copper deposits and prospects. Furthermore, no intrusive rocks are exposed in either the Jamieson Volcanic Group or Licola Volcanics. Therefore, this sub-tract was not quantitatively assessed for porphyry copper resources. A qualitative assessment concludes that the Victoria sub-tract is unlikely to contain significant undiscovered porphyry copper resources.

Tasmania Sub-tract (009pCu8001c)

The Tasmania sub-tract in western Tasmania (fig. B1) is defined by the distribution of the calc-alkaline Mount Read Volcanics of Middle to Late Cambrian age (fig. B2). This sub-tract also contains relatively minor granitoid intrusions along the eastern margin of the Mount Read Volcanics. Volcanic rocks of this sub-tract include shoshonitic basaltic to andesitic rocks (table B2). This sub-tract also contains relatively minor intermediate to felsic volcanic and granitoid intrusive rocks, which are considered permissive for porphyry copper deposits.

Although the Mount Read Volcanics contain many volcanic-hosted massive sulfide deposits, this permissive sub-tract contains no known porphyry copper deposits or prospects, and may not represent an appropriate geologic setting for porphyry copper deposits.

Known Deposits

No porphyry copper deposits are known to occur in the Delamerian permissive tract. However, there are stratabound copper deposits in metasedimentary strata of the Adelaide fold and thrust belt (in the Adelaide sub-tract). There also are copper-bearing volcanic-hosted massive sulfide deposits in the Mount Wright Volcanics (near the north end of the Adelaide sub-tract) and in the Mount Read Volcanics (in the Tasmania sub-tract). Also, just east of the Mount Stavely Volcanic Complex, epigenetic gold deposits are present in the Stawell Zone, east of the Moyston Fault (fig. B2). However, none of these deposits appears to be related to, or associated with, intrusion-centered porphyry copper systems.

Initially, we misinterpreted the circular open-pit on the Kanmantoo copper deposit as a porphyry copper mine. However, Seccombe and others (1985) described the Kanmantoo deposit as a swarm of discordant lenses containing chalcopyrite, pyrrhotite, magnetite, and pyrite in pyritized metasedimentary schists. They interpreted the Kanmantoo copper deposit as a deformed and metamorphosed feeder zone beneath a nearby stratabound sedimentary-exhalative lead-zinc occurrence.

Stratabound sediment-hosted copper ore zones of the Anabama Copper Mine are near the Anabama Complex, which hosts the Anabama Hill porphyry copper prospect. Because their names are similar, however, references to these sediment-hosted copper ore zones and porphyry copper prospects have been confused. Ore zones at the Anabama Copper Mine are hosted in Neoproterozoic metasedimentary strata, about 4 km southeast of the Anabama Granite pluton and about 12 km from the Anabama Hill porphyry copper prospect.

Only sub-economic concentrations of copper have been found at the Anabama Hill porphyry copper prospect. By contrast, stratabound ore zones at the Anabama Copper Mine site are estimated to contain at least 4.2 Mt of ore with an average grade of 0.52 percent copper.

Prospects, Mineral Occurrences, and Related Deposit Types

Four significant porphyry copper prospects occur in the Adelaide sub-tract (fig. B1). They are the Thursdays Gossan, Netley Hill, Anabama Hill, and Kitticoola porphyry copper prospects (table B3).

Thursdays Gossan Prospect

The Thursdays Gossan porphyry copper prospect, near Stavely, Victoria, is hosted by subvolcanic, pyroclastic, and volcanic-derived sedimentary rocks of the Mount Stavely Volcanic Complex. The southeastern part of the prospect is exposed, but its northwestern part is mostly covered by colluvial deposits, which overlie a lateritic regolith developed on bedrock. Mineralized host rocks include andesitic breccia, andesitic to dacitic tuffs, volcaniclastic sandstone to siltstone, and subvolcanic intrusions (Radojkovic, 2003). Intrusions of dacitic porphyry and surrounding sedimentary and volcanic strata are mineralized, but younger intrusions of tonalite and monzodiorite are barren (Rajagopalan, 1999).

According to Radojkovic (2003, p. 1), “Air core drilling at Thursdays Gossan identified extensive (3 × 1.2 km) quartz-sericite-pyrite alteration with associated chalcocite mineralization believed to be related to the intrusion of several quartz-feldspar porphyries.” According to Rajagopalan (1999), an inner zone of advanced argillic alteration minerals passes outward to intermediate argillic, silicic, sericitic, and propylitic alteration mineral assemblages.

Primary ore minerals at the Thursdays Gossan prospect are chalcopyrite, molybdenite, and bornite (Rajagopalan, 1999). These minerals are associated with pyrite in veins, fractures and shear zones, and are sparsely disseminated throughout ore-related intrusions. Primary copper concentrations generally range from 0.1 to 0.3 percent copper. A cross section of the Thursdays Gossan prospect indicates that the best drilled intercept was 229 m with an average grade of 0.22 percent copper in altered volcanic and sedimentary rocks above a barren tonalite porphyry stock.

The oxide zone of weathering and copper leaching at the Thursdays Gossan prospect generally ranges from 20 to 40 m deep, but extends to 150 m in the zone of intermediate argillic alteration. The highest-grade copper intercept was 15 m of drill core containing 1.8 percent copper from the chalcocite-bearing zone of supergene enrichment below the weathered, oxidized, and leached cap of the mineralized zone.

Netley Hill and Anabama Hill Prospects in the Anabama Granite

The Netley Hill and Anabama Hill prospects are in the Anabama Complex, a composite pluton of granitoid composition including the Anabama Granite, granodiorite, tonalite, and adamellite (or monzogranite) that is exposed in hills northeast of the northeastern end of the Mount Lofty Ranges (figs. B1, B2). This pluton is 45 km long (northeast-southwest) and 10 km wide. It is elongate parallel to the structural grain of its tightly folded Neoproterozoic metasedimentary host strata. The Netley Hill prospect is in the southern part of the Anabama Granite pluton. The Anabama Hill prospect is about 23 km northeast of the Netley Hill prospect, near the eastern margin of the central part of the Anabama Granite pluton. Foden and others (2002) suggested that the Anabama Granite was emplaced during the Delamerian Orogeny, which according to Foden and others (2006) probably occurred in Middle to Late Cambrian time, between about 514 and 490 Ma.

According to Morris (1979), a whole-rock strontium-isotopic isochron on samples from drill core indicates an age of 468±62 Ma for Anabama Granite at Anabama Hill, and K-Ar age determinations on muscovite from greisens at Anabama Hill indicate a minimum age of 450 Ma. These age determinations and their ranges of uncertainty bracket the age of the granite and greisen at Anabama Hill between 530 and 450 Ma, between Early Cambrian and Late Ordovician.

Foden and others (2002) reported $^{87}Sr/^{86}Sr$ (at 500 Ma) = 0.70431 to 0.71340 and $\varepsilon_{Nd(I)}$ (the initial neodymium isotopic ratio) = +0.4 to −7.8 for tonalite and granodiorite of the Anabama Complex, which includes the Anabama Granite. They interpreted these rocks as products of mantle-derived I-type magma batches, which underwent different degrees of crustal assimilation and fractional crystallization and different combinations of deformation, hydrothermal mineralization, and alteration.

Netley Hill Prospect

At the Netley Hill prospect, quartz veins containing pyrite, chalcopyrite, and subordinate molybdenite are associated with hydrothermally altered granite (Morris, 1979). Drilling at the Netley Hill prospect recovered a 40-m intercept averaging 0.3 percent copper and 0.05 percent molybdenum (table B3). This is apparently the best intercept reported in prospects hosted in Anabama Granite, but we have no indication of the angle of intersection between the drill hole and the mineralized zone.

Anabama Hill Prospect

Morris (1979) mapped the geology of the Anabama Hill prospect. His maps show a core of relatively unaltered and unmineralized granite to granodiorite and adamellite. The core is cut by a dacite dike and surrounded by phyllically altered to partially greisenized granite. A semicircular rind

Table B2*A*. Map units that define the Adelaide sub-tract (009pCu8001a), Delamerian tract, New South Wales, South Australia, and Victoria, Australia.

[Based on Raymond, Liu, and Kilgour (2007), Raymond, Liu, Kilgour, Retter, and Connolly (2007), Raymond, Liu, Kilgour, Retter, Stewart, and Stewart (2007), and Whitaker and others (2008); for additional information about named map units, see Geoscience Australia, Stratigraphic Units Database at http://dbforms.ga.gov.au/www/geodx.strat_units.int/]

Map unit	Map symbol	Lithology	Age range
		Intrusive rocks	
Felsic intrusives 73466	Єgv	muscovite granite and biotite granite, magnetic to non-magnetic	Cambrian
Kadnook Creek Granodiorite	Єg449	biotite-muscovite granodiorite with magnetite	Late Cambrian
Chetwynd Tonalite	Єg433	biotite tonalite with magnetite, allanite	Cambrian
Ferres Creek Tonalite	Єg423	biotite-hornblende tonalite with magnetite, epidote	Cambrian
Kooreelah Gabbro-Diorite	Єg428	quartz diorite, quartz monozodiorite,	Middle to Late Cambrian
Cairns Creek Granodiorite	Og432	hornblende-biotite granodiorite with magnetite, sphene, allanite	Cambrian to Ordovician
Glenelg River Metamorphic Complex	Єygd	hornblende-plagioclase metagabbro, metadolerite, amphibolite	Cambrian
Snake River Tonalite	Єg437	hornblende-biotite tonalite with magnetite, sphene, allanite	Cambrian
Brimboal Granodiorite	Єg438	biotite-hornblende granodiorite with magnetite	Early to Middle Cambrian
Wando Tonalite	Єg421	biotite-hornblende granodiorite with magnetite, epidote, sphene, allanite	Late Cambrian
Tuloona Granodiorite	Єg425	biotite granite with accessory muscovite, magnetite	Late Cambrian
Torah Granodiorite	Єg427	biotite granodiorite	Cambrian
Wennicott Tonalite	Єg429	biotite tonalite with magnetite, epidote; hornblende migrogranite enclaves	Cambrian
Lalkaldarno Porphyry	Єgsl	hornblende quartz diorite	Late Cambrian
Nargoon Group	Єyga	meta-quartz-diorite, amphibolite, volcaniclastic metasandstone, breccia	Cambrian
Bushy Creek Granodiorite	Єg395	hornblende granodiorite	Late Cambrian
Buckeran Diorite	Єgbk	diorite	Cambrian
Anabama Granite	ЄOgan	granite to granodiorite	Cambrian to Ordovician
Granite 37500	Єg4	felsic intrusives	Cambrian
Mafic rocks 73012	ЄOd5	mafic igneous	Cambrian
Kaiserstuhl Granite	ЄOgka	biotite-hornblende granite	Cambrian to Ordovician
Mount Crawford Granite Gneiss	Onmc	granite	Cambrian
Rathjen Gneiss	Єnrj	granite to granodiorite orthogneiss	Early Cambrian
Palmer Granite	Ogpa	granodiorite, aplite, monzogranite	Middle Cambrian to Middle Ordovician
Summerfield Intrusive Suite	ЄOgsi	I-type granitoids, gabbro, diorite	Late Cambrian to Early Ordovician
Monarto Granite	ЄOgmo	monzogranite	Cambrian to Early Ordovician
Monzogranite, granite 73014	Єggp	hornblende-biotite monzogranite, granite	Cambrian
		Volcanic rocks	
Gnalta Group (Mount Wright Volcanics)	Єwg	mafic, intermediate, and felsic volcanic and sedimentary rocks	Early to Middle Cambrian
Acid volcanic rocks 73013	Єf	felsic volcanic	Cambrian
Ponto Group	Єyp	mafic to felsic volcanic rocks, sedimentary rocks	Early to Middle Cambrian
Fairview Andesitic Breccia	Єasf	andesitic breccia, minor andesite and basalt lava	Cambrian

Table B2*B*. Map units that define the Victoria sub-tract (009pCu8001b), Delamerian tract, Victoria, Australia.

[Based on Raymond, Liu, Kilgour, Retter, and Connolly (2007); for additional information about named map units, see Geoscience Australia, Stratigraphic Units Database at http://dbforms.ga.gov.au/www/geodx.strat_units.int/]

Map unit	Map symbol	Lithology	Age range
		Volcanic rocks	
Jamieson Volcanic Group	Ꞓaj	andesite lava and breccia, rhyolite and dacite lava and breccia, volcaniclastic sandstone, shale and conglomerate	Middle to Late Cambrian
Licola Volcanics	Ꞓflc	rhyolite lava, rhyolitic volcaniclastic rocks, andesite breccia and lava, sandstone, phosphatic shale with limestone clasts	Cambrian
Dookie Igneous Complex	Ꞓbd	tholeiitic metabasalt, metagabbro, marine sedimentary rocks	Cambrian
Maitland Beach Volcanics	Ꞓbmb	tholeiitic basalt, gabbro	Cambrian
Lickhole Volcanic Group	Ꞓbl	pillowed and massive tholeiitic basalt, boninitic lavas, gabbro, dolerite, andesite, volcaniclastic sandstone	Early to Middle Cambrian
Heathcote Volcanic Group	Ꞓbh	pillowed and massive basalt and andesite flows, metadolerite dikes, sills	Early Cambrian

Table B2*C*. Map units that define the Tasmania sub-tract (009pCu8001c), Delamerian tract, Tasmania, Australia.

[Based on Raymond, Liu, and Kilgour (2007); for additional information about named map units, see Geoscience Australia, Stratigraphic Units Database at http://dbforms.ga.gov.au/www/geodx.strat_units.int/]

Map unit	Map symbol	Lithology	Age range
		Intrusive rocks	
Beulah Granite	Ꞓgbu	biotite-hornblende monzogranite	Late Cambrian
Dove Granite	Ꞓgdv	biotite monzogranite	Late Cambrian
Quartz-feldspar porphyry	Ꞓgrq	quartz-feldspar porphyry, mostly intrusive	Middle to Late Cambrian
Elliott Bay Granite	Ꞓgeb	biotite monzogranite	Middle to Late Cambrian
Tonalite	Ꞓgt	tonalite	Cambrian
Darwin Granite	Ꞓgdw	biotite-alkali-feldspar granite	Cambrian
Murchison Granite	Ꞓgmr	biotite granite	Early to Middle Cambrian
		Volcanic rocks	
Felsic to intermediate volcanics	Ꞓfr	felsic to intermediate volcanic, volcaniclastic, and intrusive rocks	Middle to Late Cambrian
Tyndall Group	Ꞓfrt	felsic volcanic and volcaniclastic rocks	Middle to Late Cambrian
Mafic volcanics	Ꞓbr	shoshonitic basaltic to andesitic volcanics; dolerite, gabbro	Middle to Late Cambrian

Table B3. Significant porphyry copper prospects and occurrences in the Adelaide sub-tract (009pCu8001a), Delamerian tract, New South Wales, South Australia, and Victoria, Australia.

[Ma, million years; m, meters; %, percent; t, metric tons; prospect ranking criteria listed in table 2]

Name	Latitude	Longitude	Age (Ma)	Comments	Rank	Reference
Thursdays Gossan	-37.608	142.612	503	229 m at 0.22% Cu	3	Rajagopalan (1999), Radojkovic (2003), Singer and others (2008), Geoscience Australia (2010)
Netley Hill	-32.807	140.043	503	40 m at 0.3% Cu, 0.05% Mo	3	South Australian Resources Information Geoserver (SARIG), 2010
Anabama Hill	-32.719	140.206	503	5 m at 0.1% Cu; 4 m at 0.1% Mo	4	Morris (1979)
Kitticoola	-34.874	139.152	490	past production, 740 t Cu	6	Ewers and others (2002), Geoscience Australia (2010)

of greisen occupies the southern margin of the Anabama Hill prospect. Weathered greisen consists mostly of quartz and muscovite with cubic, limonite-stained pits after weathered-out pyrite. Supergene limonite, malachite, chrysocolla, and turquoise occur in the leached cap, which underwent oxidative weathering. Chalcocite and covellite occur below the leached cap.

Beneath weathered greisen, mineralized and altered biotite granite contains copper-bearing quartz veins and breccias with greisenized envelopes. Chalcopyrite and traces of molybdenite are the primary ore minerals, accompanied by pyrite and magnetite. An inner potassic zone grades outward through a medial phyllic to partially greisenized zone, a partial ring of greisen, and an outer propylitic zone. Morris (1979, p. 23) noted that “copper mineralization is concentrated on the inner margin of the pyritic greisen zone.”

Morris (1979) reports that 3 test holes were drilled, each to about 200 m deep. The best intercepts were 5 m with 0.1 percent of copper and 4 m with 0.1 percent of molybdenum (table B3). Morris (1979, p. 22–23) concluded “the hydrothermal episode at Anabama Hill was not violent enough to shatter and fracture the host rocks sufficiently for large-scale, pervasive, hydrothermal alteration to take place . . . and unaltered granite appears to be unmineralised.”

Kitticoola Prospect

The Kitticoola porphyry copper prospect, in the Mount Lofty Ranges about 75 km east of Adelaide (fig. B1), is hosted in a pluton of Palmer Granite. The Palmer Granite is a Delamerian I-type granite with $^{87}Sr/^{86}Sr$ (at 500 Ma) = 0.70655 and $\varepsilon_{Nd(I)} = -2.6$ (Foden and others, 2002).

According to Morris (1979, p. 23) “the Palmer Granite is unmineralised, except where the Palmer Fault crosses the granite,” where it is “shattered, sericitised, and chloritised.” At the Kitticoola Mine, copper and gold were mined from this altered granite (Morris, 1979). The OZMIN mineral deposits database (Ewers and others, 2002) states that 740 t of copper and 0.2 t of gold were recovered from the Kitticoola Mine.

Exploration History

Although there has been little recent exploration for porphyry copper deposits in the Delamerian tract, covered parts of the Adelaide sub-tract are now being explored for copper-bearing ore deposits of any type, using geology, geochemistry, geophysics, and drilling. The four documented porphyry copper prospects in this tract are in the Adelaide sub-tract.

Sources of Information

The principal sources of information used by the assessment team for delineation of the Delamerian tract are listed in table B4.

Grade and Tonnage Model Selection

The Delamerian tract includes three sub-tracts, but only the Adelaide sub-tract (009pCu8001a) shows sufficient evidence of porphyry copper systems to support quantitative estimation of undiscovered resources. Best intercepts in three prospects in the Adelaide sub-tract have average copper grades of 0.1–0.3 percent copper. Such grades are less than the median grade of the global model for porphyry copper deposits. However, these grades are similar to those of some deposits included in the custom grade-tonnage model for Australian porphyry copper deposits of the East Tasmanide and Yeoval permissive tracts (appendix A). Consequently, we selected the custom grade-tonnage model for Australian porphyry copper deposits to represent grades and tonnages of undiscovered deposits in the Adelaide sub-tract.

Estimate of the Number of Undiscovered Deposits

Only the Adelaide sub-tract was assessed quantitatively. The Victoria and Tasmania sub-tracts contain no known porphyry copper deposits or prospects and are qualitatively judged to have low potential for undiscovered deposits.

Table B4. Principal sources of information used for the Delamerian tract (009pCu8001), Australia.

[NA, not applicable]

Theme	Name or Title	Scale	Citation
Geology	Surface geology of Australia, New South Wales—2nd edition	1:1,000,000	Raymond, Liu, Kilgour, Retter, Stewart, and Stewart (2007)
	Surface geology of Australia, Victoria—3rd edition	1:1,000,000	Raymond, Liu, Kilgour, Retter, and Connolly (2007)
	Surface geology of Australia, Tasmania—3rd edition	1:1,000,000	Raymond, Liu, and Kilgour (2007)
	Surface geology of Australia, South Austalia	1:1,000,000	Whitaker and others (2008)
	Geodynamic synthesis of the Phanerozoic of eastern Australia and implications for metallogeny	NA	Champion and others (2009)
	The Tasmanides of eastern Australia	NA	Glen (2005)
	Timing of subduction and exhumation along the Cambrian East Gondwana margin and the formation of Paleozoic back-arc basins	NA	Foster and others (2005)
	Granite production in the Delamerian Orogen, South Australia	NA	Foden and others (2002)
Mineral occurrences	Porphyry copper deposits of the world: database and grade and tonnage models	NA	Singer and others (2008)
	Australian Atlas of mines and mineral deposits	NA	Geoscience Australia (2010)
	OZMIN mineral deposits database	1:2,500,000	Ewers and others (2002)
	OZPOT geoprovince-scale assessment of mineral potential	NA	Jaireth and Miezitis (2004b)
	PIRSA minerals, copper	NA	Primary Industries and Resources South Australia (2010)
	Intierra	NA	Interra (2009)
Geophysics	Total magnetic anomaly (TMI) grids of Australia, fourth edition	NA	Geoscience Australia (2004)
	Australian National gravity database 0.5 minute offshore-onshore gravity grid	NA	Geoscience Australia (2009)
Exploration	Australian mineral exploration	NA	Geoscience Australia (2005–2009)
	Advanced mineral projects and exploration highlights in New South Wales	NA	NSW Industry and Investment (2010)

Before estimating numbers of undiscovered deposits, the assessment panel reviewed the geology, known deposits, locations and qualities of significant porphyry prospects and occurrences, exploration status of the tract, and geophysical evidence for undiscovered deposits in relatively unexplored or underexplored parts of the tract. Then panel members were asked to list and weigh positive factors which favor the existence of undiscovered deposits, versus negative factors, which limit possibilities for undiscovered porphyry copper deposits in the permissive tract.

Rationale for the Estimate

The rationale for the estimate was that it should be guided by comparing prospects to known deposits, by counting and assigning probabilities to prospects and occurrences, by consideration of spatial constraints, and by weighing positive versus negative factors listed by the panel members.

Positive Factors

Positive factors that indicate the possible presence of undiscovered porphyry copper deposits in the Adelaide sub-tract include:

1. Lithologic assemblages provide evidence of I-type magmatism, which occurred before, during, and after the Delamerian Orogeny, probably in subduction-related magmatic-arc to back-arc settings. Such lithologic assemblages are considered permissive for the formation of porphyry copper deposits.

2. Four porphyry copper prospects are known to exist in the Adelaide sub-tract. Three of these are in synorogenic granitoid plutons, and one is in postorogenic volcanic and subvolcanic rocks. Two of these prospects are rank-3 prospects (table 2) with drilled intercepts of more than 20 m at grades of 0.2 percent or more of copper.

3. Although the exposed part of the Adelaide sub-tract is well explored, much of this sub-tract is covered and underexplored. Volcanic and intrusive rocks of the Mount Stavely Volcanic Complex are mostly covered, but exposures at the southern end of this belt indicate that volcanic and intrusive rocks of this belt probably are eroded to about the right level for preservation of porphyry copper systems beneath cover.

4. The magmatic arcs that contain these prospects were recognized only in the past 10 years, and they currently contain many active exploration tenements.

Negative Factors

Negative factors that may limit the number of undiscovered porphyry copper deposits in Adelaide sub-tract include:

1. Most of the known ore deposits in volcanic belts of the Delamerian tract are volcanic-related massive sulfide deposits rather than porphyry copper deposits. This indicates low potential for undiscovered porphyry copper deposits in volcanic arcs of the Delamerian tract.

2. Synorogenic I-type granitoid plutons (which host three of the four known porphyry copper prospects in the Adelaide sub-tract) are predominantly phaneritic, and probably are too deeply eroded for preservation of porphyry copper deposits related to the tops of porphyro-aphanitic intrusions.

3. Generally low grades of mineralized zones in the known prospects in the Adelaide sub-tract indicate that small and low-grade deposits are more likely than are the larger and higher grade deposits included in the global grade-tonnage model of Singer and others (2008).

4. The known prospects are of subeconomic grade, and they probably are generally representative of what can be expected in the Adelaide sub-tract.

Estimates of numbers of undiscovered deposits were guided by weighing positive versus negative factors, by counting and assigning ranks and probabilities to prospects and occurrences, and by considering process constraints implied by a high ratio of intrusive to preserved volcanic rocks and a lack of tight stockworks of closely spaced and well mineralized veinlets in the known prospects. However, strict application of process constraints was tempered by consideration of the amount of cover and the possibility that small intrusions and associated zones of altered and mineralized rocks may not be portrayed on geologic maps at 1:1,000,000 scale, which do not indicate areas of hydrothermally altered rocks.

Each of five estimators (Bookstrom, Glen, Hammarstrom, Robinson, and Zientek) gave an independent estimate of the number of undiscovered deposits expected at three levels of subjective probability (at 90-, 50-, and 10-percent probability levels for example, or if 0 deposits at 90-percent probability, then at 50-, 10-, and 5-percent probability levels). After an anonymous first round of estimation, the high and low estimators explained their reasoning, and consensus was achieved by negotiation.

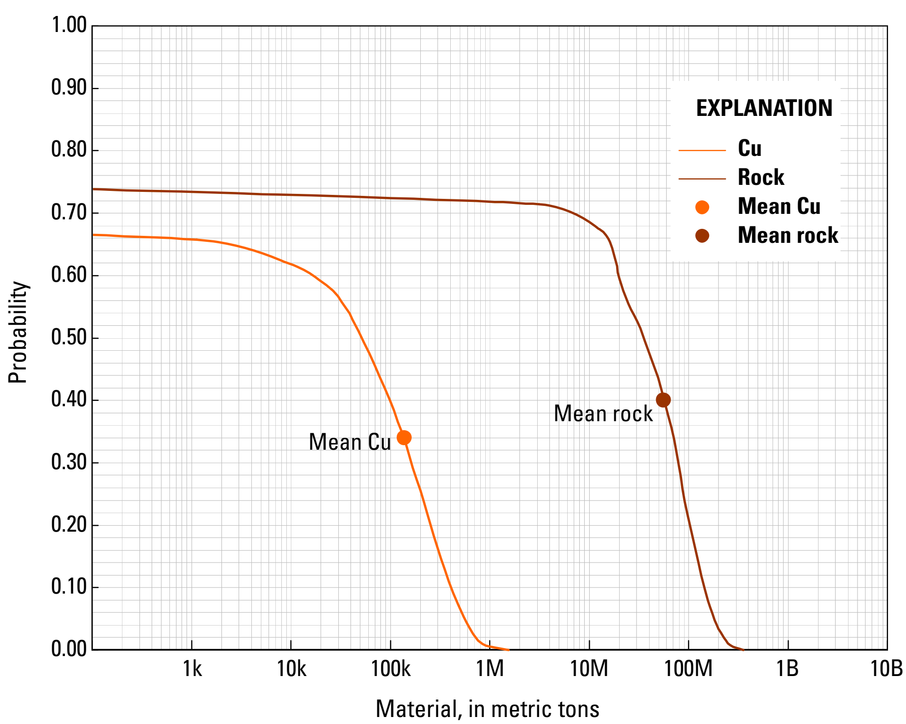

Figure B4. Cumulative frequency plot showing the results of Monte Carlo computer simulation of undiscovered resources in Adelaide sub-tract (009pCu8001a), Delamerian tract, New South Wales, South Australia, and Victoria, Australia. k=thousands, M=millions, B=billions.

Table B5. Undiscovered deposit estimates, tract area, and deposit density for the Adelaide sub-tract (009pCu8001a), Delamerian tract, New South Wales, South Australia, and Victoria, Australia.

[N_{XX}, estimated number of deposits associated with the xxth percentile; N_{und}, expected number of undiscovered deposits; *s*, standard deviation; C_v%, coefficient of variance; N_{known}, number of known deposits in the tract that are included in the grade and tonnage model; N_{total}, total of expected number of deposits plus known deposits; Tract area, area of permissive tract in square kilometers; Deposit density, total number of deposits per 100,000 km². N_{und}, *s*, and C_v% are calculated using a regression equation (Singer and Menzie, 2005)]

Consensus undiscovered deposit estimates					Summary statistics					Tract area (km²)	Deposit density (N_{total}/100,000 km²)
N_{90}	N_{50}	N_{10}	N_{05}	N_{01}	N_{und}	*s*	C_v%	N_{known}	N_{total}		
0	2	5	7	7	2.5	2.2	91	0	2.5	50,747	4.9

Table B6. Results of Monte Carlo simulations of undiscovered resources for the Adelaide sub-tract (009pCu8001a), Delamerian tract, New South Wales, South Australia, and Victoria, Australia.

[Cu, copper in metric tons (t); Rock, in million metric tons (Mt)]

Material	Probability of at least the indicated amount						Probability of	
	0.95	0.9	0.5	0.1	0.05	Mean	Mean or greater	None
Cu (t)	0	0	52,000	410,000	560,000	140,000	0.34	0.27
Rock (Mt)	0	0	36	150	180	56	0.40	0.21

Consensus Estimates

Summary statistics, based on the consensus estimate, indicate 2.5±2.2 expected undiscovered deposits in the Adelaide sub-tract of the Delamerian permissive tract (table B5). The coefficient of variation (C_v) of 91 percent indicates a fairly high degree of uncertainty in the expected number of undiscovered deposits. Adding the mean estimate of 2.5 undiscovered deposits to 0 known deposits indicates a total of 2.5 porphyry copper deposits expected to occur within 1 km of the surface. The area of this sub-tract is 50,747 km². Therefore the estimated spatial density of deposits is 4.9 per 100,000 km².

Probabilistic Assessment Simulation Results

Undiscovered resources for the tract were estimated (table B6) by combining consensus estimates for numbers of undiscovered porphyry copper deposits with a custom Australian porphyry model (appendix A), using the EMINERS program (Root and others, 1992; Duval, 2012; Bawiec and Spanski, 2012). Cumulative probability graphs show expected amounts of the commodities through a range of levels of subjective probabilities (fig. B4).

References Cited

Bawiec, W.J., and Spanski, G.T., 2012, Quick-start guide for version 3.0 of EMINERS—Economic Mineral Resource Simulator: U.S. Geological Survey Open-File Report 2009–1057, 26 p., available at http://pubs.usgs.gov/of/2009/1057/. (This report supplements USGS OFR 2004–1344.)

Betts, P.G., Giles, D., Lister, G.S., and Frick, L.R., 2002, Evolution of the Australian lithosphere: Australian Journal of Earth Sciences, v. 49, no. 4, p. 661–695.

Champion, D.C., Kositcin, N., Huston, D.L., Mathews, E., and Brown, C., 2009, Geodynamic synthesis of the Phanerozoic of eastern Australia and implications for metallogeny: Geoscience Australia, Record 2009/18, GeoCat#68866, 222 p., digital, accessed October 4, 2010, at http://www.ga.gov.au/products/.

Clark, D.A., 1999, Magnetic petrology of igneous intrusions—Implications for exploration and magnetic interpretation: Exploration Geophysics, v. 30, p. 5–26.

Cooke, D.R., Heithersay, P.S., Wolfe, Rohan, and Calderon, A.L., 1998, Australian and western Pacific porphyry Cu-Au deposits—Exploration model: AGSO Journal of Australian Geology and Geophysics, v. 17, no. 4, p. 97–104.

Cox, D.P., 1986a, Descriptive model of porphyry Cu (model 17), *in* Cox, D.P. and Singer, D.A., eds., Mineral deposit models: U.S. Geological Survey Bulletin 1693, p. 76.

Cox, D.P., 1986b, Descriptive model of porphyry Cu-Au (model 20c), *in* Cox, D.P. and Singer, D.A., eds., Mineral deposit models: U.S. Geological Survey Bulletin 1693, p. 110.

Cox, D.P., 1986c, Descriptive model of porphyry Cu-Mo (model 21a), *in* Cox, D.P., and Singer, D.A., eds., Mineral deposit models: U.S. Geological Survey Bulletin 1693, p. 115.

Crawford, A.J., Cameron, W.E. and Keays, R.R., 1984, The association boninite-low-Ti andesite-tholeiite in the Heathcote Greenstone Belt, Victoria—Ensimatic setting for the Early Lachlan Fold belt: Australian Journal of Earth Sciences, v. 31, p. 161–177.

Crawford, A.J., Meffre, S., and Symonds, P.A., 2003, 120 to 0 Ma tectonic evolution of the southwest Pacific and analogous geological evolution of the 600 to 220 Ma Tasman fold belt system: Geological Society of Australia, Special Publication 22, and Geological Society of America Special Paper 372, p. 383–403.

Crawford, A.J., Stevens, B.P.J., and Fanning, M., 1997, Geochemistry and tectonic setting of some Neoproterozoic and Early Cambrian volcanics in western New South Wales: Australian Journal of Earth Sciences, v. 44, 831–852.

Duval, J.S., 2012, Version 3.0 of EMINERS— Economic Mineral Resource Simulator: U.S. Geological Survey Open-File Report 2004–1344, available at http://pubs.usgs.gov/of/2004/1344/.

Ewers, G.R., Evans, N., and Hazell, M., (Kilgour, B., compiler), 2002, OZMIN Mineral Deposit Database [Digital GIS Dataset]: Canberra, Geoscience Australia, accessed 2010 at http://www.ga.gov.au/meta/ANZCW0703003393.html.

Foden, J.D., Elburg, M.A., Dougherty-Page, J., and Burtt, A., 2006, The timing and duration of the Delamerian Orogeny—Correlation with the Ross Orogen and implications for Gondwana assembly: The Journal of Geology, v. 114, p. 189–210.

Foden, J.D., Elburg, M.A., Turner, S.P., Sandiford, M., O'Callaghan, J., and Mitchell, S., 2002, Granite production in the Delamerian orogen, South Australia: Journal of the Geological Society of London, Lyell Collection, v. 159, p. 557–575.

Foster, D.A., Gray, D.R., and Spaggiari, C., 2005, Timing of subduction and exhumation along the Cambrian east Gondwana margin, and the formation of Paleozoic backarc basins: Geological Society of America Bulletin, v. 117, p. 105–116.

Geoscience Australia, 2004, Fourth edition total magnetic anomaly (TMI) grids of Australia: Canberra, Geoscience Australia, accessed May 19, 2010, at http://www.geoscience.gov.au/.

Geoscience Australia, 2005–2009, Australian mineral exploration, a review of exploration for the years 2005 to 2009: Canberra, Geoscience Australia, accessed May 25, 2010, at http://www.geoscience.gov.au/.

Geoscience Australia, 2009, Australian national gravity database 0.5 minute offshore-onshore gravity grid: Canberra, Geoscience Australia, accessed May 19, 2010, at http://www.geoscience.gov.au/.

Geoscience Australia, 2010, Australian atlas of mines and mineral deposits: Canberra, Geoscience Australia, accessed October 20, 2010, to December 27, 2010, at http://www.australianminesatlas.gov.au/.

Glen, R.A., 2005, The Tasmanides of eastern Australia, *in* Vaughan, A.P.M., Leat, P.T., and Pankhurst, R.J., eds., Terrane Processes at the Margins of Gondwana: Geological Society of London, Special Publications, v. 246, p. 23–96.

Greenfield, J.E., Musgrave, R.J., Bruce, M.C., Gilmore, P.J., and Mills, K.J., 2011, The Mount Wright arc—A Cambrian subduction system developed on the continental margin of east Gondwana, Koonenberry belt, eastern Australia: Gondwana Research, v. 19, p. 650–669.

Intierra, 2009, Intierra home page: accessed December 10, 2010, at http://www.intierra.com/Homepage.aspx/.

Jaireth, S., and Miezitis, Y., 2004a, Porphyry copper-gold, *in* Jaireth, Subhash, and Miezitis, Yanis, compilers, OZPOT Geoprovince-scale assessment of mineral potential [1:2,500,000 scale GIS]: Canberra, Geoscience Australia, product description accessed 2010 at http://www.australianminesatlas.gov.au/build/common/minpot.html.

Jaireth, S., and Miezitis, Y., 2004b, OZPOT Geoprovince-scale assessment of mineral potential [1:2,500,000 scale GIS]: Canberra, Geoscience Australia, product description accessed 2010 at http://www.australianminesatlas.gov.au/build/common/minpot.html.

John, D.A., Ayuso, R.A., Barton, M.D., Blakely, R.J., Bodnar, R.J., Dilles, J.H., Gray, Floyd, Graybeal, F.T., Mars, J.C., McPhee, D.K., Seal, R.R., Taylor, R.D., and Vikre, P.G., 2010, Porphyry copper deposit model, chapter B *of* Mineral deposit models for resource assessment: U.S. Geological Survey Scientific Investigations Report 2010–5070–B, 169 p., accessed January 15, 2011, at http://pubs.usgs.gov/sir/2010/5070/b/.

Morris, B.J., 1979, Porphyry style copper/molybdenum mineralization at Anabama Hill: Mineral Resources Review, South Australia, no. 150, p. 5–24.

Noble, R.R.P., Dugdale, J., Mele, S., and Scott, K.M., 1980, The Stawell Au deposits, western Victoria, *in* Butt, C.R.M., and Smith, R.E., Conceptual models in Exploration Geochemistry, 4: Australia—Cooperative Research Centre for Landscape Environments and Mineral Exploration (CRC LEME), 4 p., accessed 2012 at http://crcleme.org.au/RegExpOre/Stawell.pdf.

NSW Industry and Investment, 2010, Advanced mineral projects and exploration highlights in New South Wales: New South Wales Government, Department of Industry and Investment, New Frontiers, accessed 2010 at http://www.industry.nsw.gov.au/.

Page, N.J, 1986, Descriptive model of synorogenic-synvolcanic Ni-Cu, *in* Cox, D.P. and Singer, D.A., eds., Mineral deposit models: U.S. Geological Survey Bulletin 1693, p. 28.

Panteleyev, A., 1995a, Porphyry Cu±Mo±Au (model L04), *in* Lefebure, D.V., and Ray, G.E., eds., Selected British Columbia mineral deposit profiles, vol. 1—Metallics and coal: British Columbia Ministry of Energy of Employment and Investment, Energy and Minerals Division, Open File 1995–20, p. 87–92, accessed April 5, 2012, at http://www.empr.gov.bc.ca/Mining/Geoscience/MineralDepositProfiles/.

Panteleyev, A., 1995b, Porphyry Cu-Au—Alkalic (model L03), *in* Lefebure, D.V., and Ray, G.E., eds., Selected British Columbia mineral deposit profiles, vol. 1—Metallics and coal: British Columbia Ministry of Employment and Investment, Energy and Minerals Division, Open File 1995–20, p. 83–86, accessed April 5, 2012, at http://www.empr.gov.bc.ca/Mining/Geoscience/MineralDepositProfiles/.

Panteleyev, A., 2005a, Porphyry Cu±Mo±Au L04., *in* Fonseca, A., and Bradshaw, G., compilers, Yukon mineral deposits profiles: Yukon Geological Survey Open File 2005–5, 175 p., accessed July 28, 2009, at http://www.geology.gov.yk.ca/mineral_deposit_profiles.html; http://ygsftp.gov.yk.ca/publications/openfile/2005/of2005_5.pdf; http://www.geology.gov.yk.ca/pdf/l04_porphyry_cu_mo_au.pdf.

Panteleyev, A., 2005b, Porphyry Cu-Au—Alkalic L03., *in* Fonseca, A., and Bradshaw, G., compilers, Yukon mineral deposits profiles: Yukon Geological Survey Open File 2005–5, 175 p., accessed July 28, 2009, at http://www.geology.gov.yk.ca/mineral_deposit_profiles.html; http://ygsftp.gov.yk.ca/publications/openfile/2005/of2005_5.pdf; http://www.geology.gov.yk.ca/pdf/l03_alkalic_porphyry_cu_au.pdf.

Preiss, W.V., 2000, The Adelaide geosyncline of South Australia and its significance in Neoproterozoic continental reconstruction: Precambrian Research, v. 100, p. 21–63.

Primary Industries and Resources South Australia (PIRSA), 2010, Copper [Digital Dataset]: Government of South Australia, accessed 2010 at http://pir.sa.gov.au/minerals/geology/minerals_mines_and_quarries/commodities/.

Radojkovic, A., 2003, Thursdays porphyry copper prospect, western Victoria, *in* Butt, C.R.M, Cornelius, M., Scott, K.M., and Robertson, I.D.M., Regolith Expression of Australian Ore Systems—A compilation of geochemical case histories and conceptual models: Cooperative Research Centre for Landscape Environments and Mineral Exploration (CRC LEME), 3 p., accessed February 16, 2011, at http://crcleme.org.au/RegExpOre/ThursdaysGossan.pdf

Rajagopalan, S., 1999, Thursdays Gossan prospect, *in* Willocks, A.J., Haydon, S.J., Asten, M.W., and Moore, D.H., eds., Geology and geophysical exploration of base metals in Victoria: Geological Survey of Victoria, GSV Report 119, p. 129–135.

Raymond, O.L., Liu, S.F., and Kilgour, P., 2007, Surface geology of Australia, 1:1,000,000 scale, Tasmania, 3rd edition [Digital Dataset]: Canberra, Geoscience Australia, accessed May 9, 2010, at http://www.ga.gov.au/.

Raymond, O.L., Liu, S.F., Kilgour, P., Retter, A.J., and Connolly, D.P., 2007, Surface geology of Australia, 1:1,000,000 scale, Victoria, 3rd edition [Digital Dataset]: Canberra, Geoscience Australia, accessed May 9, 2010, at http://www.ga.gov.au/.

Raymond, O.L., Liu, S.F., Kilgour, P., Retter, A.J., Stewart, A.J., and Stewart, G., 2007, Surface geology of Australia, 1:1,000,000 scale, New South Wales, 2nd edition [Digital Dataset]: Canberra, Geoscience Australia, accessed May 9, 2010, at http://www.ga.gov.au/.

Root, D.H., Menzie, W.D., and Scott, W.A., 1992, Computer Monte Carlo simulation in quantitative resource estimation: Natural Resources Research, v. 1, no. 2, p. 125–138.

Scotese, C.R., 2002, Paleomap project: accessed January 12, 2012, at http://www.scotese.com/.

Seccombe, P.K., Spry, P.G., Both, R.A., Jones, M.T., and Schiller, J.C., 1985, Base metal mineralization in the Kanmantoo Group, South Australia—A regional sulfur isotope study: Economic Geology, v. 80, p. 1824–1841.

Singer, D.A., Berger, V.I., and Moring, B.C., 2008, Porphyry copper deposits of the world—Database and grade and tonnage models, 2008: U.S. Geological Survey Open-File Report 2008–1155, 45 p., available at http://pubs.usgs.gov/of/2008/1155/.

Singer, D.A., and Menzie, W.D., 2005, Statistical guides to estimating the number of undiscovered mineral deposits—An example with porphyry copper deposits, *in* Cheng, Qiuming, and Bonham-Carter, Graeme, eds., Proceedings of IAMG—The annual conference of the International Association for Mathematical Geology: Toronto, Canada, Geomatics Research Laboratory, York University, p. 1028–1033.

South Australian Resources Information Geoserver (SARIG), 2010, Mineral deposit information: accessed November, 2010 at http://egate.pir.sa.gov.au/minerals/.

U.S. Department of State, 2009, Small-scale digital international land boundaries (SSIB)—Lines, edition 10, and polygons, beta edition1, *in* Boundaries and Sovereignty Encyclopedia (B.A.S.E.): U.S. Department of State, Office of the Geographer and Global Issues.

Whitaker, A.J., Champion, D.C., Sweet, I.P., Kilgour, P., and Connolly, D.P., 2007, Surface geology of Australia 1:1,000,000 scale, Queensland [Digital Dataset]: Canberra, Geoscience Australia, accessed May 9, 2010, at http://www.ga.gov.au/.

Whitaker, A.J., Glanville, H.D., English, P.M., Stewart, A.J., Retter, A.J., Connolly, D.P., Stewart, G.A., and Fisher, C.L., 2008, Surface geology of Australia 1:1,000,000 scale, South Australia [Digital Dataset]: Canberra, Geoscience Australia, accessed May 9, 2010, at http://www.ga.gov.au/.

Appendix C. Porphyry Copper Assessment for Tract 009pCu8002, Macquarie, Australia

By Arthur A. Bookstrom[1], Richard A. Glen[2], Jane M. Hammarstrom[3], Gilpin R. Robinson, Jr.[3], and Michael L. Zientek[1]

Deposit Type Assessed

Deposit type: Porphyry Cu-Au

Descriptive models: Porphyry Cu-Au (Cox, 1986a), porphyry Cu-Au (Panteleyev, 1995a and 2005a), porphyry Cu-Au (Cooke and others, 1998), porphyry Cu-Au (Jaireth and Miezitis, 2004a), porphyry copper (Cox, 1986b), porphyry Cu ± Mo ± Au (Panteleyev, 1995b and 2005b), and porphyry copper (John and others, 2010)

Grade and tonnage model: Porphyry Cu-Au (Singer and others, 2008)
Table C1 summarizes selected assessment results.

Table C1. Summary of selected resource assessment results, Macquarie tract (009pCu8002), New South Wales, Australia.

[km, kilometers; km^2, square kilometers; t, metric tons]

Date of assessment	Assessment depth (km)	Tract area (km^2)	Known copper resources (t)	Mean estimate of undiscovered copper resources (t)	Median estimate of undiscovered copper resources (t)
September 2010	1	41,463	13,000,000	21,000,000	13,000,000

Location

The Macquarie tract is in southeastern Australia, west of Sydney and north of Canberra, in eastern New South Wales (fig. C1).

Geologic Feature Assessed

Igneous rocks of the Macquarie Arc, an accreted island-arc complex of Ordovician to Early Silurian age.

[1]U.S. Geological Survey, Spokane, Washington, United States.

[2]Geological Survey of New South Wales, Hunter Region Mail Centre, New South Wales, Australia.

[3]U.S. Geological Survey, Reston, Virginia, United States.

Delineation of the Permissive Tract

The fundamental feature that defines the Macquarie tract is the Macquarie Arc, an accreted oceanic volcanic-arc complex of Ordovician to Early Silurian age. Figure C2 shows the areal extent of the Macquarie Arc, as indicated by mapped exposures (after Raymond, Liu, Kilgour, Retter, Stewart, and Stewart, 2007) and inferred from aeromagnetic anomalies (after Glen, Crawford, and Cooke, 2007).

Macquarie Arc

The Macquarie Arc is in the Lachlan Orogen, west of the Sydney Basin (fig. C2). Volcanic, volcaniclastic, and minor intrusive rocks of the Macquarie Arc are exposed in north-trending and structurally bounded volcanic belts. From the west, these are the Junee-Narromine Volcanic Belt, the Kiandra Volcanic Belt, the Molong Volcanic Belt, and the Rockley-Gulgong Volcanic Belt. The eastern margin of the Macquarie Arc is partly covered by Permian strata of the Sydney Basin, and its northern part is mostly covered by Mesozoic to Cenozoic strata of the Great Artesian Basin (fig. C2).

The exposed part of the Macquarie Arc consists mostly of volcanic and volcaniclastic rocks, interlayered sedimentary rocks, and relatively small intrusions. As shown in figure C3, the ratio of mapped volcanic (v) to intrusive (i) rocks is very high (79v/1i). Volcanic rock types include basalt to andesite, trachyandesite, latite, and trachyte lavas. Volcaniclastic rocks include breccia, tuff, and volcanic-derived sedimentary rocks. Interlayered sedimentary strata include sandstone, siltstone,

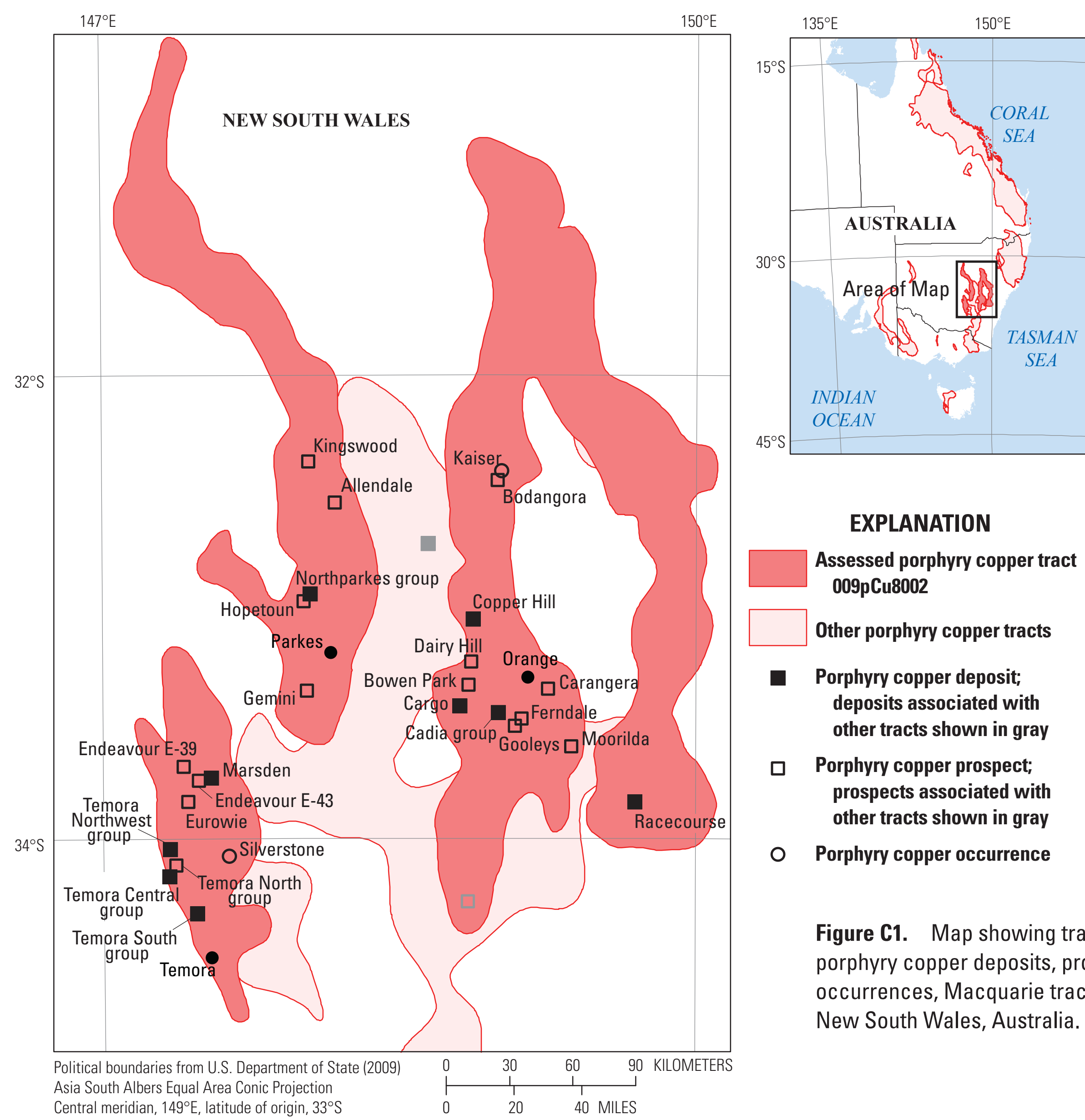

Figure C1. Map showing tract location and porphyry copper deposits, prospects, and occurrences, Macquarie tract (009pCu8002), New South Wales, Australia.

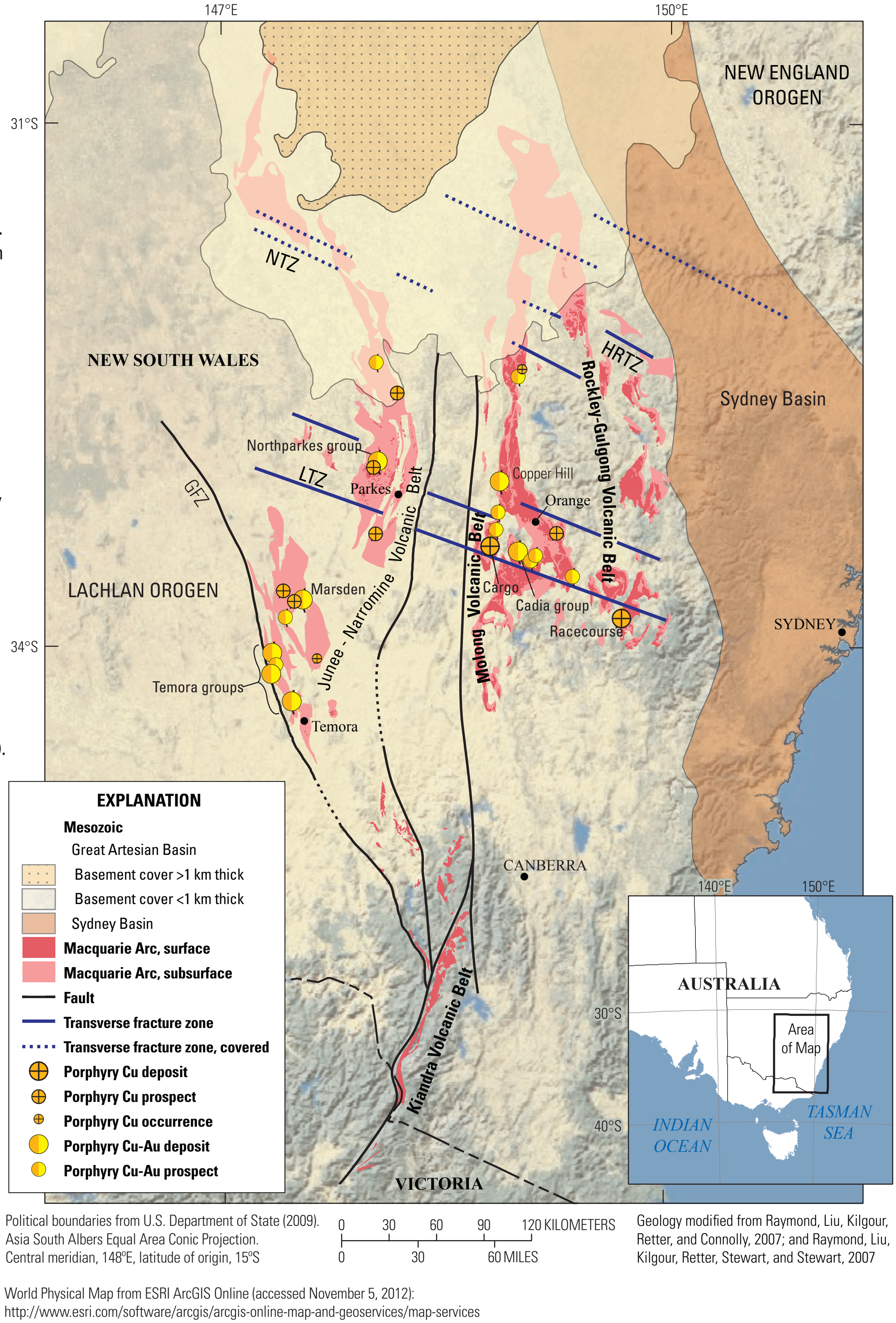

Figure C2. Map showing geologic setting and distribution of porphyry copper deposits, prospects, and occurrences for the Macquarie tract (009pCu8002), New South Wales, Australia. The surface expression of the Macquarie Arc is defined by mapped volcanic and intrusive rocks of Ordovician to Early Silurian age. The subsurface expression of the Macquarie Arc, as inferred from geologic maps and aeromagnetic-anomaly patterns, is from Glen, Crawford, and Cooke (2007). GFZ, Gilmore Fault (or Suture) Zone; HRTZ, Hunter River Transverse Zone; LTZ, Lachlan Transverse Zone; NTZ, Nyngan Transverse Zone (after Glen and Walshe, 1999).

shale, and limestone. Minor intrusive rocks include gabbro, monzodiorite, diorite, monzonite, quartz monzonite, and syenite (table C2).

Most major porphyry Cu-Au deposits in the Macquarie Arc are associated with monzonitic to quartz monzonitic intrusions of latest Ordovician to Early Silurian age (447–433 Ma). However, a few porphyry copper sites are associated with intrusions of tonalitic to granodioritic composition. Such intrusions are too small to be mapped at 1:1,000,000 scale and are not listed in table C2.

According to Percival and Glen (2007), Ordovician to Early Silurian igneous rocks of the Kiandra, Junee-Narromine, Molong, and Rockley-Gulgong Volcanic Belts formed during four successive phases of magmatism. Correlation of these phases between volcanic belts supports the conclusion that these four volcanic belts were once contiguous parts of a single Macquarie Arc.

A tectonic reconstruction by Glen and others (2009) shows the Macquarie Arc was tectonically inserted between two meta-turbidite terranes. This geometry “requires either rifting or orogen-parallel, strike-slip duplication” of the metasedimentary terranes that are east and west of the Macquarie Arc. Amalgamation of these terranes probably occurred during the Benambran Orogeny, in Late Ordovician to earliest Silurian time. These amalgamated terranes were later accreted to the continental margin, and the Macquarie Arc was tectonically fragmented to form the Junee-Naromine, Kiandra, Molong, and Rockley-Gulgong Volcanic Belts during the Tabberabberan Orogeny, in Late Silurian to Middle Devonian time.

Magmatism and Metallogenesis in the Macquarie Arc

Glen, Meffre, and Scott (2007, p. 405) suggested that the Macquarie Arc formed above a west-dipping subduction zone in the proto-Pacific Ocean. According to Glen, Crawford, and others (2007, p. 167), the earliest magmatism in the Macquarie Arc was dominated by high-K calc-alkaline to shoshonitic basalt, basaltic andesite, and andesite. Age corrected εNd values of lavas range from +6.2 to +7.8, indicating an “absence of any old continental crustal component.” Meffre and others (2007) showed that the Macquarie Arc is generally not conformable with neighboring Ordovician turbidites, but is bounded by major faults.

Despite the Early Paleozoic age of the Macquarie Arc, volcanic belts of the Macquarie Arc are characterized by moderate dips, sub-greenschist to lower-greenschist metamorphic facies, and preservation of late-stage shallowly emplaced porphyries and associated porphyry Cu-Au deposits.

According to Crawford, Meffre, and others (2007), Early Ordovician volcanic rocks of phase 1 of Macquarie Arc magmatism (~490–474 Ma) are mainly high-K calc-alkaline volcanics, overlain by conglomerate and siltstone in the Junee-Narromine and Kiandra Volcanic Belts. According to Glen (2009, p. 208–209), “Phase 2 began in the latest Middle Ordovician (~466–457/4 Ma) and was terminated by local uplift and erosion. It is capped by a widespread 456–450 Ma carbonate platform that overlaps in age with the Phase 3 dacites.”

Phase 3 of Macquarie Arc magmatism (~456–443 Ma) produced the calc-alkalic Copper Hill Suite of tonalitic to granodioritic and dacitic intrusions. According to Percival and Glen (2007), ages of most rocks in the Copper Hill Suite cluster around 451–448 Ma. Such intrusions are associated with the calc-alkalic Copper Hill porphyry Cu-Au deposit in the Molong Volcanic Belt and the Marsden porphyry Cu-Au deposit (447 Ma) in the Junee-Narromine Volcanic Belt (fig. C2).

Phase 4 magmatism comprises a Late Ordovician volcanic phase and an Early Silurian intrusive phase. Shoshonitic volcanic rocks include the Late Ordovician Goonumbla Volcanics in the Junee-Narromine Volcanic Belt, the Forest Reefs Volcanics and Junction Reefs Monzodiorite in the Molong Volcanic Belt, and the upper Sofala Volcanics in the Rockley-Gulgong Belt.

Early Silurian intrusions emplaced during late phase 4 magmatism (mostly 440–435 Ma) include (1) shoshonitic to high-K calc-alkaline intrusions associated with porphyry Cu-Au deposits of the Goonumbla Complex (~440 Ma), (2) shoshonitic intrusions associated with the giant Cadia composite porphyry Cu-Au deposit (~440–437 Ma), and (3) high-K calc-alkaline intrusions associated with porphyry Cu-Au deposits in the Temora area (~436 Ma), as recorded in appendix F.

Phase 4 intrusions also are associated with the Big and Little Cadia Cu-Au skarns, Junction Reefs Monzodiorite-related skarns and Comobella skarns, and with low-sulfidation epithermal Au-Ag deposits near the Cowal Mine (fig. C2). High-sulfidation epithermal Au-Ag deposits in and near the Macquarie Arc yield age determinations that range from 446 to 401 Ma (as determined by a variety of methods cited in appendix F).

Squire and Crawford (2007, p. 293) likened shoshonitic rocks of Macquarie phase 4 to Pliocene shoshonitic rocks of the Tavua Caldera in Fiji. There, such rocks “were emplaced following arc magmatism when the arc moved into an extensional phase.” They suggested that “pre-processing of the mantle above a subduction zone prior to extension and fragmentation of arc lithosphere” led to “generation of subduction-modified shoshonite magmas.” Richards (2009, p. 249) suggested further that “Porphyry- and epithermal-style mineral deposits associated with postsubduction magmatism are Au-rich relative to many arc-related deposits, a characteristic that may reflect remelting of small amounts of residual sulfide left in the deep lithosphere by arc magmatism.”

The Cadia and Northparkes Cu-Au deposits are aligned along the Lachlan Transverse Zone (LTZ, fig. C2) of Glen and Walshe (1999). Corbett and Leach (1998) interpreted west-northwest-oriented swarms of fractures as transtensional fault jogs, splays, and pull-apart grabens. Harris and others (2010) showed that porphyry Cu-Au deposits of the Cadia group of deposits are localized within a west-northwest-trending half-graben, interpreted as a pull-apart graben. Inasmuch as

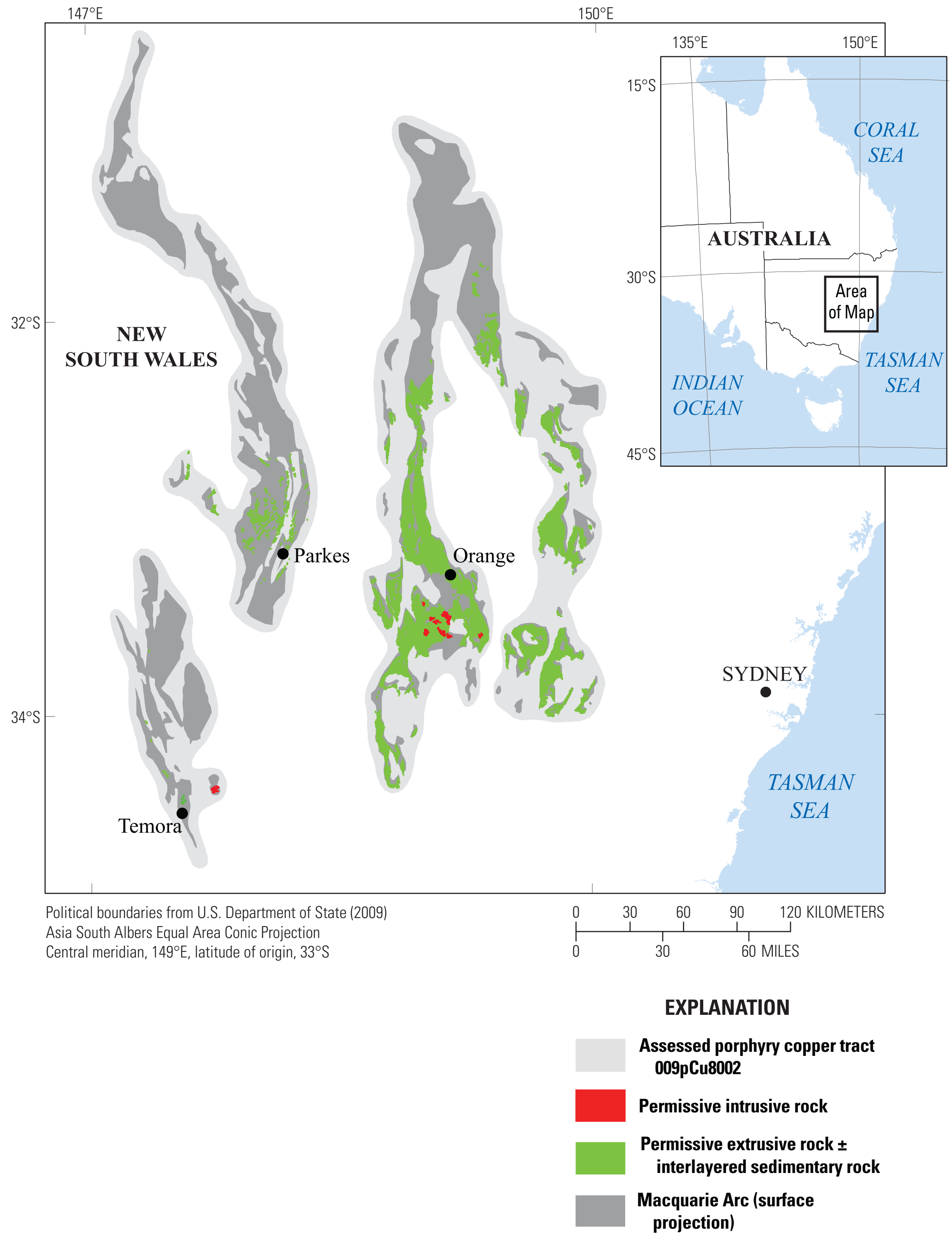

Figure C3. Map showing areas of permissive intrusive and extrusive rocks assigned to the Macquarie permissive tract (009pCu8002), New South Wales, Australia. The subsurface expression of the Macquarie Arc, as inferred from geologic maps and aeromagnetic-anomaly patterns, is from Glen, Crawford, and Cooke (2007).

Table C2. Map units that define the Macquarie tract (009pCu8002), New South Wales, Australia.

[Based on Raymond, Liu, Kilgour, Retter, Stewart, and Stewart (2007) and Glen, Crawford, and Cooke (2007); for additional information about named map units, see Geoscience Australia, Stratigraphic Units Database at http://dbforms.ga.gov.au/www/geodx.strat_units.int/]

Map unit	Map symbol	Lithology	Age range
		Intrusive rocks	
Specimen Hill Gabbroic Diorite	Sdsm	gabbroic diorite, noritic gabbro, quartz-hornblende diorite	Early Silurian
Cadia Hill Monzonite	Ogch	monzonite, monzodiorite, orthoclase porphyry	Late Ordovician
Errowan Monzonite	Oger	monzonite, syenite	Late Ordovician
Glen Ayr Syenite	Ogga	monzonite, syenite	Late Ordovician
Moorilda Monzonite	Ogmm	monzonite, syenite	Late Ordovician
Tallwood Monzodiorite	Ogtw	porphyritic monzonite, diorite	Late Ordovician
Tettenhall Monzodiorite	Ogte	porphyritic monzonite, diorite	Late Ordovician
Stokefield Metagabbro	Odst	metagabbro, plagioclase-phyric	Middle to Late Ordovician
		Volcanic rocks	
Coomber Formation	Ojcc	basalt, dolerite, gabbro and diorite sills or lavas, volcaniclastic sedimentary rocks	Late Ordovician to Early Silurian
Cowal Igneous Complex	Owl	intermed to mafic volcanic, volcaniclastic sedimentary rocks, and igneous intrusions	Late Ordovician to Early Silurian
Gidginbung Volcanics	Owlg	andesite, trachyandesite, chert, breccia	Late Ordovician to Early Silurian
Kenyu Formation	Owkk	andesite, tuff, siltstone, shale, limestone	Late Ordovician to Early Silurian
Temora Volcanics	Oatm	andesite, trachyandesite, latite, basaltic andesite	Late Ordovician to Early Silurian
Burranah Formation	Owcu	latite, basalt, andesitic volcanic and intrusive rocks, sedimentary rocks	Late Ordovician
Byng Volcanics	Owcy	basalt, volcaniclastic sedimentary rocks	Late Ordovician
Cheesemans Creek Formation	Owcc	basaltic andesite, mafic latite, quartz latite, volcaniclastic sedimentary rocks	Late Ordovician
Northparkes Volcanic Group	Own	andesite, basalt, trachyte lavas, volcanic breccias, monzonitic intrusions, sedimentary rocks	Late Ordovician
Oakdale Formation	Owco	basalt, basaltic andesite, latite lavas and intrusions, volcaniclastic sedimentary rocks	Late Ordovician
Raggatt Volcanics	Oarv	andesite lavas, volcaniclastic sedimentary rocks	Late Ordovician
Rockley Volcanics	Owcr	mafic schists, andesite, peridotite, pyroxenite, volcaniclastic sedimentary rocks	Late Ordovician
Sofala Volcanics	Owcs	basalt, andesite, volcaniclastic sedimentary rocks, chert	Late Ordovician
Tucklan Formation	Owct	basalt, andesite, dolerite, latite, volcaniclastic sedimentary rocks	Late Ordovician
Forest Reefs Volcanics (Subgroup)	Owcf	basalt, trachybasalt, latite, sandstone, siltstone, conglomerate, chert limestone	Middle Ordovician to Early Silurian
Blayney Volcanics	Owcb	clinopyroxene basalt, volcaniclastic sedimentary rocks	Middle to Late Ordovician
Fairbridge Volcanics	Owkf	basaltic, andesitic, latitic volcanics, tuff, sandstone, conglomerate, siltstone, limestone	Middle to Late Ordovician
Narrugudgil Volcanics	Obna	andesite, gabbro, diorite (greenstone to amphibolite metamorphic facies)	Middle to Late Ordovician
Walli Volcanics	Owkw	plagioclase basalt, volcaniclastic sandstone, conglomerate	Middle Ordovician
Nelungaloo Volcanics, Yarrimbah Fm	Owuy	basalt to andesite lavas, volcaniclastic conglomerate, arkose, sandstone, siltstone	Early Ordovician

west-northwest-trending fractures of the Lachlan Transverse Zone cut Ordovician rocks but host Early Silurian porphyry Cu-Au systems, these fractures must have formed during the Late Ordovician-Early Silurian Benambran Orogeny.

Permissive Igneous Rocks and Map Units of the Macquarie Arc

Cooke and others (1998) listed the following geologic criteria for identification of permissive areas for porphyry Cu-Au deposits in Australia and the western Pacific:

1. Volcanic and volcaniclastic country rocks in island-arc tectonic settings,
2. Oxidized I-type intrusive porphyries,
3. Known porphyry Cu-Au systems, indicating permissive levels of exposure,
4. Intersections of arc-parallel and arc-oblique structures to localize porphyry Cu-Au deposits, and
5. Minor clastic sediments ± limestones to host Cu-Au skarn deposits.

The geology of the Macquarie Arc meets all of these criteria for identification of permissive areas for porphyry Cu-Au deposits. It also is one of the areas on which these criteria were based.

The descriptive model for porphyry Cu-Au deposits by Cox (1986a) indicates that such deposits are associated with intrusions of tonalitic to monzogranitic, or monzonitic to syenitic, composition. The descriptive model for alkalic porphyry Cu-Au deposits by Panteleyev (1995a) more specifically indicates that such deposits are associated with intrusions of gabbro, diorite, monzodiorite, monzonite, syenite and foidal syenite, or their microcrystalline to porphyro-aphanitic equivalents, including basalt, andesite, trachyandesite, latite, trachyte, and foidal trachyte.

Most of the porphyry copper deposits and prospects in the Macquarie tract are alkalic porphyry Cu-Au deposits, associated with generally monzonitic intrusions. On a triangular quartz-alkali feldspar-plagioclase (QAP) diagram (after Le Maitre, 2002), compositions of mesoscopically crystalline rocks of the porphyry Cu-Au-related intrusions of the Cadia and Northparkes areas are mostly in the fields of monzodiorite, monzonite, quartz monzodiorite, and quartz monzonite. Nevertheless, intrusions of gabbro, diorite, quartz syenite, and monzogranite also occur in association with some of these deposits (Blevin, 2002).

On a total alkali-silica (TAS) diagram (after Le Maitre and others, 2002), predominantly aphanitic rocks of the Cadia and Goonumbla complexes span the compositional fields of trachybasalt, basaltic trachyandesite, trachyandesite, and trachyte (Blevin, 2002). This reflects increasing total alkalis ($Na_2O + K_2O$) with increasing silica (SiO_2), from about 6.5 weight percent of alkalis at 50 weight percent of silica to about 11 weight percent of alkalis at 65 weight percent of silica. Some synmineral potassic quartz monzonite porphyry and post-mineral aplites in the Northparkes porphyry Cu-Au system contain over 70 weight percent of silica and plot in the rhyolite field of the TAS diagram (Lickfold and others, 2007).

Blevin (2002) found that mineralized igneous complexes of porphyry Cu-Au systems (of the Macquarie Arc) in the Lachlan Fold Belt vary from quartz-poor, high-K to ‘shoshonitic’ monzodioritic to monzonitic complexes (in the Cadia and Northparkes groups of deposits, for example) to quartz-rich, medium-K dacites (at Copper Hill, for example). According to Blevin (2002, p. 87), these igneous suites have high K/Rb ratios, “low mantle-compatible element abundances, and marked depletions in Ti, Nb and Ta, which is consistent with a subduction-related tectonic setting.”

Blevin (2002) also found that magnetite is the dominant Fe-Ti oxide phase, that Fe_2O_3/FeO ratios are high, and that magmatic biotite is Mg-rich in igneous suites associated with porphyry Cu-Au deposits of the Macquarie Arc. These characteristics indicate high magmatic oxidation states, which favor retention and concentration of copper and gold in residual magma during fractional crystallization (Blevin and others, 1996).

Porphyry copper deposits generally are associated with porphyryitic intrusions characterized by phenocrysts in a microcrystalline to aplitic groundmass. However, such rocks commonly occur below (or are intrusive into) widespread bodies of volcanic rocks, and above (or are intrusive into) bodies of coarser-grained plutonic rocks of similar age and composition. Therefore, rocks of appropriate composition and age are considered permissive, whether or not they are intrusive porphyries. However, gabbro and basalt are considered permissive only where they occur with other permissive rock types in a setting interpreted to represent subduction-related magmatism.

Geologic map units included in Macquarie tract (009pCu8002) are listed in table C2. Any geologic map unit that represents a lithologic assemblage that is of Ordovician to Silurian age and contains any of the permissive rock types listed above is considered permissive. All areas that represent such a map unit are therefore included in the Macquarie tract (fig. C3).

Igneous rocks of the Kiandra Volcanic Belt are almost entirely volcanic and formed during phase 1 and early phase 2 volcanism on the southwestern flank of the Macquarie Arc. No known porphyry Cu-Au sites are related to volcanic rocks of phases 1 and 2 in the Kiandra Volcanic Belt.

Subsurface Extension of Permissive-Tract Boundaries

I-type igneous rocks of the magnetite series generally are ferromagnetic and can therefore be detected by magnetic surveys, according to Clark (1999). Consequently, reduced-to-pole aeromagnetic maps can be interpreted to indicate subsurface extensions of permissive bodies of I-type igneous rocks of the magnetite series. Glen, Dawson, and Colquhoun (2006, 2007) interpreted mapped exposures, drill intercepts, and magnetic anomaly patterns to indicate surface and subsurface expressions of the Macquarie volcanic belts. A small-scale version of their map of the Junee-Narromine, Molong, Rockley Gulgong, and Kiandra Volcanic Belts was published by Glen, Crawford, and Cooke (2007).

We geo-registered the small-scale map of the Macquarie volcanic belts by Glen, Crawford, and Cooke (2007) to the 1:1,000,000-scale geologic map of New South Wales and used these two maps to delineate the surface and subsurface expressions of the Macquarie Arc. To insure inclusion of permissive rocks beneath outward-dipping structural contacts to a depth of 1 km, we added a 3-km buffer. Figure C2 shows mapped surface expressions of the Macquarie Arc in red. Subsurface expressions of the Macquarie Arc, interpreted from buffered aeromagnetic anomalies (as described above), are shown in pink.

According to a depth-to-basement contour map by Hind and Helby (1969), the northern ends of the Junee-Narromine and Molong Volcanic Belts are covered. However, depth to basement probably is 1 km in areas underlain by volcanic belts of the Macquarie Arc.

Known Deposits

Known porphyry Cu-Au deposits of the Macquarie Arc tend to be clustered. Where they are grouped according to the 2-km rule of Singer and others (2005), we refer to them as deposit groups, and we aggregate their resources for purposes of grade-tonnage and spatial-density modeling. The Cadia group of deposits includes at least five individual porphyry Cu-Au deposits and two skarn Cu-Au deposits. The Northparkes group of deposits includes at least four porphyry Cu-Au deposits. Temora central group of porphyry copper sites includes three known deposits and several prospects. Two other deposits in the Temora area are grouped with nearby porphyry copper prospects.

Figure C1 shows the location of each known deposit or group of deposits in the Macquarie tract. Table C3 lists tonnages of ore, average grades, and tonnages of copper contained in known porphyry Cu-Au deposits in the Macquarie tract. It also lists total resources of groups of deposits.

Cadia Group of Porphyry Cu-Au and Skarn Cu-Au Deposits

The giant Cadia group of porphyry Cu-Au and skarn Cu-Au deposits is in the Cadia mining district located in the Molong Volcanic Belt, about 20 km southwest of Orange, New South Wales. For consistency in modeling of grade, tonnage, and spatial density of deposits, known deposits of the Cadia group of deposits are grouped, and their resources aggregated according to the 2-km rule of Singer and others (2005). The Cadia group of at least five porphyry Cu-Au deposits and two porphyry skarn Cu-Au skarn deposits is now estimated to contain total resources of at least 9,550,000 t of copper and 1,510 t of gold (table C3 and appendix F). This qualifies the Cadia group of deposits as a world-class giant resource of both copper and gold, according to the criteria of Singer (1995). It amounts to about 71 percent of the copper and 89 percent of the gold in identified resources of known porphyry Cu-Au deposits in the Macquarie Arc.

At least five porphyry Cu-Au deposits and two porphyry-related Cu-Au skarn deposits are now known to occur in a northwest-southeast elongate area within the Lachlan Transverse Zone (LTZ) of northwest-trending shear zones and faults (fig. C2). According to Porter and Glen (2005, p. 287), the Cadia group of deposits is spatially associated with shoshonitic, porphyrytic monzodioritic to quartz monzonitic intrusions of Late Ordovician to Early Silurian age in the Cadia Intrusive Complex. Long sections of the Cadia Intrusive Complex by Harris and others (2010) and Wood (2012a, b) show a broad, composite central stock, dismembered by reverse faults, some of which splay upward into multiple thrust faults. At depths between about 2 and 3 km, the central stock of the Cadia Intrusive Complex widens downward to broad shoulders that extend to the northwest and southeast. Swarms of plugs and dikes in the Ridgeway and Cadia East deposits are interpreted as cupolas and apophyses that rose above the shoulders of the Cadia Intrusive Complex.

As shown in figure C4 (*A* and *B*), the Cadia group of deposits and their associated alteration zones are at least 5 km long and 1.7 km wide. The Cadia Hill and Cadia Quarry porphyry Cu-Au deposits are hosted in and around the Cadia Intrusive Complex, parts of which are exposed in the central part of the Cadia group. The deep Ridgeway porphyry Cu-Au deposit is about 1.5 km northwest of the Cadia Quarry deposit, and the shallow-to-deep Cadia East-to-Far East set of porphyry Cu-Au ore zones extends at least 2 km southeastward from the Cadia Hill deposit. The porphyry-related Big Cadia and Little Cadia skarn Cu-Au deposits are about 0.5 km northeast of the Cadia Intrusive Complex, where they are hosted in beds of limestone and calcareous sandstone, which strike northwest, and dip southeastward, toward the Cadia Intrusive Complex (fig. C5*A*).

According to Wood (2012a, b), the Cadia group of deposits has been prospected since 1851, and mined locally and intermittently on a small scale for copper-oxide, gold, and hematite-magnetite rock. However, it was not until 1992 that potential for a large porphyry Cu-Au system was recognized by geologists of Newcrest Mining Ltd. This recognition was based on their discovery of geochemical anomalies for copper and gold in a poorly exposed part of the Cadia Intrusive Complex, and their recognition of Cu-Au-bearing garnet-magnetite-hematite rocks at Big and Little Cadia as porphyry-related skarns, similar to those associated with the Ok Tedi porphyry Cu-Au deposit in Papua New Guinea (Wood, 2012a, b).

Chalcopyrite, native gold, and bornite are important ore minerals of the Cadia group of deposits. Wilson, Cooke, Harper, and Deyell (2007) noted that the Ridgeway and Cadia East deposits have bornite-rich cores surrounded by chalcopyrite-rich halos and peripheral pyritic zones. In

Table C3. Porphyry copper deposits in Macquarie tract (009pCu8002), New South Wales, Australia.

[Ma, million years; Mt, million metric tons; %, percent; t, metric ton; g/t, gram per metric ton; Cu-Au subtype, deposits that have Au/Mo ratios > 30 or average Au grades >0.2 g/t; NA; not applicable; contained Cu in metric tons is computed as tonnage (Mt × 1,000,000) × Cu grade (%) ÷ 100; -, no data. Group totals are reported as weighted averages]

Group	Name	Latitude	Longitude	Subtype	Age (Ma)	Tonnage (Mt)	Cu (%)	Mo (%)	Au (g/t)	Ag (g/t)	Contained Cu (t)	Reference
Cadia	Cadia East (underground)	-33.457	149.012	Cu-Au	437	2,348	0.285	-	0.43	0.47	6,690,000	Wilson, Cooke, Harper, and Deyell (2007), Wilson, Cooke, Stein, and others (2007), Cooke and others (2007), Geoscience Australia (2010)
Cadia	Cadia East (open pit)	-33.463	149.009	Cu-Au	437	300	0.37	-	-	-	1,110,000	Wilson and others (2003), Collett (2007), Cooke and others (2007), Wilson, Cooke, Stein, and others (2007), Geoscience Australia (2010)
Cadia	Ridgeway	-33.435	148.976	Cu-Au	456	154	0.385	-	0.73	0.81	593,000	Fredricksen (2006), Cooke and others (2007), Wilson, Cooke, Stein, and others (2007), Geoscience Australia (2010)
Cadia	Cadia Hill (open pit)	-33.457	148.996	Cu-Au	437	490.3	0.117	-	-	-	573,000	Holliday and others (2002), Fredricksen (2006), Cooke and others (2007), Wilson, Cooke, Stein, and others (2007), Geoscience Australia (2010)
Cadia	Cadia Far East	-33.461	149.016	Cu-Au	437	63	0.48	-	-	-	302,000	Wilson, Cooke, Harper, and Deyell (2007), Wilson, Cooke, Stein, and others (2007), Cooke and others (2007), Geoscience Australia (2010)
Cadia	Cadia Quarry	-33.448	148.992	Cu-Au	437	50	0.23	-	-	-	115,000	Cooke and others (2007), Wilson, Cooke, Stein, and others (2007), Geoscience Australia (2010)
Cadia	Big Cadia + Little Cadia (resources)	-33.440	148.990	Cu-Au skarn	437	42.3	0.398	-	-	-	168,000	Forster and others (2004), Holliday and others (2002), Cooke and others (2007), Wilson, Cooke, Harper, and Deyell (2007), Wilson, Cooke, Stein, and others (2007), Geoscience Australia (2010)
Cadia	Little Cadia (location only)	-33.459	149.015	Cu-Au skarn	-	-	-	-	-	-		Forster and others (2004), Holliday and others (2002), Cooke and others (2007), Wilson, Cooke, Stein, and others (2007)
Cadia	**total, Cadia**	**-33.457**	**148.997**	**Cu-Au**	**-**	**3,447.6**	**0.277**	**-**	**0.33**	**0.36**	**9,550,000**	Holliday and others (1999, 2002), Fredricksen (2006), Collett (2007), Cooke and others (2007), Wilson, Cooke, Stein, and others (2007), Crawford, Meffre, and others (2007), Glen, Crawford, and Cooke (2007)
Northparkes	Endeavour E-26	-32.907	148.033	Cu-Au	440	87.3	0.885	-	0.325	-	1,440,000	Heithersay and Walshe (1995), Cooke and others (2007), Perkins and others (1995), Ewers and others (2002), Geoscience Australia (2010)
Northparkes	Endeavour E-48	-32.920	148.045	Cu-Au	440	33.4	1.04	-	0.59	-	347,000	Perkins and others (1995), Hooper and others (1996), Lickfold and others (2003, 2007), Arundell (2004), Cooke and others (2007)
Northparkes	Endeavour E-22	-32.910	148.038	Cu-Au	440	18.6	0.71	-	0.61	-	132,000	Jones (1985), Perkins and others (1995), Lickfold and others (2003, 2007), Cooke and others (2007)
Northparkes	Endeavour E-27	-32.908	148.048	Cu-Au	440	14.4	0.71	-	0.73	-	102,000	Perkins and others (1995), Arundell (2004), Lickfold and others (2003, 2007), Cooke and others (2007), Geoscience Australia (2010)

Table C3. Porphyry copper deposits in Macquarie tract (009pCu8002), New South Wales, Australia.—Continued

Group	Name	Latitude	Longitude	Subtype	Age (Ma)	Tonnage (Mt)	Cu (%)	Mo (%)	Au (g/t)	Ag (g/t)	Contained Cu (t)	Reference
Northparkes	Endeavour E-37	-32.929	147.993	NA	440	6.8	0.66	-	0.02	-	44,900	Perkins and others (1995), Arundell (2004), Lickfold and others (2003, 2007), Cooke and others (2007), Geoscience Australia (2010)
Northparkes	Endeavour E-28	-32.933	148.048	NA	440	8.1	0.35	-	0.04	-	28,400	Cooke and others (2007), Perkins and others (1995)
Northparkes	Endeavour E-31N	-32.928	148.063	Cu-Au	440	6.6	0.35	-	0.39	-	23,100	Perkins and others (1995), Arundell (2004), Cooke and others (2007)
Northparkes	**total, Northparkes**	**-32.941**	**148.048**	**Cu-Au**	**440**	175.2	**0.828**	**-**	**0.411**	**-**	**2,120,000**	Jones (1985), Perkins and others (1990, 1995), Heithersay and others (1990), Heithersay and Walshe (1995), Hooper and others (1996), Lickfold and others (2003), Arundell (2004), Lye and others (2006)
Temora Central	Mandamah	-34.166	147.330	Cu-Au	436	28.4	0.35	0.003	0.4	-	99,400	MacCorquodale (1997), Lawrie and others (2007), Mowat (2007), Goldminco Corp. (2008), Geoscience Australia (2010)
Temora Central	Culingerai	-34.211	147.394	Cu-Au	436	8.7	0.28	0.002	0.37	-	24,400	Cooke and others (2007), Lawrie and others (2007), Mowat (2007), Goldminco Corp. (2008)
Temora Central	Estoril	-34.245	147.414	Cu-Au	436	10.8	0.22	0.001	0.37	-	23,800	Lawrie and others (2007), Mowat (2007), Goldminco Corp. (2008), Geoscience Australia (2010)
Temora Central	**total, Temora central**	**-34.166**	**147.330**	**Cu-Au**	**436**	47.9	**0.308**		**0.388**	**-**	**148,000**	Cooke and others (2007), Lawrie and others (2007), Mowat (2007), Geoscience Australia (2010)
Temora Northwest	Yiddah	-34.047	147.334	Cu-Au	436	61.2	0.35	0.004	0.13	-	214,000	Lawrie and others (2007), Mowat (2007), Goldminco Corp. (2008)
Temora South	Dam	-34.328	147.469	Cu-Au	436	33.1	0.314	0.003	0.431	-	104,000	Lawrie and others (2007), Mowat (2007), Goldminco Corp. (2008)
	Marsden	-33.737	147.543	NA	447	224	0.32	-	0.166	-	717,000	Blevin (2002), Porter and Glen (2005), McInnes (2006), Cooke and others (2007), Crawford, Cooke, and Fanning (2007), Champion and others (2009), Lehany (2007), Geoscience Australia (2010)
	Copper Hill	-33.053	148.869	Cu-Au	446	132.5	0.32	-	0.302	-	424,000	Scott (1978), Perkins and others (1995), Scott and Torrey (2003), Torrey and Burrell (2006), Coianiz and Burrell (2007), Geoscience Australia (2010)
	Racecourse	-33.842	149.689	NA	442	27.7	0.45	-	-	1.855	125,000	Lachlan Star (2007), Geoscience Australia (2010)
	Cargo	-33.429	148.801	Cu-Au	433	27	0.2	-	-		54,000	Torrey and White (1998), Golden Cross Resources (2009), Singer and others (2008), Geoscience Australia (2010)
Total	9 known deposits										13,456,000	
rounded total	9										13,000,000	

addition to copper and gold, silver also is reported in ores of the Ridgeway and Cadia East deposits (table C3). Ore minerals occur in sheeted quartz veins, stockworks of quartz veins, and disseminations in both intrusive, volcanic host rocks. Associated ore-bearing skarns are hosted in carbonate-bearing metasedimentary host rocks (Holliday and others, 2002; Forster and others, 2004).

According to Wilson, Cooke, Harper, and Deyell (2007, p. 465), alteration mineral assemblages include inner potassic (biotite-orthoclase), peripheral propylitic (albite-chlorite-carbonate-epidote), and late phyllic (sericite-pyrite), restricted to fault zones. They also noted that "hematite dusting is characteristic, and has produced a distinctive reddening" of altered rocks in the propylitic zone. Sulfur isotopic studies by Wilson, Cooke, Harper, and others (2007, p. 465) showed that "deposit cores are characterized by low $\delta^{34}S$ sulfide values (–10 to –4‰), consistent with sulfide precipitation from an oxidized (sulfate-predominant) magmatic fluid at 450 to 400 °C." There is, however, "a gradual increase in $\delta^{34}S$ sulfide values outwards from the deposit cores to near 0‰" in pyrite from the propylitic zone. Wilson, Cooke, Harper, and Deyell (2007) suggested that this increase probably was caused by sulfate reduction during water-rock interaction, which also produced characteristically reddened propylitic alteration halos containing hematite and epidote.

Cadia Hill and Cadia Quarry Deposits

The Cadia Hill and smaller Cadia Quarry deposits are estimated to contain a total of 688,000 t copper and 123 t gold. This amounts to about 7 percent of the copper and 1 percent of the gold contained in the Cadia group of deposits. The Cadia Hill deposit is near the center of the Cadia group of deposits, in a fault-bounded cupola of the composite central stock of the Cadia Intrusive Complex of porphyritic monzodiorite to quartz monzonite and local syenite. Much of the Cadia Hill deposit was concealed beneath metasedimentary rocks of the Middle Silurian Waugoola Group (Harris and others, 2010). The up-faulted Cadia Quarry deposit is about 600 m northwest of the Cadia Hill deposit, where it is hosted in rocks of the Cadia Intrusive Complex (fig. C5*A* and *B*).

According to Wilson, Cooke, Harper, and Deyell (2007), "The Cadia Hill and Cadia Quarry deposits have chalcopyrite-rich cores and pyrite-rich halos, and Cadia Hill contains a high-level bornite-rich zone." Hydrothermal albite and biotite-orthoclase are irregularly distributed and are commonly overprinted by propylitic chlorite-calcite-epidote-hematite. A late phyllic alteration assemblage of illite, muscovite, and pyrite is grade-destructive but is restricted to large fault zones.

The Cadia Quarry, Cadia Hill, and Cadia East deposits were mineralized at about 442 Ma, as indicated by Re-Os dates on molybdenite. Mineralization may have continued at Cadia East until about 437 Ma, as indicated by a U-Pb age determination on zircon from an intermineral dike (Wilson, Cooke, Stein, and others, 2007). Thus, the Cadia Quarry, Cadia Hill, and Cadia East deposits formed during very late stages of phase 4 Macquarie-Arc magmatism (~457–438 Ma, according to Percival and Glen, 2007).

Big and Little Cadia Cu-Au Skarns

The Big Cadia Cu-Au skarn is northeast of the Cadia Quarry porphyry Cu-Au deposit (fig. C4*A*), and the Little Cadia skarn is northeast of the Cadia East porphyry Cu-Au ore zone (fig. C4*A*). The Big Cadia and Little Cadia Cu-Au skarns are hosted in beds of limestone and calcareous sandstone to conglomerate. These calcareous beds are interlayered with island-arc volcanic and volcaniclastic rocks of the Late Ordovician Forest Reefs Volcanics, which dip toward the Cadia Intrusive Complex (fig. C5*A*). Thus, although the Big and Little Cadia Cu-Au skarns are spatially separated from the Cadia Intrusive Complex at the surface, they are contiguous with the Cadia Intrusive Complex in the sub-surface, as shown in figure C5 (*A* and *B*), (after Forster and others, 2004).

According to Forster and others (2004), proximal stage-1 garnet skarn (near the intrusive contact) grades outward and up-dip to medial stage-1 garnet-pyroxene skarn, and thence to distal stage-1 and stage-2 hematite-magnetite skarn, containing chalcopyrite and native gold. Stage-2 epidote is locally superimposed on stage-1 mineral assemblages, and stage-3 epidote, chlorite, quartz, and calcite are locally superimposed on stage-1 and stage-2 mineral assemblages (fig. 6*B*). Inasmuch as the Big Cadia and Little Cadia skarns are associated with nearby porphyry Cu-Au deposits, and copper and gold have higher per-unit economic values than iron, we characterize the Big and Little Cadia deposits as porphyry-related Cu-Au skarns with iron-oxide matrices.

Ridgeway Deposit

The Ridgeway deposit is about 2 km northwest of the Cadia Quarry deposit, where it is completely hidden beneath about 50±30 m of Miocene basalt, a 50-m thick zone of barren weathered rock, and about 400 m of Ordovician Forest Reef Volcanics (fig. C4*A* and *B*). The Ridgeway deposit was discovered in 1996 by deep drilling to test an induced-polarization (IP) chargeability anomaly, which probably detected disseminated pyrite above the ore zone (Wood, 2012b).

The Ridgeway ore body is pipe-like and nearly vertical. It is up to 250 m across (horizontally) and at least 800 m long (vertically). It is localized in and around a swarm of steep monzonite porphyry plugs and pyroxene porphyry dikes. Host rocks to these intrusions are gently dipping strata in the lower part of the Late Ordovician Forest Reefs Volcanics, which consist mostly of volcaniclastic rocks, lavas, and subvolcanic intrusions.

According to Holliday and others (1999), the Ridgeway deposit contains gold, chalcopyrite, bornite, and magnetite in

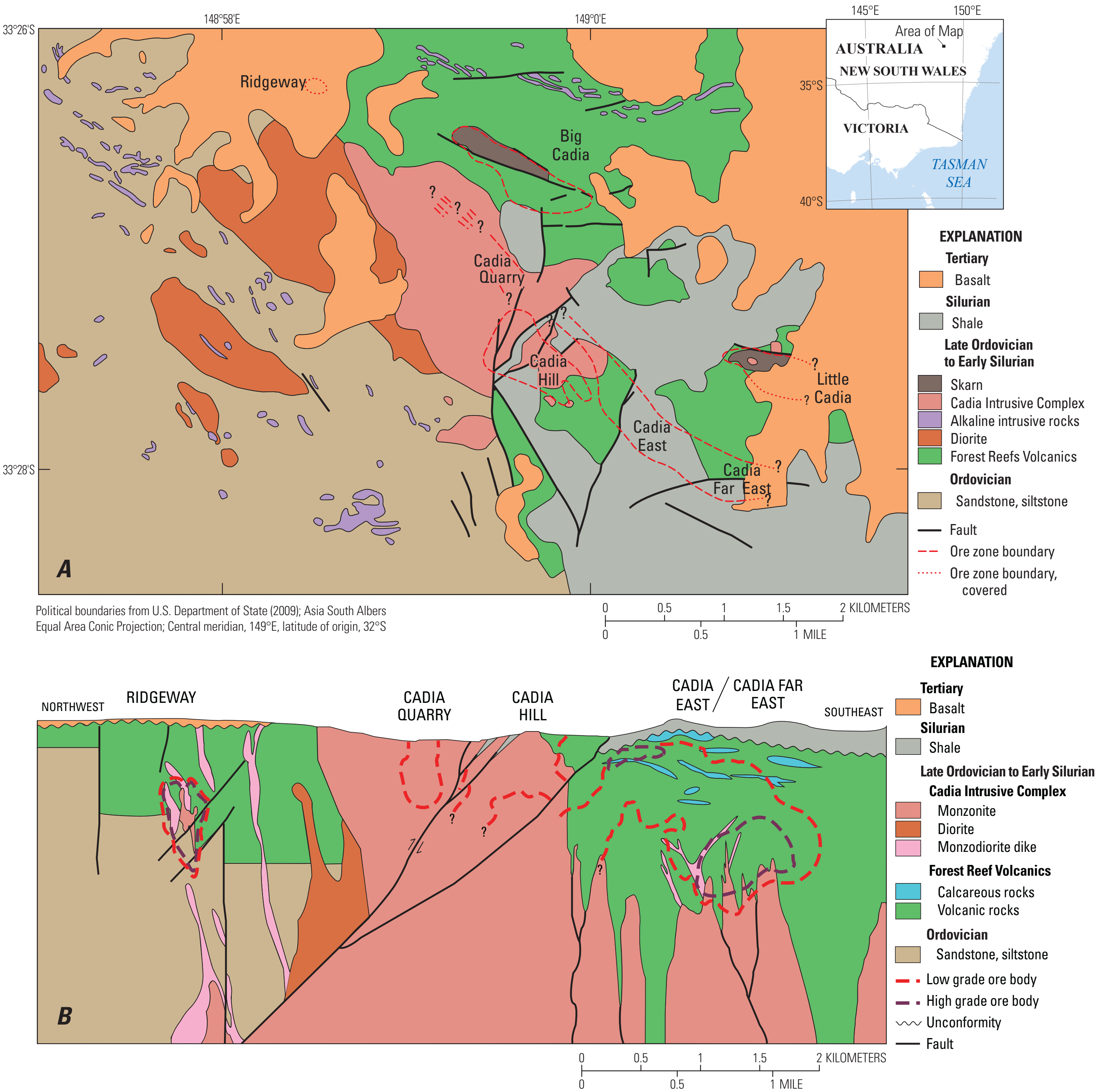

Figure C4. Geologic map and composite NW-SE long section of the Cadia group of deposits. *A*, Geologic map showing locations of porphyry Cu-Au deposits and porphyry-related Cu-Au skarn deposits of the Cadia group (after Wood, 2012b). *B*, Vertical geologic section along the northwest-southeast-trending long axis of the Cadia group of porphyry Cu-Au deposits (after Wood, 2012b).

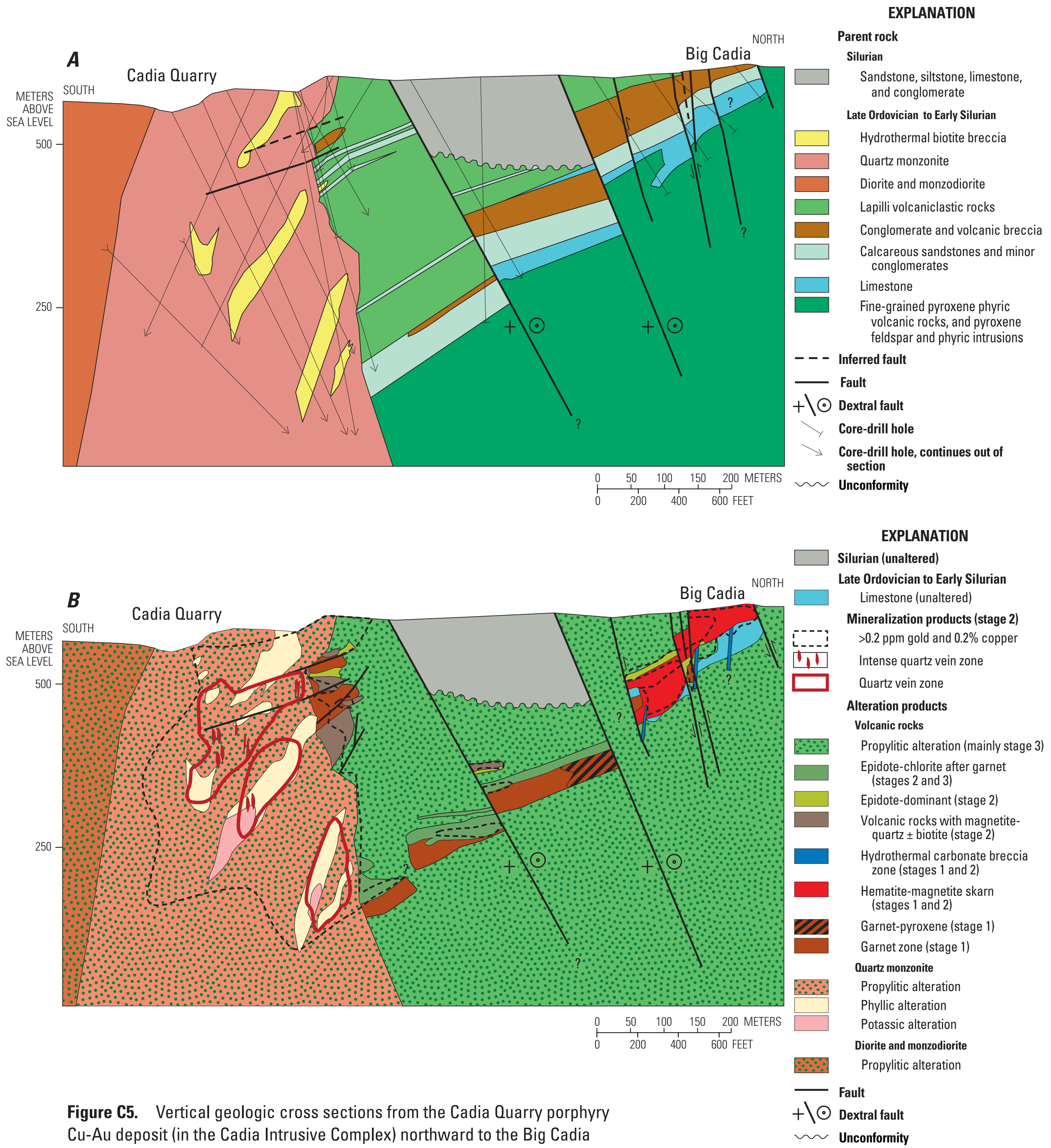

Figure C5. Vertical geologic cross sections from the Cadia Quarry porphyry Cu-Au deposit (in the Cadia Intrusive Complex) northward to the Big Cadia Cu-Au skarn deposit (after Forster and others, 2004). *A*, Parent host-rock types, faults, and core-drill holes; *B*, Alteration products resulting from thermal metamorphism, hydrothermal mineralization, and hydrothermal alteration of parent host-rocks. %, percent; ppm, parts per million.

veins and disseminations. Abundances of veins, ore minerals, and alteration products decrease both inward and outward from contacts of ore-related monzonitic intrusions. Highest ore grades are associated with hydrothermal orthoclase, albite, actinolite, magnetite, and biotite. These are commonly overprinted by later epidote, chlorite, iron-carbonate, and a characteristic pinkish hematite dusting.

Harris and others (2007) described comb-layered magnetite (± quartz) textures in intrusions associated with ore-bearing hydrothermal mineral assemblages in the Ridgeway deposit. They suggested that thickly stacked magnetite-quartz comb-layered structures indicate that large volumes of extremely iron-rich volatiles streamed through the intrusive plugs and dikes related to the Ridgeway deposit (fig. C4*B*) transporting and depositing ore-forming metals to form the Ridgeway porphyry Cu-Au deposit. The Ridgeway porphyry Cu-Au deposit is estimated to contain about 593,000 t copper and 112 t gold, which amounts to about 6 percent of the copper and 8 percent of the gold contained in the Cadia group of deposits. It is now the site of an operating block-cave mine.

Wilson, Cooke, Stein, and others (2007) reported U-Pb age determinations of 456–454 Ma for a quartz monzonitic stock thought to be related to the Ridgeway deposit. However, the dated stock is older than the ore-related intrusions, the ages of which may be closer to about 440±3 Ma.

Cadia East and Cadia Far East Deposits

Exploration of the Cadia East deposit began in 1994 with drilling in a zone of pyritic rocks with quartz-tourmaline and phyllic alteration-mineral assemblages, southeast of Cadia Hill and southwest of the Little Cadia skarn (fig. C4*A* and *B*). The discovery hole was drilled in 1996, but the project was delayed in order to follow up on discovery of higher-grade intercepts at Ridgeway. After 1996, drilling resumed in the Cadia East area, and this led to discovery of the Cadia Far East deposit, and definition of the combined resources of the Cadia East and Cadia Far East deposits (Wood, 2012b).

The combined Cadia East and Cadia Far East deposits extend about 2.5 km from the Cadia Hill deposit, but they are only about 100–300 m wide, and their southwest side is bounded by a normal fault, which bounds the southern margin of a northwest-elongate half-graben (Harris and others, 2010).

As suggested by Corbett and Leach (1998), northwest-trending faults and sheeted veins of the Cadia porphyry Cu-Au deposits can be interpreted as transtensional features, formed during northwest compression and north-striking left-lateral faulting, and accompanied by subvolcanic magmatism and porphyry Cu-Au mineralization. Such magmatism and mineralization apparently followed island-arc volcanism, and probably accompanied amalgamation of the Macquarie Arc with turbidite terranes of the Lachlan Orogen. This would be consistent with evidence for the regionally extensive Lachlan Transverse Zone identified and described by Glen and Walshe (1999), and with a model for assembly of Ordovician terranes in the Lachlan Orogen by Glen and others (2009).

The upper and lower boundaries of the Cadia East deposit are arch-shaped in long section, and the deeper Cadia Far East deposit is below the southeastern limb of the Cadia East ore zone, where it appears to be localized above multiple cupolas of a subsurface stock in the southeastern part of the Cadia Intrusive Complex (fig. C4*B*).

The relatively shallow Cadia East deposit is comparatively copper rich and contains replacement-style disseminated chalcopyrite and pyrite ± bornite ± molybdenite (Harris and others, 2010). Semistratabound concentrations of ore minerals are preferentially concentrated in relatively permeable volcanic conglomerates and breccias. These rocks are interlayered with gently dipping intermediate to mafic volcanic strata of the Late Ordovician Forest Reefs Volcanics. Phyllic alteration minerals (sericite, quartz, and pyrite) accompany disseminated chalcopyrite in the upper ore zone, where they overprint an upward-flared zone of propylitic alteration minerals (chlorite and hematite ± calcite ± epidote ± albite). This propylitic zone extends up section and surrounds the garnet-skarn zone in the calcareous sandstone layer that contains the nearby Little Cadia Cu-Au skarn.

The deeper Cadia Far East deposit is relatively gold-rich. It contains swarms of sheeted quartz-sulfide veins that strike west-northwest and dip steeply. These veins contain quartz, calcite, feldspar, bornite, and chalcopyrite ± molybdenite. Potassic alteration assemblages around the veins contain secondary K-feldspar, magnetite, and biotite ± actinolite (Harris and others, 2010). Similar mineral assemblages surround steeply dipping monzonitic dikes. The dikes and the Cadia East ore zone extend upward from the top of a composite monzonitic stock that rose above the deep eastern shoulder of the Cadia Intrusive Complex (Harris and others, 2010).

The combined Cadia East and Far East ore zones constitute the largest deposit in the Cadia group of porphyry Cu-Au deposits. Total estimated tonnages of copper and gold contained in the upper and lower parts of these ore zones are 7,800,000 t copper and 1,148 t gold. This amounts to about 82 percent of the copper and 82 percent of the gold contained in the Cadia group of deposits. The relatively copper-rich upper Cadia East ore zone will be mined by open-pit methods. The relatively gold-rich lower Cadia Far East ore zone will become the site of Australia's largest underground panel-cave mine (Collett, 2007).

Northparkes Group of Porphyry Cu-Au Deposits

The Northparkes group of porphyry Cu-Au deposits is in the northern part of the Junee-Narromine Volcanic Belt (fig. C2). The Northparkes group of porphyry Cu-Au deposits is within the Lachlan Transverse Zone, north of Parkes and about 100 km west-northwest of the Cadia deposits. Much of the northern Junee-Narromine Volcanic Belt underlies flat agricultural land, which is deeply weathered to saprolite, and covered by up to 70 m of transported sediments. The saprolite is generally about 20–30 m thick, and copper is leached from the upper saprolite. However, copper concentrations above weathered porphyry copper deposits increase downward in the lower saprolite (Arundell, 2004).

The Northparkes area is known to contain seven porphyry Cu-Au deposits, which are grouped by the 2-km rule of Singer and others (2005). These have total estimated resources of at least 2,120,000 t of copper and 72 t of gold (table C3 and appendix F). This amounts to about 16 percent of the copper and 4 percent of the gold contained in known porphyry Cu-Au deposits of the Macquarie permissive tract.

Four of the known porphyry Cu-Au deposits in the Northparkes group of deposits have been mined. In order of decreasing size, these are the Endeavour 26, 48, 22, and 27 (E-26, E-48, E-22, and E-27) deposits. The Northparkes mining operation includes mines on these four deposits, which feed a single processing plant near the E-26 deposit. Production from the E-22 and E-27 open pits and the E-26 underground block-cave mine began in 1992–1993. The E-48 deposit was discovered in 1992 and is the site of an underground block-cave mine. The E-37, E-28, and E-31N deposits are smaller, and have not been put into production.

Porphyry Cu-Au deposits of the Northparkes group are pipe-like bodies of altered and mineralized volcanic and volcaniclastic rocks around narrow, subvertical, cylindrical intrusions of shoshonitic quartz monzonite porphyries. Syn-ore intrusions at each deposit are pinkish to reddish K-feldspar quartz monzonite porphyries with about 30–40 percent phenocrysts. These intrusions and their associated Cu-Au deposits are hosted in volcanic and volcaniclastic rocks of Middle to Late Ordovician age (Porter and Glen, 2005; Simpson and others, 2005). Lickfold and others (2003) showed that the four economic porphyry Cu-Au deposits of the Northparkes group of deposits are remarkably consistent in terms of the sequences of intrusive emplacement, veining, and alteration. Therefore, they suggested that intrusions related to these deposits were all connected to a single mid- or upper-crustal magma chamber during their formation.

Zones of hydrothermally mineralized and altered intrusive and volcanic host rocks typically surround and extend up to 750 m outward from ore-related intrusions. Heithersay and Walshe (1995) documented the following sequence of igneous and hydrothermal products at E-26 North:

1. quartz monzonite porphyry intrusions
   - 1.1 vein-dikes (quartz veins with aplite fill)
   - 1.2 albite
   - 1.3 biotite, magnetite, albite and K-feldspar
   - 1.4 K-feldspar with disseminated bornite and fine quartz-sulfide-anhydrite veins
   - 1.5. quartz stockwork with disseminated bornite ± gold, chalcopyrite, anhydrite, and minor sericite
2. quartz monzonite porphyry intrusions
   - 2.1. vein-dikes
   - 2.2. K-feldspar, disseminated bornite, and quartz-sulfide-anhydrite veins
   - 2.3. quartz stockwork with disseminated bornite ± gold, chalcopyrite, anhydrite, and minor sericite
   - 2.4. quartz-sericite
   - 2.5. gypsum and anhydrite veins with minor sulfides

According to Heithersay and Walshe (1995), phlogopitic compositions of hydrothermal biotite and very saline compositions of fluid inclusions indicate separation of saline fluid and vapor from a silicate melt at temperatures of about 800–1,000 °C. Fluid inclusion homogenization temperatures show a series of pronounced temperature peaks. Peaks at 750–800 °C occurred during K-feldspar flooding with disseminated bornite, which closely followed emplacement of ore-related quartz monzonite porphyries 1 and 2. Peaks at about 500–650 °C occurred with quartz-stockwork veining and sulfide deposition. Late veins formed at temperatures between about 600 and 200 °C.

Perkins and others (1990) reported a U-Pb date of 438.5±3.6 Ma on zircon from the groundmass of an ore-related intrusion and a $^{40}Ar/^{39}Ar$ date of 439.2±1.2 Ma on vein sericite intergrown with quartz and bornite. Lickfold and others (2003) documented nine phases of shoshonitic quartz monzonite porphyry intrusions in intrusive complexes associated with the Endeavour porphyry Cu-Au deposits. These include pre-ore, syn-ore, and post-ore intrusions with ages that range from Late Ordovician to Early Silurian, as indicated by $^{40}Ar/^{39}Ar$ dates on biotite and hornblende, which range from 446 to 437 Ma.

Jones (1985) showed that the Wombin Volcanics are roughly co-spatial with a negative gravity anomaly, which has a diameter of nearly 20 km, and the Northparkes deposits are within the northeastern lobe of this anomaly. Lye (2010) inverted this gravity anomaly and modeled it as a representation of the top of a large upper crustal monzonite pluton. This model is consistent with drill-hole intercepts of such a pluton beneath the Northparkes Mines area and its surroundings. It also is consistent with the suggestion by Lickfold and others (2003) that the Northparkes deposits were all connected to a single magma chamber during their formation.

Temora Group of Porphyry Cu-Au Deposits

The Temora group of porphyry Cu-Au deposits extends north-northeastward from the town of Temora, which is about 160 km southwest of Parkes, and is near the fault-bounded southwestern margin of the Junee-Narromine Volcanic Belt (fig. C2). The Temora area is generally flat lying, and is mostly covered by colluvium and alluvium, deposited on saprolite, which grades downward to saprock and bedrock. Outcropping bedrock is exposed only locally, in and around the Gidginbung Mine, which is in low hills at the south end of the Temora area.

The Temora porphyry Cu-Au deposits and prospects are along the eastern margin of the terrane-bounding Gilmore Fault Zone (fig. C2). Glen (1992) interpreted this north-northwest-trending fault zone as a suture zone between the Macquarie Arc to the east and Ordovician turbiditic metasedimentary rocks to the west. The Temora group of porphyry Cu-Au deposits parallels the Gilmore Fault Zone. Geochemical anomalies associated with individual deposits and prospects in this area also are elongate to the north-northwest (Mowat, 2007).

The five known porphyry Cu-Au deposits of the Temora group of deposits contain a total of 466,000 t copper and 40.9 t gold. This amounts to about 3 percent of the copper and 2 percent of the gold estimated to be contained in known porphyry Cu-Au deposits of the Macquarie Arc. The Mandamah, Culingerai, and Estoril deposits comprise the Temora Central group of deposits. The Temora Northwest group comprises the grouped Yiddah deposit and the Yiddah west prospect. The Dam deposit is grouped with several prospects and occurrences in the Temora South group. These deposits and prospects were grouped according to the 2-km rule for grouping of porphyry copper deposits, as explained in the introductory report, and illustrated in figure 2.

Porphyry Cu-Au deposits of the Temora group are hosted in Ordovician to Silurian volcaniclastic rocks, interlayered with minor volcanic rocks, and intruded by dikes of mafic to intermediate composition. Porphyry Cu-Au deposits of the Temora cluster are spatially and temporally associated with dikes of medium- to high-K calc-alkaline porphyritic monzodiorite (Mowat, 2007). They are less potassic and less felsic than some of the ore-related monzonitic to quartz monzonitic intrusions of the Cadia and Northparkes porphyry Cu-Au systems.

Mowat (2007) summarized vein paragenesis and alteration-mineral assemblages typical of porphyry Cu-Au deposits of the Temora cluster. Early quartz + magnetite + pyrite ± K-feldspar ± chalcopyrite veins occur as seam-like, high-temperature veinlets. Late coarse quartz + carbonate + chlorite + chalcopyrite veinlets are wider and more planar. Chalcopyrite also occurs in irregular patches marginal to veins. The potassic alteration assemblage consists of K-feldspar + hematite + magnetite + chlorite + albite ± secondary biotite ± actinolite. The phyllic assemblage consists of albite + sericite + chlorite. The propylitic assemblage consists of sericite + chlorite + epidote.

Mowat (2007) classified the Dam deposit as a porphyry Cu-Au deposit on the basis of mineralized and altered rocks discovered by drilling. The mean of U-Pb age determinations on magmatic zircons from an intermediate subvolcanic intrusion near the Dam porphyry Cu-Au deposit and the Gidginbung high-sulfidation epithermal Au-Ag-(Cu) deposit is 435±2.5 Ma (Perkins and others, 1990). Similarly, Lawrie and others (2007) reported a weighted mean age of 436±3.1 Ma for hydrothermal zircon grains from the Gidginbung deposit. These age determinations seem to indicate that porphyry Cu-Au deposits and prospects of the Temora area formed in association with subvolcanic intrusions, emplaced during Early Silurian time, between about 439 and 433 Ma.

Marsden Porphyry Copper Deposit

The Marsden porphyry copper deposit is in the Junee-Narromine Volcanic Belt of the Macquarie Arc (figs. C1, C2). It is on the eastern margin of a large positive aeromagnetic anomaly that is interpreted to represent the Cowal Igneous Complex. It is about 50 km southwest of the Northparkes group of deposits and 20 km northeast of the Yiddah deposit, which is at the north end of the Temora cluster of deposits (fig. C2).

The Marsden deposit was discovered in 1997 beneath about 100 m of clay-rich alluvium. It has been sufficiently explored by drilling to support estimation of its resources (indicated and inferred), as listed in table C3. The Marsden deposit is estimated to contain about 717,000 t copper and 37.2 t gold. That amounts to about 5 percent of the copper and 2 percent of the gold currently estimated to be contained in known porphyry Cu-Au deposits of the Macquarie Arc.

Cooke and others (2007) listed Marsden as a calc-alkalic porphyry Cu-Au deposit, comparable to those of Copper Hill and the Temora cluster of deposits. They noted that Marsden is the largest of these deposits, even though its lower part is truncated by a post-ore thrust fault.

A generalized geologic map by Crawford, Cooke, and Fanning (2007) shows Marsden to be near the northeastern end of a composite body of monzonites and granodiorites of phases 2 and 3 of the Cowal Igneous Complex. They suggested that most of the igneous rocks of the Marsden area are broadly comparable with those of the Narromine Igneous Complex, but that some of the more evolved quartz diorites to quartz monzonites may be better correlated with the Copper Hill Intrusive Complex. They reported SHRIMP U-Pb zircon ages for 12 zircons from a granodiorite in the Cowal Igneous Complex. The mean age was 447±11 Ma (Late Ordovician to Early Silurian), cores of zircon grains yielded ages from 474 to 460 Ma (Ordovician), and rims yielded an average age of 445 Ma (Late Ordovician).

A vertical north-south section through the Marsden deposit (Lehany, 2007) shows drill-indicated geology and ore intercepts. About 100 m of transported alluvial cover overlie about 100–140 m of mineralized diorite. The mineralized diorite is underlain by barren Devonian sedimentary strata beneath a sub-horizontal thrust fault.

Copper Hill Porphyry Cu-Au Deposit

The Copper Hill porphyry Cu-Au deposit is in the Molong Volcanic Belt, about 45 km north-northwest of the Cadia group of deposits, and 5 km north of the town of Molong. The Copper Hill deposit consists of quartz-pyrite-chalcopyrite and quartz-magnetite-chalcopyrite stockworks and veins. These are spatially and temporally associated with intrusions of early quartz diorite to tonalite, and later porphyritic dacite. The mineralized zone is about 2 km long and 1 km wide and is in the central part of the intrusive complex (Scott and Torrey, 2003).

According to Torrey and Burrell (2006), “Copper Hill is a large, multiphase system, in which well-mineralised, early porphyry phases have been intruded and disrupted by a series of weakly mineralised, intramineral porphyry bodies. This results in high-grade material being diluted, leading to the formation of a large, but relatively low grade porphyry deposit. Potential remains for the discovery and (or) expansion of high grade remnants of the early mineralization.” Crawford, Meffre, and others (2007) characterized the Copper Hill intrusions as a suite of medium-K calc-alkalic intrusions.

The Copper Hill deposit was mined on a small scale from 1845 to 1851, producing about 40 t of copper from about 3,300 t of supergene-enriched ore with an average grade of 1.2 percent copper. Modern exploration of the deposit began in the 1960s and is ongoing. Results of recent drilling have increased estimated open-pit mineable resources from 424,000 t of contained copper and 40 t of contained gold (table C3, appendix F) to 527,000 t of contained copper and 44,000 t of contained gold (Stanton-Cook, 2011; Golden Cross Resources, 2011). Furthermore, recent preliminary economic modeling indicates that the Copper Hill deposit may be profitably mineable.

Illustrations by Torrey and Burrell (2006) show a swarm of northwest-elongate ore zones within and around phase 1 and phase 2 dacite porphyry intrusions that also are elongate to the northwest. Photographs of drill core show greenish gray rocks, locally hematite-stained, and cut by early stockworks of quartz veinlets and later swarms of subparallel sheeted veins, some of which contain high concentrations of chalcopyrite.

Furthermore, Torrey and Burrell (2006) show that rocks of a central phyllic zone contain pyrite, chalcocite, chalcopyrite, and bornite. This central zone is surrounded by a sericite-chlorite-magnetite zone, containing chalcopyrite and pyrite. Within this zone are cognate inclusions of earlier quartz veined K-feldspar-biotite-magnetite-altered rock, containing chalcopyrite ± bornite. An outer sericite-chlorite-calcite zone contains local concentrations of chalcopyrite and pyrite. A peripheral propylitic assemblage of epidote, chlorite, and calcite is superimposed on early tonalite and surrounding andesitic country rocks.

Sequential timeframe cross sections by Torrey and Burrell (2006) summarize the history of igneous intrusion, mineralization, and alteration at Copper Hill. Andesitic host rocks of the Molong Volcanic Belt were invaded by a vertical stock of pre-ore diorite to quartz diorite. This dioritic stock was intruded by a stock of early tonalite (dated 450±6 Ma, according to Cooke and others, 2007). The early tonalite stock developed a carapace of copper-bearing quartz veins. The early tonalite and its mineralized carapace were subsequently intruded by two sequential phases of intramineral dacite porphyry. Phase 1 intramineral intrusions are mineralized but contain cognate inclusions of previously mineralized tonalite. Phase 2 intramineral intrusions cut phase 1 intramineral intrusions and are less well mineralized than phase 1 intrusions. Perkins and others (1995) reported a minimum K-Ar age determination of 446±6 Ma (Late Ordovician to Early Silurian) on hornblende from phase 2 dacite porphyry at Copper Hill. Post-ore intrusions invaded and disrupted the previously mineralized ore zones.

Weathering of the deposit produced a saprolitic leached cap, underlain by a supergene enriched zone. Copper and gold are depleted in the leached zone and enriched in the supergene zone, which contains chalcocite, digenite, native copper, malachite, and azurite. The supergene zone blankets the northeastern part of the deposit, where it is about 5 m thick and lies at depths between 30 and 40 m (Scott and Torrey, 2003; Torrey and Burrell, 2006).

Cargo Porphyry Copper Deposit

The Cargo porphyry Cu-Au system consists of a central low-grade porphyry copper deposit and a peripheral radial set of late gold-bearing quartz-carbonate veins. Early production of 0.318 t gold was from epithermal veins and gold placers. The Cargo copper and gold deposits are about 35 km southwest of Orange, New South Wales, and about 20 km west-northwest of the Cadia group of porphyry Cu deposits (fig. C1). They are on the west-central margin of the Molong Volcanic Belt, where they lie in a north-trending, doubly plunging anticline in the hanging wall of a west-dipping thrust with an unknown amount of displacement.

Singer and others (2008) listed tonnage and grade of Cargo copper resources as 27 Mt, averaging 0.2 percent copper. The Australian Mines Atlas (Geoscience Australia, 2010) listed the tonnage and grade of Cargo gold resources as 3.7 Mt, averaging 1.24 g/t gold. Recent exploration activity has focused mainly on gold, because the copper grades are subeconomic. Most of the gold is in epithermal quartz veins peripheral to the copper zone.

According to Torrey and White (1998), the Cargo porphyry Cu-Au system is associated with the Cargo Intrusive Complex, which is hosted by andesitic to trachyandesitic island-arc volcanics and sedimentary rocks of the Middle to Late Ordovician Cargo Andesite. The Cargo Intrusive Complex consists of calc-alkaline diorites, quartz diorites, and dacite to rhyodacite porphyries. In the center of the intrusive complex is an intrusion breccia with fragments of the other rock types in an alkalic igneous matrix of quartz monzonite and monzodiorite to syenite.

According to Simpson and others (2007, p. 350), “Initial emplacement of monzonites and monzodiorites at Cargo is constrained to the interval 453–451 Ma, although compositionally similar intrusions elsewhere in the Molong Volcanic Belt were mostly emplaced at or shortly after 440 Ma.”

Torrey and White (1998) described the Cargo porphyry Cu-Au system as a large concentrically zoned mineralized and altered igneous complex that is half-circular in plan, with a diameter of about 3 km. The western half of the system apparently is faulted away. A central zone contains chalcopyrite, molybdenite, and lesser bornite in breccias and stockwork veins in potassically altered rocks. A peripheral gold halo corresponds to a radial set of quartz-carbonate veins, which cross the outer potassic, phyllic, and inner propylitic zones.

Racecourse Porphyry Copper Deposit

The Racecourse porphyry copper deposit is near the south end of the Rockley Gulgong Volcanic Belt. It is about 75 km southeast of the Cadia group of deposits (fig. C1).

The mineralized zone at the Racecourse deposit is tabular, about 1 km long and from 30 to 130 m wide. Drill results indicate that it extends to a depth of at least 350 m. The Racecourse deposit is presently estimated to contain about 125,000 t copper (table C3). This amounts to about 1 percent of the presently estimated resources of known porphyry Cu-Au deposits of the Macquarie Arc.

According to Lachlan Star, Ltd., (2007), pyrite and chalcopyrite occur as fine-grained disseminations, fracture coatings, stringer veins, and veinlets. These are hosted in Ordovician volcaniclastic and volcanic rocks, adjacent to a shoshonitic monzonite intrusion. Inasmuch as this intrusion may resemble ore-related Early Silurian intrusions of the Cadia, Northparkes, and Temora groups of deposits, we assume that this intrusion and the associated Racecourse deposit probably are of Early Silurian age (about 436±3 Ma).

Prospects, Mineral Occurrences, and Other Deposit Types

Porphyry Copper Prospects and Copper Occurrences

About half the significant porphyry copper prospects in the Macquarie tract are located within groups of known porphyry Cu-Au deposits and prospects. These prospects are therefore considered potential extensions to known deposits (table C4*A*) and are not counted as potential undiscovered deposits.

The Northparkes group of deposits includes the Brazen, GRP314, and Veedas prospects. The Temora northwest group contains the Yiddah west occurrence (appendix F). The Temora north group contains the Kangaroo Hill prospect and the Bull Plain occurrence. The Temora central group contains the significant Chicane, Homer, and Monza prospects, as well as the Harold Bell, Horse Paddock, Punch, Rain Hill, and Spiers occurrences. The Temora south group contains the Greens Creek, Mag H1, Rosevale, and Woolshed prospects, as well as the Fields and Steinke occurrences (table C4*A* and appendix F).

About half the significant porphyry Cu-Au prospects in the Macquarie tract are spatially independent, and each of these represents a potential undiscovered porphyry Cu-Au deposit. Such prospects in the Molong Volcanic Belt include the Bodangora, Dairy Hill, Bowen Park, Carangara, Ferndale, Gooleys, and Moorilda prospects. Such prospects in the Junee-Narromine Volcanic Belt include the Kingswood, Allendale, Hopetoun, Gemini, Endeavour E-39, Endeavour E-43, and Eurowie prospects (figs. C1, C2, and table C4*A*).

The Kaiser copper occurrence is in the northern part of the Molong Volcanic Belt. The Silverstone copper occurrence is about 20 km east of the Temora cluster of porphyry copper deposits and prospects (fig. C1).

Other Relevant Types of Deposits

Other types of deposits that are relevant to exploration for undiscovered porphyry copper deposits include skarns, replacement deposits, and epithermal veins and breccias. Any of these deposit types may occur in association with porphyry copper deposits.

Skarns and replacement deposits commonly occur in calcareous rocks in and around porphyry copper deposits, as illustrated in figure C6. Early exploration in the Cadia area focused on the Big Cadia skarn, and this led to wider exploration for associated porphyry Cu-Au deposits, according to Wood (2012a).

Replacement-style deposits may also occur in association with porphyry copper deposits. The discovery of relatively copper-rich replacement-style ore in the upper part of the East Cadia deposit contributed to later discovery of relatively gold-rich sheeted quartz vein ore in the deeper Far East Cadia deposit.

Epithermal veins and breccias also occur in and around some porphyry Cu-Au systems, as illustrated in figure C6. Late, high-sulfidation epithermal veins occur above and around some porphyry Cu-Au deposits. Late, medium-sulfidation epithermal veins occur in and around most porphyry copper deposits. Although low-sulfidation epithermal veins and breccias commonly occur in regions that contain porphyry copper deposits, they generally are spatially independent from particular porphyry copper deposits.

Known skarn Cu-Au, vein and replacement Cu, and epithermal deposits and prospects within the Macquarie permissive tract are listed in table C4*B*, where they are arranged in order of decreasing age. Although some skarns, replacement deposits, and epithermal veins and breccias are spatially and temporally associated with porphyry copper systems, others are not. In order to discriminate between those that are porphyry-copper related, and those that are not, other indications of porphyry-copper-style deposits are required. Such indications might include proximity to intrusive porphyries or to over-sized patterns of alteration products, typical of the upper and outer parts of intrusion-centered porphyry copper systems.

Epithermal veins that are younger than 433 Ma are younger than the youngest known porphyry Cu-Au deposit in the Macquarie tract. Nevertheless, porphyry copper deposits are commonly cut by epithermal veins, so such veins generally are younger than the porphyry copper deposits with which they are spatially associated. Therefore, such relatively young veins can indicate potential for spatially associated porphyry copper deposits, which are likely to be somewhat older than their spatially associated epithermal veins.

Skarn and Replacement Deposits

Several skarn Au ± Cu deposits and prospects are present in the Junction Reefs area, which is in the Molong Volcanic Belt, about 20 km south of the Cadia group of porphyry Cu-Au and skarn Cu-Au deposits. The Comobella skarn Au-Cu prospect is in the northern part of the Molong Volcanic Belt (table C4*B*).

The previously mined copper deposit at Lloyds Copper Mine was a semistratabound replacement deposit, hosted in Ordovician volcanic rocks near the south end of the Rockley-Gulgong Volcanic Belt (table C4*B* and fig. C7). This semistratabound Lloyds Copper orebody may have resembled the relatively copper-rich, volcanic-hosted upper ore zone of the Cadia East deposit, which lies above the larger, more gold-rich Cadia Far East deposit. By analogy, it seems possible that an undiscovered porphyry Cu-Au deposit could be present beneath the previously mined Lloyds Copper deposit.

High-Sulfidation Epithermal Deposits

According to Allibone (1998, p. 509) “The development of high-sulfidation hydrothermal systems, synchronous with deformation along brittle-ductile shear zones, is a predictable consequence of intrusive activity during deformation.” Nevertheless, the localization of such deposits may be more influenced by fracture zones and regionally high thermal gradients, than by proximity to specific igneous intrusions or porphyry copper systems.

Gidginbung Au-Ag-(Cu) Deposit and Dobroyde Au Prospect

The Gidginbung high-sulfidation epithermal Au-Ag-(Cu) deposit was mined from the Temora open pit, which is near Temora, in the southeastern part of the Junee-Narromine Volcanic Belt and at the southern end of the Temora groups of porphyry Cu-Au deposits and prospects (figs. C2, C7, and table C4*B*). The Temora mine produced about 21 t of gold (Mowat and Smith, 2006; Cooke and others, 2007).

The Dobroyde gold prospect is south-southeast of Temora, and is similar to the Gidginbung deposit (fig. C7). Allibone and others (1995) described the Gidginbung deposit as a shear-zone-hosted magmatic-hydrothermal Au-Ag deposit in which economic gold grades were associated with barite-sulfide veins. Such veins generally were confined to the silica-pyrite-altered core of an earlier quartz-rich advanced-argillic alteration zone, localized along a north-striking, steeply dipping shear zone.

Lawrie and others (2007) reported an Early Silurian age determination of 436.4±3.1 Ma for hydrothermal zircons from the Gidginbung ore zone. This overlaps with an age determination of 435±2.5 Ma, reported by Perkins and others (1990) for intermediate subvolcanic intrusions near the Gidginbung deposit. Lawrie and others (2007) interpreted this

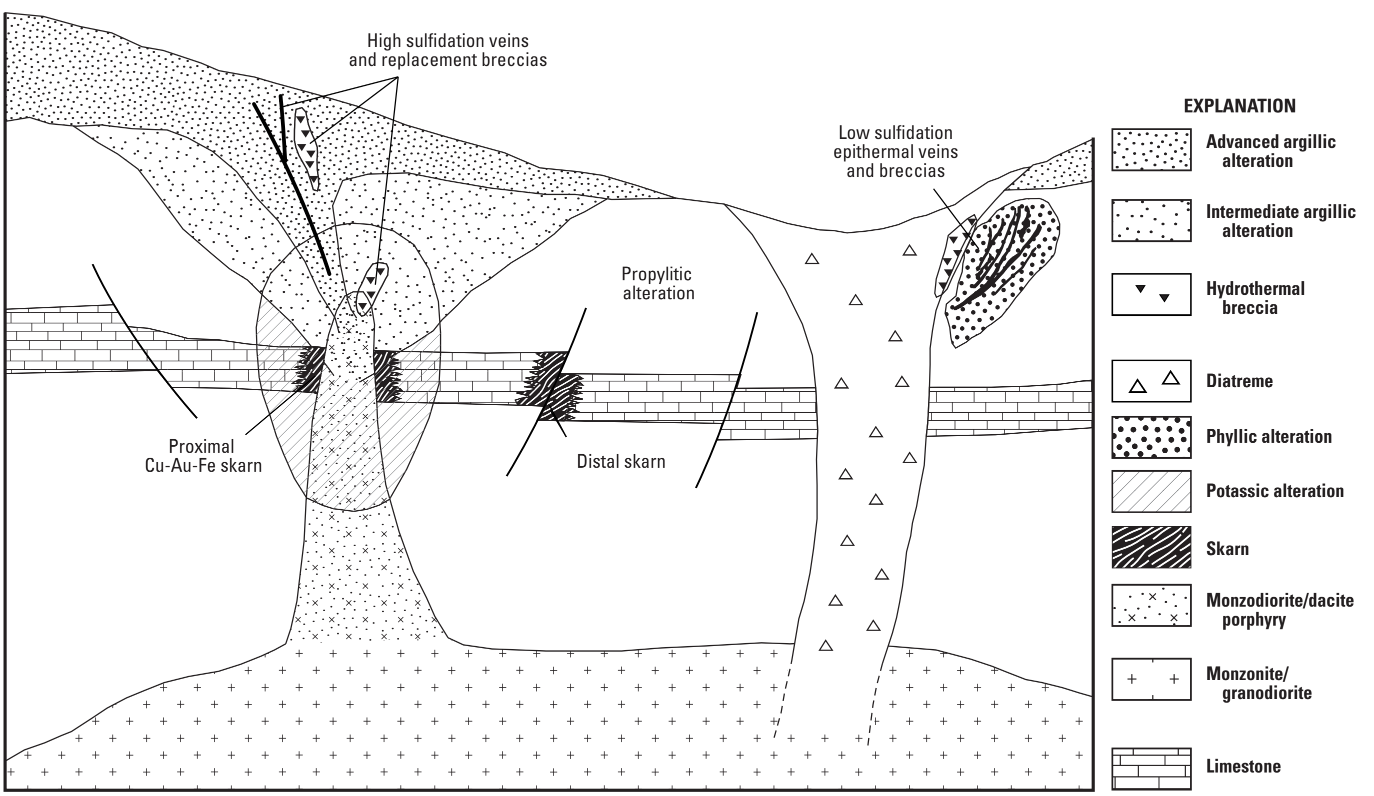

Figure C6. Schematic ore deposit model for western Pacific porphyry Cu-Au deposits, showing possible associations with carbonate-hosted skarn and replacement deposits, high-sulfidation and low-sulfidation epithermal veins and breccias, and diatremes (after Cooke and others, 1998; and Sillitoe, 1989).

Table C4*A*. Significant porphyry copper prospects in the Macquarie tract (009pCu8002), New South Wales, Australia.

[Ma, million years; m, meters; %, percent; ppm, parts per million; prospect ranking criteria listed in table 2; -, no data]

Group	Name	Latitude	Longitude	Age (Ma)	Comments	Rank	Reference
Northparkes	Veedas	-32.921	147.998	440	102 m at 0.47% Cu, 0.05 ppm Au	3	Lye and others (2006), Cooke and others (2007)
Temora Central	Monza	-34.235	147.405	437	27 m at 0.8% Cu, 0.3 ppm Au	3	Lawrie and others (2007), Mowat (2007)
Temora North	Kangaroo Hill	-34.115	147.362	437	28 m at 0.2% Cu, 0.0018% Mo, 0.26 ppm Au, 2 ppm Ag	3	Mowat (2007), Goldminco Corp. (2008)
	Bodangora	-32.452	148.994	443	45 m at 0.24% Cu, 0.9 ppm Au	3	Alkane Resources, Ltd. (2011a)
	Bowen Park	-33.335	148.845	443	33 m at 0.31% Cu, 0.21 ppm Au	3	Alkane Resources, Ltd. (2004)
	Dairy Hill	-33.234	148.859	443	48 m at 0.35% Cu, 0.31% Au	3	Alkane Resources, Ltd. (2004)
	Endeavour E-43	-33.748	147.480	440	490 m at 0.19% Cu	3	Cooke and others (2007), Perkins and others (1995), McInnes and Freer (2007)
	Eurowie	-33.841	147.425	443	27 m at 0.27% Cu, 0.15 ppm Au	3	Clancy Exploration, Ltd. (2010)
	Ferndale	-33.482	149.115	443	68 m at 0.3% Cu, 0.18 ppm Au	3	Bird (1999), Maynard (2003), Geoscience Australia (2010)
	Gooleys	-33.513	149.081	443	44 m at 0.55% Cu, 1.3 ppm Au	3	Cooke and others (2007), Crawford and others (2007)
	Kingswood	-32.373	148.038	443	52 m at 0.67% Cu, 0.2 ppm Au	3	Clancy Exploration, Ltd. (2009)
	Moorilda	-33.604	149.365	443	19 m at 0.2% Cu, 1.23 ppm Au	3	Alkane Exploration, Ltd. (2003)
	Carangera	-33.353	149.250	443	10 m at 0.29% Cu	4	NSW Industry and Investment (2010)
	Gemini	-33.360	148.030	443	1 m at 0.19% Cu, 0.02 ppm Au	4	Clancy Exploration, Ltd. (2010)
Temora Central	Chicane	-34.227	147.399	437	10 m at 0.33% Cu, 0.0076% Mo, 0.13 ppm Au, 0.9 ppm Ag	4	Goldminco Corp. (2010)
	Homer	-34.197	147.337	437	geochemical anomaly, > 1,000 ppm Cu, > 0.5 ppm Au	5	Mowat (2007), Goldminco Corp. (2008)
Temora South	Greens Creek	-34.317	147.460	437	geochemical anomaly, > 1,000 ppm Cu, > 0.5 ppm Au	5	Mowat (2007), Goldminco Corp. (2008)
	Mag H1	-34.310	147.442	437	geochemical anomaly, > 1,000 ppm Cu, > 0.5 ppm Au	5	Mowat (2007), Goldminco Corp. (2008)
	Rosevale	-34.300	147.400	437	geochemical anomaly, > 1,000 ppm Cu, > 0.5 ppm Au	5	Mowat (2007), Goldminco Corp. (2008)
	Woolshed	-34.301	147.418	437	geochemical anomaly, > 1,000 ppm Cu, > 0.5 ppm Au	5	Mowat (2007), Goldminco Corp. (2008)
Northparkes	Brazen	-32.930	148.055	440	bornite, chalcopyrite, gold, pyrite near known porphyry Cu-Au	5	Lye and others (2006), Cooke and others (2007)
	GRP314	-32.934	148.056	440	bornite, chalcopyrite, gold, pyrite near known porphyry Cu-Au	5	Lye and others (2006), Cooke and others (2007)
	Endeavour E-39	-33.688	147.404	440	prospect in Goonumbla district with chalcopyrite, gold, pyrite	6	Miles and Brooker (1998), McInnes and Freer (2007), Perkins and others (1995)
	Allendale	-32.550	148.173	443	widespread low-grade gold and base metals in altered rocks	6	Alkane Resources, Ltd. (2004)
	Hopetoun	-32.975	148.013	439	-	-	Lye and others (2006), Cooke and others (2007)

Table C4*B*. Deposits and prospects of types that may be related to porphyry copper systems in the Macquarie tract (009pCu8002), New South Wales, Australia.

[Ma, million years; prospect ranking criteria listed in table 2]

Name	Latitude	Longitude	Age (Ma)	Comments	Rank	Reference
Lloyds Copper Mine (Burraga)	-33.962	149.534	443	Volcanic-hosted Cu, vein and replacement-style (past producer)	5	Republic Gold, Ltd. (2010), Burraga Copper, Ltd. (2012), Stanton (1953)
Comobella	-32.364	148.983	443	Skarn Au-Cu	5	Taylor (1983), Perkins and others (1995), Jaireth and Miezitis (2004b), Cube Consulting (2006), Alkane Resources, Ltd. (2004), Geoscience Australia (2010)
Junction Reefs	-33.617	148.980	440	Skarn Au + Cu	5	Gray and others (1995)
Endeavour E-42	-33.635	147.404	440	Low-sulfidation epithermal gold + silver + copper	8	Miles and Brooker (1998), Cooke and others (2007), McInnes and Freer (2007), Perkins and others (1995), Ewers and others (2002), Geoscience Australia (2010)
Dobroyde	-34.759	147.651	415	High-sulfidation epithermal gold + copper + zinc	5	Perkins and others (1995), Allibone (1997), Geoscience Australia (2010)
Peak Hill	-32.719	148.191	410	High-sulfidation epithermal gold + silver + copper	5	Bowman and Richardson (1983), Perkins and others (1995), Masterman and others (2002), Cooke and others (2007), Squire and Crawford (2007), Singer and others (2008), Alkane Resources, Ltd. (2006)
Gidginbung	-34.314	147.450	409	High-sulfidation epithermal gold + silver + copper	5	Perkins and others (1995), Masterman and others (2002), Cooke and others (2007), Lawrie and others (2007), Mowat (2007), Geoscience Australia (2010)

to indicate that the epithermal gold deposits at Gidginbung formed in association with coeval subvolcanic intrusions.

Perkins and others (1995) reported Ar-Ar age determinations of 417–401 Ma for alunite in the epithermal gold deposits. This may indicate that there were at least two episodes of mineralization at Gidginbung—a late Early Silurian episode related to nearby shallowly emplaced intrusions (dated about 435–436 Ma), and an Early Devonian episode of shear-zone-hosted high-sulfidation mineralization, presumably related to more distant and deeply emplaced intrusions.

Peak Hill

The Peak Hill high-sulfidation epithermal Au-Cu deposit is in the northern part of the Junee-Narromine Volcanic Belt (figs. C2, C7). It is about 27 km north-northeast of the Northparkes group of porphyry copper deposits. Estimated production from 1904 to 1917 was 1.87 t gold from 500,000 t ore. Estimated resources are 11.27 Mt of ore at 1.29 g/t gold and 0.11 weight percent copper (Chapman, 2003; Alkane Resources Ltd., 2006).

According to Allibone (1998), economically significant gold grades in excess of 1 g/t are coincident with concentrations of veins rich in barite and pyrite. Native gold, calaverite, Te-rich tennantite-tetrahedrite, chalcopyrite, covellite, and chalcocite occur in the barite-pyrite veins. Such veins cut advanced-argillic alteration-mineral assemblages of quartz, kaolinite, and pyrite ± alunite ± illite, which occur throughout the core of the deposit. The veins and altered rocks are in and around north-striking, steeply dipping shear zones, which cut volcanic and sedimentary rocks of Ordovician age. Ore shoots parallel nearly vertical lineation in the shear zones.

Although the barite-pyrite veins at Peak Hill contain both gold- and copper-bearing minerals, it has not been shown that these veins are related to a porphyry Cu-Au system, or even to any particular igneous intrusion. Furthermore, an Ar-Ar age determination of 408.7±2.4 Ma on K-mica from Peak Hill by Perkins and others (1995) indicates that the Peak Hill deposit formed significantly later than most of the porphyry Cu-Au systems in the Macquarie Arc, most of which formed between about 445 and 435 Ma (appendix F).

Masterman and others (2002, p. 14) estimated that the Peak Hill deposit formed at a minimum depth of 700–800 m if the pressure was hydrostatic and the minimum temperature at the core of the deposit was 280 °C, as indicated by the core pyrophyllite-diaspore assemblage. They suggested that gold-copper mineralization and alteration-mineral zonation resulted from wall-rock reaction that neutralized acid fluids, which dispersed laterally from the axis of flow "like seepage along a leaky pipe." They suggested further that "the Peak Hill deposit is a deeply eroded example of a typical high-sulfidation deposit and that there may have been significantly more gold and copper higher up along the direction of flow."

Low-Sulfidation Epithermal Deposits

Endeavour E-42

The Endeavour E-42 deposit is a low-sulfidation epithermal gold deposit, which is in the northern part of the southern segment of the Junee-Narromine Volcanic Belt (figs. C2, C7). This deposit is mined from the large open-pit Cowal Mine. According to Miles and Brooker (1998), the E-42 deposit is a fracture-controlled low-sulfidation epithermal deposit that contains free native gold, as well as gold in association with sulfides in quartz-carbonate-adularia-bearing veins. Associated sulfides are pyrite and sphalerite ± minor galena, pyrrhotite, and chalcopyrite. Estimated resources of the E-42 deposit are 105 t gold in 108.5 Mt of ore with an average grade of 0.97 g/t gold (Geoscience Australia, 2010).

Host rocks of the E-42 deposit include three volcanic-volcaniclastic units—a lower volcaniclastic conglomerate unit, a middle unit of trachyandesitic lava and hyaloclastic breccia, and an upper unit of redeposited volcaniclastic debris. These units are intruded by a dioritic pluton, dated 465±5 Ma, and by dikes of porphyritic diorite and andesite (Miles and Brooker, 1998). A west-east vertical cross section by McInnes and Freer (2007) indicates that a western ore zone occurs in steeply east-dipping shear zones in monzogranite, whereas a larger central ore zone consists of sheeted veins and disseminations in volcaniclastic rocks and diorite. The sheeted veins strike northwest and dip moderately southwest.

Miles and Brooker (1998) cited $^{40}Ar/^{39}Ar$ plateau age determinations of about 438 Ma for sericite-silica ± carbonate samples from the E-42 deposit, based on information from Perkins (unpub. data, 1993). This is within the age range of porphyry Cu-Au deposits of the Northparkes group of deposits (439±1.2 Ma, according to Perkins and others, 1990). However, such low-sulfidation epithermal deposits are too distal to be ascribed to a hidden porphyry copper system nearby.

Exploration History

According to Fredricksen (2006), copper was discovered in the Cadia Valley in 1851. Gold was being mined there by 1870, and the Iron Duke (Big Cadia) magnetite skarn was mined from 1919 to 1929 and from 1942 to 1945. The Cadia Hill and Cadia Quarry porphyry Cu-Au deposits were discovered in 1992 and were put into production by open-pit mining in 1998 (Wilson, Cooke, Harper, and Deyell, 2007). Between 2008 and 2010 the estimated copper resources of the Cadia group increased

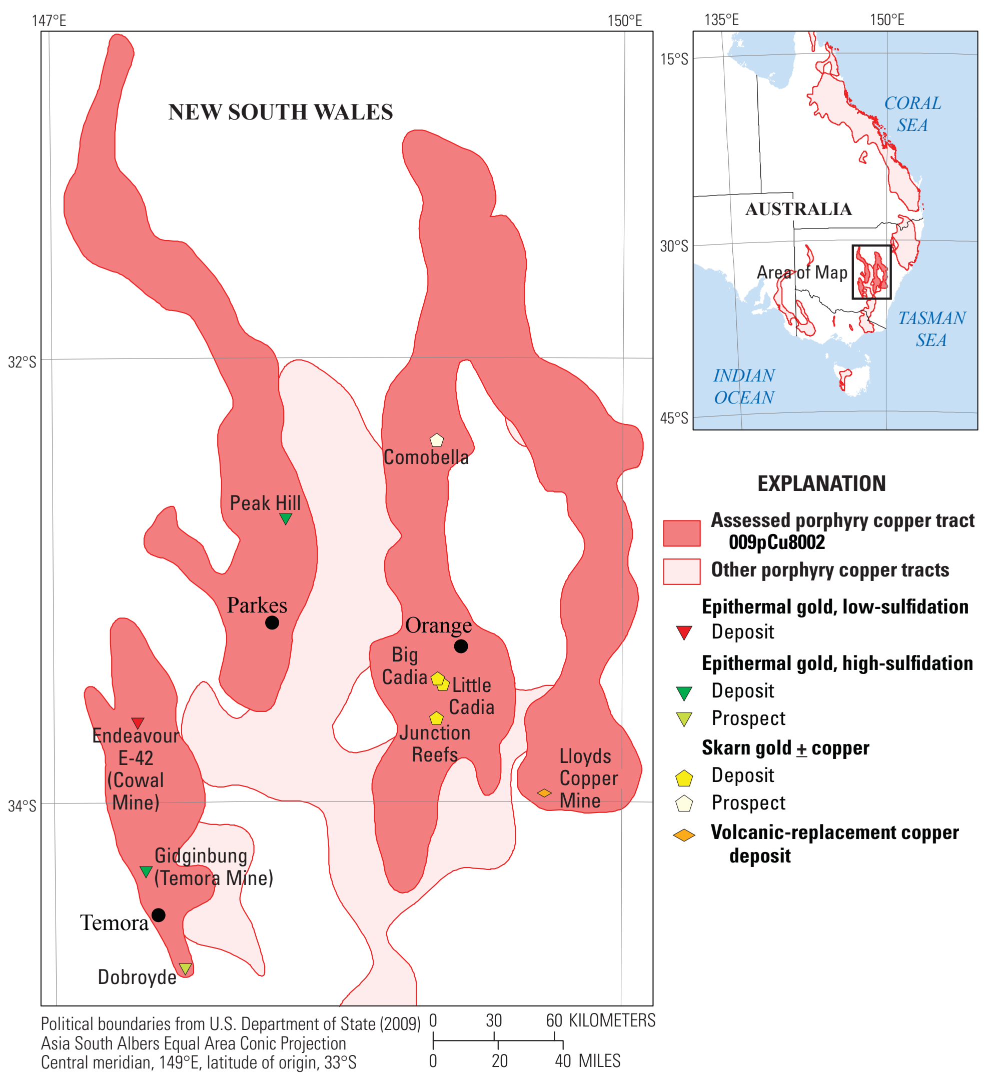

Figure C7. Map of the Macquarie permissive tract, showing locations of deposits and prospects of types that may or may not be associated with porphyry copper systems (as suggested in figure C6).

by 247 percent, from 3,872,000 t copper (according to Singer and others, 2008) to 9,550,000 t copper (according to tonnages and grades reported in the Australian Mines Atlas (Geoscience Australia, 2010)). Most of this increase resulted from analysis of data obtained during deep drilling to discover the downward extent of the Cadia East and Cadia Far East deposits, which are still not completely defined.

In the Northparkes area, copper showings in weathered outcrops of andesitic volcanic rocks have been known since the late 19th century, but porphyry copper exploration did not begin until 1964 (Jones, 1985). According to Lye and others (2006), Geopeko explored for volcanic-hosted massive sulfide deposits in Goonumbla Volcanics from 1972 to 1976. In 1976, a west-to-east traverse of auger-core holes, drilled at 1 km centers, intersected the eastern margin of the Endeavour 22 (E-22) porphyry Cu-Au deposit. This led to the discovery of three other Endeavour deposits (E-26, E-27, and E-48) of the Northparkes mining operation. Three additional porphyry Cu-Au deposits (E-28, E-31N, and E-37) also have been discovered and sufficiently explored to support estimation of tonnage and grade.

Each of the Endeavour porphyry Cu-Au deposits of the Northparkes group of deposits was discovered beneath transported sediments and saprolite. The first two discoveries were made by drilling at 1 km intervals along a road perpendicular to the north-south structural grain. Geophysical surveys over these deposits showed that they are associated with positive magnetic anomalies. A circular reduced-to-pole magnetic anomaly with a diameter of less than about 1 km might correspond to a pencil-like magnetite-bearing intrusion or the top of a hydrothermal system not breached by erosion. A circular magnetic high with a central magnetic low might correspond to a pipe-like body of magnetite-bearing ore around an intrusion in which magnetite was hydrothermally destroyed.

Porphyry Cu-Au deposits that were once exposed and weathered, but are now covered, may nevertheless be associated with detectable geochemical anomalies. In locally derived colluvial or alluvial cover, concentrations of lead, zinc, arsenic, and copper may be detectable. In saprolite, concentrations of copper and gold generally increase downward, from barely detectable in the upper leached zone to ore grade in the lower transition from saprock to bedrock (Tonui and others, 2002).

In the Cadia area, soil and rock-chip geochemical surveys led to discovery of the Cadia Hill and Cadia Quarry deposits, and an IP chargeability anomaly led to discovery of the Ridgeway porphyry Cu-Au deposit. Magnetic anomalies and sub-surface geochemical anomalies led to discoveries of seven Endeavour deposits in the Northparkes area and to discoveries of five deposits in the Temora area.

Positive reduced-to-pole aeromagnetic anomalies in the region of the Macquarie Arc generally coincide with mafic and intermediate rocks of the Macquarie volcanic belts (fig. C8). Such anomalies can therefore be used to indicate subsurface extensions of the Macquarie volcanic belts. Magnetic anomalies with short wave lengths can be isolated by filtering anomalies by wave length. This provides a way to identify relatively small diameter subvolcanic intrusions of oxidized (magnetite-series) porphyry, like those that are associated with porphyry Cu-Au systems in the Cadia and Northparkes areas. Figure C9 shows more than 150 small-diameter magnetic spikes, each buffered to a radius of 2 km, within the boundaries of the Macquarie volcanic belts. Some of these spikes are spatially separate, but others form linear strings or irregular clusters of small-scale magnetic anomalies. More-detailed magnetic surveys in areas of such small-scale magnetic anomalies might show that some are donut-shaped in map view, as are magnetic anomalies associated with the E-27 and E-48 porphyry Cu-Au deposits (according to Lye and others, 2006). Such a donut-shaped magnetic high might indicate an intrusion-centered hydrothermal system, in which magnetite was hydrothermally displaced from a source intrusion to its hydrothermal halo.

Positive gravity anomalies in the region of the Macquarie Arc also generally coincide with bodies of mafic to intermediate rocks of the Macquarie volcanic belts (fig. C9). However, porphyry Cu-Au deposits of the Cadia and Northparkes areas are associated with quartz monzonitic intrusive complexes with lower densities than those of their mafic to intermediate host rocks. As shown in figure C9, the quartz monzonitic Cadia Intrusive Complex is expressed as a subtle west-northwest-elongate trough across the broad north-trending gravity high along the Molong Volcanic Belt. Similarly, quartz monzonite-related deposits of the Northparkes group rim the margins of a gravity embayment in the western margin of a north-trending gravity high. This embayment is interpreted to represent a relatively felsic pluton, hosted in mafic to intermediate rocks of the north-trending Junee-Narromine Volcanic Belt. The Temora cluster of porphyry Cu-Au deposits lies along the eastern edge of a gravity high that is elongate to the north-northwest. These porphyry Cu-Au deposits appear to be associated with small-scale intrusions, emplaced near the margin of a larger body of mafic to intermediate rocks with higher densities.

One way to prioritize the multitude of possible targets indicated by small magnetic anomalies would be to favor those that coincide with relative gravity lows or the margins of gravity highs shown in figure C9. This would favor about 10–20 percent of the small magnetic highs, yielding about 16–32 geophysical targets.

Sources of Information

Principal sources of information used by the assessment team for delineation of Macquarie tract 009pCu8002 are listed in table C5.

Grade and Tonnage Model Selection

The porphyry Cu-Au grade-tonnage model (20c) for porphyry Cu-Au deposits of the world, by Singer and others (2008), best represents undiscovered porphyry Cu-Au deposits of the Macquarie Arc. This choice was made on the basis of a statistical comparison of 9 known deposits in the Macquarie tract against a population of 112 other porphyry Cu-Au deposits included in the global model by Singer and others (2008). To make this comparison, it was necessary to aggregate the identified resources of known deposits, as grouped by the 2-km rule of Singer and others (2005). This yielded a preliminary total of nine Macquarie porphyry Cu-Au systems with known ore tonnages and average grades of copper and gold. Student's *t*-tests at a 1 percent screening threshold yielded *p*-values > 0.05, indicating that the means of the two populations are not statistically different in terms of tonnage of ore, copper grade, or gold grade (table A1). We therefore accept the global model for porphyry Cu-Au deposits as an appropriate grade-tonnage model for estimation of copper and gold resources in undiscovered porphyry Cu-Au deposits of the Macquarie Arc.

Estimate of the Number of Undiscovered Deposits

Before assessment panel members were asked to estimate numbers of undiscovered deposits in a tract, the panel reviewed the geology, known deposits, locations, and qualities of significant porphyry prospects and occurrences, as well as the exploration status of the tract, and geophysical evidence for undiscovered deposits in relatively unexplored

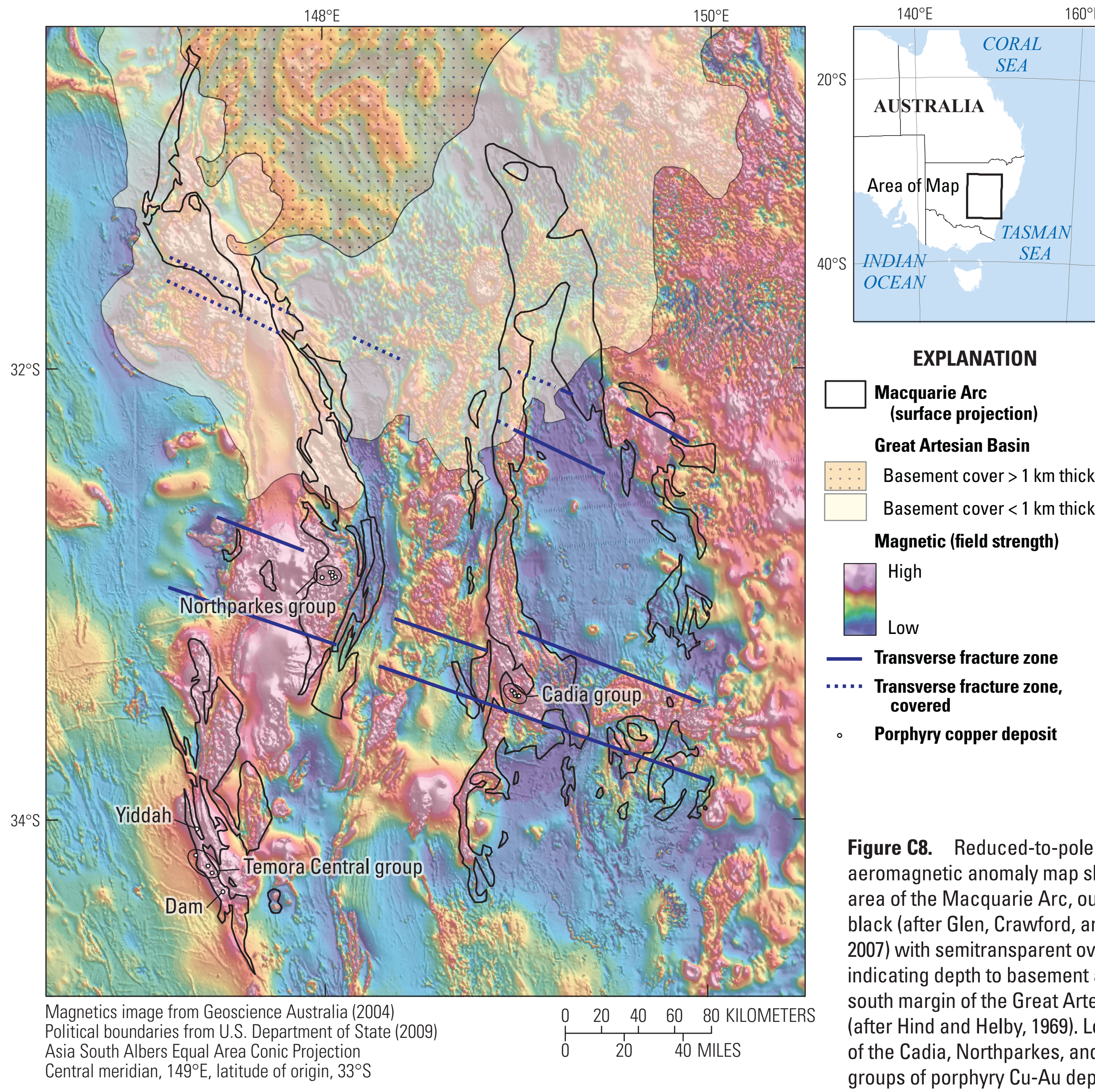

Figure C8. Reduced-to-pole aeromagnetic anomaly map showing the area of the Macquarie Arc, outlined in black (after Glen, Crawford, and Cooke, 2007) with semitransparent overlays indicating depth to basement along the south margin of the Great Artesian Basin (after Hind and Helby, 1969). Locations of the Cadia, Northparkes, and Temora groups of porphyry Cu-Au deposits also are shown. See figure C2 for names of transverse fracture zones. km, kilometer.

or underexplored parts of the tract. Then panel members were asked to list and weigh positive factors, which may indicate undiscovered deposits, versus negative factors, which may limit the number of undiscovered deposits in the permissive tract.

Rationale for the Estimate

The rationale for the estimate was that it should be guided by comparing prospects to known deposits, by counting and assigning probabilities to prospects and occurrences, by consideration of spatial constraints, and by weighing positive versus negative factors listed by the panel members, as follows.

Positive Factors

Positive factors supporting the probability of undiscovered porphyry Cu-Au deposits in the Macquarie tract include:

1. Nine known porphyry Cu-Au systems are present in this tract, and one of them (Cadia) is a giant. About a dozen prospects are spatially associated with known deposits, indicating good potential for extension of known deposits.
2. Compositions of igneous intrusions of Late Ordovician to Early Silurian age are generally favorable for the concentration of copper and gold and for the formation of porphyry Cu-Au deposits.
3. Levels of emplacement and erosion are right for the generation and preservation of subvolcanic intrusions and associated hydrothermal systems within 1 km of the surface.
4. Many skarns, replacement deposits, and epithermal veins are present in this tract, and some could be associated with undiscovered porphyry copper systems.
5. At least a dozen spatially separate porphyry copper prospects are present in this tract, and the majority of these have drilled intercepts of at least 20 m, containing at least 0.15 percent Cu.

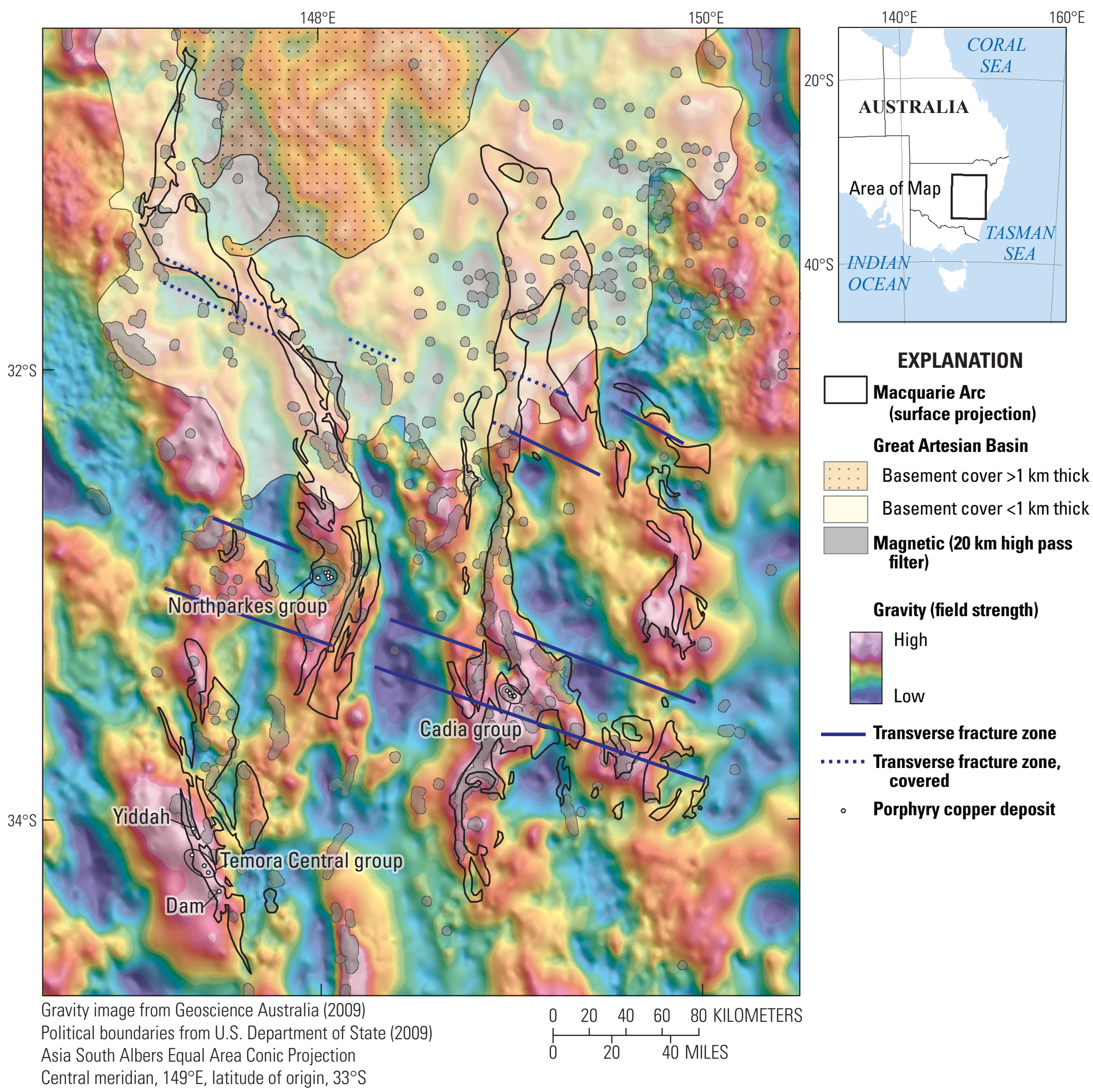

Figure C9. Bouguer gravity anomaly map showing the area of the Macquarie Arc, outlined in black (after Glen, Crawford, and Cooke, 2007) with semitransparent overlays indicating depth to basement along the south margin of the Great Artesian Basin (after Hind and Helby, 1969). Small gray areas indicate magnetic highs that pass a 20-km high-pass filter. Locations of the Cadia, Northparkes, and Temora groups of porphyry Cu-Au deposits also are shown. See figure C2 for names of transverse fracture zones.

Table C5. Principal sources of information used for the Macquarie tract (009pCu8002), New South Wales, Australia.

[NA, not applicable]

Theme	Name or Title	Scale	Citation
Geology	Surface geology of Australia 1:1,000,000 scale, New South Wales—2nd edition	1:1,000,000	Raymond, Liu, Kilgour, Retter, Stewart, and Stewart (2007)
	Surface geology of Australia 1:1,000,000 scale, Victoria—3rd edition	1:1,000,000	Raymond, Liu, Kilgour, Retter, and Connolly (2007)
	The Great Artesian Basin in New South Wales		Hind and Helby (1969)
	Eastern Lachlan Orogen geoscience database version 2	NA	Glen, Dawson, and Colquhoun (2006)
	The Tasmanides of eastern Australia	NA	Glen (2005)
	Geodynamic synthesis of the Phanerozoic of eastern Australia and implications for metallogeny	NA	Champion and others (2009)
	Tectonic setting of porphyry Cu-Au mineralisation in the Ordovician-Early-Silurian Macquarie Arc, eastern Lachlan Orogen, New South Wales	NA	Glen, Crawford, and Cooke (2007)
	Middle and Late Ordovician magmatic evolution of the Macquarie Arc, Lachlan Orogen, New South Wales	NA	Crawford, Cooke, and Fanning (2007)
	Benambran orogeny in the eastern Lachlan Orogen, Australia	NA	Glen, Meffre, and Scott (2007)
	Metallogenic episodes of the Tasman fold belt system, eastern Australia	NA	Perkins and others (1995)
Mineral occurrences	Porphyry copper deposits of the world: database and grade and tonnage models	NA	Singer and others (2008)
	Mineral systems of Australia: An overview of resources, settings and processes	NA	Jaques and others (2002)
	OZMIN mineral deposits database	NA	Ewers and others (2002)
	OZPOT geoprovince-scale assessment of mineral potential	1:2,500,000	Jaireth and Miezitis (2004a, b)
	Intierra	NA	Intierra (2009)
	Australian mines atlas	NA	Geoscience Australia (2010)
	Alkalic porphyry Au-Cu and associated mineral deposits of the Ordovician to Early Silurian Macquarie arc, New South Wales	NA	Cooke and others (2007)
	A review of the metallogeny and tectonics of the Lachlan orogen	NA	Hough and others (2007)
Geophysics	Total magnetic anomaly (TMI) grids of Australia, fourth edition	NA	Geoscience Australia (2004)
	Australian National gravity database 0.5 minute offshore-onshore gravity grid	NA	Geoscience Australia (2009)
Exploration	Australian mineral exploration	NA	Geoscience Australia (2005–2009)
	Advanced mineral projects and exploration highlights in New South Wales	1:3,000,000	NSW Industry and Investment (2010)

6. The northern 30 percent of the permissive tract is covered by overburden less than 1 km thick on the southern margin of the Great Artesian Basin. This area remains to be explored for porphyry Cu-Au.
7. The Nyngan and Hunter River transverse zones are north of but subparallel to the Lachlan Transverse Zone, along which the Cadia and Northparkes porphyry Cu-Au deposits are localized. These transverse zones are mostly covered and have not yet been explored for porphyry Cu-Au deposits.
8. South of the southern margin of the Great Artesian Basin the spatial density of known deposits is 9 deposits in an area of 28,905 km^2, 31 deposits per 100,000 km^2. If the covered area to the north had the same spatial density, that would add three undiscovered deposits.
9. There is plenty of room for hidden undiscovered deposits south of the Great Artesian Basin. South of this covered area, much of the Macquarie tract is deeply weathered to saprolite, and covered by a few to tens of meters of relatively unconsolidated overburden, locally capped by basalt. Mapped surface expressions of permissive units therefore comprise only a small percentage of the southern part of the permissive tract. The remainder is hidden, except in drill-tested areas near known deposits and prospects.
10. Hidden deposits have been found recently by persistent exploration using geologic, geophysical, and geochemical knowledge and methods, combined with drilling, sampling, and assaying.

Negative Factors

Negative factors that may limit the number of undiscovered deposits in the Macquarie tract include:

1. The number of undiscovered deposits is limited by the relatively small size and structural discontinuity of the Maqua-

Table C6. Undiscovered deposit estimates, deposit numbers, tract area, and deposit density for the Macquarie tract (009pCu8002), New South Wales, Australia.

[N_{XX}, estimated number of deposits associated with the xxth percentile; N_{und}, expected number of undiscovered deposits; s, standard deviation; C_v%, coefficient of variance; N_{known}, number of known deposits in the tract that are included in the grade and tonnage model; N_{total}, total of expected number of deposits plus known deposits; Tract area, area of permissive tract in square kilometers; Deposit density, total number of deposits per 100,000 km^2. N_{und}, s, and C_v% are calculated using a regression equation (Singer and Menzie, 2005)]

Consensus undiscovered deposit estimates					Summary statistics					Tract area (km^2)	Deposit density (N_{total}/100,000 km^2)
N_{90}	N_{50}	N_{10}	N_{05}	N_{01}	N_{und}	s	C_v%	N_{known}	N_{total}		
2	7	12	12	12	6.9	3.5	52	9	15.9	41,463	39

Table C7. Results of Monte Carlo simulations of undiscovered resources for the Macquarie tract (009pCu8002), New South Wales, Australia.

[Cu, copper, Mo, molybdenum, Au, gold, and Ag, silver, in metric tons (t); Rock, in million metric tons (Mt)]

Material	Probability of at least the indicated amount						Probability of	
	0.95	0.9	0.5	0.1	0.05	Mean	Mean or greater	None
Cu (t)	350,000	1,500,000	13,000,000	52,000,000	72,000,000	21,000,000	0.34	0.04
Mo (t)	0	0	45,000	370,000	570,000	120,000	0.27	0.15
Au (t)	38	140	1,100	3,500	4,500	1,500	0.36	0.04
Ag (t)	0	0	2,800	18,000	32,000	6,900	0.25	0.10
Rock (Mt)	89	340	2,900	11,000	13,000	4,300	0.36	0.04

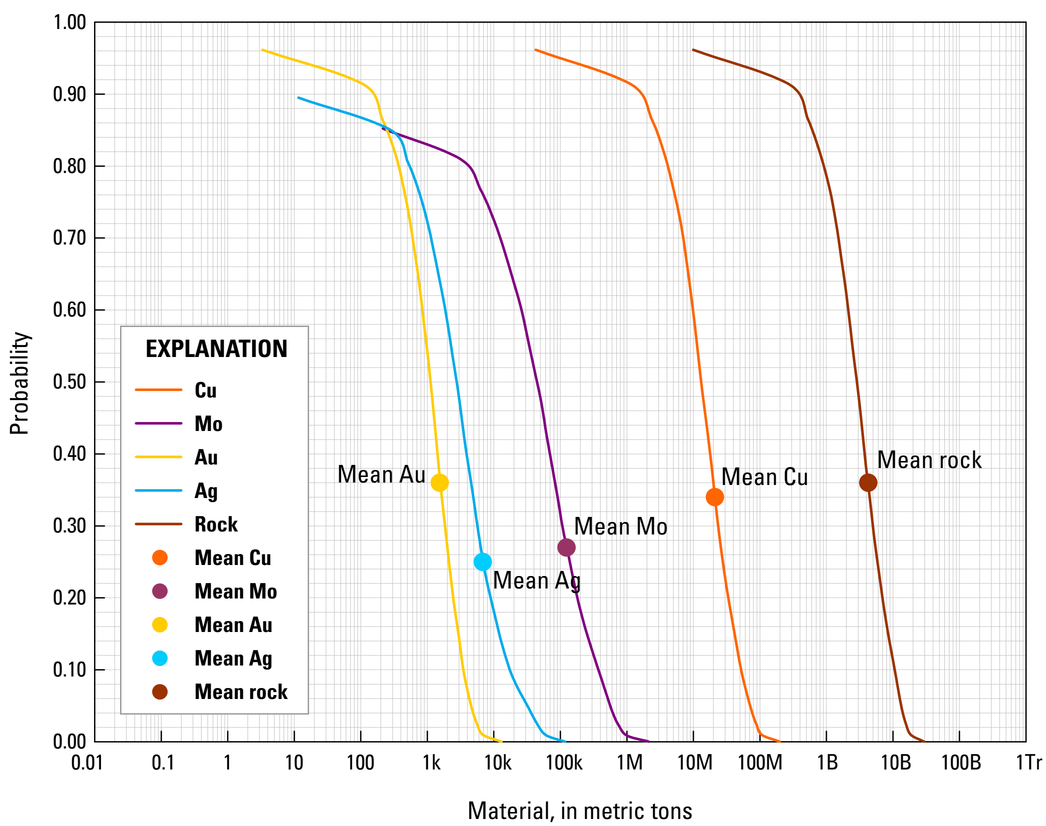

Figure C10. Cumulative frequency plot showing the results of a Monte Carlo computer simulation of undiscovered resources in the Macquarie tract (009pCu8002), New South Wales, Australia. k=thousands, M=millions, B=billions, Tr=trillions.

rie tract. This tract is presently known to contain nine deposits in an area of about 41,500 km^2. Thus, the density of known deposits is equivalent to 22 known deposits per 100,000 km^2, which is within the range of densities of known deposits as a function of tract size, as modeled by Singer and others (2008).

2. The most prospective part of the exposed part of the Macquarie tract is in zones of intersection of the Lachlan Transverse Zone with the Molong and Junee-Narromine Volcanic Belts, and these areas have been quite thoroughly explored for porphyry Cu-Au deposits.

3. Recently discovered deposits outside of the Cadia group are much smaller than recently discovered extensions to known deposits in the Cadia group.

Estimation Process

Each of five estimators (Bookstrom, Glen, Hammarstrom, Robinson, and Zientek) made an independent estimate of the number of undiscovered deposits expected at three levels of subjective probability (90, 50, and 10 percent levels of probability, for example, or if 0 deposits at 90 percent, then at 50, 10, and 5 percent levels of probability). After an anonymous first round of estimation, the high and low estimators explained their reasoning. This led to discussion, negotiation, and settlement on a consensus set of estimates (table C6).

Consensus Estimates

Summary statistics, based on this set of consensus estimates, indicate a mean and standard deviation of 6.9±3.5 undiscovered deposits. The C_v of 52 percent indicates a moderate degree of uncertainty in the consensus-based number of undiscovered deposits expected in the Macquarie tract. Adding the mean estimate of 6.9 undiscovered deposits to the 9 known deposits indicates a total of 15.9 porphyry Cu-Au deposits expected to occur within 1 km of the surface in the Macquarie tract. Inasmuch as the area of the Macquarie tract is 41,463 km^2, this indicates an estimated spatial density of 0.00039 porphyry Cu-Au deposits/km^2 (or about 39 deposits per 100,000 km^2). This estimated density of 39 deposits per 100,000 km^2 for the Macquarie tract is a little below the 90th percentile of spatial densities of porphyry copper deposits as a function of size, as modeled by Singer and others (2008).

Probabilistic Assessment Simulation Results

Undiscovered resources for the tract were estimated (table C7) by combining consensus estimates for numbers of undiscovered porphyry copper deposits with the global porphyry Cu-Au model of Singer and others (2008) using the EMINERS program (Root and others, 1992; Duval, 2012; Bawiec and Spanski, 2012). Cumulative probability graphs show expected amounts of the commodities through a range of levels of subjective probabilities (fig. C10).

References Cited

Alkane Exploration, Ltd., 2004, Prospect acquisitions—New South Wales: Alkane Exploration, Ltd., ASX Announcement, 8 January 2004, accessed May 25, 2010, at http://www.alkane.com.au/reports/asx/pdf/20040108.pdf.

Alkane Resources, Ltd., 2003, Reconnaissance drilling results from Moorilda: Alkane Exploration, Ltd., ASX Announcement—23 June 2003, accessed November 2, 2010, at http://www.alkane.com.au/reports/asx/pdf/20030623.pdf.

Alkane Resources, Ltd., 2006, Peak Hill gold mine: Alkane Exploration, Ltd., Web site, accessed November 18, 2010, at http://www.alkane.com.au/projects/nsw/peak-hill/.

Alkane Resources, Ltd., 2008, Core results from the Caloma and Wyoming Three gold deposits: Alkane Resources, Ltd., ASX Announcement—7 August 2008, accessed November 2, 2010, at http://www.alkane.com.au/reports/asx/pdf/20080807.pdf.

Alkane Resources, Ltd., 2010, McPhillamys first resource estimate—2.96 million oz. gold: Alkane Resources, Ltd., ASX Announcement, 5 July, 2010, accessed November 2, 2010, at http://www.alkane.com.au/reports/asx/pdf/20100705.pdf.

Alkane Resources, Ltd., 2011a, Discovery of porphyry style gold-copper mineralization at Bodangora: Alkane Resources, Ltd., ASX Announcement, 19 April, 2011, accessed January 26, 2012, at http://www.alkane.com.au/reports/asx/pdf/20110419.pdf.

Alkane Resources, Ltd., 2011b, Tomingley gold project, environmental assessment, public exhibition: Alkane Resources, Ltd., Web site accessed January 26, 2012, at http://www/alkane.com.au/.

Allibone, A., 1997, Gold mineralization and advanced argillic alteration at the Dobroyde prospect, central New South Wales: Australian Journal of Earth Sciences, v. 44, no. 6, p. 727–742.

Allibone, A., 1998, Synchronous deformation and hydrothermal activity in the shear zone hosted high-sulphidation Au-Cu deposit at Peak Hill, NSW, Australia: Mineralium Deposita, v. 33, p. 495–512.

Allibone, A.H., Cordery, G.R., Morrison, G.W., Jaireth, Subhash, and Lindhorst, J.W., 1995, Synchronous advanced argillic alteration and deformation in a shear zone-hosted magmatic hydrothermal Au-Ag deposit at the Temora

(Gidginbung) mine, New South Wales, Australia: Economic Geology, v. 90, p. 1570–1603.

Arundell, M.C., 2004, Northparkes Cu-Au mines, central NSW, *in* Butt, C.R.M, Cornelius, M., Scott, K.M., and Robertson, I.D.M., Regolith expression of Australian ore systems—A compilation of geochemical case histories and conceptual models: Cooperative Research Centre for Landscape Environments and Mineral Exploration (CRC LEME), 3 p., accessed May 18, 2011, at http://crcleme.org.au/RegExpOre/Northparkes.pdf.

Bawiec, W.J., and Spanski, G.T., 2012, Quick-start guide for version 3.0 of EMINERS—Economic Mineral Resource Simulator: U.S. Geological Survey Open-File Report 2009–1057, 26 p., available at http://pubs.usgs.gov/of/2009/1057/. (This report supplements USGS OFR 2004–1344.)

Bird, D., 1999, The Ferndale copper-gold project—A case study on exploring for Ordovician porphyry systems beneath Tertiary cover: accessed November 29, 2010, at http://www.smedg.org.au/Sym99bird.htm.

Blevin, P.L., 2002, The petrographic and compositional character of variably K-enriched magmatic suites associated with Ordovician porphyry Cu-Au mineralization in the Lachlan fold belt, Australia: Mineralium Deposita, v. 37, p. 87–99.

Blevin, P.L., Chappell, B.W., and Allen, C.M., 1996, Intrusive metallogenic provinces in eastern Australia based on granite source and composition: Transactions of the Royal Society of Edinburgh—Earth Sciences, v. 87, p. 281–290.

Bowman, H.N., and Richardson, S.J., 1983, Alteration zoning at the Peak Hill disseminated copper-gold deposit: New South Wales Geological Survey Records, v. 21, no. 2, p. M75–M83.

Burraga Copper, Ltd., 2012, Burraga Copper corporate background: Burraga Copper, Ltd., Web page, accessed June 26, 2012, at http://www.burragacopper.com.au/about/company/.

Chalmers, D.I., Ransted, T.W., Kairaitis, R.A., and Meates, D.G., 2007, The Wyoming gold deposits—Volcanic-hosted lode-type gold mineralization in the eastern Lachlan Orogen, Australia: Mineralium Deposita, v. 42, p. 505–513.

Champion, D.C., Kositcin, N., Huston, D.L., Mathews, E., and Brown, C., 2009, Geodynamic synthesis of the Phanerozoic of eastern Australia and implications for metallogeny: Geoscience Australia, Record 2009/18, GeoCat#68866, 222 p., accessed October 4, 2010, at http://www.ga.gov.au/products/.

Chapman, J.R., 2003, Peak Hill Au deposit, Peak Hill, NSW, *in* Butt, C.R.M, Cornelius, M., Scott, K.M., and Robertson, I.D.M., Regolith Expression of Australian Ore Systems—A compilation of geochemical case histories and conceptual models: Cooperative Research Centre for Landscape Environments and Mineral Exploration (CRC LEME), 3 p., accessed March 26, 2013, at http://crcleme.org.au/RegExpOre/PeakHill.pdf.

Clancy Exploration, Ltd., 2009, Myall Exploration Lease 6913 (Kingswood prospect), *in* Quarterly activities report for the period ending 30 June 2009: Clancy Exploration, Ltd., accessed August 11, 2010, at http://www.clancyexploration.com/Shared/Sites/clancy/Assets/Your%20Files/News/press_releases/June%202009%20Qly%20activities.pdf.

Clancy Exploration, Ltd., 2010, Annual report 2010: Clancy Exploration, Ltd., Web site, accessed May 19, 2011, at http://www.clancyexploration.com/Shared/Sites/clancy/Assets/Your%20Files/Clancy%20Exploration%202010%20Annual%20Report%20LowResNew.pdf.

Clark, D.A., 1999, Magnetic petrology of igneous intrusions—Implications for exploration and magnetic interpretation: Exploration Geophysics, v. 30, p. 5–26.

Coianiz, G., and Burrell, P., 2007, Update on the Copper Hill porphyry project: Mines and Wines Symposium, Mineral Exploration in the Tasmanides, Australian Institute of Geoscientists, AIG Bulletin 46, p. 27–30.

Collett, D.K., 2007, The Cadia East deposit—Ensuring at least 30 more years of mining at Cadia Valley—Newcrest Mining [abs.]: Mines and Wines Symposium, 2007, Mineral Exploration in the Tasmanides, Orange, NSW, AIG Bulletin 46, p. 31.

Cooke, D.R., Heithersay, P.S., Wolfe, R., and Calderon, A.L., 1998, Australian and western Pacific porphyry Cu-Au deposits—Exploration model: Australian Geological Survey Organisation Journal of Australian Geology and Geophysics, v. 17, no. 4, p. 97–104.

Cooke, D.R., Wilson, A.J., House, M.J., Wolfe, R.C., Walshe, J.L., Lickfold, V.., and Crawford, A.J., 2007, Alkalic porphyry Au-Cu and associated mineral deposits of the Ordovician to Early Silurian Macquarie Arc, New South Wales: Australian Journal of Earth Sciences, v. 54, p. 445–463.

Corbett, G.J, and Leach, T.M., 1998, Gold-copper systems in porphyry environments, *in* Corbett, G.J. and Leach, T.M. eds., Southwest Pacific Rim gold-copper systems—Structure, alteration, and mineralization: Society of Economic Geologists Special Publication 06, 236 p. [CD ROM] (Also available at http://www.segweb.org/store/info/SP06.doc/.)

Cox, D.P., 1986a, Descriptive model of porphyry Cu-Au (model 20c), *in* Cox, D.P. and Singer, D.A., eds., Mineral deposit models: U.S. Geological Survey Bulletin 1693, p. 110–111.

Cox, D.P., 1986b, Descriptive model of porphyry Cu (model 17), *in* Cox, D.P., and Singer, D.A., eds., Mineral deposit models: U.S. Geological Survey Bulletin 1693, p. 76–79.

Crawford, A.J., Cooke, D.R., and Fanning, C.M., 2007, Geochemistry and age of magmatic rocks in the unexposed Narromine, Cowal and Fairholme igneous complexes in the Ordovician Macquarie Arc, New South Wales: Australian Journal of Earth Sciences, v. 54, p. 243–271.

Crawford, A.J., Meffre, S., Squire, R.J., Barron, L.M., and Falloon, T.J., 2007, Middle and Late Ordovician magmatic evolution of the Macquarie Arc, Lachlan Orogen, New South Wales: Australian Journal of Earth Sciences, v. 54, p. 181–214.

Cube Consulting Pty. Ltd., 2006, Discovery Ridge gold project NSW, Australia: Perth, Western Australia, NI-43–101 compliant Independent Technical Report for Goldminco Corporation, March, 2006, 68 p., accessed May 24, 2011, at http://www.sedar.com/.

Duval, J.S., 2012, Version 3.0 of EMINERS—Economic Mineral Resource Simulator: U.S. Geological Survey Open-File Report 2004–1344, available at http://pubs.usgs.gov/of/2004/1344/.

Ewers, G.R., Evans, N., and Hazell, M., (Kilgour, B., compiler), 2002, OZMIN Mineral Deposit Database [Digital GIS Dataset]: Canberra, Geoscience Australia, CD ROM. (Also available at http://www.ga.gov.au/meta/ANZCW0703003393.html.)

Fredricksen, D., 2006, Sustainable gold and copper production, Cadia Valley operations: Mines and Wines Symposium, 2006, Orange, NSW, Speaker Program, Dean Fredricksen, 36-slide Powerpoint presentation, accessed July 22, 2010, at http://www.smedg.org.au/M&WProg.htm.

Forster, D.B., Seccombe, P.K., and Phillips, David, 2004, Controls on skarn mineralization and alteration at the Cadia deposits, New South Wales, Australia: Economic Geology, v. 99, p. 761–788.

Geoscience Australia, 2004, Fourth edition total magnetic anomaly (TMI) grids of Australia: Canberra, Geoscience Australia, accessed May 19, 2010, at http://www.geoscience.gov.au/.

Geoscience Australia, 2005–2009, Australian mineral exploration—A review of exploration for the years 2005 to 2009: Canberra, Geoscience Australia, accessed May 25, 2010, at http://www.geoscience.gov.au/.

Geoscience Australia, 2009, Australian national gravity database 0.5 minute offshore-onshore gravity grid: Canberra, Geoscience Australia, accessed May 19, 2010, at http://www.geoscience.gov.au/.

Geoscience Australia, 2010, Australian atlas of mines and mineral deposits: Canberra, Geoscience Australia, accessed October 20, 2010, to December 27, 2010, at http://www.australianminesatlas.gov.au/.

Glen, R.A., 1992, Thrust, extensional and strike-slip tectonics in an evolving Palaeozoic orogen—A structural synthesis of the Lachlan Orogen of southeastern Australia: Tectonophysics, v. 214, p. 341–380.

Glen, R.A., 2005, The Tasmanides of eastern Australia, *in* Vaughn, A.P.M., Leat, P.T., and Pankhurst, R.J., eds., Terrane processes at the margins of Gondwana: Geological Society, London, Special Publications, v. 246, p. 23–96.

Glen, R.A., convener, 2009, The third and final workshop of IGCP-542—Continent-island arc collisions—How anomalous is the Macquarie arc? Conference Report, Orange, New South Wales, Australia, April 13–22, 2009: Episodes, Journal of International Geoscience, v. 32, no. 3, p. 208–210.

Glen, R.A., and Walshe, J.L., 1999, Cross-structures in the Lachlan Orogen—The Lachlan transverse zone example: Australian Journal of Earth Sciences, v. 46, p. 641–658.

Glen, R.A, Crawford, A.J., and Cooke, D.R., 2007, Tectonic setting of porphyry Cu-Au mineralization in the Ordovician-Early Silurian Macquarie Arc, eastern Lachlan Orogen, New South Wales: Australian Journal of Earth Sciences, v. 54, p. 465–479.

Glen, R.A., Crawford, A.J., Percival, I.G., and Barron, L.M., 2007, Early Ordovician development of the Macquarie Arc, Lachlan Orogen, New South Wales: Australian Journal of Earth Sciences, v. 54, p. 167–179.

Glen, R.A., Dawson, M.W., and Colquhoun, G.P., 2006, Eastern Lachlan Orogen Geoscience Database (DVD-ROM), Version 2: NSW, Department of Primary Industries—Minerals, Geological Survey of New South Wales, Maitland, New South Wales, Australia.

Glen, R.A., Dawson, M.W., and Colquhoun, G.P., 2007, Solid geology of the Eastern Lachlan Orogen, New South Wales, Australia: Sydney, Geological Survey of New South Wales, Department of Primary Industries, GIS compilation on CD-ROM.

Glen, R.A., Meffre, S., and Scott, R.J., 2007, Benambran Orogeny in the Eastern Lachlan Orogen, Australia: Australian Journal of Earth Sciences, v. 54, no. 2, p. 385–415.

Glen, R.A., Percival, I.G., and Quinn, C.D., 2009, Ordovician continental margin terranes in the Lachlan Orogen, Australia—Implications for tectonics in an accretionary orogen along the east Gondwana margin: Tectonics, v. 28, 17 p.

Goldminco Corp., 2008, Goldminco acquires ground along strike from the Dam porphyry copper-gold deposit, at its 100% owned Temora Project: Goldminco Corp., accessed October 2010 at http://www.goldminco.com/images/stories/newsrelease/2008/Goldminco_acquires_ground_along_strike_from_the%20_DAM_Porphyry_Coopper-Gold_Deposit,_at_its_100_owned_Temora_Project_%2120080229.pdf.

Goldminco Corp., 2010, Additional strong copper and gold intersection recorded at Culingerai: Goldminco Corp., accessed October 2010, at http://www.goldminco.com/media/files/new_releases/2010/Additional_Strong_Copper_and_Gold_Intersection_Recorded_at_Culingerai_!20100726.pdf.

Golden Cross Resources, 2011, Copper Hill: Golden Cross Resources Web site, accessed January 26, 2012, at http://www.goldencross.com.au/projects/australian-projects/copper-hill/.

Gray, N., Mandyczewsky, Alex, and Hine, Richard, 1995, Geology of the zoned gold skarn system at Junction Reefs, New South Wales: Economic Geology, v. 90, p. 1533–1552.

Harris, A.C., Cooke, D.R., Fox, N., Cuison, A.L, Tosdal, R., Groome, M., Percival, I., Dunham, P., Collett, D., Holliday, J., and Allen, C.M., 2010, Architectural controls on Palaeozoic porphyry Au-Cu mineralization in the Cadia Valley, NSW: Arc Mineral Systems, Mines and Wines Symposium, 2010, Mudgee, NSW, 20-slide presentation, accessed January 31, 2010, at http://smedg.org.au/M&W%202010/Harris%20Cadia%20Au-Cu%20Mineralization.pdf.

Harris, A.C., Cuison, A.L.G., Chang, S., Cooke, D.R., Bonnici, N. Faure, K., and Cross, C., 2007, Fe-rich magmatic volatiles in the Ridgeway Au-cu porphyries—Evidence from magnetite-quartz comb-layered textures, *in* Andrew, C.J., ed., Digging Deeper: Proceedings of the Ninth Biennial Society for Geology Applied to Mineral Deposits Meeting, Dublin, p. 415–418.

Heithersay, P.S., O'Neill, W.J., van der Helder, P., Moore, C.R., and Harbon, P.G., 1990, Goonumbla porphyry copper district—Endeavour 26 North, Endeavour 22 and Endeavour 27 copper-gold deposits: Australasian Institute of Mining and Metallurgy Monograph 14, p. 1385–1398.

Heithersay, P.S., and Walshe, J.L., 1995, Endeavour 26 North—A porphyry copper-gold deposit in the Late Ordovician shoshonitic Goonumbla Volcanic Complex, New South Wales, Australia: Economic Geology, v. 90, p. 1506–1532.

Hind, M.C., and Helby, R.J., 1969, The Great Artesian Basin in New South Wales: Australian Journal of Earth Sciences, v. 16, no. 1, p. 481–497.

Holliday, J., McMillan, C., and Tedder, I., 1999, Discovery of the Cadia-Ridgeway gold-copper porphyry deposit: Mines and Wines Symposium, 1999, accessed August 17, 2010, at http://www.smedg.org.au/Sym99cadia.htm/.

Holliday, J.R., Wilson, A.J., Blevin, P.L., Tedder, I.J., Dunham, P.D., and Pfitzner, Michael, 2002, Porphyry gold-copper mineralization in the Cadia district, eastern Lachlan Fold Belt, New South Wales, and its relationship to shoshonitic magmatism: Mineralium Deposita, v. 37, p. 100–116.

Hooper, B., Heithersay, P.S., Mills, M.B., Lindhorst, J.W, and Freyberg, J., 1996, Shoshonite-hosted Endeavour 48 porphyry copper-gold deposit, Northparkes, central New South Wales: Australian Journal of Earth Sciences, v. 43, p. 279–288.

Hough, M.A., Bierlein, F.P., and Wilde, A.R., 2007, A review of the metallogeny and tectonics of the Lachlan Orogen: Mineralium Deposita, v. 42, p. 435–448.

Intierra, 2009, Intierra home page: accessed 2009 at http://www.intierra.com/Homepage.aspx.

Jacques, A.L., Jaireth, S., and Walshe, J.L., 2002, Mineral systems of Australia—An overview of resources, settings and processes: Australian Journal of Earth Sciences, v. 49, no. 4, p. 623–660.

Jaireth, S., and Miezitis, Y., 2004a, Porphyry copper-gold, *in* Jaireth, Subhash, and Miezitis, Yanis, compilers, OZPOT Geoprovince-scale assessment of mineral potential [1:2,500,000 scale GIS]: Canberra, Geoscience Australia, accessed June 15, 2010, at http://www.australianminesatlas.gov.au/build/common/minpot.jsp.

Jaireth, S., and Miezitis, Y., 2004b, OZPOT Geoprovince-scale assessment of mineral potential [1:2,500,000 scale GIS]: Canberra, Geoscience Australia, accessed June 21, 2010, to December 27, 2010, at http://www.australianminesatlas.gov.au/build/common/minpot.jsp.

John, D.A., Ayuso, R.A., Barton, M.D., Blakely, R.J., Bodnar, R.J., Dilles, J.H., Gray, F., Graybeal, F.T., Mars, J.C., McPhee, D.K., Seal, R.R., Taylor, R.D., and Vikre, P.G., 2010, Porphyry copper deposit model, chapter B *of* Mineral deposit models for resource assessment: U.S. Geological Survey Scientific Investigations Report 2010–5070–B, 169 p., accessed January 15, 2011, at http://pubs.usgs.gov/sir/2010/5070/b/.

Jones, G.J., 1985, The Goonumbla porphyry copper deposits, New South Wales: Economic Geology, v. 80, p. 591–613.

Lachlan Star, Ltd., 2007, Bushranger project, Racecourse prospect: accessed September 30, 2010, at http://www.Lachlanstar.com.au/.

Lawrie, K.C., Mernagh, T.P., Ryan, C.G., van Achterbergh, E., and Black, L.P., 2007, Chemical fingerprinting of hydrothermal zircons—An example from the Gidginbung high sulphidation Au-Ag-(Cu) deposit, New South Wales, Australia: Proceedings of the Geologists' Association, v. 118, p. 37–46.

Lehany, T., 2007, Marsden Project—Presentation to Diggers and Dealers, 2007: accessed 2010, at http://www.newcrest.com/au/.

Le Maitre, R.W., ed., 2002, Igneous Rocks—A classification and glossary of terms—Recommendations of the International Union of Geological Sciences, Subcommission on the Systematics of Igneous Rocks, 2nd Edition: Cambridge University Press, 236 p.

Lickfold, V., Cooke, D.R., Crawford, A.J., and Fanning, C.M., 2007, Shoshonitic magmatism and the formation of the Northparkes porphyry Cu-Au deposits, New South Wales: Australian Journal of Earth Sciences, v. 54, p. 417–444.

Lickfold, V., Cooke, D.R., Smith, S.G., and Ullrich, T.D., 2003, Endeavour copper-gold porphyry deposits, Northparkes, New South Wales—Intrusive history and fluid evolution: Economic Geology, v. 98, p. 1607–1636.

Lye, A., 2010, Northparkes—Still prospective almost 40 years later: Arc Mineral Systems, Mines and Wines Symposium, 2010, Mudgee, New South Wales, Program and Presentations, accessed December 31, 2010, at http://smedg.org.au/M&W%202010/Lye%20Northparkes.pdf.

Lye, A., Crook, G., and van Oosterwijk, L.K., 2006, The discovery history of the Northparkes deposits: Mines and Wines Symposium, 2006, Cessnock, New South Wales, Speaker Programme, Abstracts and Presentations, accessed September 29, 2010, at http://smedg.org.au/M&WProg.htm.

MacCorquodale, F., 1997, The Mandamah porphyry Cu-Au prospect: Geological Society of Australia Abstracts, v. 51, p. 51.

Masterman, G.J., White, N.C., Wilson, C.J.L., and Pape, Daniel, 2002, High-sulfidation gold deposits in ancient volcanic terranes—Insights from the mid-Paleozoic Peak Hill Deposit, NSW: Society of Economic Geologists, SEG Newsletter, no. 51, p. 1 and p. 10–16.

Maynard, A.J., 2003, Blayney porphyry gold-copper project, New South Wales, Australia, exploration license 5922 (including the Discovery Ridge and Ferndale prospects): Independent Geologist's Report for Goldminco Corp, 29 p., accessed May 24, 2011, at http://www.sedar.com/.

McInnes, B., 2006, Exploration reviews, Australasia, New South Wales: Society of Economic Geologists Newsletter, no. 67, p. 35.

McInnes, P., and Freer, L., 2007, The Cowal gold corridor—Opening other doors: Mineral Exploration in the Tasmanides, Mines and Wines Symposium, 2007, Orange, New South Wales, Australian Institute of Geoscientists Bulletin 46, p. 95–100, accessed June 18, 2010, at http://smedg.org.au/M&W/.

Meffre, S., Scott, R.J., Glen, R.A., and Squire, R.J., 2007, Re-evaluation of contact relationships between Ordovician volcanic belts and the quartz-rich turbidites of the Lachlan Orogen: Australian Journal of Earth Sciences, v. 54, p. 363–383.

Miles, I.N., and Brooker, M.R., 1998, Endeavour 42 deposit, Lake Cowal, New South Wales—A structurally controlled gold deposit: Australian Journal of Earth Sciences, v. 45, p. 837–847.

Mowat, B., 2007, Characteristics of porphyry copper-gold mineralization in the Gidginbung Volcanics: Mineral Exploration in the Tasmanides, Mines and Wines Symposium, 2007, Orange, New South Wales, Australian Institute of Geoscientists Bulletin 46, p. 107–112, and Powerpoint presentation, accessed June 18, 2010, at http://smedg.org.au/M&W/.

Mowat, B., and Smith, S., 2006, Characteristics of porphyry Au-Cu systems in the Ordovician Macquarie arc of NSW: Mines and Wines Symposium, 2006, Cessnock, New South Wales, Speaker Programme, Abstracts and Presentations, accessed September 29, 2010, at http://smedg.org.au/M&WProg.htm.

NSW Industry and Investment, 2010, Advanced mineral projects and mineral exploration highlights: New South Wales Department of Primary Industries, geologic map, showing operational mines and active exploration sites, with estimated resources and best intercepts, accessed October 11, 2010, at http://www.industry.nsw.gov.au/.

Panteleyev, A., 1995a, Porphyry Cu-Au—Alkalic (model L03), *in* Lefebure, D.V., and Ray, G.E., eds., Selected British Columbia mineral deposit profiles, vol. 1—Metallics and coal: British Columbia Ministry of Employment and Investment, Energy and Minerals Division, Open File 1995–20, p. 83–86, accessed April 5, 2012, at http://www.empr.gov.bc.ca/Mining/Geoscience/MineralDepositProfiles/.

Panteleyev, A., 1995b, Porphyry Cu±Mo±Au (model L04), *in* Lefebure, D.V., and Ray, G.E., eds., Selected British Columbia mineral deposit profiles, vol. 1—Metallics and coal: British Columbia Ministry of Energy of Employment and Investment, Energy and Minerals Division, Open File 1995–20, p. 87–92, accessed April 5, 2012, at http://www.empr.gov.bc.ca/Mining/Geoscience/MineralDepositProfiles/.

Panteleyev, A., 2005a, Porphyry Cu-Au—Alkalic L03, *in* Fonseca, A., and Bradshaw, G., compilers, Yukon mineral deposits profiles: Yukon Geological Survey Open File 2005–5, 175 p., accessed July 28, 2009, at http://www.geology.gov.yk.ca/mineral_deposit_profiles.html; http://ygsftp.gov.yk.ca/publications/openfile/2005/of2005_5.pdf; http://www.geology.gov.yk.ca/pdf/l03_alkalic_porphyry_cu_au.pdf.

Panteleyev, A., 2005b, Porphyry Cu±Mo±Au L04., *in* Fonseca, A., and Bradshaw, G., compilers, Yukon mineral deposits profiles: Yukon Geological Survey Open File 2005–5, 175 p., accessed July 28, 2009, at http://www.geology.gov.yk.ca/mineral_deposit_profiles.html; http://ygsftp.gov.yk.ca/publications/openfile/2005/of2005_5.pdf; http://www.geology.gov.yk.ca/pdf/l04_porphyry_cu_mo_au.pdf.

Percival, I.G., and Glen, R.A., 2007, Ordovician to earliest Silurian history of the Macquarie Arc, Lachlan Orogen, New South Wales: Australian Journal of Earth Sciences, v. 54, p. 143–165.

Perkins, C., McDougall, I., Claoue-Long, J., and Heithersay, P.S., 1990, $^{40}Ar/^{39}Ar$ and U-Pb geochronology of the Goonumbla porphyry Cu-Au deposits, New South Wales, Australia: Economic Geology, v. 85, p. 1808–1824.

Perkins, C., Walshe, J.L., and Morrison, G., 1995, Metallogenic episodes of the Tasman fold belt system, eastern Australia: Economic Geology, v. 90, p. 1443–1466.

Porter, T.M., and Glen, R.A., 2005, The porphyry Cu-Au deposits and related shoshonitic magmatism of the Palaeozoic Macquarie volcanic arc, eastern Lachlan orogen in New South Wales, Australia—A review, *in* Porter, T.M., ed., Super porphyry copper & gold deposits—A global perspective: PGC Publishing, Adelaide, v. 2, p. 287–312.

Raymond, O.L., Liu, S.F., Kilgour, P., Retter, A.J., and Connolly, D.P., 2007, Surface geology of Australia, 1:1,000,000 scale, Victoria, 3rd edition [Digital Dataset]: Canberra, Geoscience Australia, accessed May 9, 2010, at http://ga.gov.au/.

Raymond, O.L., Liu, S.F., Kilgour, P., Retter, A.J., Stewart, A.J., and Stewart, G., 2007, Surface geology of Australia, 1:1,000,000 scale, New South Wales, 2nd edition [Digital Dataset]: Canberra, Geoscience Australia, accessed June 7, 2010, at http://ga.gov.au/.

Republic Gold, Ltd., 2010, Burraga copper project presents significant development potential—New drilling programme planned: Republic Gold, Ltd., ASX Announcement, accessed October 6, 2010, at http://www.republicgold.com.au/projects/nsw/.

Richards, J.P., 2009, Postsubduction porphyry Cu-Au and epithermal Au deposits—Products of remelting of subduction-modified lithosphere: Geology, v. 37, no. 3, p. 247–250.

Root, D.H., Menzie, W.D., and Scott, W.A., 1992, Computer Monte Carlo simulation in quantitative resource estimation: Natural Resources Research, v. 1, no. 2, p. 125–138.

Scott, K.M., 1978, Geochemical aspects of the alteration-mineralization at Copper Hill, New South Wales, Australia: Economic Geology, v. 73, p. 966–976.

Scott, K.M., and Torrey, C.E., 2003, Copper Hill porphyry Cu-Au prospect, central NSW, *in* Butt, C.R.M, Cornelius, M., Scott, K.M., and Robertson, I.D.M., Regolith expression of Australian ore systems—A compilation of geochemical case histories and conceptual models: Cooperative Research Centre for Landscape Environments and Mineral Exploration (CRC LEME), 3 p., accessed January 26, 2012, at crcleme.org.au/Pubs/Monographs/RegExpOre.html.

Seedorf, E., Dilles, J.H., Proffett, J.M., Jr., Einaudi, M.T., Zurcher, Lukas, Stavast, W.J.A., Johnson, D.A., and Barton, M.D., 2005, Porphyry deposits—Characteristics and origin of hypogene features *in* Hedenquist, J.W., Thompson, J.F.W., Goldfarb, R.J., and Richards, J.P., eds., One hundredth anniversary volume 1905–2005: Littleton, Colo., Society of Economic Geologists, p. 251–298.

Sillitoe, R.H., 1989, Gold deposits in western Pacific island arcs—The magmatic connection, *in* Keays, R.R., Ramsay, W.R.H., and Groves, D.I., eds., The geology of gold deposits—The perspective in 1988: Economic Geology Monograph 6, p. 274–291.

Simpson, C.J., Cas, R.A.F., and Arundell, M.C., 2005, Volcanic evolution of a long-lived Ordovician island-arc province in the Parkes region of the Lachlan Fold Belt, southeastern Australia: Australian Journal of Earth Sciences, v. 52, p. 863–886.

Simpson, C.J., Scott, R.J., Crawford, A.J., and Meffre, S., 2007, Volcanology, geochemistry and structure of the Ordovician Cargo Volcanics in the Cargo-Walli region, central New South Wales: Australian Journal of Earth Sciences, v. 54, p. 315–352.

Singer, D.A., 1995, World class base and precious metal deposits—A quantitative analysis: Economic Geology, v. 90, p. 88–104.

Singer, D.A., Berger, V.I., Menzie, W.D., and Berger, B.R., 2005, Porphyry copper density: Economic Geology, v. 100, no. 3, p. 491–514.

Singer, D.A., Berger, V.I., and Moring, B.C., 2008, Porphyry copper deposits of the world—Database and grade and tonnage models, 2008: U.S. Geological Survey Open-File Report 2008–1155, 45 p., available at http://pubs.usgs.gov/of/2008/1155/.

Singer, D.A., and Menzie, W.D., 2005, Statistical guides to estimating the number of undiscovered mineral deposits—An example with porphyry copper deposits, *in* Cheng, Qiuming, and Bonham-Carter, Graeme, eds., Proceedings of IAMG—The annual conference of the International Association for Mathematical Geology: Toronto, Canada, Geomatics Research Laboratory, York University, p. 1028–1033.

Squire, R.J., and Crawford, A.J., 2007, Magmatic characteristics and geochronology of Ordovician igneous rocks from the Cadia-Neville region, New South Wales—Implications for tectonic evolution: Australian Journal of Earth Sciences, v. 54, p. 293–314.

Stanton, R.L., 1953, The Lloyd copper mine, Burraga, *in* Edwards, A.B., ed., Geology of Australian Ore Deposits: Melbourne, Australasian Institute of Mining and Mettalurgy, p. 906–909.

Stanton-Cook, K., 2011, Golden Cross Resources Copper Hill porphyry Cu-Au deposits: accessed January 26, 2012, at http://smedg.org.au/Kim_Stanton-Cook_Copper_Hill.pdf.

Taylor, G.R., 1983, Copper and gold in skarn at Brown's Creek, Blayney, NSW: Australian Journal of Earth Sciences, v. 30, no. 3, p. 431–442.

Tonui, E., Jones, R., and Scott, K., 2002, Regolith mineralogy and geochemical dispersion at the Northparkes Cu-Au deposits, New South Wales, Australia: Geological Society, London, Geochemistry—Exploration, Environment, Analysis, v. 2, p. 345–360.

Torrey, C., and Burrell, P., 2006, Geology and mineralization of the Copper Hill area: Orange, New South Wales, Mines and Wines Symposium 2006, Mineral exploration in the Tasmanides, Speaker Program, Abstracts and Presentations, accessed July, 22, 2010, at http://www.smedg.org.au/M&WProg.htm.

Torrey, C.E., and White, P.D., 1998, Porphyry copper and gold mineralization at Cargo, NSW: Geological Society of Australia, 14th Australian Geological Convention, Townsville, July 1998, Abstracts No. 49, p. 442.

U.S. Department of State, 2009, Small-scale digital international land boundaries (SSIB)—Lines, edition 10, and polygons, beta edition 1, *in* Boundaries and Sovereignty Encyclopedia (B.A.S.E.): U.S. Department of State, Office of the Geographer and Global Issues.

Wilson, A.J., Cooke, D.R., and Harper, B.L., 2003, The Ridgeway gold-copper deposit—A high-grade alkalic porphyry deposit in the Lachlan fold belt, New South Wales, Australia: Economic Geology, v. 98, p. 1637–1666.

Wilson, A.J., Cooke, D.R., Harper, B.J., and Deyell, C.L., 2007, Sulfur isotopic zonation in the Cadia district, southeastern Australia—Exploration significance and implications for the genesis of alkalic porphyry gold-copper deposits: Mineralium Deposita, v. 42, p. 465–487.

Wilson, A.J., Cooke, D.R., Stein, H.J., Fanning, M.C., Holliday, J.R., and Tedder, I.J., 2007, U-Pb and Re-Os geochronologic evidence for two alkalic porphyry ore-forming events in the Cadia district, New South Wales, Australia: Economic Geology, v. 102, p. 3–26.

Wood, D., 2012a, Discovery of the Cadia deposits, NSW, Australia (part 1): Littleton, Colorado, Society of Economic Geologists Newsletter, no. 88, p. 1 and p. 13–18.

Wood, D., 2012b, Discovery of the Cadia deposits, NSW, Australia (part 2): Littleton, Colorado, Society of Economic Geologists Newsletter, no. 89, p. 1 and p. 17–22.

Appendix D. Porphyry Copper Assessment for Tract 009pCu8003, Yeoval, Australia

By Arthur A. Bookstrom[1], Richard A. Glen[2], Jane M. Hammarstrom[3], Gilpin R. Robinson, Jr.[3], and Michael L. Zientek[1]

Deposit Type Assessed

Deposit type: Porphyry copper

Descriptive models: Porphyry copper (Cox, 1986, John and others, 2010), porphyry Cu ± Mo ± Au (Panteleyev, 1995, 2005)

Grade and tonnage model: Eastern Australian porphyry copper (appendix A)
Table D1 summarizes selected assessment results.

Table D1. Summary of selected resource assessment results for Yeoval tract (009pCu8003), New South Wales and Victoria, Australia.

[km, kilometers; km^2, square kilometers; t, metric tons]

Date of assessment	Assessment depth (km)	Tract area (km^2)	Known copper resources (t)	Mean estimate of undiscovered copper resources (t)	Median estimate of undiscovered copper resources (t)
September 2010	1	53,157	49,700	71,000	25,000

Location

The Yeoval permissive tract is on the western side of the Great Dividing Range in southeastern Australia. It extends nearly north-south, from eastern New South Wales to southeastern Victoria (fig. D1).

Geologic Feature Assessed

Permissive igneous rocks of Late Silurian to Devonian age in and around the Cowra-Buchan Rift Complex (as informally named here, and outlined in figure D2*A*).

[1]U.S. Geological Survey, Spokane, Washington, United States.

[2]Geological Survey of New South Wales, Hunter Region Mail Centre, New South Wales, Australia.

[3]U.S. Geological Survey, Reston, Virginia, United States.

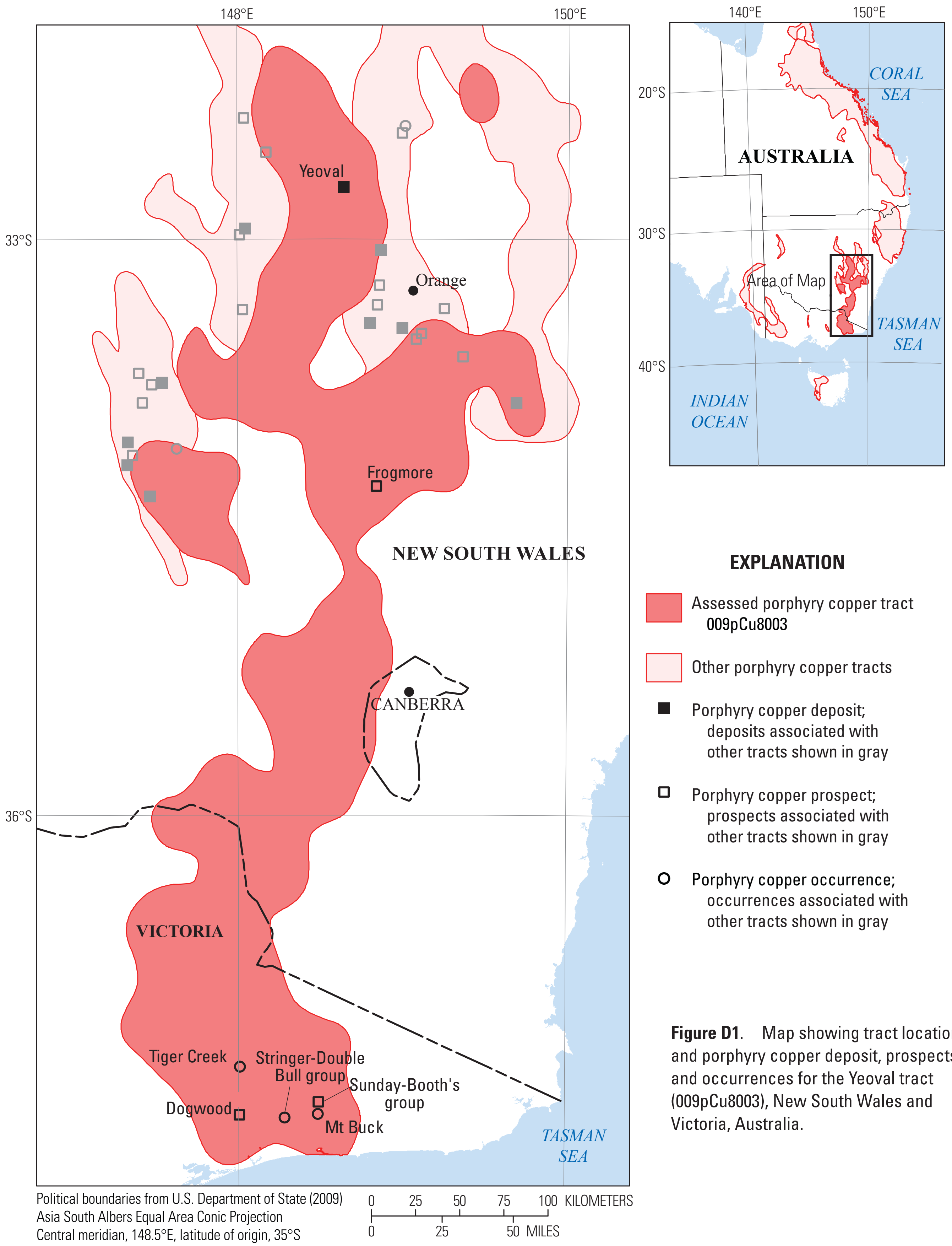

Figure D1. Map showing tract location and porphyry copper deposit, prospects, and occurrences for the Yeoval tract (009pCu8003), New South Wales and Victoria, Australia.

Delineation of the Permissive Tract

Geologic Criteria

The Yeoval tract is in the eastern part of the Lachlan Orogen. It is defined by a belt of volcanic and intrusive igneous rocks of Late Silurian to Devonian age in and around the north-south-elongate Cowra-Buchan Rift Complex, which is about 600 km long and 100–260 km wide. From north to south, the Cowra-Buchan Rift Complex is comprised of the Cowra Trough, the Tumut Trough, and the Buchan Rift (fig. D2*A* and *B*).

The Yeoval porphyry copper deposit (figs. D1, D2*B*) is associated with dioritic to dacitic intrusions of Early Devonian age in the Cowra Trough. The Dogwood and Sunday Creek porphyry copper prospects are associated with granitoid intrusions of Devonian age in and around the Buchan Rift (fig. D2*B*).

Geologic Setting and History of the Cowra-Buchan Rift Complex

The Silurian-Devonian Cowra-Buchan Rift Complex is in the eastern part of New South Wales, where it is superimposed on the Late Ordovician-Early Silurian Macquarie Arc (fig. D2*A*). According to Champion and others (2009), north-south elongate rifts formed after the Benambran Orogeny (440–430 Ma) in the eastern part of the Lachlan Orogen. Such rifts filled with shallow- to deep-marine sediments and predominantly felsic volcanics of Silurian age before the Bindian Orogeny (420–410 Ma). During the latest Silurian to Early Devonian Bindian Orogeny, rift-fill strata were folded and intruded by plutons of dioritoid to granitoid composition. Bindian folding and magmatism affected only the eastern part of the Lachlan Orogen, but the Late Devonian Tabberabberan Orogeny affected most of the Lachlan Orogen.

Porphyry copper sites and a Cu-Au skarn site in the Yeoval tract formed in association with dioritic to dacitic intrusions, emplaced during and after the Bindian Orogeny. Permissive plutons of Devonian age could have been emplaced during either the Bindian Orogeny or the Tabberabberan Orogeny.

Alternative Plate Tectonic Models

Interpretation of the assembly of the Lachlan Orogen has involved two contrasting sets of models—those that involve progressive orogen-normal addition of sediment in accretionary complexes across multiple back-arc subduction zones inboard from the plate boundary, and those that involve orogen-parallel transport (Glen and others, 2009). In the orogen-parallel-transport plate-tectonic model of Glen and others (2009), amalgamation of the eastern Lachlan terranes is explained by a combination of west-dipping subduction beneath the Macquarie Arc and left-lateral displacements along a northwest-trending strike-slip margin southeast of the Macquarie Arc. According to this model, the western Lachlan terranes were accreted to the Delamerian Orogen (fig. B1) in Ordovician time, and the eastern Lachlan terranes were amalgamated during the Early Silurian Benambran Orogeny, but were not accreted to the previously accreted western terranes until the Late Devonian Tabberabberan Orogeny. This explains how the Bindian Orogeny affected the amalgamated but still offshore eastern Lachlan terranes without affecting the previously accreted western Lachlan terranes. However, the orogen-parallel-transport model of Glen and others (2009) does not directly address the origin of post-Benambran rifts or the plate-tectonic setting and cause of the Bindian Orogeny.

In the orogen-normal accretionary plate-tectonic model of Gray and Foster (2004), the time interval from 450 to 410 Ma includes the Benambran Orogeny, Silurian rifting, and the Bindian Orogeny. The Macquarie Arc is shown to be between an outboard southwest-dipping sinistral, transpressional subduction zone to the northeast and an inboard northeast-dipping subduction zone to the southwest. According to Gray and Foster (2004, p. 809), "oblique convergence on the outboard subduction system led to sinistral transpressional deformation in the Macquarie Arc . . . with development of Early Silurian extensional basins in the arc" (possibly in response to subduction rollback after the Benambran Orogeny). Strike-slip pull-apart basins may also have formed in association with "limited southwards translation of the metamorphic belt" (along the inboard margin of the inboard subduction zone), according to Gray and Foster (2004, p. 809).

Such basins filled with Silurian sedimentary and volcanic deposits, and were then deformed and invaded by igneous intrusions during the Bindian and Tabberabberan Orogenies. Both of these orogenies probably occurred in response to west-dipping subduction. The Bindian Orogeny (about 420–410 Ma) occurred before the amalgamated eastern Lachlan terranes were accreted to the previously accreted western Lachlan terranes. The Tabberabberan Orogeny (about 485–475) occurred during accretion of the eastern Lachlan terranes to the western Lachlan terranes (time intervals of these orogenies are from Champion and others, 2009). Orogen-normal accretionary models do not account for meta-turbidite terranes east and west of the Macquarie Arc.

Permissive igneous rocks of the Yeoval permissive tract are spatially associated with the Cowra-Buchan Rift Complex. The magmatism that produced them probably occurred in response to west-dipping subduction associated with the Bindian and Tabberabberan orogenies. To the east and west of the Cowra-Buchan Rift Complex, there are large plutons of permissive composition. These have been well mapped and explored, and they contain no known porphyry copper deposits or significant porphyry copper prospects.

Within the Cowra-Buchan Rift Complex, the ratio of Silurian to Devonian volcanic to intrusive rocks is 1v/1.1i, both stocks and larger plutons are exposed, and several porphyry copper sites are present (fig. D2*B*). This indicates a permissive level of erosion for both preservation and exposure of porphyry copper deposits in the Yeoval permissive tract.

East of the Cowra-Buchan Rift Complex, batholithic plutons of Silurian to Devonian age are exposed, as shown in figure D2*B*. There, the ratio of volcanic to related intrusive rocks is very low (1v/8.7i), which indicates very deep levels of exposure, probably much too deep for the preservation of porphyry copper deposits.

West of the Yeoval permissive tract, large plutons and smaller stocks are exposed, and the ratio of volcanic to related intrusive rocks is 1v/2.7i (fig. D2*B*). This together with a lack of known porphyry copper deposits and prospects indicates that levels of exposure west of the Yeoval permissive tract are too deep for preservation of typical porphyry copper deposits. Nevertheless, quartz-molybdenite veins at the Everton Molybdenite Mine and minor copper occurrences in the Strathbogie granodiorite pluton (fig. D2*B*) indicate that this western area may contain remnants of the lower parts of intrusion-related magmatic-hydrothermal systems.

Igneous Rocks of the Yeoval Permissive Tract

The Yeoval Diorite Complex, which hosts the Yeoval porphyry copper deposit, was emplaced into folded rift-fill volcanic and sedimentary strata of Silurian age that were previously folded during the Bindian Orogeny. Gulson (1972) described the Yeoval Diorite Complex as a calc-alkaline suite of rocks ranging from gabbro through diorite to granodiorite, with associated fine-grained rock types ranging from andesite to dacite. Ambler and Facer (1975) showed a photomicrograph of porphyro-aphanitic dacite from the Yeoval Diorite Complex.

Gulson and Bofinger (1972) reported a whole-rock Rb-Sr isochron age determination of 411±2 Ma and an initial $^{87}Sr/^{86}Sr$ = 0.705 for rocks of the Yeoval Diorite Complex. This age determination corresponds to the end of the Bindian Orogeny, during which post-Benambran rift-fill sediments were folded from about 420 to 410 Ma (Champion and others, 2009). Gabbroic phases and the low Sr-isotopic initial ratio of the Yeoval Diorite Complex indicate mafic parent magmas with relatively little assimilation of older crustal constituents.

Gulson (1972) suggested that the Yeoval Diorite Complex is chemically similar to high-K andesites in orogenic zones associated with Benioff seismic zones (associated with subduction zones) around the Pacific margin, as described by Dickinson and Hatherton (1967). A linear regression of K_2O versus SiO_2 based on average compositions of low-Si diorites, normal diorites, and high-K diorites and granodiorites from the Yeoval Diorite Complex, reported by Gulson (1972), indicates that K_{55} = 1.4 (K_2O = 1.4 percent at SiO_2 = 55 percent), and K_{60} = 2.7 (K_2O = 2.7 percent at SiO_2 = 60 percent).

Dickinson and Hatherton (1967) graphed percent K_2O versus Benioff-zone depth at K_{55} and K_{60} for andesites of the Pacific. These graphs show that K_2O increases with increasing depth to the Benioff zone to about 160 km, decreases from about 160 to 200 km, and increases from 200 to 280 km. A line at K_{55} = 1.4 percent K_2O crosses the K_{55} depth-to-Benioff trend at depths of 140, 165, and 185 km. A line at K_{60} = 2.7 percent K_2O crosses the K_{60} depth-to-Benioff trend at a depth of 270 km. These data indicate that if the origin of the Yeoval Diorite Complex was related to subduction, the depth to the Benioff zone beneath it probably was between about 185 and 270 km.

Horizontal distance from the Yeoval Diorite Complex to the subduction zone trench would depend not only on depth to the Benioff zone, but also on dip of the subduction slab, which may have steepened during subduction rollback at the close of the Bindian Orogeny. Nevertheless, such depths to a Benioff zone would be consistent with the hypothesis that the Yeoval Diorite Complex intruded the Cowra Trough in the back-arc region of a west-dipping subduction zone, the trench of which was outboard from the agglomerated eastern Lachlan terranes during late stages of the post-rift Bindian Orogeny.

The nearby Yeoval Granite comprises a younger pluton, dated 370 Ma (Gulson and Bofinger, 1972). This younger granite probably is postorogenic with respect to the Tabberabberan Orogeny, which occurred in Late Devonian time (about 385–375 Ma; Champion and others, 2009). Some rocks of permissive composition are classified only as Devonian in age, so it is impossible to tell whether they are temporally associated with the Late Silurian-Early Devonian Bindian orogeny or the Late Devonian Tabberabberan Orogeny.

Permissive rocks of the Boggy Plain Supersuite are mostly of Late Silurian to Early Devonian age, and are mostly in and around the northern part of the Cowra-Buchan Rift Complex. According to Wyborn and others (1987), mafic to felsic rocks of the Boggy Plain Supersuite have relatively low strontium isotopic initial ratios mostly in the range 0.704 to 0.705. This indicates either a mantle source or a mafic crustal source that was young at the time of magma genesis or mixing between mantle and mafic lower crustal sources, possibly at the base of the Macquarie Arc. Furthermore, rocks of the Boggy Plain Supersuite with less than 70 wt. percent SiO_2 generally have higher concentrations of potassium, barium, strontium, and copper than similar rocks of most other I-type igneous suites in the Lachlan Orogen (Wyborn and others, 1987).

In southeastern Victoria, nearly 600 km south of the Yeoval deposit, the Dogwood and Sunday Creek porphyry copper prospects are hosted in granitoid plutons of the Bete Bolong Suite. Like permissive igneous rocks of the Boggy Plain Supersuite, those of the Bete Bolong Suite are mostly of Late Silurian to Early Devonian age. They occur mostly in and around the southern part of the Cowra-Buchan Rift Complex.

Table D2 lists permissive map units of the Yeoval tract. These are map units that are spatially associated with the Cowra-Buchan Rift Complex, represent igneous rocks of permissive composition, and are of Silurian to Devonian age. According to descriptive models by Cox (1986) and Panteleyev (1995, 2005), permissive rock types for porphyry copper and porphyry Cu ± Mo ± Au deposits include diorite, quartz diorite, and I-type granitoid rock types such as hornblende-bearing tonalite, granodiorite, quartz monzonite, monzogranite, and biotite granite of calc-alkaline affinity. Porphyro-aphanitic equivalents include andesite, quartz andesite, dacite, and I-type rhyodacite, quartz latite, and rhyolite porphyries of calc-alkaline affinity.

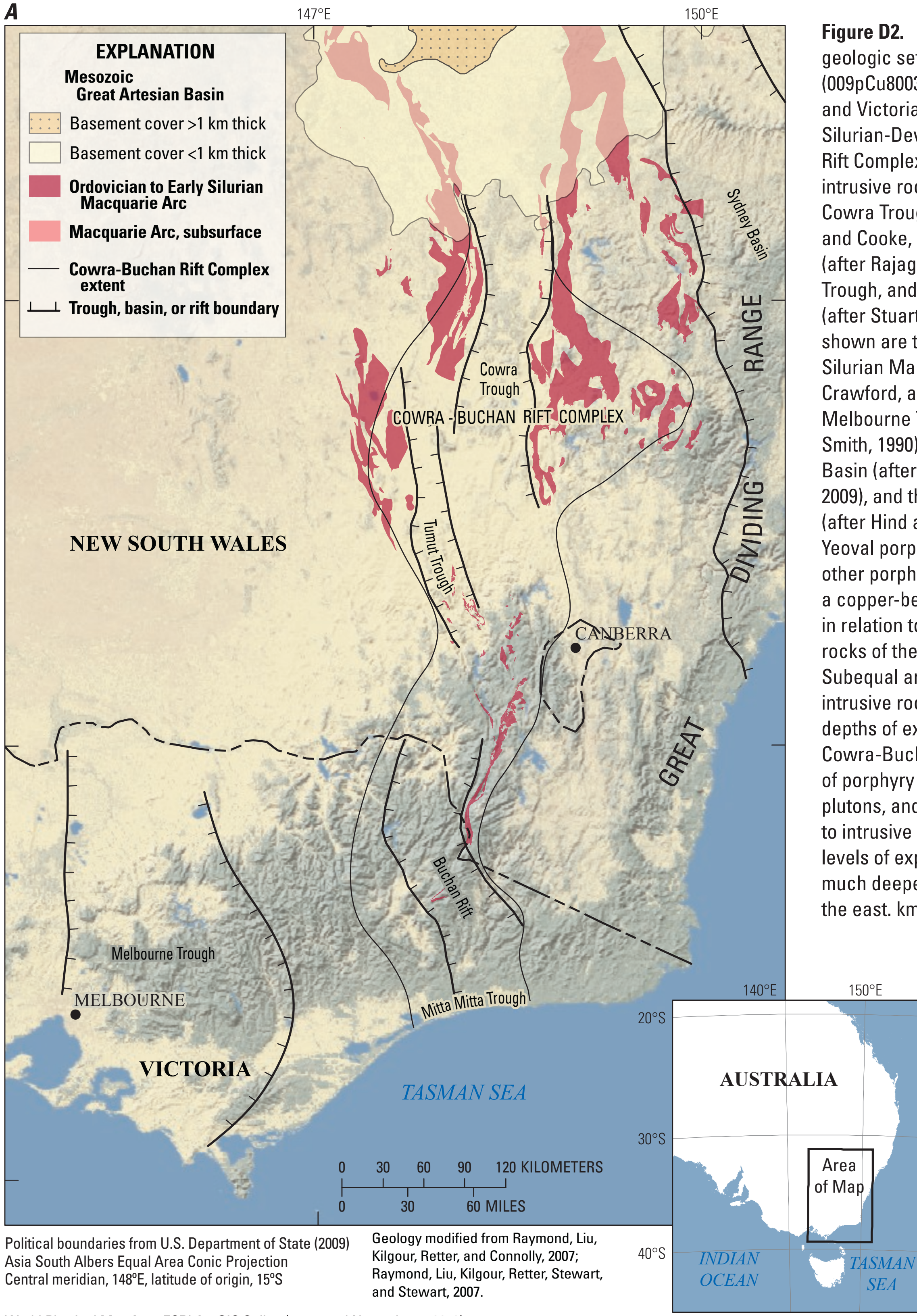

Political boundaries from U.S. Department of State (2009)
Asia South Albers Equal Area Conic Projection
Central meridian, 148°E, latitude of origin, 15°S

Geology modified from Raymond, Liu, Kilgour, Retter, and Connolly, 2007; Raymond, Liu, Kilgour, Retter, Stewart, and Stewart, 2007.

World Physical Map from ESRI ArcGIS Online (accessed November 5, 2012): http://www.esri.com/software/arcgis/arcgis-online-map-and-geoservices/map-services

Figure D2. Maps showing geologic setting of the Yeoval tract (009pCu8003), New South Wales and Victoria, Australia. *A*, The Silurian-Devonian Cowra-Buchan Rift Complex, including volcanic and intrusive rocks associated with the Cowra Trough (after Glen, Crawford, and Cooke, 2007), the Buchan Rift (after Rajagopolan, 1999), the Tumut Trough, and the Mitta Mitta Trough (after Stuart-Smith, 1990). Also shown are the Ordovician-Early Silurian Macquarie Arc (after Glen, Crawford, and Cooke, 2007), the Melbourne Trough (after Stuart-Smith, 1990), parts of the Sydney Basin (after Champion and others, 2009), and the Great Artesian Basin (after Hind and Helby, 1969). *B*, The Yeoval porphyry copper deposit, other porphyry copper sites, and a copper-bearing skarn deposit in relation to permissive igneous rocks of the Yeoval permissive tract. Subequal areas of volcanic and intrusive rocks indicate permissive depths of exposure within the Cowra-Buchan Rift Complex. Lack of porphyry copper sites, larger plutons, and lower ratios of volcanic to intrusive rocks indicate deeper levels of exposure to the west and much deeper levels of exposure to the east. km, kilometer.

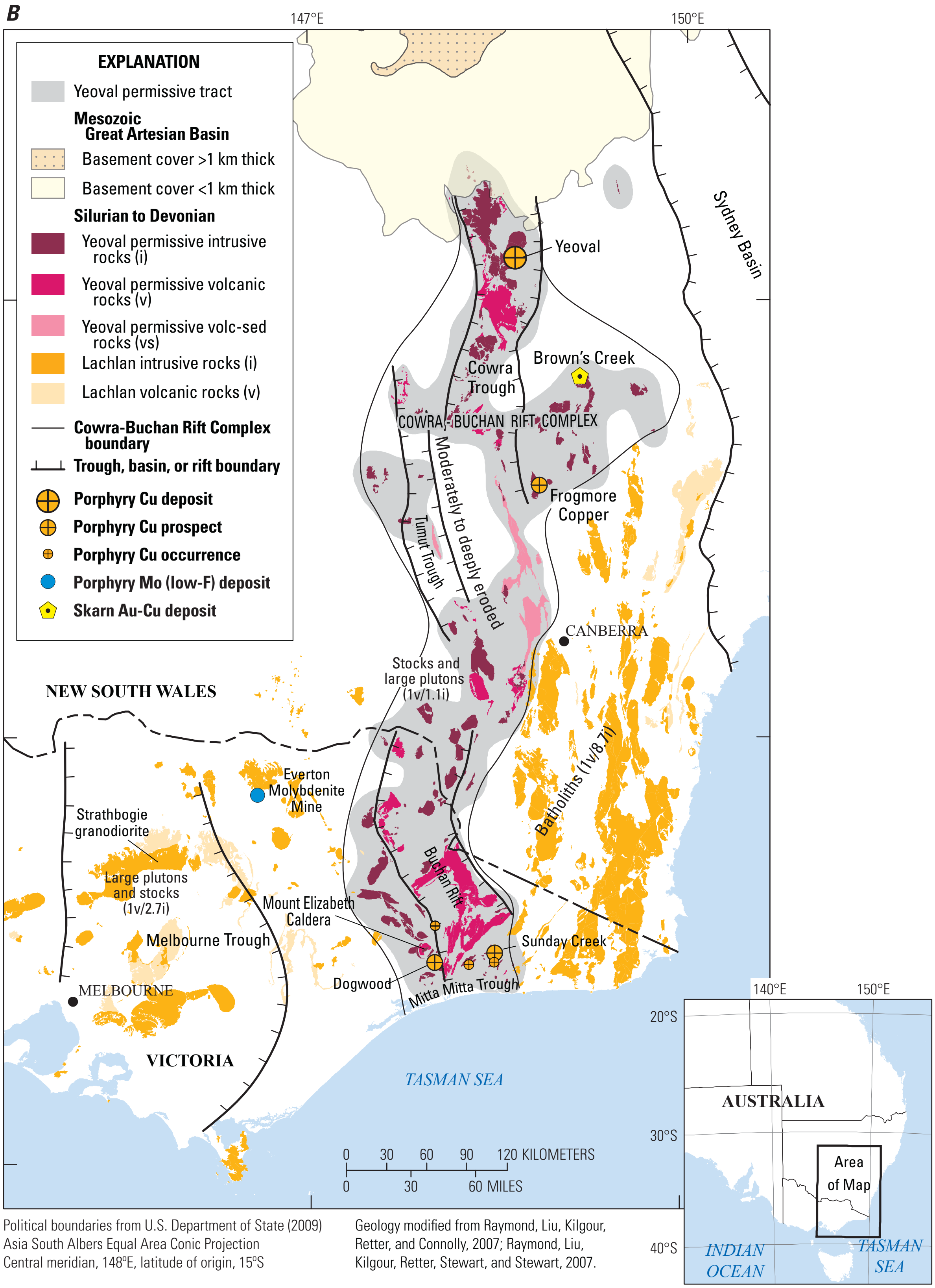

Figure D2.—Continued

Table D2. Map units that define the Yeoval tract (009pCu8003), New South Wales and Victoria, Australia.

[Based on Raymond, Liu, Kilgour, Retter, Stewart, and Stewart (2007) and Raymond, Liu, Kilgour, Retter, and Connolly (2007); for additional information about named map units, see Geoscience Australia, Stratigraphic Units Database at http://dbforms.ga.gov.au/www/geodx.strat_units.int/]

Supersuite, Suite	Map unit	Map symbol	Lithology	Age range
Barmedman Suite	Barmedman Granite	Dgbm	igneous felsic intrusive	Late Devonian
Bete Bolong Suite	Feltis Farm Tonalite	Dg47	hornblende-biotite tonalite, I-type	Late Devonian
	Cambrai Granite	Dgca	igneous felsic intrusive	Late Devonian
	Chellington Quartz Syenite	Dgch	igneous felsic intrusive	Late Devonian
	Pinehurst Granite	Dgpi	igneous felsic intrusive	Late Devonian
	Stone Boat Hill Granite	Dgsb	igneous felsic intrusive	Late Devonian
	Thurungly Granite	Dgty	igneous felsic intrusive	Late Devonian
	Trungley Hall Granite	Dgtg	igneous felsic intrusive	Late Devonian
	Weedallion Granophyre	Dgwe	igneous felsic intrusive	Late Devonian
	Yerna Granite	Dgya	igneous felsic intrusive	Late Devonian
Boggy Plain Supersuite	Grenfell Granite	Dgge	igneous felsic intrusive	Middle Devonian
	mafic intrusives 42017	Dd	igneous mafic intrusive	Devonian
	Mowamba and Silver Flat Porphyries	Dgmx	intrusive quartz-feldspar porphyry	Devonian
Bindogandri Suite	Bindogandri Granite	Dgbd	igneous felsic intrusive	Early to Middle Devonian
Boggy Plain Supersuite	Gumble Granite	Dgeg	igneous felsic intrusive	Early to Middle Devonian
	Mount Unicorn Porphyry	Dg582	quartz-feldspar porphyry, altered	Early to Middle Devonian
Boggy Plain Supersuite	Anglers Rest Granite	Dg114	biotite-muscovite granite, magnetic, I-type	Early Devonian
Boggy Plain Supersuite	Banimboola Quartz Monzodiorite	Dg110	hornblende-biotite quartz diorite, I-type	Early Devonian
Boggy Plain Supersuite	Boggy Plain Granitic Complex	Dgob	igneous felsic intrusive	Early Devonian
Boggy Plain Supersuite	Bogong Granite	Dgbb	igneous felsic intrusive	Early Devonian
Boggy Plain Supersuite	Burrinjuck Granite	Dgbu	igneous felsic intrusive	Early Devonian
Boggy Plain Supersuite	Burrungabugge Granodiorite	Dg96	hornblende granodiorite, I-type, altered	Early Devonian
Boggy Plain Supersuite	Charlestown Tonalite	Dg106	hornblende-biotite-(pyroxene) quartz diorite	Early Devonian
Boggy Plain Supersuite	Clear Hills Monzodiorite	Dgec	igneous intermediate intrusive	Early Devonian
Boggy Plain Supersuite	Coolamine Igneous Complex	Dgcl	igneous felsic intrusive, igneous mafic intrusive	Early Devonian
Boggy Plain Supersuite	Eugowra Granite	Dgeu	igneous felsic intrusive	Early Devonian
Boggy Plain Supersuite	Gocup Granite	Dggu	igneous felsic intrusive	Early Devonian
Boggy Plain Supersuite	Gurrangorambla Granophyre	Dgcu	igneous felsic intrusive	Early Devonian
Boggy Plain Supersuite	Guys Forest Granodiorite	Dg572	biotite granodiorite, minor hornblende, I-type	Early Devonian
Boggy Plain Supersuite	Guys Forest Granodiorite	Dg572	biotite granodiorite, minor hornblende, I-type	Early Devonian
Boggy Plain Supersuite	Hell Hole Creek Adamellite	Dgoh	igneous felsic intrusive	Early Devonian
Boggy Plain Supersuite	Jackson Granite	Dgjk	igneous felsic intrusive	Early Devonian
Boggy Plain Supersuite	Killimicat Granite	Dgbk	igneous felsic intrusive	Early Devonian
Boggy Plain Supersuite	Kynuna Granite	Dgyk	igneous felsic intrusive	Early Devonian
Boggy Plain Supersuite	Lock Lomond Granite	Dgel	igneous felsic intrusive	Early Devonian
Boggy Plain Supersuite	Lords Granite	Dgeo	igneous felsic intrusive	Early Devonian
Boggy Plain Supersuite	Milandra Granite	Dgei	igneous felsic intrusive	Early Devonian
Boggy Plain Supersuite	Naringla Granodiorite	Dgyn	igneous felsic intrusive	Early Devonian
Boggy Plain Supersuite	Obley Granite	Dgyo	igneous felsic intrusive	Early Devonian
Boggy Plain Supersuite	Post Office Granite	Dg113	granite, magnetic, I-type	Early Devonian
Boggy Plain Supersuite	Sorronto Granite	Dgys	igneous felsic intrusive	Early Devonian
Boggy Plain Supersuite	Timbrebongie Granite	Dgtb	felsic intrusive	Early Devonian
Boggy Plain Supersuite	Yennora Granite	Dgyy	igneous felsic intrusive	Early Devonian
Boggy Plain Supersuite	Yeoval Complex	Dgy	igneous felsic intrusive	Early Devonian
Caragabal Suite	Caragabal Granite	Dgcr	igneous felsic intrusive	Early Devonian
Karoopa Suite	Karoopa Granite	Dgkp	igneous felsic intrusive	Early Devonian

Table D2. Map units that define the Yeoval tract (009pCu8003), New South Wales and Victoria, Australia.—Continued

Supersuite, Suite	Map unit	Map symbol	Lithology	Age range
Mannus Creek Suite	Bogandyera Granite	Dgbo	igneous felsic intrusive	Early Devonian
Mannus Creek Suite	Munderoo Granodiorite	Dgmz	igneous felsic intrusive	Early Devonian
Mannus Creek Suite	Prison Farm Granodiorite	Dgps	igneous felsic intrusive	Early Devonian
Mount Elizabeth Caldera Complex	Mount Elizabeth Granodiorite	Dg126	hornblende-biotite granodiorite, magnetic, I-type	Early Devonian
Mount Elizabeth Caldera Complex	Saint Patricks Creek Granite	Dg133	biotite granite, magnetic, I-type	Early Devonian
Three Rocks Suite	Three Rocks Tonalite	Dgtr	igneous felsic intrusive	Early Devonian
	Broula Granite	Dgbr	igneous felsic intrusive	Early Devonian
	Crowther Monzodiorite	Dgcw	igneous intermediate intrusive	Early Devonian
	Lower Tableland Granite	Dg116	biotite granite, magnetic, I-type?	Early Devonian
	Marengo Granodiorite	Dg120	hornblende-biotite tonalite, magnetic, I-type	Early Devonian
	Moonshine Granite	Dgmh	igneous felsic intrusive	Early Devonian
	Tallawang Granite	Dgtl	granite	Early Devonian
	Willawong Creek Granite	Dgwg	igneous felsic intrusive	Early Devonian
Bete Bolong Suite	Double Bull Granodiorite	SDg56	granodiorite, I-type	Late Silurian to Early Devonian
Bete Bolong Suite	Dysentery Tonalite	SDg48	biotite tonalite, I-type	Late Silurian to Early Devonian
Bete Bolong Suite	Jarrahmond Granite	SDg45	hornblende-biotite granodiorite, I-type	Late Silurian to Early Devonian
Bete Bolong Suite	Orbost Tonalite	SDg44	biotite tonalite, I-type	Late Silurian to Early Devonian
Boggy Plain Supersuite	Mount Mittamatite Granite	Dg98	biotite granite, magnetic, altered	Late Silurian to Early Devonian
Boggy Plain Supersuite	Mount Nugong Tonalite	Dg123	biotite-hornblende tonalite, I-type, mafic enclaves	Late Silurian to Early Devonian
Boggy Plain Supersuite	Scammels Adamellite	Dgsa	felsic intrusive	Late Silurian to Early Devonian
Ensay Suite	Connors Creek Tonalite	Dg135	biotite-hornblende tonalite, I-type	Late Silurian to Early Devonian
Ensay Suite	Reedy Flat Tonalite	Dg128	biotite-hornblende tonalite, I-type	Late Silurian to Early Devonian
Ensay Suite	Tambo Crossing Tonalite	Dg134	biotite-hornblende tonalite, I-type	Late Silurian to Early Devonian
Free Damper Suite	Dargals Adamellite	Dgfd	felsic intrusive	Late Silurian to Early Devonian
Free Damper Suite	Free Damper Adamellite	Dgff	felsic intrusive	Late Silurian to Early Devonian
Free Damper Suite	Pennyweight Adamellite	Dgfp	felsic intrusive	Late Silurian to Early Devonian
Free Damper Suite	Welumba Adamellite	Dgfw	felsic intrusive	Late Silurian to Early Devonian
Gundibindyal Suite	Gundibindyal Granite	Dgun	felsic intrusive	Late Silurian to Early Devonian
Khancoban Suite	Khancoban Granodiorite	Dgkc	felsic intrusive	Late Silurian to Early Devonian
Ogilvies Suite	Ogilvies Adamellite	Dgog	felsic intrusive	Late Silurian to Early Devonian
Pinnak Suite	Broken Leg Granite	SDg46	hornblende-biotite granodiorite, I-type	Late Silurian to Early Devonian
Polar Star Suite	Livingstone Creek Tonalite	Dg144	biotite tonalite, I-type	Late Silurian to Early Devonian

Table D2. Map units that define the Yeoval tract (009pCu8003), New South Wales and Victoria, Australia.—Continued

Supersuite, Suite	Map unit	Map symbol	Lithology	Age range
Rileys Creek Suite	Mungobabba Tonalite	Dg143	biotite tonalite, I-type	Late Silurian to Early Devonian
Rileys Creek Suite	Old Sheep Station Granodiorite	Dg136	biotite granodiorite, magnetic dikes	Late Silurian to Early Devonian
Rileys Creek Suite	Rileys Creek Granodiorite	Dg137	biotite-hornblende granodiorite to quartz diorite, I-type	Late Silurian to Early Devonian
Surveyors Creek Suite	Coynallan Tonalite	Dg579	hornblende tonalite, magnetic, I-type	Late Silurian to Early Devonian
	Bete Bolong Granodiorite	SDg57	hornblende granodiorite, I-type, altered	Late Silurian to Early Devonian
	Bunroy Hut Granite	Dg91	porphyritic biotite granite, granodiorite, I-type	Late Silurian to Early Devonian
	Case Granite	Dg513	granite, altered, I-type	Late Silurian to Early Devonian
	Colquhoun Granite	Dg130	biotite granite, I-type	Late Silurian to Early Devonian
	Cooney Ridge Granodiorite	SDg512	hornblende-biotite granite, I-type	Late Silurian to Early Devonian
	Eleven Bob Granodiorite	SDg55	granodiorite, I-type	Late Silurian to Early Devonian
	Hermit Granite	Dg580	biotite granite, I-type, porphyritic	Late Silurian to Early Devonian
	Kenny Creek Diorite	Dg129	hornblende diorite-granodiorite, I-type	Late Silurian to Early Devonian
	mafic intrusives 42021	SDd	mafic intrusive	Late Silurian to Early Devonian
	Mollys Plain Granite	Dg514	biotite granite, I-type	Late Silurian to Early Devonian
	Mount Raymond Granite	Dg43	hornblende-biotite granite, I-type	Late Silurian to Early Devonian
	Rocky Jack Granite	Dg509	granite, I-type, altered	Late Silurian to Early Devonian
	Twins Creek Granodiorite	Dgtc	felsic intrusive	Late Silurian to Early Devonian
	Waratah Flat Granite	SDg61	hornblende granite, I-type	Late Silurian to Early Devonian
Ballyhooley Suite	Ballyhooley Granite	Sgly	felsic intrusive	Late Silurian
Barry Suite	Barry Granodiorite	Sgry	felsic intrusive	Late Silurian
Carcoar Suite	Carcoar Granodiorite	Sgca	felsic intrusive	Late Silurian
Garland Suite	Garland Granodiorite	Sggl	felsic intrusive	Late Silurian
Grants Corner Suite	Grants Corner Granodiorite	Sggc	felsic intrusive	Late Silurian
Mount Misery Suite	Mount Misery Granite	Sgmi	felsic intrusive	Late Silurian
Neville Suite	Sunset Hills Granite	Sgsh	felsic intrusive	Late Silurian
Streamville Suite	Streamville Granodiorite	Sgst	felsic intrusive	Late Silurian
Swan Ponds Tonalite, Lucan Complex	Swan Ponds Tonalite, Lucan Complex	Sgsl	felsic intrusive	Late Silurian
Thorkidaan Volcanics	Mitta Mitta Rhyolite	Sfet	rhyolite	Late Silurian
Tintern Granodiorite, Padua Granodiorite	Tintern Granodiorite, Padua Granodiorite	Sgtp	felsic intrusive	Late Silurian
	Asylum Granite	Sgas	felsic intrusive	Late Silurian
	Bartletts Creek Granite	Sgak	felsic intrusive	Late Silurian

Table D2. Map units that define the Yeoval tract (009pCu8003), New South Wales and Victoria, Australia.—Continued

Supersuite, Suite	Map unit	Map symbol	Lithology	Age range
	Blackmans Creek Granite, Spring Road Granite	Sgks	felsic intrusive	Late Silurian
	Bugs Ridge Granite	Sgrg	felsic intrusive	Late Silurian
	Davies Creek Granite	Sgdc	granite	Late Silurian
	Goonoonglah Monzodiorite, Yewangara and Sentry Box Granites	Sggy	felsic intrusive	Late Silurian
	Kempfield Granodiorite	Sgkp	felsic intrusive	Late Silurian
	Licking Gully Granite	Sglg	felsic intrusive	Late Silurian
	Yarra Granite	Sgyt	felsic intrusive	Late Silurian
	Bull Run Gap Adamellite	SDg62	biotite monzogranite	Middle Silurian to Early Devonian
	Powder Horn Hill Microgranite	Dgph	felsic intrusive	Silurian to Early Devonian
Boggy Plain Supersuite	Boebuck Granodiorite	Sg90	hornblende granodiorite, porphyritic diorite, I-type	Silurian
	felsic intrusives 42022	Sg	felsic intrusive	Silurian
	Volcanic rocks			
Rocky Ponds Group	Dulladerry Volcanics	Dfrd	ignimbrite	Middle Devonian
Rocky Ponds Group	Warrumba Volcanics	Dfrw	ignimbrite	Middle Devonian
Mount Burrowa Volcanic Group	Jemba Ignimbrite	Dfje	ignimbrite	Early to Middle Devonian
Black Range Group	Mountain Creek Volcanics	Dfbm	rhyolite, ignimbrite, sandstone	Early Devonian
Black Range Group	Pilleuil Andesite, Waynes Knob Rhyolite	Dwbp	andesite, rhyolite, conglomerate	Early Devonian
Black Range Group	Warrangong Volcanics	Dabw	andesite	Early Devonian
Boggy Plain Supersuite	Boraig Group	Dfb	rhyolite	Early Devonian
Boggy Plain Supersuite	Gatelee Ignimbrite	Dfog	ignimbrite, conglomerate	Early Devonian
Boggy Plain Supersuite	Hyandra Creek Group	Dfh	dacite	Early Devonian
Boggy Plain Supersuite	Minjary Volcanics	Dfom	dacite	Early Devonian
Cootamundra Group	Cowcumbala Rhyolite	Dfcw	rhyolite	Early Devonian
Dartella Volcanic Group	Besford Ignimbrite	Dfab	ignimbrite	Early Devonian
Dartella Volcanic Group	Dartella Volcanic Group	Dfa	ignimbrite	Early Devonian
Mount Elizabeth Caldera Complex	Mount Elizabeth Caldera Complex	Dfe	ignimbrite	Early Devonian
Snowy River Volcanics	Avonmore Subgroup	Dfsv	ignimbrite, conglomerate	Early Devonian
Snowy River Volcanics	Castor Oil Lava	Dfso	rhyolite	Early Devonian
Snowy River Volcanics	Little River Subgroup	Dfsl	ignimbrite, rhyolite	Early Devonian
Snowy River Volcanics	Marroo Subgroup	Dfsm	ignimbrite	Early Devonian
Snowy River Volcanics	Mount Dawson Subgroup	Dfsd	ignimbrite	Early Devonian
Snowy River Volcanics	Ninnie Subgroup	Dfsn	ignimbrite	Early Devonian
Snowy River Volcanics	Snowy River Volcanics	Dfs	rhyolite	Early Devonian
Snowy River Volcanics	Tara Range Subgroup	Dfsr	ignimbrite, sandstone	Early Devonian
Snowy River Volcanics	Trendale Formation	Dfst	ignimbrite	Early Devonian
Snowy River Volcanics	Tulloch Ard Ignimbrite	Dfsa	ignimbrite	Early Devonian
Trundle Group	Carawandool Volcanics	Dftc	rhyolite	Early Devonian
White Monkey Volcanics	White Monkey Volcanics	Dfwm	ignimbrite	Early Devonian
	Coonambro Volcanics	Dvco	andesite	Early Devonian
	Rolling Grounds Latite	Darg	latite	Early Devonian
	Kellys Plain Volcanics	Dfkp	ignimbrite	Late Silurian to Early Devonian

Nonpermissive Igneous Rocks East and West of the Yeoval Tract

Igneous rocks of permissive composition and of Silurian to Devonian age also are abundant to the east and west of the Yeoval permissive tract (fig. D2*B*). These eastern and western Lachlan belts of igneous rocks have been well mapped and thoroughly explored, but they have not been found to contain porphyry copper deposits or significant prospects. These otherwise permissive igneous rocks are therefore considered non-permissive for porphyry copper resources, and they are not included in a permissive tract for porphyry copper.

In general, such non-permissive rocks (of permissive composition) are visibly crystalline granitoid rocks in plutons of large to batholithic proportions. Most of these are too deeply eroded for preservation of porphyry copper deposits. For example, the Middle to Late Devonian Strathbogie Granite contains copper occurrences, according to a mineral assessment by the Commonwealth Forests Taskforce (1998). However, these occurrences apparently are scattered minor copper showings, unlikely to represent a porphyry copper system in such a large granitic pluton. Also, some granitic plutons are so differentiated that they are more likely to have concentrated molybdenum than copper, as experimentally demonstrated by Blevin and others (1996). For example, quartz-molybdenite veins and disseminated molybdenite occur with minor pyrite, chalcopyrite, pyrrhotite, and arsenopyrite at the Everton Molybdenite Mine, which is hosted in Middle to Late Devonian granite in north-central Victoria (Catalyst Metals, Ltd., 2008).

Subsurface Extension of Permissive-Tract Boundaries

We added a 10-km buffer to mapped bodies of permissive igneous intrusive rocks, and a 2-km buffer to mapped bodies of permissive volcanic rocks (fig. D3). The rationale for use of such buffers is explained in the main body of this report. A spatial modeling algorithm was applied to connect permissive areas less than 20 km apart and smooth the permissive-tract boundaries. See the metadata associated with the tracts for additional details.

Known Deposits

The Yeoval porphyry copper deposit is hosted in the Yeoval Diorite Complex, which is exposed in the Cowra Trough, near the northern end of the Yeoval permissive tract (figs D1, D2*B*). The Yeoval deposit is estimated to contain about 49,700 t copper, 1,550 t molybdenum, 1.8 t gold, and 28 t silver in 12.9 Mt of ore with average grades of 0.38 percent copper, 0.012 percent molybdenum, 0.14 g/t gold, and 2.2 g/t silver (table D3 and appendix F). According to Augur Resources, Ltd., (2009), these estimates were based on 8,112 m of core from 45 drill holes. Assay results from drill holes indicate that higher grade zones exist within the deposit.

Four pipe-like mineralized zones have been tested by drilling—two Yeoval ore zones, the Sterling zone to the west, and the Sovereign zone to the east. These ore zones are open below the 250 m depth, and the Sovereign zone also is open to the east, north, and south. The Lady Lizzy, Crown, and Cyclops prospects are near enough to the Yeoval deposit to be considered as potential additions to the resources of the known deposit.

The Yeoval deposit is hosted in dioritic to granodioritic rocks of the composite Yeoval Batholith, which ranges in composition from gabbro to high-K diorite, granodiorite, and granite. According to Ambler and Facer (1975), the distribution of copper in soils of the Yeoval mine area appears to be spatially related to small porphyritic dacite intrusions. Thus, the pipe-like ore zones described by Augur Resources, Ltd., (2009) probably surround plug-like intrusions of dacite porphyry. Ambler and Facer (1975) noted that the dacite porphyry consists of phenocrysts of intermediate plagioclase (An45), quartz, hornblende, and biotite in a fine-grained matrix. Plagioclase is commonly altered to potassium feldspar, sericite, and clay, whereas hornblende and biotite are commonly altered to chlorite and epidote.

Chalcopyrite is the most common ore mineral in the mineralized rocks of the Yeoval deposit (Ambler and Facer, 1975). The chalcopyrite occurs in veins and veinlets, and is disseminated in altered rocks around them. Subordinate bornite occurs as disseminated grains, intergrown with chalcopyrite in altered mafic-mineral sites. Minor digenite occurs as inclusions and exsolution lamellae in bornite. Pyrite is sparsely disseminated in potassically altered rocks. Fractured pyrite grains are partly healed by chalcopyrite. Molybdenite is intergrown with chalcopyrite and bornite in extremely K-feldspathized rocks and coats some fractures.

Ambler and Facer (1975) described at least two generations of veins, which are up to 1 cm wide and commonly contain sulfides and hydrothermal silicate minerals, such as quartz, potassium feldspar, epidote, and prehnite. Veins commonly are surrounded by an inner envelope of K-feldspathized rock, a medial envelope of sericitized plagioclase, and an outer envelope of clay-sericite alteration of plagioclase.

Porphyry Copper Prospects, Mineral Occurrences, and Related Deposit Types

Figures D1 and D2*B* show locations of porphyry copper prospects and occurrences in the Yeoval permissive tract. Selected information about each prospect is listed in table C4, and appendix F contains additional information about each prospect.

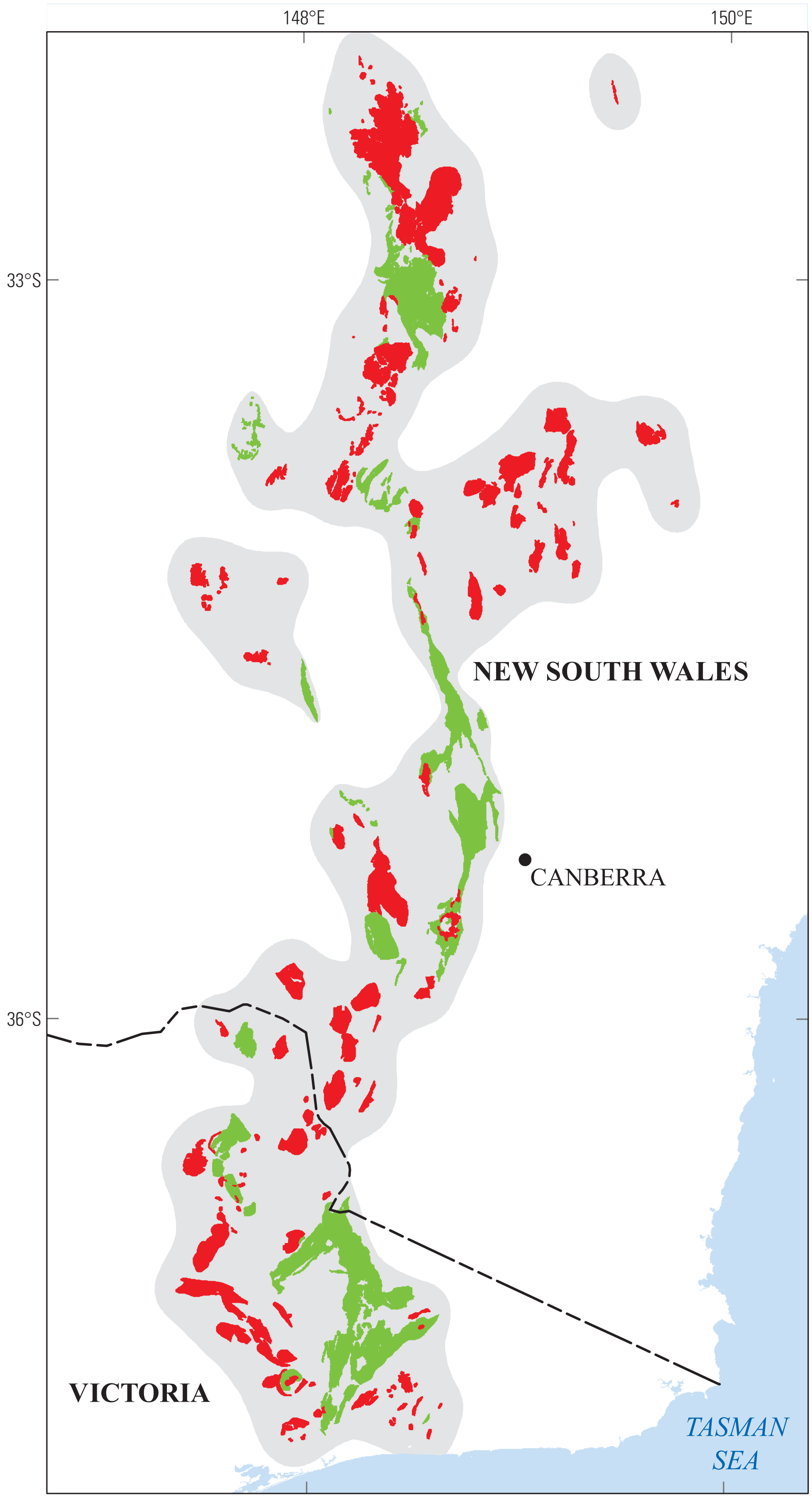

EXPLANATION

- Assessed porphyry copper tract 009pCu8003
- Permissive intrusive rock
- Permissive extrusive (volcanic) rock ± interlayered sedimentary rock

Political boundaries from U.S. Department of State (2009)
Asia South Albers Equal Area Conic Projection
Central meridian, 148.5°E, latitude of origin, 35°

0 25 50 75 100 KILOMETERS
0 25 50 MILES

Figure D3. Map showing distribution of map units representing permissive intrusive and extrusive igneous rocks used to define the Yeoval tract (009pCu8003), New South Wales and Victoria, Australia.

Table D3. Porphyry copper deposit in the Yeoval tract (009pCu8003), New South Wales and Victoria, Australia.

[Ma, million years; Mt, million metric tons; %, percent; t, metric ton; g/t, gram per metric ton; NA, not applicable. Contained Cu in metric tons is computed as tonnage (Mt × 1,000,000) × Cu grade (%) ÷ 100]

Name	Latitude	Longitude	Subtype	Age (Ma)	Tonnage (Mt)	Cu (%)	Mo (%)	Au g/t)	Ag (g/t)	Contained Cu (t)	References
Yeoval	-32.728	148.643	NA	411	12.88	0.38	0.012	0.140	2.2	49,000	Gulson (1972), Gulson and Bofinger (1972), Ambler and Facer (1975), Bowman and others (1983), Paterson and others (1983), Ewers and others (2002), Singer and others (2008), Augur Resources, Ltd., (2009), Geoscience Australia (2010)

Dogwood Porphyry Copper Prospect

The Dogwood porphyry copper prospect is on the western margin of the Buchan Rift, near the southern end of the Cowra-Buchan Rift Complex, in southeastern Victoria (fig. D2B). According to Maher (2003), subeconomic porphyry Cu-Mo mineralization at the Dogwood prospect is hosted in Kaerwut Granodiorite and Ordovician sandstones. The Kaerwut Granodiorite, which Rajagopalan (1999) classified as trondhjemite and Maher (2003) described as granodiorite-tonalite, belongs to the Bete Bolong Suite of granodiorite-tonalite stocks of probable Early Devonian age.

Magnetic surveys at Dogwood indicate that the Kaerwut granodiorite-tonalite intrusion is about 1 km long (east-west) and 0.8 km wide (Rajagopalan, 1999). Induced polarization results indicate very high induced polarization effects around a magnetic high in the southern part of the inferred granitoid intrusion.

Chalcopyrite and molybdenite occur in stockwork veins and disseminations within the Kaerwut Granodiorite and above it in contact-metamorphosed sandstone. According to Rajagopalan (1999) the area of the soil geochemical anomaly containing more than 400 ppm copper is about 4 km long (west-northwest) and 2 km wide (north-northeast), with peak anomalies of 1,000 ppm copper and 32.5 ppm molybdenum.

The Dogwood prospect has been tested by six core-drill holes. The most significant drill intercept of primary sulfides was 34 m that averaged 0.39 percent copper and 0.002 percent molybdenum (table D4). Maximum grades were encountered in a 1-m intercept that contained 1.65 percent copper, and another 1-m intercept that contained 0.275 percent molybdenum (Maher, 2003).

A vertical geological cross section constructed by Maher (2003) on the basis of drilling results indicates that the Dogwood prospect is related to a sill-like granodiorite intrusion that dips about 15° northeast. The granodiorite intrusion, which is about 100 m thick, terminates up-dip (to the southwest) at about 100 m below the surface. It is hosted in sandstone, which is contact-metamorphosed near the intrusion. Drill intercepts show relatively high molybdenum grades within the intrusion, and relatively high copper grades in host rocks above the terminus of the intrusion and around a vertical apophysis above the main intrusion.

According to Maher (2003), a blanket of supergene-enriched ore developed over sericitized ore in the contact-metamorphosed sandstone. The supergene zone is thickest and has the highest grade along a deeply weathered fault zone. The best intercept in the supergene chalcocite blanket was 24 m containing 0.8 percent copper. The drill hole that encountered that intercept ended in ore.

Sunday Creek Porphyry Copper Prospect and Booth's Fancy Copper Mine

The Sunday Creek porphyry copper prospect is on the eastern margin of the Buchan Rift, in a pluton of Feltis Farm Tonalite, which belongs to the Bete Bolong Suite of I-type igneous intrusions. The Feltis Farm Tonalite comprises a large pluton (about 10 km by 7 km), which locally contains roof pendants of Pinnak Sandstone. The Sunday Creek prospect is located near a north-trending fault that separates the Feltis Farm intrusion into western and eastern parts (Rajagopalan, 1999).

At the Sunday Creek prospect, pyrite, chalcopyrite, bornite, and magnetite are disseminated, and occur along fine fractures in the tonalite. Results of soil geochemical and induced polarization surveys outlined two areas of coincident copper and chargeability anomalies. Five core holes were drilled to test these anomalies. The best intercept of primary copper was 50 m that averaged 0.13 percent copper in a mineralized shear zone. The best intercept of supergene-enriched copper was 27 m averaging 0.3 percent copper (Rajagopalan, 1999).

Booth's Fancy Copper Mine is about 4 km north of the Sunday Creek prospect and is at the contact of the same Feltis Farm Tonalite pluton that hosts the Sunday Creek prospect. Inasmuch as it is less than about 4.3 km from the Sunday Creek prospect, we group Booth's Fancy Copper Mine with the Sunday Creek prospect. At Booth's Fancy Copper Mine, a quartz vein, about 20–60 cm wide, contains abundant chalcopyrite, with pyrite, gold, and some galena. Sampling from the dump of the small mine on this vein returned maximum assays of 1.9 percent copper and 7.8 g/t gold (Rajagopalan, 1999, p. 122).

Table D4. Significant porphyry copper prospects and occurrences in the Yeoval tract (009pCu8003), New South Wales and Victoria, Australia.

[Ma, million years; m, meter; %, percent; ppm, parts per million; prospect ranking criteria listed in table 2]

Group	Name	Latitude	Longitude	Age (Ma)	Comments	Rank	References
	Frogmore	-34.276	148.842	422	14 m at 1.0% Cu (veins), alternatively classified as orogenic base-metal veins	4	Ackerman (2003), Paradigm Metals (2011), Singer and others (2008), Lewis and Downes (2008)
	Brown's Creek	-33.527	149.159	421	skarn Au-Cu	5	Taylor (1983), Perkins and others (1995), Jaireth and Miezitis (2004), Cube Consulting (2006), Geoscience Australia (2010)
Stringer-Double Bull	Double Bull Creek	-37.574	148.316	407	chalcopyrite, pyrite	7	Rajagopalan (1999)
Stringer-Double Bull	Stringer Knob	-37.601	148.282	407	chalcopyrite, pyrite	7	Rajagopalan (1999), Singer and others (2008)
Sunday-Booth's	Sunday Creek	-37.519	148.489	407	50 m at 0.13% Cu to supergene 0.3% Cu	4	Rajagopalan (1999)
Sunday-Booth's	Booth's Fancy Copper Mine	-37.480	148.485	407	0.4 m at 1.9% Cu, 7.8 ppm Au (vein)	7	Rajagopalan (1999)
	Dogwood	-37.588	148.004	407	34 m at 0.39% Cu, 0.003% Mo (stockwork)	3	Rajagopalan (1999), Maher (2003), Singer and others (2008)
	Mount Buck	-37.583	148.487	407	chalcopyrite, pyrite	7	Rajagopalan (1999)
	Tiger Creek	-37.330	148.009	407	chalcopyrite, pyrite	7	Rajagopalan (1999)

Frogmore

The Frogmore copper prospect is on the eastern margin of the Cowra Trough (fig. D2*B*). Copper occurrences at Frogmore are hosted in Middle Silurian Hawkins Volcanics, adjacent to a stock of Licking Gully Granite, which is part of the Wyangalla batholith, of Late Silurian age (Ackerman, 2003).

Ackerman (2003, p. 3) described "Narrow zones of quartz vein-hosted primary Cu sulfides" in sheared porphyritic quartz dacite at Frogmore. Chalcopyrite and pyrite with minor sphalerite and galena are the primary sulfide minerals. The zone of mineralized rock is about 200 m long (north-northwest) and 50–100 m wide (east-northeast). It is surrounded by a phyllic zone, which is about 300 m long and 200 m wide, and a propylitic zone that is more than 700 m long and 100–600 m wide.

Copper sulfides were discovered at Frogmore in the 1860s, and were mined from the Pride of Frogmore and South Frogmore mines before 1907 (Ackerman, 2003). Since 1950 the Frogmore area has been explored for porphyry copper by geochemical sampling, geophysical surveys, and drilling.

Paradigm Metals (2008, 2011) reported a reverse-circulation percussion-drill hole intercept of 14 m containing 1.0 percent copper, including 2 m of 3.1 percent copper. They interpret the Frogmore veins as being similar to base-metal deposits in the Cobar region. Such deposits have recently been classified as orogenic base-metal deposits by Lewis and Downes (2008).

We are not sure whether the Frogmore prospect represents part of a porphyry copper system, or a set of orogenic base-metal veins. We tentatively include it here as a possible porphyry copper occurrence, with the caveat that its classification and origin are controversial.

Porphyry Copper Occurrences

Rajagopalan (1999, fig. 8) showed and briefly described the locations of several other porphyry copper occurrences in southeastern Victoria. Like the Sunday Creek and Booth's Fancy Copper prospects, the Mount Buck, Stinger Knob, and Double Bull Creek occurrences are associated with granodioritic to tonalitic intrusions of Late Silurian to Devonian age along the eastern margin of the Buchan Rift.

Mount Buck

The Mount Buck occurrence is about 7 km south of the Sunday Creek prospect. It is near the northern end of the 1- to 3-km wide hornfels zone that surrounds the Eleven Bob Granodiorite pluton. That pluton is about 4 km long (northwest-southeast) and 1 km wide. It consists of I-type granodiorite of Late Silurian to Early Devonian age.

Stringer Knob and Double Bull Creek

The Stringer Knob and Double Bull Creek occurrences are both along the northwestern contact of the Double Bull Granodiorite pluton with its surrounding hornfels zone. The Double Bull Granodiorite pluton is elongate northeast, and is about 6 km long and 1–1.5 km across. We grouped the Stringer Knob and Double Bull Creek occurrences, because they are only about 4 km apart, and they are related to the same pluton. That pluton consists of I-type granodiorite, and it is less than 1 km southeast of the larger Bete Bolong Granodiorite pluton, with which it may be connected at depth.

Tiger Creek

The Tiger Creek occurrence is on the eastern margin of the Buchan Rift, and is about 30 km north of the Dogwood prospect. We have almost no information about the Tiger Creek occurrence, except that Rajagopalan (1999) described it as a porphyry copper occurrence in Nunniong Granite, which is an S-type biotite-muscovite-cordierite granitoid with gneissic enclaves. This S-type granite may represent mineralized country rock, rather than a porphyry-copper-related intrusion, which may not be exposed, or may be too small to be mapped at 1:1,000,000 scale.

Deposits and Prospects of Types Possibly Related to Porphyries

Brown's Creek Cu-Au Skarn Deposit

The Brown's Creek Au-Cu skarn is a deposit that has been mined as a skarn, but we include it here as a porphyry copper prospect, with the idea that it might indicate porphyry copper potential. It is about 25 km south-southeast of Orange, NSW. According to a geologic map and vertical sections by Taylor (1983), the mineralized skarn is above the northern end of the Carcoar Granodiorite pluton. Ore is hosted in calc-silicate skarn, present in three layers of limestone, and interlayered with mudstones and tuffs that overlie andesitic lava flows of Ordovician age. A cross section of the deposit shows that the mineralized skarns are up to about 5 m thick, and they are arched over the north end of the Carcoar Granodiorite pluton.

At Brown's Creek, coarse-textured skarn is composed of wollastonite, garnet, diopside, sulfide minerals (including pyrrhotite, chalcopyrite, arsenopyrite, tennantite), and gold. In vein-like skarn, these minerals are accompanied by bornite, chalcopyrite, tetrahedrite, and gold. Chalcocite, covellite, copper oxides, native copper, and silver sulphosalts occur in supergene-enriched zones along faults that cut skarn.

Estimated resources of the Brown's Creek skarns are 2 Mt of ore, averaging 0.36 percent copper, and 4 g/t gold (Geoscience Australia, 2010). Past production from the Brown's Creek skarns was 7,200 t copper and 8.2 t gold (Cube Consulting Pty Ltd., 2006).

Although the Brown's Creek deposit is in the Molong Volcanic Belt of the Ordovician Macquarie Arc, it is spatially and temporally related to the Carcoar Granodiorite, which is Late Silurian to Early Devonian in age (421±6 Ma) (Perkins and others, 1995). Because of its post-Macquarie Arc age, the Brown's Creek deposit is assigned to the Yeoval permissive tract.

Exploration History

The presence of copper at the site of the Yeoval porphyry copper deposit has been known since 1908, but the first exploration for a bulk-mineable porphyry copper deposit occurred from 1970 to 1974 (Ambler and Facer, 1975). By 1975, the Yeoval resource was estimated to contain at least 20 Mt of sub-economic ore, averaging 0.2 percent copper (based on results from six drill holes).

Recent exploration drilling at the Yeoval deposit has spurred new interest and additional drilling. The current resource estimate, almost 13 Mt averaging 0.38 percent copper, is based on results from 45 drill holes. Exploration drilling is likely to continue at Yeoval, where two pipe-like ore zones are open below 250 m. One of these ore zones also is open laterally, and nearby prospects probably also will be tested.

We know of no new exploration activity at any of the other porphyry copper prospects described above. Results of past exploration activities in the southern part of the Yeoval permissive tract apparently were not sufficiently positive to generate renewed interest, even as metal prices have increased over the past few years.

Sources of Information

Principal sources of information used by the assessment team for delineation of the Yeoval porphyry copper permissive tract (009pCu8003) are listed in table D5. The source geologic maps and map-unit descriptions are excellent. The availability and quality of information about known deposits and prospects are very good.

Grade and Tonnage Model Selection

The custom grade-tonnage model for Australian porphyry copper deposits of the East Tasmanide and Yeoval permissive tracts (appendix A) was designed to represent undiscovered porphyry copper deposits of the Yeoval tract. We made this model on the basis of a statistical comparison, which showed that the 15 known porphyry copper deposits of the East Tasmanide and Yeoval permissive tracts have tonnages and grades that are significantly lower than those of the global grade-tonnage model for porphyry copper deposits by Singer and others (2008).

Although the Yeoval deposit contains molybdenum, gold, and silver, most of the deposits represented in the custom Australian grade-tonnage model lack data to indicate average grades of gold, molybdenum, or silver. Therefore, the custom model can be used only to estimate copper resources of undiscovered deposits in the Yeoval permissive tract.

Estimate of the Number of Undiscovered Deposits

Before estimating numbers of undiscovered deposits in the tract, the assessment panel reviewed the geology, known deposits, locations, and qualities of significant porphyry prospects and occurrences, as well as the exploration status of the tract, and geophysical evidence for undiscovered deposits in relatively unexplored or underexplored parts of the tract. Then panel members were asked to list and weigh positive factors, which may indicate undiscovered deposits, versus negative factors, which may limit the number of undiscovered porphyry copper deposits in the permissive tract.

Table D5. Principal sources of information used for the Yeoval tract (009pCu8003), New South Wales and Victoria, Australia.

[NA, not applicable]

Theme	Name or Title	Scale	Citation
Geology	Surface geology of Australia, New South Wales—2nd edition	1:1,000,000	Raymond, Liu, Kilgour, Retter, Stewart, and Stewart (2007)
	Surface geology of Australia, Victoria—3rd edition	1:1,000,000	Raymond, Liu, Kilgour, Retter, and Connolly (2007)
	Eastern Lachlan orogen geoscience database, version 2	NA	Glen and others (2006)
	Chemistry, origin, and evolution of mineralized granites in the Lachlan fold belt, Australia: the metallogeny of I- and S-type granites		Blevin and Chappell (1995)
	Intrusive metallogenic provinces in eastern Australia based on granite source and composition	NA	Blevin and others (1996)
Mineral occurrences	Porphyry copper deposits of the world: database and grade and tonnage models	NA	Singer and others (2008)
	Australian mines atlas	NA	Geoscience Australia (2010)
	OZMIN mineral deposits database	NA	Ewers and others (2002)
	OZPOT geoprovince-scale assessment of mineral potential	1:2,500,000	Jaireth and Miezitis (2004)
	Intierra	NA	Intierra (2009)
	A Silurian porphyry copper prospect near Yeoval, NSW	NA	Ambler and Facer (1975)
	Porphyry-type copper deposits, eastern Victoria	NA	Rajagopalan (1999)
Geophysics	Total magnetic anomaly (TMI) grids of Australia, fourth edition	NA	Geoscience Australia (2004)
	Australian national gravity database 0.5 minute offshore-onshore gravity grid	NA	Geoscience Australia (2009)
Exploration	Australian mineral exploration	NA	Geoscience Australia (2005–2009)
	Advanced mineral projects and mineral exploration highlights	NA	NSW Industry and Investment (2010)

Rationale for the Estimate

The rationale for the estimate was that it should be guided by comparing prospects to known deposits, by counting and assigning probabilities to prospects and occurrences, by consideration of spatial constraints, and by weighing positive versus negative factors listed by the panel members, as follows.

Positive Factors

Positive factors that may indicate undiscovered porphyry copper deposits in the Yeoval permissive tract include:

1. The Yeoval porphyry copper deposit, the Dogwood and Sunday Creek porphyry copper prospects, and the Brown's Creek Au-Cu skarns indicate that intrusion-related, copper-bearing hydrothermal systems operated during Silurian to Devonian time in the Yeoval tract.
2. Each of two ore zones at the Yeoval deposit is associated with small plug-like intrusions of dacite porphyry that are too small to be shown on source geologic maps at 1:1,000,000 scale, so similar unmapped intrusions with associated porphyry copper deposits could exist elsewhere in the Yeoval tract.
3. I-type igneous rocks of the Yeoval tract probably formed by partial melting of calc-alkaline to shoshonitic, mafic to intermediate igneous rocks, such as those that probably underlie the region of the accreted Macquarie Arc, which contains multiple major porphyry Cu-Au systems.
4. The spatial density of known porphyry copper deposits and prospects is low, compared to the area of this permissive tract, and that leaves plenty of space for undiscovered deposits.
5. Much of the area of the Yeoval tract is covered, and the covered areas have not been thoroughly explored for indications of hidden porphyry copper deposits.

Negative Factors

Negative factors that limit the number of undiscovered porphyry copper deposits in the Yeoval permissive tract include:

1. The Yeoval deposit is relatively small and of subeconomic to marginally economic grade.
2. The known porphyry copper prospects appear to be smaller and lower grade than the Yeoval deposit.

Table D6. Undiscovered deposit estimates, deposit numbers, tract area, and deposit density for the Yeoval tract (009pCu8003), New South Wales and Victoria, Australia.

[N_{XX}, estimated number of deposits associated with the xxth percentile; N_{und}, expected number of undiscovered deposits; s, standard deviation; C_v%, coefficient of variance; N_{known}, number of known deposits in the tract that are included in the grade and tonnage model; N_{total}, total of expected number of deposits plus known deposits; Tract area, area of permissive tract in square kilometers; Deposit density, total number of deposits per 100,000 km^2. N_{und}, s, and C_v% are calculated using a regression equation (Singer and Menzie, 2005)]

Consensus undiscovered deposit estimates					Summary statistics					Tract area (km^2)	Deposit density (N_{total}/100,000 km^2)
N_{90}	N_{50}	N_{10}	N_{05}	N_{01}	N_{und}	s	C_v%	N_{known}	N_{total}		
1	1	2	3	3	1.3	0.75	57	1	2.3	53,157	4.3

Table D7. Results of Monte Carlo simulations of undiscovered resources for the Yeoval tract (009pCu8003), New South Wales and Victoria, Australia.

[Cu, copper, in metric tons (t); Rock, in million metric tons (Mt)]

Material	Probability of at least the indicated amount						Probability of	
	0.95	0.9	0.5	0.1	0.05	Mean	Mean or greater	None
Cu (t)	0	0	25,000	210,000	310,000	71,000	0.30	0.24
Rock (Mt)	0	0	20	80	91	30	0.34	0.07

3. The Dogwood prospect appears to be related to the upper part of a shallow sill-like intrusion and small apophyses above it, rather than the porphyritic cupola of a stock, which would better concentrate hydrothermal fluid and focus porphyry-style stockwork fracturing and mineralization.
4. Most of the mapped I-type intrusions in the Yeoval permissive tract are phaneritic, whereas most porphyry copper deposits are associated with porphyro-aphanitic intrusions.
5. Pyrite appears to predominate over chalcopyrite in areas of induced-polarization anomalies associated with porphyry copper prospects in southern Victoria (Rajagopalan, 1999).
6. Although the Frogmore prospect has been interpreted as a porphyry copper prospect, it has not been shown to be related to a porphyritic intrusion, leading some to interpret it as an orogenic base-metal prospect.
7. Porphyry copper prospects in southern Victoria lack strong radiometric responses expected in porphyry copper systems with K-feldspathized rocks, which are generally associated with major porphyry copper systems (Rajagopalan, 1999).

Estimation Process

In preparation for estimation of numbers of undiscovered deposits, the assessment team reviewed, discussed, and considered key geologic information about the permissive tract and its known porphyry copper deposits and prospects. Process constraints implied by predominantly phaneritic intrusions indicate that many otherwise permissive intrusions may be too deeply eroded for preservation of apical porphyry copper systems. However, strict application of depth-of-exposure as a constraint is tempered by the fact that the Yeoval deposit is associated with small dacite porphyry intrusions that are not shown on the 1:1,000,000-scale source maps for this study. The low spatial density of known deposits and prospects in this tract and the amount of cover also leave plenty of room for similar unmapped intrusions and associated undiscovered porphyry copper deposits.

Each of five estimators (Bookstrom, Glen, Hammarstrom, Robinson, and Zientek) gave an independent estimate of the number of undiscovered deposits expected at three levels of subjective probability (90, 50, and 10 percent levels of probability, for example, or if 0 deposits at 90 percent, then at 50, 10, and 5 percent levels of probability). After an anonymous first round of estimation, the high and low estimators explained their reasoning. This led to discussion, negotiation, and settlement on a consensus set of estimates.

Consensus Estimates

Summary statistics, based on this set of consensus estimates, indicate a mean and standard deviation of 1.3±0.75 undiscovered deposits (table D6). The coefficient of variation (C_v) of 57 percent indicates a moderate degree of uncertainty in the number of undiscovered deposits. Adding the mean estimate of 1.3 undiscovered deposits to the 1 known deposit indicates a total of 2.3±0.75 porphyry copper deposits expected to occur in the Yeoval tract.

The area of the tract is 53,157 km^2, so the estimated spatial density is 0.000043 porphyry copper deposits per km^2 (about 4.3 deposits per 100,000 km^2). Comparison with global models for spatial density of porphyry copper deposits (Singer and others, 2005, 2008; Singer and Menzie, 2010) indicates that this is below the 10th percentile of deposit densities as a function of tract size in the control areas from around the world that form the basis for the models (fig. 5).

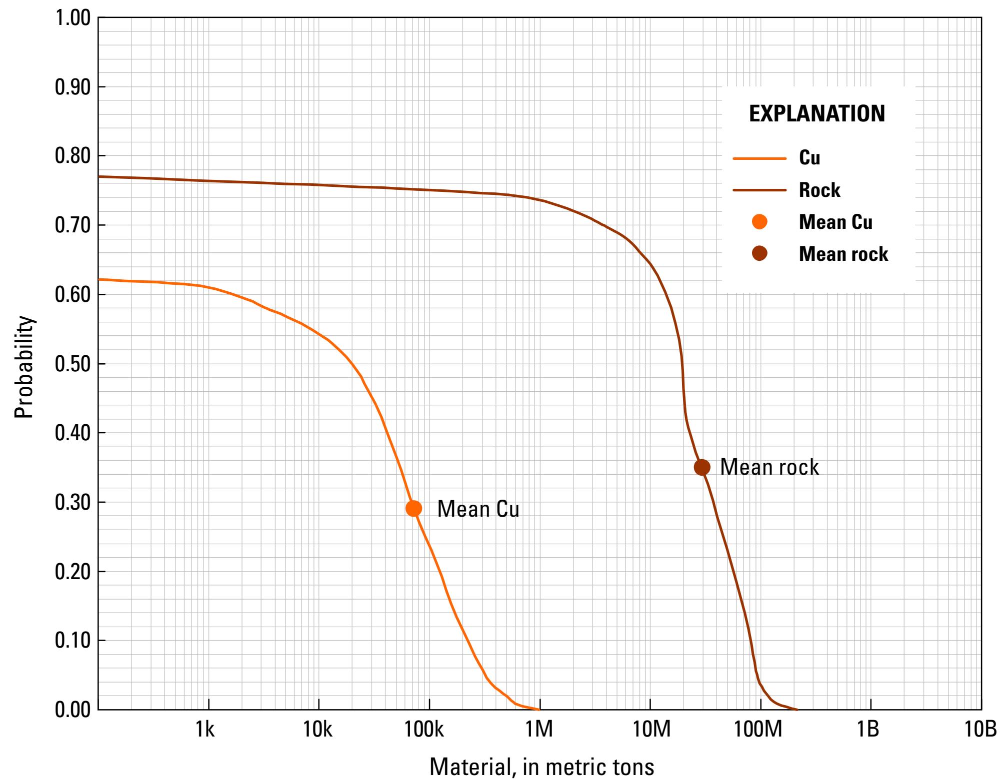

Figure D4. Cumulative frequency plot showing results of Monte Carlo computer simulation of undiscovered resources in the Yeoval tract (009pCu8003), New South Wales and Victoria, Australia. k=thousands, M=millions, B=billions.

Probabilistic Assessment Simulation Results

Undiscovered resources for the tract were estimated (table D7) by combining consensus estimates for numbers of undiscovered porphyry copper deposits with a custom grade-tonnage model for Australian porphyry copper deposits (appendix A) using the EMINERS program (Root and others, 1992; Duval, 2012; Bawiec and Spanski, 2012). Cumulative probability graphs show expected amounts of the commodities through a range of levels of subjective probabilities (fig. D4).

References Cited

Ackerman, B.R., 2003, Frogmore copper deposit, NSW, *in* Butt, C.R.M, Cornelius, M., Scott, K.M., and Robertson, I.D.M., Regolith expression of Australian ore systems—A compilation of geochemical case histories and conceptual models: Cooperative Research Centre for Landscape Environments and Mineral Exploration (CRC LEME), 3 p. (Also available at http://crcleme.org.au/Pubs/Monographs/RegExpOre.html.)

Ambler, E.P., and Facer, R.A., 1975, A Silurian porphyry copper prospect near Yeoval, New South Wales: Australian Journal of Earth Sciences, v. 22, no. 2, p. 229–241.

Augur Resources, Ltd., 2009, Maiden JORC resource estimate, Yeoval copper-gold-molybdenum-silver deposit: Augur Resources, Ltd., Web site, accessed 2010, at http://augur.com.au/Maiden%20Resource%Yeoval.

Bawiec, W.J., and Spanski, G.T., 2012, Quick-start guide for version 3.0 of EMINERS—Economic Mineral Resource Simulator: U.S. Geological Survey Open-File Report 2009–1057, 26 p., available at http://pubs.usgs.gov/of/2009/1057/. (This report supplements USGS OFR 2004–1344.)

Blevin, P.L., and Chappell, B.W., 1995, Chemistry, origin, and evolution of mineralized granites in the Lachlan Fold Belt, Australia—The metallogeny of I- and S-type granites: Economic Geology, v. 90, p. 1604–1619.

Blevin, P.L., Chappell, B.W., and Allen, C.M., 1996, Intrusive metallogenic provinces in eastern Australia based on granite source and composition: Transactions of the Royal Society of Edinburgh—Earth Sciences, v. 87, p. 281–290.

Bowman, H.N., Hobbs, J.J., and Barron, L.M., 1983, Goonumbla copper district northwest of Parkes: New South Wales Geological Survey Records, v. 21, no. 2, p. M11–M28.

Catalyst Metals, Ltd., 2008, Catalyst earns into significant molybdenum project: Catalyst Metals, Ltd., ASX release, February 18, 2008, accessed June, 2011 at http://www.catalystmetals.com/.

Champion, D.C., Kositcin, N., Huston, D.L., Mathews, E., and Brown, C., 2009, Geodynamic synthesis of the Phanerozoic of eastern Australia and implications for metallogeny: Geoscience Australia, Record 2009/18, GeoCat#68866, 222 p., digital, accessed October 4, 2010, at http://www.ga.gov.au/products/.

Commonwealth Forests Taskforce, 1998, Mineral assessment, North East Victoria: Commonwealth and Victorian Regional Forest Agreement (RFA) Steering Committee, 169 p., accessed March 15, 2012, at http://www.rfa.gov.au/.

Cox, D.P., 1986, Descriptive model of porphyry Cu (model 17), *in* Cox, D.P., and Singer, D.A., eds., Mineral Deposit Models: U.S. Geological Survey Bulletin 1693, p. 76.

Cube Consulting Pty. Ltd., 2006, Brown's Creek gold mine New South Wales, Australia: Perth, Western Australia, NI-43-101 compliant Independent Technical Report for Straits Gold Pty. Ltd., 84 p., accessed May 24, 2011, at http://www.sedar.com/.

Dickinson, W.R., and Hatherton, Trevor, 1967, Volcanism and seismicity around the Pacific: Science, v. 157, p. 801–803.

Duval, J.S., 2012, Version 3.0 of EMINERS—Economic Mineral Resource Simulator: U.S. Geological Survey Open-File Report 2004–1344/, available at http://pubs.usgs.gov/of/2004/1344/.

Ewers, G.R., Evans, N., and Hazell, M., (Kilgour, B., compiler), 2002, OZMIN mineral deposits database [Digital Datasets]: Canberra, Geoscience Australia, scale 1:1,000,000 on CD ROM. (Also available at http://www.ga.gov.au/meta/ANZCW0703003393.html.)

Geoscience Australia, 2004, Total magnetic anomaly (TMI) grids of Australia, fourth edition: Canberra, Geoscience Australia, accessed May 19, 2010, at http://www.geoscience.gov.au/.

Geoscience Australia, 2005–2009, Australian mineral exploration, a review of exploration for the years 2005 to 2009: Canberra, Geoscience Australia, accessed May 25, 2010, at http://www.geoscience.gov.au/.

Geoscience Australia, 2009, Australian national gravity database 0.5 minute offshore-onshore gravity grid: Canberra, Geoscience Australia, accessed May 19, 2010, at http://www.geoscience.gov.au/.

Geoscience Australia, 2010, Australian atlas of mines and mineral deposits: Canberra, Geoscience Australia, accessed October 20, 2010, to December 27, 2010, at http://www.australianminesatlas.gov.au/.

Glen, R.A. and Walshe, J.L., 1999, Cross-structures in the Lachlan Orogen—The Lachlan Transverse Zone example: Australian Journal of Earth Sciences, v. 46, p. 641–658.

Glen, R.A., Crawford, A.J., and Cooke, D.R., 2007, Tectonic setting of porphyry Cu-Au mineralization in the Ordovician-Early Silurian Macquarie Arc, eastern Lachlan Orogen, New South Wales: Australian Journal of Earth Sciences, v. 54, p. 465–479.

Glen, R.A., Dawson, M.W., and Colquhoun, G.P., 2006, Eastern Lachlan Orogen Geoscience Database (DVD-ROM), Version 2: New South Wales, Department of Primary Industries—Minerals, Geological Survey of New South Wales, Maitland, NSW, Australia.

Glen, R.A., Percival, I.G., and Quinn, C.D., 2009, Ordovician continental margin terranes in the Lachlan Orogen, Australia—Implications for tectonics in an accretionary orogen along the east Gondwana margin: Tectonics, v. 28, TC6012, p. 1–17.

Gray, D.R., and Foster, D.A., 2004, Tectonic evolution of the Lachlan Orogen, southeast Australia—Historical review, data synthesis and modern perspectives: Australian Journal of Earth Sciences, v. 51, no. 6, p. 773–817.

Gulson, B.L., 1972, The high-K diorites and associated rocks of the Yeoval diorite complex, N.S.W.: Contributions to Mineralogy and Petrology, v. 35, p. 173–192.

Gulson, B.L., and Bofinger, V.M., 1972, Time differences within a calc-alkaline association: Contributions to Mineralogy and Petrology, v. 36, p. 19–26.

Hind, M.C., and Helby, R.J., 1969, The Great Artesian Basin in New South Wales: Australian Journal of Earth Sciences, v. 16, no. 1, p. 481–497.

Intierra, 2009, Intierra home page: accessed 2009 at http://www.intierra.com/Homepage.aspx.

Jaireth, S., and Miezitis, Y., 2004, OZPOT Geoprovince-scale assessment of mineral potential [1:2,500,000 scale GIS]: Canberra, Geoscience Australia, accessed 2010, at http://www.australianminesatlas.gov.au/build/common/minpot.jsp.

John, D.A., Ayuso, R.A., Barton, M.D., Blakely, R.J., Bodnar, R.J., Dilles, J.H., Gray, Floyd, Graybeal, F.T., Mars, J.C., McPhee, D.K., Seal, R.R., Taylor, R.D., and Vikre, P.G., 2010, Porphyry copper deposit model, chapter B *of* Mineral deposit models for resource assessment: U.S. Geological Survey Scientific Investigations Report 2010–5070–B, 169 p., accessed January 15, 2011, at http://pubs.usgs.gov/sir/2010/5070/b/.

Lewis, P., and Downes, P.M., 2008, Mineral systems and processes in New South Wales—A project to enhance understanding and assist exploration: Geological Survey of New South Wales, Quarterly Notes, no. 128, 13 p., accessed February 2, 2012, at http://www.dpi.nsw.gov.au/__data/assets/pdf_file/0009/229914/00128-Quarterly-Notes-April-2008.pdf.

Maher, S., 2003, Dogwood porphyry Cu-Mo prospect, Benambra terrane, Victoria, *in* Butt, C.R.M, Cornelius, M., Scott, K.M., and Robertson, I.D.M., Regolith expression of Australian ore systems—A compilation of geochemical case histories and conceptual models: Cooperative Research Centre for Landscape Environments and Mineral Exploration (CRC LEME), 3 p., accessed March 2011, at http://crcleme.org.au/Pubs/Monographs/RegExpOre.html/.

NSW Industry and Investment, 2010, Advanced mineral projects and mineral exploration highlights: New South Wales Department of Primary Industries, geologic map, showing operational mines and active exploration sites, with estimated resources and best intercepts, accessed 2010 at http://www.industry.nsw.gov.au/.

Panteleyev, A., 1995, Porphyry Cu-Au—Alkalic (model L03), *in* Lefebure, D.V., and Ray, G.E., eds., Selected British Columbia mineral deposit profiles, vol. 1—Metallics and coal: British Columbia Ministry of Employment and Investment, Energy and Minerals Division, Open File 1995–20, p. 83–86, accessed April 5, 2012, at http://www.empr.gov.bc.ca/Mining/Geoscience/MineralDepositProfiles/.

Panteleyev, A., 2005, Porphyry Cu±Mo±Au L04., *in* Fonseca, A., and Bradshaw, G., compilers, Yukon mineral deposits profiles: Yukon Geological Survey Open File 2005–5, 175 p., accessed July 28, 2009, at http://www.geology.gov.yk.ca/mineral_deposit_profiles.html; http://ygsftp.gov.yk.ca/publications/openfile/2005/of2005_5.pdf; http://www.geology.gov.yk.ca/pdf/l04_porphyry_cu_mo_au.pdf.

Paradigm Metals, 2008, Frogmore—High-grade copper intersections in RC drilling including 6 m @ 3.1% Cu from 80m depth: Paradigm Metals, ASX release, 10 June 2008, accessed 2011 at http://www.paradigmgold.com/.

Paradigm Metals, 2011, Projects, Base Metals—Frogmore: Paradigm Metals Web site, accessed March 23, 2011, at http://www.paradigmgold.com.au/.

Paterson, I. B. L., Bowman, H. N., and Hobbs, J. J., 1983, Yeoval copper-gold-molybdenum district: Geological Survey of New South Wales Records v. 21, no. 2, p. M53–M73.

Perkins, C., Walshe, J.L., and Morrison, G., 1995, Metallogenic episodes of the Tasman fold belt system, eastern Australia: Economic Geology, v. 90, p. 1443–1466.

Rajagopalan, S., 1999, Porphyry-type copper deposits, eastern Victoria, *in* Willcocks, A.J., Haydon, S.J., Asten, M.W., and Moore, D.H., eds., Geophysical signatures of base metal deposits in Victoria: Geological Survey of Victoria Report 119 and Australian Society of Exploration Geophysicists, Special Publication No. 11, p. 113–127.

Raymond, O.L., Liu, S.F., Kilgour, P., Retter, A.J., and Connolly, D.P., 2007, Surface geology of Australia, 1:1,000,000 scale, Victoria, 3rd edition [Digital Dataset]: Canberra, Geoscience Australia, accessed 2009 at http://ga.gov.au.

Raymond, O.L., Liu, S.F., Kilgour, P., Retter, A.J., Stewart, A.J., and Stewart, G., 2007, Surface geology of Australia, 1:1,000,000 scale, New South Wales, 2nd edition [Digital Dataset]: Canberra, Geoscience Australia, accessed 2009, at http://ga.gov.au.

Root, D.H., Menzie, W.D., and Scott, W.A., 1992, Computer Monte Carlo simulation in quantitative resource estimation: Natural Resources Research, v. 1, no. 2, p. 125–138.

Singer, D.A., Berger, V.I., Menzie, W.D., and Berger, B.R., 2005, Porphyry copper density: Economic Geology, v. 100, no. 3, p. 491–514.

Singer, D.A., Berger, V.I., and Moring, B.C., 2008, Porphyry copper deposits of the world—Database and grade and tonnage models, 2008: U.S. Geological Survey Open-file Report 2008–1155, 45 p., available at http://pubs.usgs.gov/of/2008/1155/.

Singer, D.A., and Menzie, W.D., 2005, Statistical guides to estimating the number of undiscovered mineral deposits—An example with porphyry copper deposits, *in* Cheng, Qiuming, and Bonham-Carter, Graeme, eds., Proceedings of IAMG—The annual conference of the International Association for Mathematical Geology: Toronto, Canada, Geomatics Research Laboratory, York University, p. 1028–1033.

Singer, D.A., and Menzie, W.D., 2010, Quantitative mineral resource assessments—An integrated approach: New York, Oxford University Press, 219 p.

Stuart-Smith, P.G., 1990, Evidence for extensional tectonics in the Tumut Trough, Lachlan Fold Belt, NSW: Australian Journal of Earth Sciences, v. 37, p. 147–167.

Taylor, G.R., 1983, Copper and gold in skarn at Brown's Creek, Blayney, NSW: Australian Journal of Earth Sciences, v. 30, no. 3, p. 431–442.

U.S. Department of State, 2009, Small-scale digital international land boundaries (SSIB)—Lines, edition 10, and polygons, beta edition 1, *in* Boundaries and sovereignty encyclopedia (B.A.S.E.): U.S. Department of State, Office of the Geographer and Global Issues.

Wyborn, D, Turner, B.S., and Chappell, B.W., 1987, The Boggy Plain Supersuite—A distinctive belt of I-type igneous rocks of potential economic significance in the Lachlan Fold Belt: Australian Journal of Earth Sciences, v. 34, no. 1, p. 21–43.

Appendix E. Porphyry Copper Assessment for Tract 009pCu8004, East Tasmanide, Australia

By Arthur A. Bookstrom[1], Richard A. Glen[2], Jane M. Hammarstrom[3], Michael L. Zientek[1], and Gilpin R. Robinson, Jr.[3]

Deposit Type Assessed

Deposit type: Porphyry copper

Descriptive models: Porphyry copper, Cu-Mo, and Cu-Au (Cox, 1986a, b, c); porphyry Cu ± Mo ± Au (Panteleyev, 1995a, 2005a), porphyry Cu-Au (Panteleyev, 1995b, 2005b), Cooke and others (1998), Jaireth and Miezitis (2004a), and porphyry copper (John and others, 2010)

Grade and tonnage model: Eastern Australian porphyry copper (appendix A)

Table E1 summarizes selected assessment results.

Table E1. Summary of selected resource assessment results for the Central sub-tract (009pCu8004b), East Tasminide tract, Queensland, Australia.

[km, kilometers; km^2, square kilometers; t, metric tons]

Date of assessment	Assessment depth (km)	Tract area (km^2)	Known copper resources (t)	Mean estimate of undiscovered copper resources (t)	Median estimate of undiscovered copper resources (t)
September 2010	1	290,646	2,300,000	280,000	190,000

Location

The East Tasmanide tract extends along the eastern margin of Australia from the northern tip of the Cape York Peninsula to the northeastern corner of New South Wales (fig. E1).

Geologic Features Assessed

Igneous rocks related to pre-accretionary subduction beneath accreted island arcs and igneous rocks related to west-dipping subduction beneath the continental margin of eastern Australia.

[1]U.S. Geological Survey, Spokane, Washington, United States.

[2]Geological Survey of New South Wales, Hunter Region Mail Centre, New South Wales, Australia.

[3]U.S. Geological Survey, Reston, Virginia, United States.

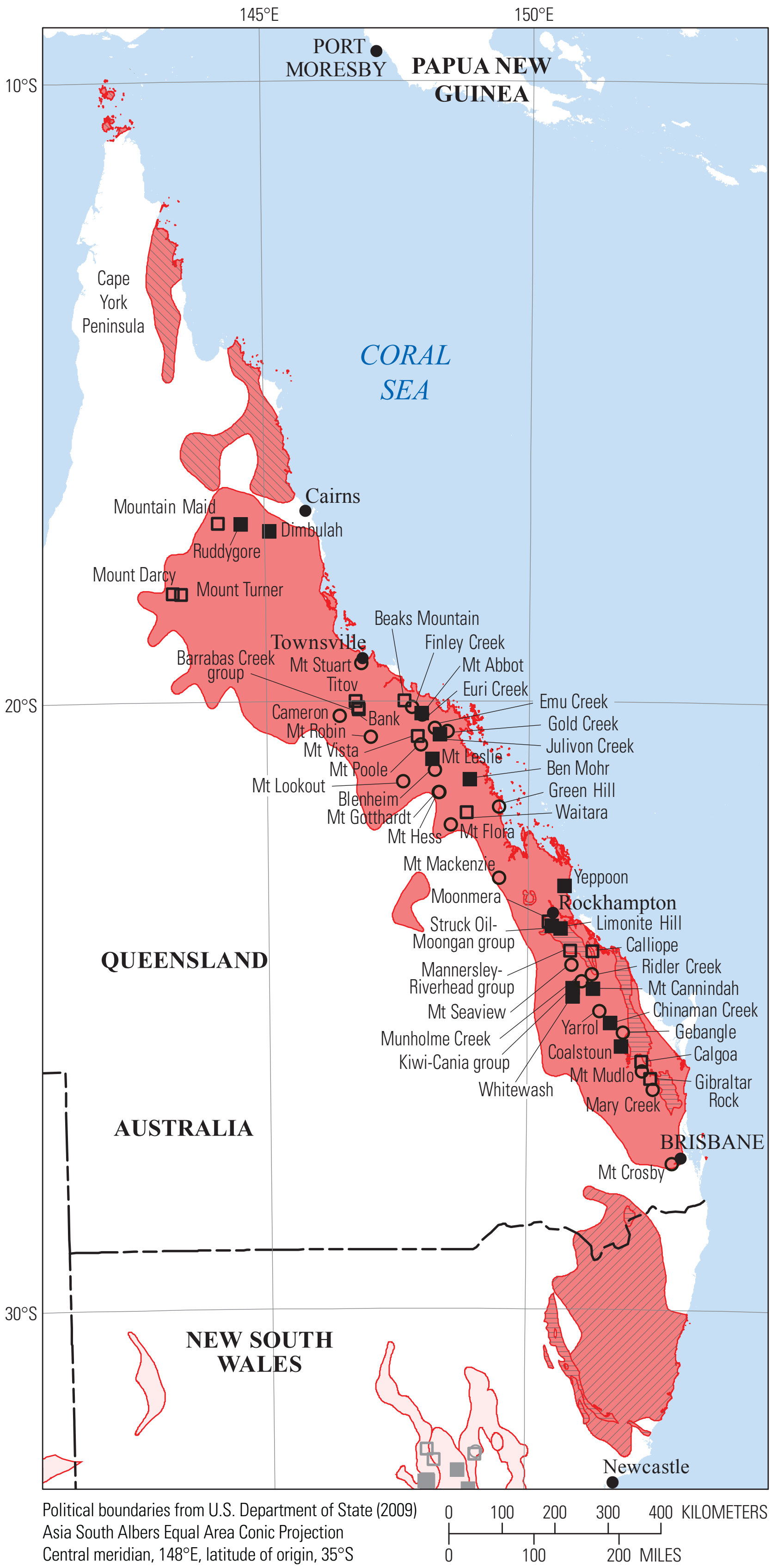

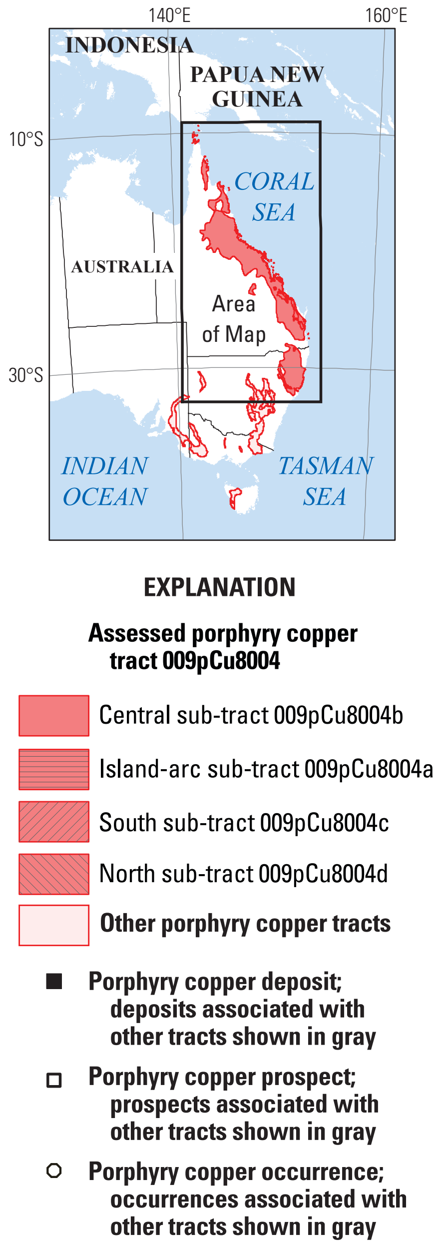

Figure E1. Map showing the East Tasmanide permissive tract (009pCu8004) and sub-tracts. Also shown are known porphyry copper deposits, significant prospects, and occurrences in the East Tasmanide tract, New South Wales and Queensland, Australia.

Delineation of the Permissive Tract

Geologic Criteria

The East Tasmanide tract includes permissive intrusive and extrusive rocks of accreted island-arc terranes (fig. E2) and continental magmatic arcs (fig. E3). These are distributed along the eastern margin of the Australian continent. Four sub-tracts were delineated, based on the nature and history of igneous rocks and the presence or absence of porphyry copper deposits and significant prospects in these sub-tracts (fig. E1).

The Island-arc sub-tract of the East Tasmanide permissive tract includes permissive rocks in subduction-related island-arc terranes, accreted to the continental margin (fig. E2). The Central, North, and South sub-tracts include permissive rocks in subduction-related magmatic belts along the eastern continental margin. The Central sub-tract contains all of the known porphyry copper deposits and significant prospects in the East Tasmanide permissive tract (fig. E1). Map units that define these subtracts are listed in table E2.

Permissive Rock Types

Descriptive models by Cox (1986a, b, c), Panteleyev (1995a, b and 2005a, b), Cooke and others (1998), and Jaireth and Miezitis (2004a) indicate that alkaline suites of I-type igneous rocks are permissive for porphyry Cu-Au deposits and calc-alkaline suites of I-type igneous rocks are permissive for porphyry copper deposits. Alkaline suites occur in some island-arcs and in some continental back-arc regions. Such alkaline suites may include gabbro, diorite, monzodiorite, monzonite, syenite, and foidal syenite or their microcrystalline to porphyro-aphanitic equivalents, including basalt, andesite, trachyandesite, latite, trachyte, and foidal trachyte. These rock types are considered permissive for porphyry Cu-Au deposits.

Permissive calc-alkaline suites occur in some island arcs and are typical of most subduction-related continental magmatic arcs. Such calc-alkaline suites may include diorite, quartz diorite, tonalite, granodiorite, quartz monzonite, monzogranite, and granite of calc-alkaline affinity. Porphyro-aphanitic equivalents include andesite, quartz andesite, dacite, rhyodacite, quartz latite, and rhyolite porphyries of calc-alkaline affinity. These rock types are considered permissive for porphyry copper deposits, porphyry Cu-Mo deposits, and porphyry Cu ± Mo ± Au deposits.

Porphyry copper deposits generally are associated with porphyritic intrusions characterized by phenocrysts in a microcrystalline to aplitic groundmass. However, such rocks commonly occur below (or are intrusive into) widespread bodies of volcanic rocks, and above (or are intrusive into) bodies of coarser grained plutonic rocks of similar age and composition. Therefore, rocks of appropriate composition and age are considered permissive, whether or not they are intrusive porphyries. However, gabbro and basalt are considered permissive only where they occur with other permissive rock types in a setting interpreted to represent subduction-related magmatism.

East Tasmanide Permissive Sub-Tracts

Island-Arc Sub-Tract (009pCu8004a)

The East Tasmanide Island-arc sub-tract represents accreted fragments of island-arc terranes in the New England Orogen—the Calliope Arc and the Gympie Arc (fig. E2). The Calliope Arc is represented by the Calliope, Gamilaroi, and Silverwood terranes of Silurian-Devonian age. According to Champion and others (2009, p. 60), the “Calliope Arc consists of Late Silurian to Middle Devonian shallow marine volcaniclastic sediments with varying amounts of calc alkaline felsic to mafic volcanic rocks.” The Calliope Arc docked with the Lachlan Orogen and was accreted to the continental margin during the Late Devonian Tabberabberan Orogeny. A forearc basin assemblage lies mostly west of the Calliope Arc, and an accretionary wedge assemblage lies to the east. This arrangement indicates that west-dipping subduction was involved in accretion of the Calliope Arc to the continental margin (Champion and others, 2009).

The Silurian-Devonian Calliope terrane hosts two known porphyry copper deposits, but these are related to postaccretionary intrusions of Late Permian to Triassic age. Therefore, these porphyry copper deposits are not assigned to the Island-arc sub-tract. Instead, they are considered to belong to a continental magmatic belt of Late Permian to Triassic age, and they are included in the Central sub-tract.

The Calliope terrane also hosts the Mount Morgan Au-Cu deposit (fig. E2). According to Arnold and Sillitoe (1989), the Mount Morgan Au-Cu deposit contained approximately 280 t of gold and 360,000 t of copper in 50 Mt of ore. This deposit is hosted in a pendant of volcaniclastic and sedimentary rocks in the roof zone of a tonalitic pluton of the Mount Morgan Group. This tonalitic pluton is Late Devonian in age, and it probably was emplaced during accretion of the Calliope Arc during the Late Devonian Tabberabberan Orogeny.

Fedikow and Govett (1985) described the Mount Morgan Au-Cu deposit as a pipe-like body of pyritic massive sulfides, hosted in rhyolitic tuff. Their cross section of the deposit shows a steeply plunging pipe that widens upward into relatively flat-lying felsic porphyries, like a massive-sulfide feeder zone. Lawrence (1967, 1972) classified the Mount Morgan deposit as a metamorphosed volcanic-hosted massive sulfide deposit. Arnold and Sillitoe (1989) emphasized the spatial and temporal relation between the ore and the subjacent, post-volcanic tonalite pluton, and they therefore classified the Mount Morgan deposit as an intrusion-related replacement deposit. Ulrich and others (2003) described both volcanic-related and pluton-related features, and they suggested that the Mount Morgan Au-Cu deposit represents a unique hybrid of volcanic-hosted massive-sulfide, intrusion-related replacement, and stockwork-veinlet deposit types. In any case, we do not regard the Mount Morgan Au-Cu deposit

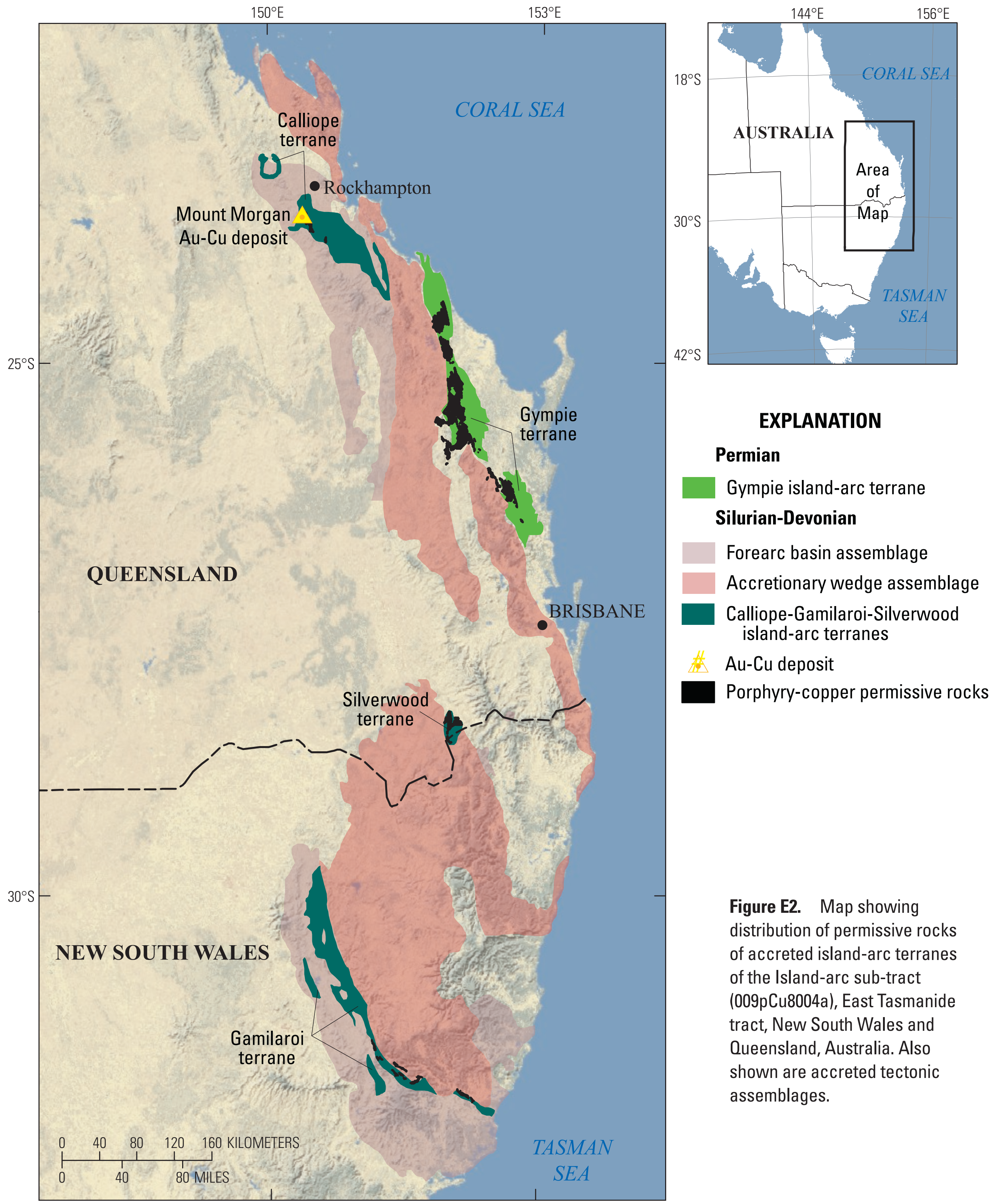

Political boundaries from U.S. Department of State (2009)
Asia South Albers Equal Area Conic Projection
Central meridian, 151°E, latitude of origin, 15°S

Geology modified from Raymond and others, 2007; Whitaker and others, 2007; and Champion and others, 2009.

World Physical Map from ESRI ArcGIS Online (accessed November 5, 2012):
http://www.esri.com/software/arcgis/arcgis-online-map-and-geoservices/map-services

Figure E2. Map showing distribution of permissive rocks of accreted island-arc terranes of the Island-arc sub-tract (009pCu8004a), East Tasmanide tract, New South Wales and Queensland, Australia. Also shown are accreted tectonic assemblages.

as a porphyry copper deposit, nor do we regard it as evidence for the presence of pre-accretionary porphyry copper deposits in the Calliope Arc.

The Gympie Arc is represented by the Gympie terrane of Permian age. The Gympie terrane consists of submarine and subaerial island-arc tholeiites, basaltic tuff breccias and lavas, and sedimentary rocks of the Gympie Group. These are overlain unconformably by andesites and dacites, which are geochemically indicative of an island-arc setting (Champion and others, 2009). The Gympie terrane was accreted to the eastern continental margin in Triassic time, and its accretion may have ended a Permian-Triassic episode of continental-arc magmatism (Champion and others, 2009). There are no porphyry copper deposits in the Gympie terrane.

Continental-Margin Sub-Tracts

Areas of permissive volcanic and intrusive rocks related to multiple episodes of west-dipping subduction beneath the continental margin of eastern Australia are shown in figure E3. In the Central sub-tract, the areal ratio of volcanic to intrusive rocks is 1v/2i, in the North sub-tract it is 1v/2.7i, and in the South sub-tract, it is 1v/9.9i. All of the known porphyry copper deposits and significant prospects are located in the Central sub-tract, which probably is the least deeply eroded, as indicated by its larger ratio of preserved volcanic rocks to exposed intrusive rocks.

The East Tasmanide tract includes four successive belts of permissive igneous rocks, as shown in figure E4. The ranges of ages of permissive rocks in these successive belts are:

- Cambrian to Devonian
- Carboniferous to Middle Permian
- Late Permian to Triassic
- Late Jurassic to Early Cretaceous.

However, the ages of some permissive rocks between Townsville and Rockhampton are less well constrained and may range from Carboniferous to Cretaceous.

Each of these magmatic belts is interpreted to be a product of an episode of west-dipping subduction beneath the eastern continental margin (as it was configured at the time of the corresponding magmatic episode). In general, each successive magmatic belt is east of (and outboard from) preceding magmatic belts. Where the belts overlap, plutons of the younger belt intrude those of the older belts.

The Cambrian-Devonian magmatic belt consists of volcanic rocks of Cambrian-Ordovician age and postvolcanic intrusions of Silurian-Devonian age. Stolz (1995) interpreted volcanic rocks and massive sulfide deposits of Cambrian to Devonian age as products of back-arc volcanism, related to west-dipping subduction beneath continental crust. This volcanic belt contains volcanic-related massive sulfide deposits. Postvolcanic intrusions host three porphyry copper prospects (fig. E4), which Horton (1978) classified as Silurian-Devonian in age, on the basis of the ages of their host granitoid intrusions.

A continental-margin magmatic belt of Carboniferous to Middle Permian age hosts porphyry copper deposits and prospects near Cairns and Townsville (fig. E4). According to Champion and others (2009), these igneous rocks and porphyry copper systems probably formed in an Andean-style continental magmatic arc that was active early in the Hunter-Bowen tectonic cycle.

Igneous rocks and porphyry copper deposits and prospects of Late Permian to Triassic age are most abundant between Stanage and Brisbane (fig. E4). These igneous rocks and porphyry copper systems probably formed in an Andean-style continental magmatic arc that was active during late stages of the Hunter-Bowen tectonic cycle. Accretion of the Gympie Arc may have ended this episode of continental-arc magmatism in Middle to Late Triassic time.

Areas of Late Jurassic to Early Cretaceous igneous rocks generally fringe, embay, and invade the eastern margins of older magmatic belts (fig. E4). Porphyry copper deposits and prospects of Early Cretaceous age occur near the coast between Townsville and Stanage (fig. E4). Allen and others (1997) interpreted geologic, geochemical, and isotopic evidence to indicate that igneous rocks of Early Cretaceous age (145–125 Ma) are subduction related. However, they interpreted younger felsic volcanic rocks (120–98 Ma) as products of postsubduction rifting along what became the present passive margin of eastern Australia.

The known porphyry copper deposits in these four successive continental magmatic belts are mutually similar in terms of their grade-tonnage and geological characteristics. As graphed in appendix A, these deposits generally are smaller and of lower copper-grades than those that define the global grade-tonnage model for porphyry copper deposits by Singer and others (2008). This reflects the geology of these deposits, most of which are characterized by stockworks of moderately spaced and moderately mineralized veinlets in moderately altered host rocks.

For purposes of assessment of undiscovered porphyry copper resources, it is appropriate to combine these four successive magmatic belts into one permissive tract for the following reasons: (1) they are spatially contiguous, (2) they formed in subduction-related continental magmatic-arc to back-arc settings, (3) they comprise mutually similar assemblages of permissive rocks, and (4) they contain mutually similar porphyry copper deposits and prospects.

All of the known porphyry copper deposits in continental magmatic belts of the East Tasmanide permissive tract are in the central segment of the tract, between about Brisbane and Cairns (fig. E1). This central segment of the tract is therefore thought to have higher potential for the presence of undiscovered porphyry copper deposits than southern and northern parts of the tract. Thus, the combined continental magmatic belts of the East Tasmanide tract are divided into three sub-tracts—the Central, South, and North sub-tracts, as described below.

Central Sub-Tract (009pCu8004b)

The Central sub-tract of the East Tasmanide tract is defined by areas of permissive igneous rocks of continental magmatic belts and by the distribution of porphyry copper deposits and prospects in those magmatic belts. The Central sub-tract extends along the eastern continental margin between Cairns and Brisbane. The Central sub-tract contains all of the known porphyry copper deposits and prospects in the East Tasmanide tract (fig. E1).

As shown in figure E3, the ratio of areas of volcanic rocks to areas of intrusive rocks in the Central sub-tract is fairly low (1v/2i). This ratio indicates deeper than optimum levels of erosion and exposure for the preservation of typical porphyry copper deposits, which form at relatively shallow depths, in and around the uppermost parts of subvolcanic stocks, or cupolas above larger plutons at greater depths. Thus, the relatively low tonnages and grades of known porphyry copper deposits in the Central sub-tract are consistent with evidence that they represent remnants of deposits that formed at greater than optimum depths, where high confining pressures suppressed development of stockworks of well-mineralized fractures.

North Sub-Tract (009pCu8004d)

The North sub-tract of the East Tasmanide tract is defined by the distribution of igneous rocks of permissive composition in continental magmatic belts of northeastern Queensland. Such rocks are sparsely scattered along the eastern margin of the Cape York Peninsula (fig. E3). However, the North sub-tract contains no known porphyry copper deposits or significant prospects. The ratio of the area of volcanic rocks to that of intrusive rocks in this sub-tract (1v/2.7i) is lower than that of the Central sub-tract. This indicates a deeper level of exposure, which may be too deep for the preservation of porphyry copper deposits.

South Sub-Tract (009pCu8004c)

The South sub-tract of the East Tasmanide tract is defined by igneous rocks of permissive composition at the southern end of the New England Orogen, in northeastern New South Wales (fig. E3). The ratio of the area of volcanic rocks to intrusive rocks in this sub-tract is very low (1v/9.9i). This sub-tract contains no known porphyry copper deposits or significant prospects (fig. E1). These observations are interpreted to indicate that the area of this sub-tract is too deeply eroded for preservation of porphyry copper deposits.

Extension of Permissive-Tract Boundaries to 1-km Depth

To extend permissive units to a depth of 1 km below the geologically mapped surface, we added a 10-km buffer to mapped bodies of igneous intrusive rocks, and a 2-km buffer to mapped bodies of permissive volcanic rocks. The rationale for use of such buffers is explained in the main body of this report. A spatial modeling algorithm was applied to connect permissive areas and smooth the permissive-tract boundaries. Additional details are provided in the metadata associated with the tracts in appendix G.

Known Deposits

The Central permissive sub-tract contains 14 known porphyry copper deposits and about that many significant porphyry copper prospects. As shown in appendix A, the tonnages and grades of the known deposits in this sub-tract are significantly lower than those of the global population of porphyry copper deposits included in the general grade-tonnage model by Singer and others (2008).

The Mount Cannindah deposit, with average grades of 0.65 percent copper and 0.16 g/t gold, and the Ruddygore deposit, with an average grade of 0.4 percent copper, may be of economic interest at current metal prices. However, average grades of the other deposits are between about 0.3 percent copper (at Yeppoon) and 0.1 percent copper (at Whitewash). Such low copper grades remain economically submarginal, especially in the absence of accompanying concentrations of molybdenum, gold, or silver. It is unlikely that the low grades of such deposits would have justified the effort and expense required to fully explore them in three dimensions; so such deposits may be larger than currently estimated.

Horton (1978, p. 904) summarized the general character of these relatively low-grade deposits as follows: “Overall, the deposits are characterized by weakly developed potassic alteration assemblages, although widespread phyllic and propylitic assemblages are almost always present. Sulfide and alteration mineralogy is predominantly fracture controlled and usually exhibits a rough zonation, commonly about a central core. Supergene enrichment is weakly developed or lacking and all deposits are at present economically submarginal.”

Horton (1978 table 2, p. 908–909) divided porphyry copper and porphyry molybdenum sites of Queensland into sets, based on age, and subsets based on character. The known deposits are listed in table E3, where they are organized into sets corresponding to the ages of related igneous intrusions or hydrothermal minerals (as isotopically dated or estimated from relative-age relationships), and listed within each set in order of decreasing average copper grade. In order of decreasing geologic age, these sets are:

1. Carboniferous to Middle Permian (two deposits),
2. Late Permian to Triassic (eight deposits), and
3. Early Cretaceous (four deposits).

Horton (1978) summarized key characteristics of each set and subset of porphyry copper sites, as follows.

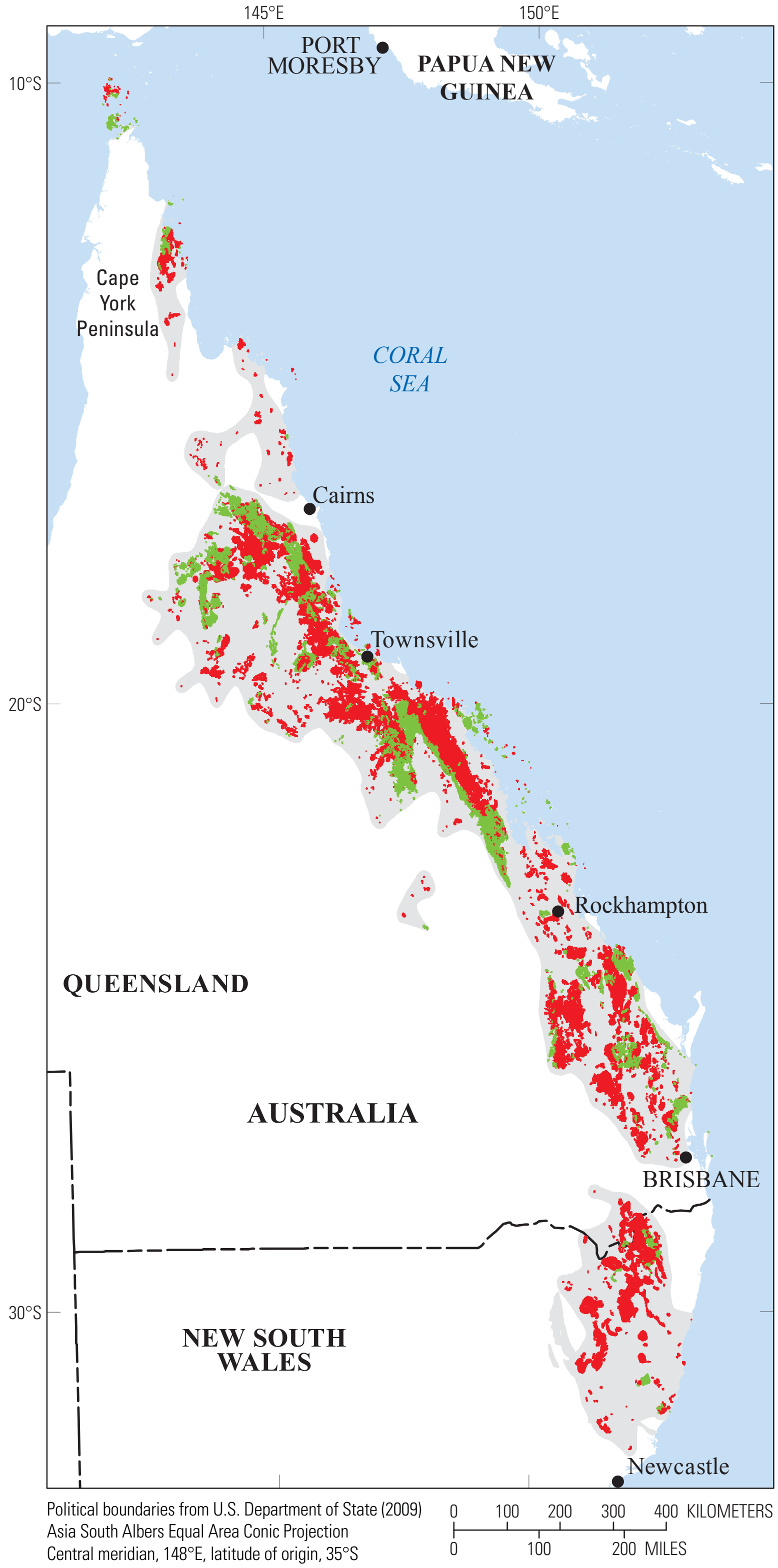

Figure E3. Map showing distribution of permissive intrusive and extrusive rocks of continental magmatic belts used to define the Central, North, and South sub-tracts of the East Tasmanide tract (009pCu8004), New South Wales and Queensland, Australia.

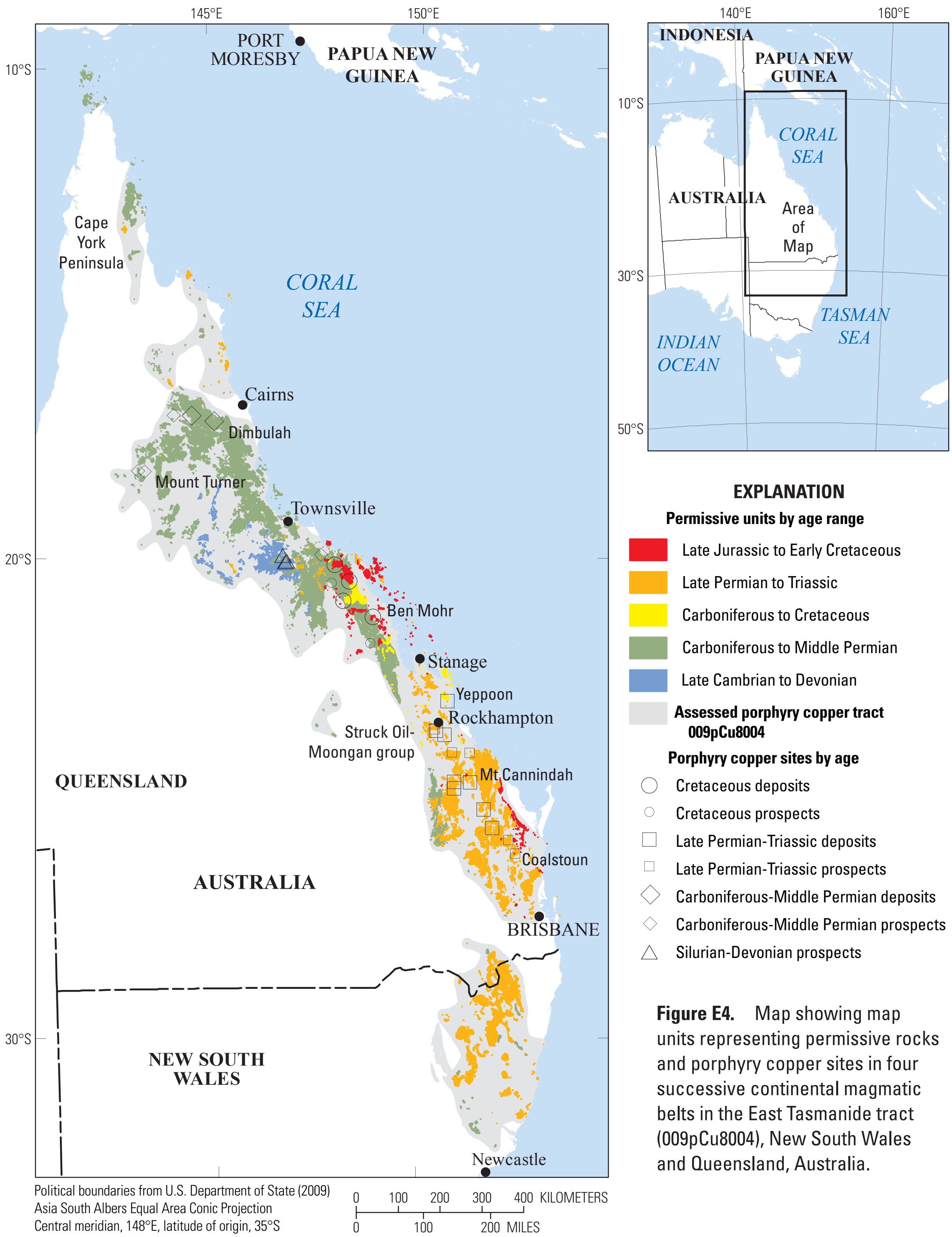

Figure E4. Map showing map units representing permissive rocks and porphyry copper sites in four successive continental magmatic belts in the East Tasmanide tract (009pCu8004), New South Wales and Queensland, Australia.

Table E2*A*. Map units that define the Island-arc sub-tract (009pCu8004a), East Tasmanide tract, New South Wales and Queensland, Australia.

[Based on Whitaker and others (2007), Raymond and others (2007), Champion and others (2009), Sivell and McCulloch (2001); for additional information about named map units, see Geoscience Australia, Stratigraphic Units Database at http://dbforms.ga.gov.au/www/geodx.strat_units.int/]

Map unit	Map symbol	Lithology	Age range
		Gympie terrane (accreted island-arc fragment)	
		Intrusive rocks	
Gympie Group		dolerite and microdiorite-shoshonite dikes	Permian
		Volcanic rocks	
Gympie Group	Pwg	basaltic to andesitic flows, pyroclastics, volcaniclastics, mudstone, siltstone, sandstone, limestone	Permian
Mant Basalt	Pbgm	basalt	Early Permian
		Calliope terrane (north part of Calliope-Gamilaroi-Silverwood island-arc assemblage)	
		Intrusive rocks	
Mount Morgan Trondhjemite	Dgor	trondhjemite	Middle Devonian
Mafic intrusives 42017	Dd	dolerite	Devonian
		Silverwood terrane (middle part of Calliope-Gamilaroi-Silverwood accreted island-arc assemblage)	
		Volcanic rocks	
Bald Hill Formation	Dwbh	mafic volcanic and subvolcanic rocks	Early Devonian
Silverwood Group	SDws	andesite, dolerite, arenite	Late Silurian to Early Devonian
Connolly Volcanics	Swsc	andesite	Late Silurian to Early Devonian
Risdon Stud Formation	Swsr	andesite, arenite	Late Silurian
		Gamilaroi terrane (south part of Calliope-Gamilaroi-Silverwood accreted island-arc assemblage)	
		Intrusive rocks	
Mafic intrusives 42021	SDd	dolerite	Late Silurian to Devonian
		Volcanic rocks	
Folly Basalt	Dbtf	basalt	Early to Middle Devonian
Mafic intrusives 42021	SDd	dolerite	Late Silurian to Early Devonian
Pitch Creek Volcanics	Dftp	basalt, andesite, dacite, felsic tuff	Late Silurian to Early Devonian

Carboniferous to Middle Permian Deposits

The Ruddygore and Dimbulah (Eureka Creek) deposits, four porphyry copper prospects, and a porphyry molybdenum prospect are of Carboniferous to Middle Permian age and are clustered about 350 km northwest of Townsville (figs. E1, E4). These are related to small elliptical granodioritic stocks of probable Permian age. Some of these stocks are hosted in metamorphic rocks of Precambrian age, and others are hosted in calc-alkaline volcanic and intrusive rocks of Carboniferous age.

According to Horton (1978, table 3), major primary sulfide minerals at the Ruddygore and Dimbulah deposits are pyrite, chalcopyrite, and subordinate bornite. Pyrite/chalcopyrite ratios are about 5:1. Minor primary sulfide minerals are arsenopyrite, pyrrhotite, galena, and subordinate molybdenite. These minerals occur in stockworks of moderately spaced and moderately mineralized fractures.

Phyllic and propylitic alteration minerals are common, but potassic alteration minerals are rare, indicating that the middle and upper parts of the deposits are exposed. Therefore, these probably are not the roots of deposits that formed at shallower depth. Instead, they probably represent deposits that formed at greater-than-normal depths for porphyry copper deposits. Supergene-enriched ore averaging less than 1.5 percent copper is present at Ruddygore.

Late Permian to Triassic Deposits

Eight known porphyry copper deposits of Late Permian to Triassic age are hosted in igneous rocks of a continental magmatic arc of that age range in southeastern Queensland, between Brisbane and Stanage (fig. E4). Horton (1978) divided these deposits into three subsets (J, K and L), according to character.

The Mount Cannindah, Limonite Hill, Coalstoun, Chinaman Creek, and Struck Oil deposits (fig. E1) are included in subset K of Horton (1978). These porphyry copper deposits are related to quartz dioritic to granodioritic intrusions of Early to Middle Triassic age. According to Horton (1978), ore-related intrusions of this subset are hosted in metasedimentary strata and andesitic volcanic rocks of Silurian to Permian age. Fracturing is weak to moderate and locally strong. Major hypogene sulfide minerals are pyrite and chalcopyrite, with minor molybdenite, magnetite, gold, galena, and sphalerite. Pyrite/chalcopyrite ratios vary from 5:1 to 20:1, and copper/molybdenum ratios vary from 10:1 to 50:1. Hydrothermal alteration products include minor inner potassic, medial phyllic, and widespread outer and late propylitic alteration-mineral assemblages. Supergene enrichment is weak.

Table E2*B*. Map units that define the Central sub-tract (009pCu8004b), East Tasmanide tract, Queensland, Australia.

[Based on Whitaker and others (2007); for additional information about named map units, see Geoscience Australia, Stratigraphic Units Database at http://dbforms.ga.gov.au/www/geodx.strat_units.int/]

Map unit	Map symbol	Lithology	Age range
		Intrusive rocks	
Felsic intrusives 39470	Kg	biotite monzogranite, quartz monzodiorite, granodiorite, diorite, rhyolite	Cretaceous
Mount Abbot Igneous Complex	Kga	alkali granite, quartz syenite	Cretaceous
Hecate Granite	Kghc	biotite-hornblende granodiorite, monzogranite, aplite, microgranite, diorite	Cretaceous
Wundaru Granodiorite	Kgwu	biotite-hornblende granodiorite	Cretaceous
Morugo Granite	Kgmo	biotite granite, hornblende-biotite granodiorite, quartz diorite, porphyritic microgranite	Cretaceous
Flat Top Diorite	Kgft	diorite	Cretaceous
Round Top Granite	Kgrt	granite	Cretaceous
Ben Mohr Igneous Complex—gabbro	Kdbm	diorite, gabbro	Cretaceous
Ben Mohr Igneous Complex—granite	Kgbm	foidal monzosyenite	Cretaceous
Mount Bridgman Igneous Complex	Kgb	biotite monzogranite, syenite, diorite, gabbro	Cretaceous
Munbura Diorite	Kgmu	diorite	Cretaceous
Mount Chelona Granite	Kgmc	biotite monzogranite to granodiorite, mafic xenoliths	Cretaceous
Swayneville Granite	Kgsw	hornblende-biotite monzogranite	Cretaceous
Cameron Creek Granite	Kgcc	granite	Cretaceous
Koumala Granite	Kgko	biotite monzogranite, syenogranite	Cretaceous
Mount Scott Granite	Kgms	hornblende-biotite monzogranite, syenogranite	Cretaceous
Tollbar Breccia	Kggt	granitoid breccia	Cretaceous
Glassford Igneous Complex—leucocratic granite	Kgg	alkali feldspar granite, rhyolite	Cretaceous
Burns Spur Nepheline Monzosyenite	Kggb	foidal monzosyenite	Cretaceous
Mount Barker Granodiorite	Kgmb	hornblende-biotite granodiorite, diorite	Early Cretaceous
Bundarra Granodiorite	Kgbu	hornblende-biotite tonalite	Early Cretaceous
Noosa Quartz Diorite	Jgno	quartz diorite	Late Jurassic to Cretaceous
Mount Bauple Syenite	Jgmb	biotite-quartz syenite	Late Jurassic to Early Cretaceous
Mount Urah Granodiorite	Jgmu	hornblende-biotite granodiorite, pyroxene-hornblende diorite	Late Jurassic to Early Cretaceous
Diorite 42029	Jgd	diorite, minor aplite, microgranite	Jurassic to Cretaceous
Felsic intrusives 42028	Jgq	granite, microgranite	Jurassic to Cretaceous
Intrusive rhyolite 68108	Mzgi	rhyolite	Mesozoic
Wonbah Granodiorite	-Rgwn	hornblende-biotite granodiorite, quartz diorite	Late Triassic
Broomfield Granite	-Rgbr	biotite granite, hornblende tonalite, diorite, quartz diorite, granodiorite	Late Triassic
Tawah Granodiorite	-Rgta	biotite-muscovite granite, hornblende tonalite, pyroxene-hornblende diorite	Late Triassic
Musket Flat Granodiorite	-Rgmk	biotite-hornblende granodiorite	Late Triassic
Degilbo Granodiorite	-Rgdg	biotite granite, hornblende-bio granite, granophyre, porphyritic granodiorite	Late Triassic
Mungore Granite	-Rgmm	biotite granite, granophyre, rhyolite	Late Triassic

Table E2*B*. Map units that define the Central sub-tract (009pCu8004b), East Tasmanide tract, Queensland, Australia.—Continued

Map unit	Map symbol	Lithology	Age range
		Intrusive rocks	
Boogooramunya Granite	-Rgby	biotite granite, granophyre, rhyolite	Late Triassic
Canoe Creek Granite	-Rgcn	biotite-hornblende granite to granodiorite	Late Triassic
Wooroonden Granodiorite	-Rgwr	hornblende-biotite granodiorite, diorite, quartz diorite, tonalite, gabbro	Late Triassic
Mount Mucki Diorite	-Rgsm	hornblende-clinopyroxene diorite, quartz diorite, monzonite	Late Triassic
Gibraltar Quartz Monzodiorite	-Rgsg	hornblende-biotite monzodiorite, quartz monzodiorite	Late Triassic
Farquharson Granite	-Rgfa	hornblende-biotite granite	Late Triassic
Cedar Pocket Porphyry	-Rgce	biotite-hornblende granite to granodiorite	Late Triassic
Woondum Granite	-Rgwd	granite, granodiorite, monzogranite, quartz diorite	Late Triassic
Eerwah Vale Tonalite	-Rgee	tonalite, diorite	Late Triassic
Tungi Creek Granodiorite	-Rgtu	biotite-hornblende granodiorite, hornblende-biotite granite	Late Triassic
Avoca Creek Granodiorite	-Rgav	hornblende granodiorite	Late Triassic
Neurum Complex	-Rgn	granodiorite, quartz monzonite, granite	Late Triassic
Brisbane Valley Porphyrite	-Rgbv	hornblende diorite, microdiorite	Late Triassic
Wilfred Creek Igneous Complex	-Rgw	hornblende-biotite diorite, quartz diorite, tonalite, gabbro, monzogranite	Middle to Late Triassic
Gloucester Granite	-Rggc	granite	Triassic
Felsic to intermediate intrusives 39497	-Rg	granite, granodiorite, monzogranite, quartz monzonite, tonalite, gabbro	Triassic
Kabra Quartz Monzodiorite	-Rgok	hornblende-quartz monzodiorite, gabbro, quartz gabbro	Triassic
Diorite 40152	-Rgd	diorite	Triassic
Voewood Granite	-Rgvo	biotite granite	Triassic
Diglum Granodiorite	-Rgmd	biotite-hornblende granodiorite, tonalite, quartz diorite	Triassic
Matchbox Range Granite	-Rgma	biotite quartz syenite	Triassic
Littlemore Granodiorite	-Rggi	biotite-hornblende granodiorite, quartz monzodiorite	Triassic
Monal Granodiorite	-Rggm	hornblende-biotite granodiorite, granite, quartz diorite	Triassic
Rule Gabbro	-Rdgr	gabbro, dolerite	Triassic
Deception Quartz Monzonite	-Rggd	hornblende-biotite quartz monzonite, granite	Triassic
Lawyer Granite	-Rggl	hornblende-biotite granodiorite, granite, tonalite	Triassic
Molangul Granite	-Rgmg	leucogranite	Triassic
Watalgan Granite	-Rgwa	biotite granite, biotite granodiorite, biotite-hornblende quartz diorite, aplite	Triassic
Moolyung Granodiorite	-Rgml	hornblende-biotite granodiorite	Triassic
Mount Bania Granite	-Rgbc	biotite-hornblende monzogranite	Triassic
Intrusive rhyolite 42031	-Rgi	rhyolite intrusive sill-like bodies	Triassic
Mount Saul Granite	-Rgms	biotite-hornblende monzogranite	Triassic
Boondooma Igneous Complex—granite	-Rgbd	biotite-hornblende granite to granodiorite	Triassic
Memerambi Granite	-Rgmb	hornblende-biotite granite	Triassic

Table E2*B*. Map units that define the Central sub-tract (009pCu8004b), East Tasmanide tract, Queensland, Australia.—Continued

Map unit	Map symbol	Lithology	Age range
		Intrusive rocks	
Kingaham Creek Granodiorite	-Rgki	hornblende-quartz monzodiorite, gabbro, quartz gabbro	Triassic
Taromeo Igneous Complex—granodiorite 2	-Rgtr4	biotite-hornblende granodiorite, granite, quartz monzonite, tonalite, quartz diorite	Triassic
Taromeo Igneous Complex—diorite	-Rgtr5	quartz diorite, granodiorite, gabbro, diorite, tonalite, microdiorite	Triassic
Taromeo Igneous Complex—granodiorite 1	-Rgtr6	biotite-hornblende granodiorite, tonalite	Triassic
Mount Mee Granophyre	-Rgme	granophyre	Triassic
Somerset Dam Igneous Complex—granophyre	-Rgsd	granophyre	Triassic
Somerset Dam Igneous Complex—gabbro	-Rdsd	microgabbro, leucogabbro, plagiogabbro, ferrigabbro	Triassic
Dayboro Tonalite	-Rgda	biotite-pyroxene tonalite, biotite granodiorite	Triassic
Mount Samson Granodiorite	-Rgmn	granodiorite, diorite, gabbro, granite, microgranite	Triassic
Samford Granodiorite	-Rgs	granodiorite, diorite, trondhjemite	Triassic
Enoggera Granite	-Rgeg	biotite granite, granodiorite	Triassic
Karana Quartz Diorite	-Rgkr	quartz diorite, diorite	Middle Triassic
Grevillea Granite	-Rggv	biotite syenogranite	Early to Middle Triassic
Nour Nour Granodiorite	-Rgnn	biotite-hornblende granodiorite, hornblende-biotite granodiorite	Early to Middle Triassic
Calgoa Diorite	-Rgcg	hornblende diorite, biotite-hornblende diorite to granodiorite, granite	Early to Middle Triassic
Boonara Granodiorite	-Rgbn	biotite-hornblende granodiorite, quartz diorite, diorite	Early to Middle Triassic
Rush Creek Granodiorite	-Rgsr	hornblende granodiorite to monzogranite	Early to Middle Triassic
Woolooga Granodiorite	-Rgsl	biotite-hornblende quartz monzodiorite to granodiorite	Early to Middle Triassic
Native Creek Microgranite	-Rgnc	hornblende-biotite microgranite	Early to Middle Triassic
Goomboorian Intrusive Complex—gabbro	-Rdgo	gabbro	Early to Middle Triassic
Goomboorian Intrusive Complex—diorite	-Rggo	diorite	Early to Middle Triassic
Woonga Granodiorite	-Rgsw	biotite-hornblende quartz monzodiorite to granodiorite	Early to Middle Triassic
Champion Hills Diorite	-Rgch	diorite, gabbro	Early to Middle Triassic
Buaraba Granodiorite	-Rgbu	granodiorite, tonalite, quartz diorite	Early to Middle Triassic
South Buaraba Microdiorite	-Rgsb	microdiorite	Early to Middle Triassic
Greenbank Quartz Diorite	-Rggr	biotite-hornblende quartz diorite, biotite-pyroxene quartz diorite	Early to Middle Triassic
New Moonta Diorite	-Rgnm	diorite, quartz diorite	Early to Middle Triassic
Black Snake Porphyry	-Rgbk	quartz diorite, monzodiorite, microdiorite	Early Triassic
Borilla Granite	-Rgbi	granite	Early Triassic
Eskdale Granodiorite 4	-Rges4	hornblende-biotite granodiorite, diorite	Early Triassic
Eskdale Granodiorite 3	-Rges3	hornblende-biotite granodiorite, granite, diorite, gabbro	Early Triassic
Eskdale Granodiorite-gabbro	-Rdes	gabbro	Early Triassic

Table E2*B*. Map units that define the Central sub-tract (009pCu8004b), East Tasmanide tract, Queensland, Australia.—Continued

Map unit	Map symbol	Lithology	Age range
		Intrusive rocks	
Eskdale Granodiorite 1	-Rges1	granodiorite, diorite, gabbro	Early Triassic
Eskdale Granodiorite 2	-Rges2	hornblende-biotite granodiorite	Early Triassic
Eskdale Granodiorite 5	-Rges5	granite	Early Triassic
Latite 39474	Pal	latite	Late Permian to Early Cretaceous
Pyri Pyri Granite	Pgpy	biotite-muscovite granite, hornblende-biotite monzogranite, biotite-hornblende granodiorite, dacite	Late Permian to Early Cretaceous
Mafic intrusives 42032	PKd	dolerite, gabbro, diorite	Permian to Cretaceous
Bayfield Granite	Pgba	biotite granite, biotite-hornblende monzogranite	Permian to Cretaceous
East Apple Granite	Pgea	hornblende-biotite monzogranite	Late Permian to Early Triassic
Gabbro 39477	Pdq	gabbro, diorite	Late Permian to Early Triassic
Racecourse Creek Gabbro	Pdrc	gabbro	Late Permian to Early Triassic
Wattlebank Granodiorite	Pgwa	granodiorite, pegmatite	Late Permian to Early Triassic
Ridgelands Granodiorite	Pgmr	biotite-hornblende granodiorite, tonalite, quartz diorite	Late Permian to Early Triassic
Gracemere Gabbro	Pdor	quartz-hornblende-biotite-orthopyroxene-clinopyroxene gabbro	Late Permian to Early Triassic
Bundaleer Tonalite	Pgob	hornblende-biotite tonalite, biotite granite	Late Permian to Early Triassic
Quarry Gabbro	Pdoq	gabbro	Late Permian to Early Triassic
Umbrella Creek Granodiorite	Pguc	biotite-hornblende granodiorite	Late Permian to Early Triassic
Moonkan Granite	Pgom	biotite-hornblende granite	Late Permian to Early Triassic
Gavial Gabbro	Pdog	gabbro	Late Permian to Early Triassic
Bajool Quartz Diorite	Pgaj	hornblende-quartz diorite	Late Permian to Early Triassic
Targinie Quartz Monzonite	Pgta	hornblende-biotite quartz monzonite	Late Permian to Early Triassic
Cecilwood Quartz Diorite	Pgce	hornblende quartz diorite	Late Permian to Early Triassic
Miriam Vale Granodiorite	Pgmv	hornblende-quartz diorite, tonalite, granodiorite, gabbro, hornblende-biotite granite	Late Permian to Early Triassic
Sawnee Gabbro	Pdgs	biotite-hornblende granodiorite	Late Permian to Early Triassic
Dumgree Tonalite	Pggd	biotite-hornblende tonalite, quartz diorite	Late Permian to Early Triassic
Mannersley Granodiorite	Pgma	biotite-hornblende microdiorite	Late Permian to Early Triassic
Riverston Granodiorite	Pgri	biotite granodiorite, diorite, microgranite, rhyolite	Late Permian to Early Triassic
Zig Zag Tonalite	Pgmz	hornblende-biotite tonalite	Late Permian to Early Triassic
Bocoolima Granodiorite	Pggb	biotite-hornblende granodiorite	Late Permian to Early Triassic
Redshirt Granite	Pggs	hornblende-biotite granite	Late Permian to Early Triassic
Castletower Granite	Pgcs	hornblende-biotite granite	Late Permian to Early Triassic
Rocky Point Granodiorite	Pggr	biotite-hornblende granodiorite	Late Permian to Early Triassic
Wyalla Granite	Pggw	biotite granite	Late Permian to Early Triassic
Bororen Tonalite	Pgbr	biotite tonalite	Late Permian to Early Triassic
Mount Seaview Igneous Complex—diorite, gabbro	Pdms	quartz diorite, quartz gabbro	Late Permian to Early Triassic
Mount Seaview Igneous Complex—granite	Pgms	hornblende-biotite granite	Late Permian to Early Triassic
Norton Tonalite	Pgnt	hornblende-biotite tonalite	Late Permian to Early Triassic
Munholme Quartz Diorite	Pgmn	quartz diorite, tonalite, diorite	Late Permian to Early Triassic
Wingfield Granite	Pgwi	hornblende-biotite granite	Late Permian to Early Triassic

Table E2*B*. Map units that define the Central sub-tract (009pCu8004b), East Tasmanide tract, Queensland, Australia.—Continued

Map unit	Map symbol	Lithology	Age range
		Intrusive rocks	
Kariboe Layered Gabbro	Pdka	layered gabbro, diorite, tonalite, hornblendite	Late Permian to Early Triassic
Toonboro Granite	Pgto	biotite-hornblende monzogranite	Late Permian to Early Triassic
Harrami Igneous Complex	Pgh	biotite monzonite, biotite granite, hornblende gabbro	Late Permian to Early Triassic
Gaeta Diorite	Pgga	diorite	Late Permian to Early Triassic
Old Kolonga Gabbro	Pdko	gabbro	Late Permian to Early Triassic
Nulambie Granite	Pgnl	biotite-hornblende granite, granodiorite	Late Permian to Early Triassic
Colodon Granite	Pgcl	hornblende-biotite monzogranite	Late Permian to Early Triassic
Moolboolaman Granodiorite	Pgmo	biotite-hornblende granodiorite, diorite, pyroxene-hornblende tonalite, biotite-hornblende granite	Late Permian to Early Triassic
Kooyong Gabbro	Pdky	hornblende gabbro	Late Permian to Early Triassic
Tecoma Granite	Pgtc	biotite granite, granodiorite, leucogranite dikes with tourmaline	Late Permian to Early Triassic
Glencoe Gabbro	Pdgl	hornblende-clinopyroxene gabbro, hornblende gabbro with pegmatoid veins	Late Permian to Early Triassic
Marvel Creek Gabbro	Pdmc	gabbro, diorite	Late Permian to Early Triassic
Wind Mill Diorite	Pgwm	diorite, quartz diorite, gabbro, granodiorite, microgranite	Late Permian to Early Triassic
Glen View Quartz Monzodiorite	Pggv	quartz monzodiorite, diorite, quartz diorite, gabbro, granodiorite	Late Permian to Early Triassic
Crystal Vale Monzogranite	Pgcr	biotite granite, monzogranite	Late Permian to Early Triassic
Hefferon Creek Gabbro	Pdhf	pyroxene-hornblende gabbro, microgranite dikes	Late Permian to Early Triassic
Kildare Granodiorite	Pgkd	biotite granodiorite, hornblende quartz monzonite, hornblende gabbro	Late Permian to Early Triassic
Greystone Granite	Pgge	biotite granite, hornblende-biotite granite	Late Permian to Early Triassic
Tandora Granodiorite	Pgtn	hornblende-biotite granodiorite, biotite syenogranite, biotite-hornblende diorite or gabbro	Late Permian to Early Triassic
Telemark Granodiorite	Pgtm	hornblende granodiorite	Late Permian to Early Triassic
Ravenscraig Gabbro	Pdra	gabbro	Late Permian to Early Triassic
Boughyard Quartz Diorite	Pgbo	quartz diorite to granodiorite	Late Permian to Early Triassic
Culcraigie Granite	Pgcu	biotite granite, monzogranite	Late Permian to Early Triassic
Euroka Granite	Pger	hornblende-biotite granite	Late Permian to Early Triassic
Eidsvold Complex	Pge	biotite granite, hornblende-biotite granodiorite, quartz gabbro	Late Permian to Early Triassic
Yenda Granodiorite	Pgye	biotite-hornblende granodiorite, hornblende-biotite granite to granodiorite	Late Permian to Early Triassic
Morrow Granite	Pgmw	leucogranite	Late Permian to Early Triassic
Flat Range Granodiorite	Pgfr	hornblende-biotite granodiorite, gabbro, monzogabbro, monzonite	Late Permian to Early Triassic
Widbury Granite	Pgwb	granodiorite, pegmatite	Late Permian to Early Triassic
Quaggy Mountain Quartz Gabbro	Pdqm	quartz gabbro, quartz diorite, local pegmatite	Late Permian to Early Triassic
Wathonga Granite	Pgwt	biotite leucogranite	Late Permian to Early Triassic
Pollard Granodiorite	Pgpo	hornblende-biotite granodiorite	Late Permian to Early Triassic
Cadarga Creek Granodiorite	Pgca	biotite-hornblende granodiorite to monzogranite	Late Permian to Early Triassic
Cheltenham Creek Monzogranite	Pgcm	hornblende-biotite monzogranite	Late Permian to Early Triassic
Delubra Quartz Gabbro	Pdde	gabbro with hornblende phenocrysts	Late Permian to Early Triassic
Greencoat Monzonite	Pggc	hornblende-biotite quartz monzonite	Late Permian to Early Triassic
Impey Granodiorite	Pgim	hornblende-biotite granodiorite	Late Permian to Early Triassic

Table E2*B*. Map units that define the Central sub-tract (009pCu8004b), East Tasmanide tract, Queensland, Australia.—Continued

Map unit	Map symbol	Lithology	Age range
		Intrusive rocks	
Aisbetts Granodiorite	Pgai	hornblende-biotite granodiorite	Late Permian to Early Triassic
Kenmore Gabbro	Pdke	biotite-hornblende gabbro	Late Permian to Early Triassic
Yorkeys Diorite	Pgyo	diorite, quartz diorite, granite	Late Permian to Early Triassic
May Queen Gabbro	Pdmq	gabbro, andesite	Late Permian to Early Triassic
Boondooma Igneous Complex—granodiorite	Pgbd2	granodiorite, monzogranite, granite, tonalite, diorite, gabbro	Late Permian to Early Triassic
Hivesville Granite	Pghv	biotite-hornblende granite	Late Permian to Early Triassic
Kimbala Granodiorite	Pgki	biotite-hornblende granodiorite	Late Permian to Early Triassic
Monsildale Granodiorite	Pgml	biotite-hornblende granodiorite, quartz diorite, diorite, gabbro	Late Permian to Early Triassic
Taromeo Igneous Complex—granodiorite 4	Pgtr1	biotite-hornblende granodiorite	Late Permian to Early Triassic
Taromeo Igneous Complex—tonalite	Pgtr2	tonalite, granodiorite, quartz diorite, diorite, quartz gabbro	Late Permian to Early Triassic
Boondooma Igneous Complex—tonalite	Pgbd1	diorite, granodiorite, granite	Late Permian to Early Triassic
Taromeo Igneous Complex—granodiorite 3	Pgtr3	granodiorite, tonalite	Late Permian to Early Triassic
Kenewah Granodiorite	Pgke	biotite granite, granodiorite	Late Permian to Early Triassic
Djuan Tonalite	-Rgdj	tonalite, hornblende diorite, hornblendite	Late Permian to Early Triassic
Crows Nest Granite	-Rgcw	biotite granite, monzogranite	Late Permian to Early Triassic
Hogback Granite	-Rgho	biotite granite, hornblende-biotite granite	Late Permian to Late Triassic
Melrose Igneous Complex	Pgm	biotite-hornblende granite, granodiorite, diorite, quartz microdiorite	Permian to Late Triassic
Felsic intrusives 42189	P-Rg	tonalite, granodiorite, granite, monzogranite, rhyolite, microgranodiorite	Permian to Triassic
Diorite 39481	Pgd	hornblende diorite, biotite-hornblende quartz diorite, gabbro, monzodiorite, monzonite, granodiorite	Permian to Triassic
Galloway Plains Igneous Complex	Pgg	biotite-hornblende tonalite, granodiorite	Permian to Triassic
Monduran Granite	Pgmd	monzogranite	Permian to Triassic
Briggs Granodiorite	Pgbi	biotite-hornblende granodiorite, granite, tonalite	Permian to Triassic
Stuart River Granite	Pgst	biotite microgranite, metased rocks, amphibolite	Permian to Triassic
Wooroolin Granite	Pgwn	biotite leucogranite, aplite dikes	Permian to Triassic
Aitken Creek Gabbro	Pdac	gabbro	Late Permian
Magog Gabbro	Pdma	gabbro, monzonite	Late Permian
Copperville Granodiorite	Pgcv	hornblende-biotite granodiorite, quartz diorite, porphyritic microdiorite	Late Permian
Cleethorpes Granodiorite	Pgcp	hornblende-biotite granodiorite	Late Permian
Og Syenite	Pgog	biotite syenite	Late Permian
Craiglands Quartz Monzodiorite	Pgcg	hornblende-quartz monzodiorite, quartz diorite	Late Permian
Lookerbie Igneous Complex	Pgo	tonalite, granodiorite, quartz diorite, andesite	Late Permian
Bartle Frere Granite	Pgbf	hornblende-biotite granite, biotite granite with tourmaline	Permian
Yataga Granodiorite	Pgyy	hornblende-biotite granodiorite, tonalite	Permian
Flagstone Granite	Pgfg	granite, microgranite	Permian
Felsic intrusives 69832	Pgcx	granite, monzogranite, granodiorite, quartz monzonite	Permian
Dingo Diorite	Pgdd	quartz diorite	Permian

Table E2*B*. Map units that define the Central sub-tract (009pCu8004b), East Tasmanide tract, Queensland, Australia.—Continued

Map unit	Map symbol	Lithology	Age range
		Intrusive rocks	
Mundic Igneous Complex	Pgu	microgranite, leucogranite, dolerite	Permian
First Pocket Igneous Complex	Pgf	granodiorite, tonalite, quartz monzonite, quartz diorite	Permian
Ellrott Rhyolite	Pfbe	rhyolite, dacite intrusions, flows, breccias	Permian
Flaggy Quartz Monzodiorite	Pgof	quartz monzodiorite, clinopyroxene-hornblende quartz monzodiorite	Permian
Kyle Mohr Igneous Complex—gabbro	Pdkm	quartz-hornblende-biotite gabbro	Permian
Kyle Mohr Igneous Complex—granite	Pgkm	hornblende granite	Permian
Felsic intrusives 42187	Pg	granite, granodiorite, tonalite, aplite, porphyry	Permian
Wolca Granite	Pgwl	hornblende-biotite granite, quartz diorite, tonalite	Permian
Chowey Granite	Pgch	hornblende-biotite granite	Permian
Wigton Granite	Pgwg	biotite granite, K-feldspar phyric, rapakivi granite	Permian
Woolshed Mountain Granodiorite	Pgwo	granodiorite	Permian
Lags Supersuite	Pgl	microgranite to microdiorite	Early Permian
Maneater Granodiorite	Pgl1	biotite-hornblende granodiorite with pyroxene, garnet	Early Permian
Yokas Microgranite	Pgl4	microgranite with garnet	Early Permian
Bustlem Microgranite	Pgl3	clinopyroxene microgranite	Early Permian
Microgranite 68928	Pgl5	hornblende-pyroxene microgranite	Early Permian
Lags Microgranite	Pgl2	biotite microgranite	Early Permian
Saint Helena Monzogranite	Pgl6	garnet-pyroxene-biotite microgranodiorite to microgranite hornblende-biotite microgranodiorite to microdiorite	Early Permian
Three Horse Lagoon Granite	Pgtg	biotite granite, microgranite	Early Permian
Clotten Granodiorite	Pga23	granodiorite to diorite	Early Permian
Brodies Camp Supersuite	Pgb	biotite granite, hornblende-biotite granodiorite	Early Permian
Knob Camp Granodiorite	Pgik	biotite-hornblende granodiorite, diorite	Early Permian
Promise Creek Granite	Pgpr	biotite granite, microgranite, biotite-hornblende microgranite	Early Permian
Copper Bush Granite	Pgkb	biotite granite, microgranite	Early Permian
Bull Creek Granite	Pgku	hornblende-biotite granodiorite, biotite granodiorite, microgranite, microtonalite	Early Permian
Kangaroo Creek Supersuite	Pgk	biotite granodiorite to granite	Early Permian
Aylesbury Microgranite	Pgia	hornblende-biotite microgranite	Early Permian
Ancaster Granite	Pgac	hornblende-biotite granite	Early Permian
Yuccabine Granodiorite	Pgyu	biotite-hornblende granodiorite	Early Permian
Wallys Dolerite	Pdwa	dolerite	Early Permian
Awring Granodiorite	Pgaw	hornblende-biotite granodiorite, tonalite with disseminated chalcopyrite	Early Permian
Carnes Granodiorite	Pgrn	biotite granodiorite	Early Permian
West Creek Diorite	Pgwc	pyroxene-hornblende-biotite diorite, quartz diorite, hornblende-biotite tonalite	Early Permian
Gongora Granodiorite	Pggo	biotite granodiorite	Early Permian
Palm Islands Granite	Pgpi	hornblende-biotite granodiorite, biotite granodiorite, granite	Early Permian

Table E2*B*. Map units that define the Central sub-tract (009pCu8004b), East Tasmanide tract, Queensland, Australia.—Continued

Map unit	Map symbol	Lithology	Age range
		Intrusive rocks	
Jacobsens Track Granodiorite	Pgja	biotite-hornblende granodiorite	Early Permian
Connie May Dolerite	Pdcm	clinopyroxene dolerite	Early Permian
Magnetic Island Granite	Pgoa	biotite leucogranite	Early Permian
Castle Hill Granite	Pgoc	biotite leucogranite, granophyre, granodiorite	Early Permian
Muntalunga Range Granite	Pgun	leucogranite, microgranite	Early Permian
Mount Storth Granite	Pgos	granite, microgranite, granodiorite, diorite, gabbro	Early Permian
Thunderbolt Granite	Pgth	hornblende-biotite monzogranite, micromonzogranite, granite gneiss	Early Permian
Whitehorse Granite	Pgwh	biotite monzogranite to syenogranite, granophyre, pegmatite, aplite	Early Permian
Gotthardt Granodiorite	Kggo	biotite-hornblende granodiorite	Late Carboniferous to Early Cretaceous
Almaden Granodiorite	Cga6	hornblende-biotite granodiorite	Late Carboniferous to Permian
Goddard Creek Granite	Cggo	hornblende-biotite granodiorite	Late Carboniferous to Permian
Princess Hills Granite	Cgo89	biotite granite	Late Carboniferous to Permian
Gleneagle granite	Cgo79	hornblende-biotite granodiorite	Late Carboniferous to Permian
Gowrie Creek Granodiorite	Cggk	hornblende-biotite granodiorite	Late Carboniferous to Permian
Kitty O'Shea Suite	Cdk	microdiorite, dolerite, gabbro, intrusive andesite, basalt	Late Carboniferous to Permian
Surgeons Lookout Rhyolite	Cfsl	rhyolite, porphyritic granophyre	Late Carboniferous to Permian
Mount Masterson Granodiorite	Cga26	hornblende granodiorite	Late Carboniferous to Early Permian
Ingham Granite Complex	Cgin	hornblende-biotite and biotite monzogranite, granodiorite, undivided granites	Late Carboniferous to Early Permian
Mount Departure Microgranite	Cgde	biotite microgranite, intrusive rhyolite, dacite	Late Carboniferous to Early Permian
Glenleigh Granite	Cggl	biotite granite	Late Carboniferous to Early Permian
Broadlands Granite	Cgbd	biotite granite	Late Carboniferous to Early Permian
Pinedale Granite	Cgpd	biotite granite	Late Carboniferous to Early Permian
Gypsy Pocket Granodiorite	Pggp	hornblende-biotite granodiorite	Late Carboniferous to Early Permian
Little Watson Granite	Cgo69	biotite leucogranite to aplite	Late Carboniferous to Early Permian
Subkin Granodiorite	Cga18	biotite granodiorite, diorite	Late Carboniferous to Early Permian
Nightflower Dacite	Cffn	dacite to rhyodacite	Late Carboniferous to Early Permian
Prices Dam Igneous Complex	Cga22	biotite-clinopyroxene-hornblende granodiorite to tonalite	Late Carboniferous to Early Permian
Watsonville Granite	Cgo75	biotite granite	Late Carboniferous to Early Permian
Tully Granite Complex	Pgtl	hornblende-biotite granite to biotite-hornblende granodiorite, quartz gabbro, biotite granite	Late Carboniferous to Early Permian
Gunnawarra Bump Granite	Cgo82	biotite granite	Late Carboniferous to Early Permian
Lancewood Rhyolite	Cgb87	rhyolite, rhyodacite, microgranite	Late Carboniferous to Early Permian
Herbert River Granite	Cgo67	hornblende-biotite granite	Late Carboniferous to Early Permian
Goold Island Granite	Cggi	hornblende-biotite monzogranite	Late Carboniferous to Early Permian
Greasy Creek granodiorite	Cgo80	biotite-hornblende granodiorite	Late Carboniferous to Early Permian
Gorge Range Microgranite	Cggn	microgranite, granophyre	Late Carboniferous to Early Permian
Manor Creek Microgranite	Cgmr	feldspar-quartz porphyry	Late Carboniferous to Early Permian
Ingham Granite Complex—granodiorite to tonalite	Cgid	hornblende-biotite granodiorite, tonalite	Late Carboniferous to Early Permian
Expedition Creek Granodiorite	Cgex	sphene-biotite granodiorite	Late Carboniferous to Early Permian

Table E2*B*. Map units that define the Central sub-tract (009pCu8004b), East Tasmanide tract, Queensland, Australia.—Continued

Map unit	Map symbol	Lithology	Age range
		Intrusive rocks	
Elphinstone Granite	Cgel	hornblende-biotite monzogranite	Late Carboniferous to Early Permian
Bewilder Granite	Cgib	sphene-biotite granodiorite, granophyre	Late Carboniferous to Early Permian
Speed Creek Granite	Cgls	biotite granodiorite	Late Carboniferous to Early Permian
Pall Mall Granite	Cglp	biotite granite	Late Carboniferous to Early Permian
Emysland Granodiorite	Cgle	hornblende-biotite granodiorite, biotite granite	Late Carboniferous to Early Permian
Felsic intrusives 69833	Cgcx	microgranite, aplite, granite, hornblende-biotite granite, diorite, tonalite	Late Carboniferous to Early Permian
Percy Douglas Granodiorite	Cgpe	hornblende-biotite granite to granodiorite	Late Carboniferous to Early Permian
Nostone Creek Granodiorite	Pgno	hornblende-biotite granodiorite, granite	Late Carboniferous to Early Permian
Palms Lookout Granodiorite	Cgpl	hornblende granodiorite to biotite granite, cut by andesite and rhyolite dikes	Late Carboniferous to Early Permian
Finch Hatton Granite	Cgfi	biotite syenogranite	Late Carboniferous to Early Permian
Uruba Granite	Cgub	biotite granite, microgranite, aplite, pegmatite, hornblende microdiorite, biotite-hornblende granodiorite	Late Carboniferous to Early Permian
Teemburra Igneous Complex	Cge	biotite granite, leucogranite, biotite-hornblende granodiorite, diorite, or gabbro	Late Carboniferous to Early Permian
Gargett Granite	Cggr	biotite granite, hornblende-biotite granodiorite	Late Carboniferous to Early Permian
Pisgah Igneous Complex	Cgp	syenogranite, biotite-hornblende granodiorite, pegmatite, aplite, andesite and rhyolite dikes	Late Carboniferous to Early Permian
Bluegrass Creek Granite	Cglg	biotite granite, granodiorite	Late Carboniferous to Early Permian
Wirralie Granodiorite	Cgwr	biotite-hornblende granodiorite, granite	Late Carboniferous to Early Permian
Johnstone Creek Igneous Complex	Cgj	hornblende diorite to granodiorite, biotite granite, cut by microdiorite, rhyolite dikes	Late Carboniferous to Early Permian
Yarravale Creek Granite	Cgyv	hornblende granite and granodiorite, biotite-hornblende tonalite, porphyritic andesite	Late Carboniferous to Early Permian
Tally Ho Igneous Complex	Cgt	biotite granite, granodiorite, two-mica granite with tourmaline, rhyolite, dacite, andesite, diorite dikes	Late Carboniferous to Early Permian
Screaming Creek Gabbro	Cdsc	hornblende gabbro, cut by andesite, basalt, and microgranite dikes	Late Carboniferous to Early Permian
Doraville Granodiorite	Cgdv	biotite granodiorite, cut by andesite dikes	Late Carboniferous to Early Permian
Manaman Granodiorite	Cgnn	biotite-hornblende granodiorite, granite, quartz-feldspar porphyry	Late Carboniferous to Early Permian
Waitara Granite	Cgwa	biotite-hornblende monzonite, monzogranite	Late Carboniferous to Early Permian
Doreen Granite	Cgdr	hornblende-biotite granite to monzonite, felsic and andesitic dikes	Late Carboniferous to Early Permian
Tindarra Granite	Cgtd	biotite granite	Late Carboniferous to Early Permian
Woolton Granite Complex	Cgwo	leucogranite, hornblende-biotite granite, hornblende-biotite granodiorite	Late Carboniferous to Early Permian
Lyndale Diorite	Cgld	hornblende diorite	Late Carboniferous to Early Permian
Boam Creek Granite	Cgbc	hornblende-biotite and biotite granodiorite to granite	Late Carboniferous to Early Permian
Mount Appenben Granite	Cgmp	biotite granite	Late Carboniferous to Early Permian
Dawson Granite	Cgdw	hornblende-biotite granite, microgranite, diorite dikes	Late Carboniferous to Early Permian
Montour Gabbro	Cdmo	hornblende gabbro	Late Carboniferous to Early Permian
Hutchinsons Granite	Cghu	hornblende-biotite granite, aplite veins	Late Carboniferous to Early Permian
Moocoorooba Granite	Cgmc	hornblende-biotite granite, biotite granite, diorite, leucogranite	Late Carboniferous to Early Permian

Table E2*B*. Map units that define the Central sub-tract (009pCu8004b), East Tasmanide tract, Queensland, Australia.—Continued

Map unit	Map symbol	Lithology	Age range
		Intrusive rocks	
Okangal Granodiorite	Cgoa	hornblende-biotite granodiorite to tonalite, biotite granite, pegmatite, aplite, diorite, rhyolite	Late Carboniferous to Early Permian
Ten Mile Granite	Cgtm	hornblende-biotite granite	Late Carboniferous to Early Permian
Delusion Granodiorite	Cgdl	biotite-hornblende granodiorite to quartz monzodiorite, biotite granite, diorite	Late Carboniferous to Early Permian
J P Granite	Cgjp	hornblende-biotite granite, biotite leucogranite, pegmatite	Late Carboniferous to Early Permian
Tan Lies Quartz Monzodiorite	Cgtl	quartz monzodiorite to granodiorite	Late Carboniferous to Early Permian
Rockdale Granite	Cgrk	hornblende-biotite and biotite-hornblende granite to granodiorite	Late Carboniferous to Early Permian
Mungungal Granite	Cgmu	biotite granite	Late Carboniferous to Early Permian
Nine Mile Granite	Cgnm	biotite granite	Late Carboniferous to Early Permian
Jan Mar Granite	Cgjm	biotite granite	Late Carboniferous to Early Permian
Berri Berri Granite	Cgei	biotite granite, aplite	Late Carboniferous to Early Permian
Ross Granite	Cgro	biotite granite	Late Carboniferous to Early Permian
Rockybar Granodiorite	Cgrb	hornblende-biotite and biotite-hornblende granodiorite to granite	Late Carboniferous to Early Permian
Mount Cross Igneous Complex	Cdm	gabbro	Late Carboniferous to Early Permian
Urannah Igneous Complex	Cgu	hornblende-biotite monzogranite, granodiorite, diorite, quartz diorite, gabbro	Carboniferous to Cretaceous
Urannah Batholith 13	Cgu13	granite to diorite, minor gabbro, aplite, breccia	Carboniferous to Cretaceous
Urannah Batholith 14	Cgu14	granite with xenolithic screens	Carboniferous to Cretaceous
Cashmere microgranite	Cgcs	microgranite	Carboniferous to Permian
Felsic intrusives 68932	CPggh	granodiorite, monzogranite, hornblende-biotite granite, muscovite-cordierite granite, greisen, dacite	Carboniferous to Permian
Mafic intrusives 39448	CPd	dolerite, gabbro, diorite, monzonite, meladiorite	Carboniferous to Permian
Intrusive rhyolite 41758	Cgi	rhyolite and dacite intrusives	Carboniferous to Permian
Dingo Mountain Granodiorite	Cgdm	hornblende-biotite granodiorite	Carboniferous to Permian
Minnamoolka Granite	Cgo88	biotite granite	Carboniferous to Permian
Mafic intrusives 69537	Cdct	diorite, dolerite, gabbro, andesite, basalt, hornblende tonalite	Carboniferous to Permian
Sword Creek Microgranite	Cgsw	microgranite and granophyre	Carboniferous to Permian
Midway Creek Granodiorite	Cgmi	biotite granodiorite to monzogranite	Carboniferous to Permian
Mount Grey Granite	Cgmg	biotite granite, biotite-hornblende granite	Carboniferous to Permian
Ryeburn Quartz Diorite	Cgry	hornblende-biotite quartz diorite, granodiorite, gabbro	Carboniferous to Permian
Mafic intrusives 69538	Cdgh	dolerite, microdiorite, gabbro, diorite, monzonite, meladiorite	Carboniferous to Permian
Felsic intrusives 69458	CPgct	biotite granite, biotite-hornblende granodiorite, microgranitoids, microsyenite, micromonzonite, intrusive rhyolite, dacite, quartz diorite, dolerite	Carboniferous to Permian
Felsic to intermediate intrusives 39451	Cggx	monzogranite, granodiorite, granite, quartz diorite, granophyre, trondhjemite	Carboniferous to Permian
Diorite 41784	Cgd	diorite, quartz diorite, hornblende-clinopyroxene diorite, tonalite, gabbro, granodiorite	Carboniferous to Permian
Mount Success Rhyolite	Cfms	intrusive rhyolite with granitic and sed inclusions	Carboniferous to Permian
Mount Prince Charlie Granophyre	Cgcp	granophyre (miarolitic)	Carboniferous to Permian

Table E2*B*. Map units that define the Central sub-tract (009pCu8004b), East Tasmanide tract, Queensland, Australia.—Continued

Map unit	Map symbol	Lithology	Age range
		Intrusive rocks	
Drynoch Granite	Cglr	hornblende-biotite granite	Carboniferous to Permian
Barratta Granite	Cgar	biotite granite	Carboniferous to Permian
Bogie Creek Granite	Cgbg	hornblende-biotite granite	Carboniferous to Permian
Banana Microgranite	Cgbn	microgranite	Carboniferous to Permian
Molybdenite Creek Granite	Cgly	biotite granite	Carboniferous to Permian
Tuckers Igneous Complex—gabbro	Pdtu	gabbro, diorite, granodiorite, tonalite, monzogranite	Carboniferous to Permian
Tuckers Igneous Complex—granodiorite	Pgtu	biotite-hornblende granodiorite, tonalite, monzogranite, gabbro, diorite, quartz diorite, granite	Carboniferous to Permian
Robey Range Granite	Cgbr	biotite granite, ferromag microgranite, microgranodiorite	Carboniferous to Permian
Mount Canton Igneous Complex—monzogranite	Cglc	biotite monzogranite	Carboniferous to Permian
Lulu Pocket Igneous Complex	Cglu	hornblende-biotite granodiorite, biotite granodiorite, porphyritic microgranite	Carboniferous to Permian
Deep Water Creek Granophyre	Pgde	granophyre	Carboniferous to Permian
Stuart Pocket Granite	Cgst	biotite granite	Carboniferous to Permian
Billy-Can Creek Granite	Cgby	granite	Carboniferous to Permian
Joe-De-Little Granite	Cgjl	hornblende-biotite granodiorite, diorite, granite	Carboniferous to Permian
Roscow Granite	Cgrw	hornblende-biotite granite, biotite granite, granodiorite, quartz monzonite	Carboniferous to Permian
Urannah Batholith 3	Cgu3	biotite-pyroxene-hornblende granodiorite, biotite monzogranite	Carboniferous to Permian
Urannah Batholith 8	Cgu8	biotite-hornblende granodiorite	Carboniferous to Permian
Urannah Batholith 4	Cgu4	biotite-hornblende granodiorite, hornblende-biotite granodiorite to monzogranite	Carboniferous to Permian
Urannah Batholith 2	Cgu2	hornblende-biotite monzogranite, biotite-muscovite monzogranite	Carboniferous to Permian
Urannah Batholith 1	Cgu1	biotite monzogranite to granodiorite	Carboniferous to Permian
Urannah Batholith 11	Cgu11	biotite granite	Carboniferous to Permian
Urannah Batholith—monzodiorite	Cdu2	hornblende-clinopyroxene-quartz monzodiorite, hornblende-biotite granodiorite	Carboniferous to Permian
Urannah Batholith 7	Cgu7	biotite-hornblende granodiorite, hornblende-biotite granodiorite to monzogranite	Carboniferous to Permian
Urannah Batholith 6	Cgu6	biotite monzogranite	Carboniferous to Permian
Urannah Batholith 15	Cdu1	pyroxene-hornblende gabbro	Carboniferous to Permian
Boori Igneous Complex	Pgi	granodiorite, monzogranite, tonalite, diorite, leucogranite	Carboniferous to Early Permian
Almac Granodiorite	Cga17	biotite-hornblende granodiorite	Late Carboniferous
Wabaredory Granite	Cgo74	hornblende-biotite granite	Late Carboniferous
Bilch Creek Granodiorite	Cga19	biotite-hornblende granodiorite to granite	Late Carboniferous
Wotan Granodiorite	Cga16	hornblende-biotite granodiorite with dioritic xenoliths	Late Carboniferous
Ruddygore Granodiorite	Cga3	pyroxene-hornblende-biotite granodiorite to tonalite, sparse mafic enclaves	Late Carboniferous
Worcester Granodiorite	Cgo58	pyroxene-hornblende-biotite granodiorite to granite	Late Carboniferous
Belgravia Granodiorite	Cga4	clinopyroxene-biotite-hornblende granodiorite, hornblende-biotite granodiorite	Late Carboniferous
Election Granite	Cgo10	biotite monzogranite, muscovite bearing hornblende-biotite leuco-monzogranite with miarolitic cavities	Late Carboniferous

Table E2*B*. Map units that define the Central sub-tract (009pCu8004b), East Tasmanide tract, Queensland, Australia.—Continued

Map unit	Map symbol	Lithology	Age range
		Intrusive rocks	
James Creek Granite	Cgo8	biotite granite	Late Carboniferous
Sentinel Range Igneous Complex	Cgo2	hornblende-biotite granite, hornblende quartz diorite, aplite, pegmatite	Late Carboniferous
Atlanta Granite	Cgb2	biotite granite	Late Carboniferous
Parada Granite	Cgo34	biotite granite	Late Carboniferous
Barkers Creek Igneous Complex—granodiorite	Cgob2	biotite-hornblende granodiorite, pyroxene gabbro, quartz gabbro, aplite, aplitic microgranite	Late Carboniferous
Barkers Creek Igneous Complex—	Cgob1	biotite monzogranite, hornblende-biotite granodiorite, mafic enclaves	Late Carboniferous
Carrs Granite	Cgo4	hornblende-biotite monzogranite, mafic enclaves	Late Carboniferous
Quaker Granite	Cgo31	hornblende-biotite monzogranite, mafic enclaves	Late Carboniferous
Halpin Granite	Cgo13	biotite microgranite	Late Carboniferous
Lass O'Gowrie Granite	Cgb9	biotite granite	Late Carboniferous
Ootann Supersuite	Cgo	biotite granite, biotite-hornblende granite, sparse granodiorite	Late Carboniferous
Jacks Granite	Cgo12	biotite monzogranite	Late Carboniferous
Bamford Granite	Cgo9	biotite granite	Late Carboniferous
Muldiva Quartz Monzodiorite	Cga25	biotite-hornblende diorite	Late Carboniferous
Bock Granodiorite	Cga8	clinopyroxene-biotite-hornblende granodiorite	Late Carboniferous
Retire Monzodiorite	Cga5	quartz monzodiorite	Late Carboniferous
Saint Patrick Hill Granite	Cgb6	biotite granite	Late Carboniferous
Petford Granite	Cgo15	hornblende-biotite granite	Late Carboniferous
Burke Granite	Cgo30	biotite monzogranite	Late Carboniferous
Hales Siding Granite	Cgb7	sphene-hornblende-biotite granodiorite	Late Carboniferous
McCord Granite	Cgb1	biotite monzogranite with fluorite, tourmaline	Late Carboniferous
Bakerville Granodiorite	Cga9	biotite-hornblende granodiorite, hornblende-biotite granodiorite	Late Carboniferous
Stirlington Granite	Cgo11	biotite monzogranite	Late Carboniferous
Jumna Granite	Cgb8	biotite granite	Late Carboniferous
Gibbs Granite	Cgo33	hornblende-biotite microgranite	Late Carboniferous
Crystal Brook Volcanic Neck—granodiorite phase	Cga12	biotite-hornblende granodiorite, hornblende-biotite granite to granodiorite	Late Carboniferous
Kalunga Granodiorite	Cga13	hornblende-biotite granodiorite	Late Carboniferous
Crystal Brook Volcanic Neck—granite phase	Cgo64	biotite granite	Late Carboniferous
Reddicliffe Granite	Cgo29	biotite granite	Late Carboniferous
Hermit granodiorite	Cgo68	hornblende-biotite granodiorite	Late Carboniferous
Billings Granite	Cgb4	biotite granite	Late Carboniferous
Emuford Granite	Cgb3	biotite syenogranite to monzogranite	Late Carboniferous
Indicator Granite	Cgo18	hornblende-biotite monzogranite	Late Carboniferous
Saucebottle Granite	Cgo27	biotite monzogranite with K-feldspar phenocrysts	Late Carboniferous
Kitchener Granite	Cgo17	biotite monzogranite with mafic enclaves	Late Carboniferous
Madjack Granite	Cgb95	biotite monzogranite, microgranite	Late Carboniferous
Martin Creek Microgranite	Cgo28	syenogranite, monzogranite	Late Carboniferous
Sheba Granite	Cgo26	biotite syenogranite and monzogranite	Late Carboniferous
Sugar Bag Granite	Cgb27	biotite granite	Late Carboniferous

Table E2*B*. Map units that define the Central sub-tract (009pCu8004b), East Tasmanide tract, Queensland, Australia.—Continued

Map unit	Map symbol	Lithology	Age range
		Intrusive rocks	
Giblets Granite	Cgb21	biotite granite	Late Carboniferous
Oaky Creek granite	Cgo19	biotite granite	Late Carboniferous
Black Prince Granite	Cgb23	biotite granite	Late Carboniferous
Go Sam Granite	Cgb17	biotite granite	Late Carboniferous
Butterfly Granite	Cgb26	biotite granite	Late Carboniferous
Opah Granite	Cgb76	biotite granite	Late Carboniferous
Cigarette Granite	Cgb31	biotite granite	Late Carboniferous
Mount Cardwell Granite	Cgo49	biotite monzogranite	Late Carboniferous
Percy Granophyre	Cgb33	biotite granite	Late Carboniferous
Glen Granite	Cgb54	biotite granite	Late Carboniferous
Confluence Granite	Cgb56	biotite granite	Late Carboniferous
Boot Granite	Cgb45	biotite granite	Late Carboniferous
California Granite	Cgo48	biotite monzogranite	Late Carboniferous
Flynns Creek Granite	Cgb85	biotite granite	Late Carboniferous
Gurrumba Ring Complex	Cgo83	quartz diorite, gabbro, monzogranite, microgranite, rhyolite lava	Late Carboniferous
Rock of Ages Granite	Cgb50	biotite granite	Late Carboniferous
Desert Creek granite	Cgb75	biotite granite	Late Carboniferous
Excelsior Granite	Cgb57	biotite granite	Late Carboniferous
Butters Creek granite	Cgb68	biotite granite	Late Carboniferous
Brumby Granite	Cgb58	biotite granite	Late Carboniferous
Rices Creek Granite	Cgo39	biotite granite	Late Carboniferous
Nettle Granite	Cgb59	biotite granite	Late Carboniferous
Geebung Granite	Cgb48	biotite granite	Late Carboniferous
Gelaro Granite	Cgo38	biotite monzogranite	Late Carboniferous
The Gorge Rhyolite	Cgb78	microgranite, rhyolite, dacite, intrusive breccia	Late Carboniferous
Ballast Creek Dacite	Cgcc	biotite granite	Late Carboniferous
Baldick Granite	Cgo76	biotite granite	Late Carboniferous
Koogangoona Granite	Cgo84	biotite granite	Late Carboniferous
Rose Creek granite	Cgb86	biotite granite	Late Carboniferous
Three Mile Microgranite	Cgth	biotite microgranite	Late Carboniferous
Devon Microgranite	Cgb60	biotite microgranite	Late Carboniferous
Munderra Granodiorite	Cgcm	biotite-hornblende granodiorite and tonalite	Late Carboniferous
Whelan Creek Granite	Cgb94	biotite granite	Late Carboniferous
Junevale Granite	Cgo50	hornblende-biotite monzogranite, biotite monzogranite	Late Carboniferous
Wireyard Granite	Cgb66	biotite granite	Late Carboniferous
Nymbool Granite	Cgo36	biotite granite	Late Carboniferous
Wild Granite	Cgb63	biotite granite	Late Carboniferous
Shady Microgranite	Cgb61	topaz-bearing microgranite	Late Carboniferous
Mount Gibson Microgranite	Cgb37	biotite granite	Late Carboniferous
Askins Microgranite	Cgb38	microgranite	Late Carboniferous
Neds Gully Granite	Cgb40	biotite granite	Late Carboniferous
Crane Creek Granite	Cgo77	biotite granite	Late Carboniferous

Table E2*B*. Map units that define the Central sub-tract (009pCu8004b), East Tasmanide tract, Queensland, Australia.—Continued

Map unit	Map symbol	Lithology	Age range
		Intrusive rocks	
Square Rock granite	Cgb73	biotite granite	Late Carboniferous
Wurruma Granite	Cgb64	biotite granite	Late Carboniferous
Sandy Tate Granite	Cgo51	hornblende-biotite monzogranite	Late Carboniferous
Mountain Camp Granite	Cgo46	biotite monzogranite and granodiorite	Late Carboniferous
Frenchy Creek granite	Cgo57	biotite granite	Late Carboniferous
Ixe Microgranodiorite	Cgo56	biotite granite	Late Carboniferous
Rudd Granite	Cgo54	biotite granite	Late Carboniferous
Flat Rock Granite	Cgo66	biotite granite	Late Carboniferous
Sundown Granite	Cgb77	granite	Late Carboniferous
Rattler Granite	Cgo53	biotite monzogranite	Late Carboniferous
First Bull Run Granite	Cgb79	biotite granite	Late Carboniferous
Amber granite	Cgo55	biotite granite	Late Carboniferous
Pat and Peter Creek granite	Cgb69	biotite granite	Late Carboniferous
Charlies Knob granite	Cgb70	biotite granite	Late Carboniferous
Arden granite	Cgo61	hornblende-biotite granodiorite	Late Carboniferous
Frog Hollow Granite	Cgo87	biotite granite	Late Carboniferous
Angore Granite	Cgb82	biotite granite	Late Carboniferous
Barwidgi Granite	Cgo45	monzogranite cut by sheeted quartz veins	Late Carboniferous
Teddys Creek Granite	Cgo86	biotite granite	Late Carboniferous
Burlington Granite	Cgb72	biotite granite	Late Carboniferous
Dickie Hill Granite	Cgo78	biotite granite	Late Carboniferous
Bonnor Creek Granite	Cgcb	hornblende-biotite granite to granodiorite	Late Carboniferous
Mount Pudding Basin Granodiorite	Cgo70	hornblende-biotite granodiorite, mafic enclaves	Late Carboniferous
Soda Spring Granite	Cgo47	monzogranite with K-feldspar phenocrysts, mafic enclaves	Late Carboniferous
Brookers Waterhole Granite	Cgo43	hornblende-biotite monzogranite	Late Carboniferous
Elizabeth Creek Granite	Cgb65	biotite granite	Late Carboniferous
Barney Knob Granite	Cgb81	biotite granite	Late Carboniferous
Mulindie Granite	Cgo71	biotite monzogranite	Late Carboniferous
Mount Noble Granite	Cgmn	biotite granite	Late Carboniferous
Whitewater Creek Granite	Cgb96	biotite granite	Late Carboniferous
House and Kitchen Granite	Cghs	granite	Late Carboniferous
Sunbeam Granodiorite	Cgsg	granite to granodiorite	Late Carboniferous
Mia Mia Igneous Complex	Cgm	hornblende-biotite granodiorite, granite, biotite leucogranite, rhyolitic to andesitic dikes	Late Carboniferous
Mount Spencer Granodiorite	Cgsn	hornblende granodiorite, tonalite, andesite and dacite dikes	Late Carboniferous
Sambo Quartz Monzonite	Cgsb	pyroxene-biotite quartz monzonite to quartz monzodiorite	Late Carboniferous
Bora Creek Quartz Monzodiorite	Cgbo	biotite-hornblende quartz monzonite, granite	Late Carboniferous
Clement Creek Quartz Monzodiorite	Cgct	hornblende-biotite monzogranite, mafic enclaves	Late Carboniferous
Camp Creek Granite	Cgce	biotite granite	Late Carboniferous
Mount Clairvoyant Granite	Cgmv	biotite granite	Late Carboniferous
Carinya Granite	Cgcn	biotite granite, biotite-hornblende granodiorite to diorite	Late Carboniferous

Table E2*B*. Map units that define the Central sub-tract (009pCu8004b), East Tasmanide tract, Queensland, Australia.—Continued

Map unit	Map symbol	Lithology	Age range
		Intrusive rocks	
Coonambula Granodiorite	Cgco	biotite granodiorite, biotite gneiss, hornblende-biotite granodiorite, pegmatite, aplite	Late Carboniferous
Glissons Granodiorite	Cggs	sphene-hornblende-biotite granodiorite	Late Carboniferous
Dogherty Granite	Cgdg	biotite leucogranite	Late Carboniferous
Evandale Tonalite	Cgev	hornblende-biotite tonalite, granodiorite	Late Carboniferous
Ah Fat Granite Complex	Cgaf	granite, monzogranite, aplite in granodiorite to granite	Late Carboniferous
Sujeewong Gabbro	Cdsj	layered hornblende gabbro, quartz gabbro	Late Carboniferous
Chahpingah Meta-Igneous Complex	Cnc	granitic to granodioritic biotite gneiss, quartz veins, pegmatites, granitic sills, dikes	Late Carboniferous
Kooingal Granite Complex	Cgk	hornblende-bio granite to granodiorite	Middle Carboniferous to Early Permian
Glenhalvern Granite	Cggv	biotite granite, aplite, microgranite	Middle Carboniferous to Early Permian
Lonesome Creek Monzonite	Cgln	hornblende-biotite monzonite, granodiorite	Middle Carboniferous to Early Permian
Shawlands Granite Complex	Cgsl	hornblende-biotite granite to monzonite, hornblende-biotite granotiorite to diorite	Middle Carboniferous to Early Permian
Parraweena Gabbro	Cdpa	hornblende-plagioclase gabbro, leucogabbro	Middle Carboniferous to Early Permian
Jonah Vale Granite	Cgjv	biotite granite	Middle Carboniferous to Early Permian
Hildura Granodiorite	Cghd	biotite granodiorite	Middle Carboniferous to Early Permian
Kandoonan Granite	Cgkd	hornblende-biotite granite	Middle Carboniferous to Early Permian
Hainault Granodiorite	Cghn	hornblende-biotite granodiorite	Middle Carboniferous to Early Permian
Keen Creek Granite	Cgkc	biotite granite	Middle Carboniferous to Early Permian
Top Nettle Microgranite	Cgb34	microgranite	Middle to Late Carboniferous
Airport Quartz Diorite	Cga11	quartz diorite	Middle to Late Carboniferous
O'Briens Creek Microgranite	Cgb67	biotite microgranite	Middle to Late Carboniferous
Monkey Springs Granite	Cgmy	granite, leucogranite	Carboniferious
Big Watson Granodiorite	Cga20	hornblende-biotite granodiorite, gabbro, dolerite, minor diorite	Carboniferous
Bungabilly Granite	Cgo3	hornblende-biotite monzogranite, mafic enclaves, aplite, microgranite, microgranodiorite, diorite	Carboniferous
Long Gully Granite	Cga2	hornblende-biotite monzogranite, sparse mafic enclaves	Carboniferous
Beapeo Rhyolite	Cffb	hornblende-biotite-clinopyroxene dacitic ignimbrite	Carboniferous
Almaden Supersuite	Cga	hornblende-biotite and biotite-hornblende granodiorite to granite	Carboniferous
Bulluburrah Granodiorite	Cgo5	hornblende-biotite granodiorite to monzogranite	Carboniferous
Pinchgut Granite	Cgo6	biotite leucogranite, granophyre	Carboniferous
Borneo Granite	Cgo14	biotite-hornblende microgranodiorite	Carboniferous
Retchford Granite	Cgo21	hornblende-biotite monzogranite	Carboniferous
Ootann Granite	Cgo23	hornblende-biotite granite, minor granodiorite	Carboniferous
Lucy Granite	Cgo25	hornblende-biotite monzogranite, sparse mafic enclaves	Carboniferous
Koorboora Granite	Cgo22	biotite granite	Carboniferous
Billycan Granite	Cgo24	biotite monzogranite and granite	Carboniferous
Campbell Creek granodiorite	Cgo37	biotite-hornblende quartz monzodiorite to granodiorite	Carboniferous

Table E2*B*.—Map units that define the Central sub-tract (009pCu8004b), East Tasmanide tract, Queensland, Australia.—Continued

Map unit	Map symbol	Lithology	Age range
		Intrusive rocks	
Pinnacles Granite	Cgb39	biotite granite	Carboniferous
Hammonds Creek Granodiorite	Cga15	hornblende-biotite granodiorite, biotite granite	Carboniferous
Ravenshoe Granite	Cgb41	biotite granite	Carboniferous
Lubrina Granite	Cglb	biotite leucogranite	Carboniferous
Mount Sharples granite	Cgo85	biotite granite	Carboniferous
Tiger Hill Microgranite	Cgo90	biotite microgranite	Carboniferous
Greenes Spring granodiorite	Cgo81	hornblende-biotite granodiorite	Carboniferous
Carruchan Granite	Cgca	biotite monzogranite, granite	Carboniferous
Talaroo Microgranite	Cgta	biotite-hornblende microgranite	Carboniferous
Mount Darcy Microgranodiorite	Cgmd	biotite and biotite-hornblende microgranodiorite	Carboniferous
Caterpillar Microgranite	Cger	microgranite	Carboniferous
Eva Creek Microgranite	Cgec	biotite microgranite, leucogranite	Carboniferous
Rockingham Bay Granite	Cgw7	biotite monzogranite	Carboniferous
Prestwood Microgranite	Cgpr	biotite microgranite	Carboniferous
Mount Sircom Microgranodiorite	Cgus	hornblende-biotite microgranodiorite	Carboniferous
MacCallor Microgranodiorite	Cgma	microgranodiorite	Carboniferous
White Crystal Granite	Cgww	biotite granite	Carboniferous
Tenavute Microgranite	Cgtv	microgranite	Carboniferous
Poison Creek Granite	Cgpo	biotite granite	Carboniferous
Kallanda Granite	Cgw4	biotite granite	Carboniferous
Rollingstone Granite	Cgw9	biotite granite	Carboniferous
Coane Range Granite Complex	Cgw2	biotite granite	Carboniferous
Clemant Microgranite	Cgw3	biotite microgranite	Carboniferous
Spinifex Creek Granite	Cgw8	biotite granite	Carboniferous
Macauley Creek Granite	Cgw5	biotite granite	Carboniferous
Montgomery Range Igneous Complex—intrusive rhyolite	Cge1	biotite-hornblende granodiorite, microgranite, rhyolite, hornblende-biotite granite	Carboniferous
Malmesbury Microgranite	Cgw6	hornblende microgranite	Carboniferous
Montgomery Range Igneous Complex—granite	Cge2	biotite to hornblende-biotite granite and granodiorite, microgranite	Carboniferous
Baumans Camp Granite	Cgw1	biotite granite	Carboniferous
Mingoom Granite	Cglm	biotite granite	Carboniferous
Whiphole Spring Granite	Cgwp	biotite granite	Carboniferous
Mount Shields Granodiorite	Cgsh	biotite granite	Carboniferous
Toobier Granite	Cgtb	clinopyroxene-hornblende-biotite quartz monzonite to monzogranite or monzodiorite	Carboniferous
Felsic intrusives 42016	Cg	granite, granodiorite, monzonite, quartz monzonite, monzogranite, diorite	Carboniferous
Olympus Granite	Cgol	biotite quartz monzonite	Carboniferous
Dacey Granite	Cgda	biotite-hornblende granite to granodiorite	Carboniferous
Burwood Complex	Cgw	biotite-hornblende granodiorite to quartz monzodiorite, diorite, leucogranite, quartz monzonite	Carboniferous
Tooloombah Creek Granite	Cgto	biotite granite	Carboniferous
Withersfield Quartz Syenite	Cgwi	hornblende-biotite quartz syenite to granite	Carboniferous
Pandora Granite	Cgo72	biotite granite	Carboniferous

Table E2*B*.—Map units that define the Central sub-tract (009pCu8004b), East Tasmanide tract, Queensland, Australia.—Continued

Map unit	Map symbol	Lithology	Age range
		Intrusive rocks	
Bedarra Granite Complex	Cgdd	biotite granite, fine-grained biotite granite dikes	Early Carboniferous
Lochaber Granite	Cglo	biotite granite	Early Carboniferous
Sues Creek Microgranite	Cgsu	hornblende-biotite and biotite microgranite	Early Carboniferous
Noel Micromonzonite	Cgno	hornblende-pyroxene quartz micromonzonite	Early Carboniferous
Eastdale Granite	Cged	biotite granite	Early Carboniferous
Black Cap Diorite	Cgbk	hornblende-biotite microgranite ring dike	Early Carboniferous
Bagstowe Granite	Cgla	biotite granite	Early Carboniferous
Conical Knob Microgranite	Cgck	hornblende-biotite microgranite ring dike	Early Carboniferous
Cranky Creek Granodiorite	Cgcy	hornblende-biotite microgranodiorite stock in ring structure	Early Carboniferous
Culba Granodiorite	Cgcu	hornblende-biotite granodiorite, biotite granite	Early Carboniferous
Old Man Rhyolite	Cgom	biotite intrusive rhyolite to microgranite	Early Carboniferous
Cook Microgranite	Cgoc	microgranite	Early Carboniferous
Mount Rous Microgranodiorite	Cgmt	biotite-hornblende microgranodiorite	Early Carboniferous
Purkin Granite	Cgpu	biotite granite, porphyritic microgranite	Early Carboniferous
Peak John Well Granite	Cgpj	biotite granite and granodiorite	Early Carboniferous
Metamorphic rocks 40150	Dn	metagabbro, amphibolite, metased rocks	Devonian to Permian
Karin Granite	Dgkr	biotite microgranite, biotite granite	Late Devonian to Early Carboniferous
Barrabas Adamellite	Sgb	monzogranite, granodiorite, granite	Late Silurian to Early Devonian
Deane Granodiorite	Sgea	hornblende-biotite granodiorite, quartz monzodiorite	Late Silurian to Early Devonian
Meadowvale Granodiorite	Sgm11	hornblende-biotite granodiorite	Late Silurian to Early Devonian
Spondulix Granodiorite	Sgm16	biotite-hornblende granodiorite	Late Silurian to Early Devonian
Five Mile Mill Granodiorite	Sgm8	biotite-hornblende granodiorite	Late Silurian to Early Devonian
Casey Spring Creek Granodiorite	Sgcs	biotite-hornblende granodiorite	Late Silurian to Early Devonian
River View Granodiorite	Sgm15	hornblende-biotite granodiorite	Late Silurian to Early Devonian
Heathfield West Tonalite	Sgm9	biotite-hornblende granodiorite to tonalite	Late Silurian to Early Devonian
Dalmore Granodiorite	Sgm6	biotite-hornblende granodiorite	Late Silurian to Early Devonian
Yulga Tonalite	Sgm20	biotite-hornblende tonalite	Late Silurian to Early Devonian
Crescent Granodiorite	Sgm5	biotite-hornblende granodiorite	Late Silurian to Early Devonian
Urdera Granodiorite	Sgue	biotite-hornblende granodiorite	Late Silurian to Early Devonian
Two Mile Granite	Sgm17	hornblende-biotite granodiorite	Late Silurian to Early Devonian
Balfes Creek Granodiorite	Sgba	biotite-hornblende granodiorite and tonalite	Late Silurian to Early Devonian
Weaner Vale Granite	Sgaw	biotite granite, pegmatite	Late Silurian to Early Devonian
Centauri Granodiorite	Sgm3	biotite granodiorite	Late Silurian to Early Devonian
Hodgon Granodiorite	Sghh	hornblende-biotite granodiorite	Late Silurian to Early Devonian
Powlathanga Tonalite	Sgap	orthopyroxene-clinopyroxene-biotite-hornblende granodiorite, quartz diorite	Late Silurian to Early Devonian
Spider Gully Granodiorite	Sgsp	hornblende granodiorite	Late Silurian to Early Devonian
Wharleys Tonalite	Sgm19	biotite-hornblende granodiorite, biotite-hornblende tonalite	Late Silurian to Early Devonian
Mount Cuthbert Granodiorite	Sgbc	hornblende-biotite granodiorite and tonalite	Late Silurian to Early Devonian
Policeman Creek Granodiorite	Sgrp	biotite-hornblende granodiorite, granite	Late Silurian to Early Devonian
Flora Creek Trondhjemite	Sgrf	biotite trondhjemite	Late Silurian to Early Devonian

Table E2*B*. Map units that define the Central sub-tract (009pCu8004b), East Tasmanide tract, Queensland, Australia.—Continued

Map unit	Map symbol	Lithology	Age range
		Intrusive rocks	
Merriland Tonalite	Sgm12	hornblende-biotite granodiorite and tonalite	Late Silurian to Early Devonian
Goldsborough Granodiorite	Sghg	hornblende-biotite granodiorite	Late Silurian to Early Devonian
Brittania Granodiorite	Sgrr	biotite granite, hornblende-biotite granodiorite	Late Silurian to Early Devonian
Alpha Granite	Sgaa	biotite granite to alkali feldspar granite	Late Silurian to Early Devonian
Molly Darling Granodiorite	Sgm14	hornblende-biotite granodiorite and tonalite	Late Silurian to Early Devonian
Carse-O-Gowrie Granodiorite	Sgce	hornblende-biotite and biotite-hornblende granodiorite and tonalite (regional)	Late Silurian
Felsic intrusives 69541	Sggt	biotite-hornblende tonalite, trondhjemite, granodiorite, and biotite-muscovite granite	Silurian to Devonian
Emu Mill Granodiorite	Sgm7	hornblende-biotite granodiorite	Silurian to Devonian
Millchester Creek Tonalite	Sgm13	biotite-hornblende tonalite to granodiorite	Silurian to Devonian
Wellington Springs Tonalite	Sgm18	biotite-hornblende and hornblende-biotite granodiorite, minor tonalite	Silurian to Devonian
Boatswain Granodiorite	Sgm2	biotite-hornblende granodiorite, tonalite, granite	Silurian to Devonian
Scoop Holes Granodiorite	Sgsc	biotite-hornblende and hornblende-biotite granodiorite, minor tonalite	Silurian to Devonian
Rishton Granodiorite	Sgri	biotite-hornblende and hornblende-biotite granodiorite, minor tonalite	Silurian to Devonian
Kirkton Tonalite	Sgki	hornblende-biotite tonaite, cut by orogenic lode-gold veins	Silurian to Devonian
Chippendale Granodiorite	Sgm4	biotite-hornblende granodiorite (regional)	Silurian to Devonian
Kedumba Granodiorite	Sgbk	hornblende-biotite granodiorite	Silurian to Devonian
Felsic intrusives 68945	SDg	granite, granodiorite, tonalite, microdiorite, rhyolite, dolerite	Silurian to Devonian
Jessop Creek Tonalite	Sgm10	hornblende-biotite tonalite, diorite	Silurian to Middle Devonian
Felsic intrusives 69540	Sgct	biotite-hornblende granodiorite, tonalite, trondhjemite, biotite granite, leucogranite	Early Silurian to Middle Devonian
Broughton River Granodiorite	Sgbb	hornblende-biotite granodiorite, granite (regional)	Silurian to Early Devonian
Craigie Tonalite	Sgcg	hornblende-biotite tonalite	Silurian to Early Devonian
Blanders Granodiorite	Sgbs	hornblende-biotite granodiorite	Silurian to Early Devonian
Toms Hole Granodiorite	Sght	hornblende-biotite granodiorite, quartz phenocrysts, plagioclase phenocrysts	Silurian to Early Devonian
Cargoon Granodiorite	Sgco	hornblende-biotite granodiorite to tonalite	Silurian to Early Devonian
Glen Dillon Granodiorite	Sggd	biotite granodiorite	Silurian to Early Devonian
Beasley Creek Tonalite	Sgm1	biotite-hornblende granodiorite and tonalite	Silurian to Early Devonian
Big Bore Granodiorite	Sgig	biotite granodiorite	Silurian to Early Devonian
Schreibers Granodiorite	Sgss	biotite and hornblende-biotite granodiorite to granite	Silurian
Landers Igneous Complex	Ogl	microgranite; felsic, intermediate, and mafic intrusions	Ordovician to Permian
Ballabay Complex	Odb	hornblende gabbro, granodiorite, biotite granite	Ordovician to Permian
Larry Creek Complex	Pga	biotite granite, hornblende granodiorite, gabbro	Ordovician to Permian
Granite to diorite 69543	Ogdt	biotite-hornblende to biotite granite, granodiorite, microgranite, microgranodiorite; minor muscovite granite, diorite, gabbro	Ordovician to Devonian
Intermediate intrusives 69457	Ogd	diorite, quartz diorite, gabbro	Ordovician to Devonian
Mafic intrusives 69835	Odct	diorite, quartz diorite, gabbro	Ordovician to Devonian
Drinkwater Diorite	Ogdd	diorite	Ordovician to Early Devonian

Table E2*B*. Map units that define the Central sub-tract (009pCu8004b), East Tasmanide tract, Queensland, Australia.—Continued

Map unit	Map symbol	Lithology	Age range
		Intrusive rocks	
Mingela Granodiorite	Ogmi	biotite-hornblende granodiorite	Ordovician to Silurian
Sunburst Granodiorite	Ogus	biotite-hornblende granodiorite to tonalite, biotite-hornblende quartz monzodiorite	Ordovician to Silurian
Stannett Creek Gabbro	Sdst	orthopyroxene-clinopyroxene-olivine gabbro, leucogabbro, hornblende-plagioclase gabbro	Ordovician to Silurian
Hogsflesh Creek Granodiorite	Oghh	hornblende-biotite granodiorite to granite	Ordovician to Silurian
Brookdale Granite	Ogoo	hornblende-biotite granite	Ordovician to Silurian
La Villa Igneous Complex	Odl	hornblende-plagioclase gabbro, hornblende quartz diorite, biotite-hornblende diorite	Ordovician to Early Silurian
Macrossan Gabbro	Odmc	hornblende-plagioclase gabbro to diorite, quartz diorite, quartz gabbro, hornblende-biotite granodiorite	Late Ordovician
Piano Gully Granodiorite	Oglp	hornblende-biotite granodiorie, biotite granite	Early Ordovician to Silurian
Towers Hill Granite	Ogth	biotite granodiorite, biotite granite, rare hornblende	Early Ordovician to Silurian
Fenian Granite	Ogff	biotite granite	Early Ordovician to Silurian
Brook Complex	-Cgb	granodiorite, granite, metasedimentary rocks	Cambrian to Devonian
Carse Creek Complex	-Cga	hornblende-biotite tonalite or trondhjemite, biotite-muscovite granodiorite, biotite granite; schist, hornfels	Late Cambrian to Ordovician
Ringwood Park Microgranite	-Cggr	biotite microgranite, biotite granite	Late Cambrian to Early Ordovician
Fat Hen Creek Complex	-Cgf	biotite tonalite to granodiorite with cordierite, gneissic enclaves, gneissic hornblende-biotite tonalite	Late Cambrian to Early Ordovician
Shovel Creek Complex	-Cgsc	granodiorite, granite porphyry, diorite, gabbro	Late Cambrian to Early Ordovician
Black Jack Granodiorite	Sgrb	biotite granite, hornblende-biotite granodiorite	Late Cambrian to Early Ordovician
Medicine Creek Complex	-Cgm	hornblende-biotite granodiorite, microgranodiorite, microgranite, gabbro, hornfels, schist, amphibolite	Cambrian to Ordovician
Mafic intrusives 69544	-Cd	gabbro, diorite	Cambrian to Ordovician
Felsic intrusives 69545	-Cgq	granite, orthogneiss	Cambrian to Ordovician
Bucklands Hill Diorite	-Cgpb	hornblende-plagioclase-quartz metadiorite to metagabbro	Early Cambrian to Early Ordovician
Bunkers Hill Granite	Ogbu	granite	Ordovician
Bend Granodiorite	Ogen	granodiorite	Ordovician
Felsic intrusives 69456	Ogct	granodiorite	Early to Middle Ordovician
Cockie Spring Tonalite	Oggc	tonalite	Cambrian to Ordovician
		Volcanic rocks	
Greenvale Formation	Obev	tholeiitic basalt	Late Ordovician to Early Silurian
Everetts Creek Volcanics	Oaev	andesite, basalt (pillowed), volcanic breccia	Late Ordovician
Wairuna Formation	Obwa	tholeiitic basalt	Ordovician
Trooper Creek Formation	Oast	andesite, basalt of Seventy Mile Range Group	Ordovician
Trooper Creek Formation	Ofst	dacite of Seventy Mile Range Group	Ordovician
Trooper Creek Formation	Owst	andesite, basalt, dacite, and sedimentary rocks of Seventy Mile Range Group	Ordovician
Mount Windsor Volcanics	Oasw	andesite of Seventy Mile Range Group	Cambrian to Ordovician
Mount Windsor Volcanics	Ofsw	felsic volcanics of Seventy Mile Range Group	Cambrian to Ordovician
Mount Windsor Volcanics	Ogsw	rhyolite porphyry of Seventy Mile Range Group	Cambrian to Ordovician
Dry River Metavolcanics	-Crbd	rhyolitic metavolcanic rocks	Late Cambrian to Early Ordovician
Eland Metavolcanics	-Ctle	schistose metavolcanic rocks	Early Cambrian to Early Ordovician

Table E2*C*. Map units that define the South sub-tract (009pCu8004c), East Tasmanide tract, Queensland, Australia.

[Based on Raymond and others (2007) and Whitaker and others (2007); for additional information about named map units, see Geoscience Australia, Stratigraphic Units Database at http://dbforms.ga.gov.au/www/geodx.strat_units.int/]

Map unit	Map symbol	Lithology	Age range
		Intrusive rocks	
Felsic to intermediate intrusives 39497	-Rg	granitoids, dioritoids, quartz monzonite, gabbro	Triassic
Koreelan Creek Granodiorite	-Rgck	granodiorite, quartz monzodiorite, locally porphyritic	Triassic
Bookookoorara Monzogranite	-Rgso	granodiorite, quartz monzodiorite, locally porphyritic	Triassic
Dormans Flat Granite	-Rgdf	monzogranite, porphyritic	Triassic
Sailor Jack Granite	-Rgbs	hornblende-biotite monzogranite, porphyritic	Triassic
Kellys Creek Leucomonzogranite	-Rgkc	hornblende-biotite granite, porphyritic	Triassic
Botumburra Range Monzogranite	-Rgeb	hornblende-biotite granodiorite, monzogranite, leucogranite	Triassic
Yarrahapinni Adamellite	-Rgry	hornblende-biotite granitoids	Triassic
Smokey Cape Adamellite	-Rgsc	hornblende-biotite granodiorite, monzogranite, leucogranite	Triassic
Banda Banda Monzodiorite	-Rgbb	monzodiorite	Triassic
Glen Esk Adamellite	-Rgge	granitoids	Triassic
Gundle Granite	-Rgrg	granitoids and leucogranitoids	Triassic
Cairncross Adamellite	-Rgca	monzogranite porphyry	Triassic
The Brothers Granitoids	-Rgbiotite	granitoids	Triassic
Ballandean Granite	-Rgba	hornblende-biotite monzogranite, clinopyroxene-biotite-hornblende granodiorite to monzogranite	Triassic
Mount You You Granite	-Rgmy	biotite granite, aplitic leucogranite, mafic intrusives	Triassic
Sailor Jack Granite	-Rgbs	hornblende-biotite monzogranite	Triassic
Dormans Flat Granite	-Rgdf	biotite monzogranite	Triassic
Rivertree Granite	-Rgsv	biotite-hornblende granite with K-feldspar phenos	Middle Triassic
Morgans Creek Monzogranite	-Rgsg	granitoids	Middle Triassic
Bruxner Monzogranite	-Rgcb	granitoids	Middle Triassic
Billyrimba Leucomonzogranite	-Rgsi	granitoids	Middle Triassic
Dandahra Creek Leucogranite	-Rgsd	granitoids	Middle Triassic
Chaelundi Complex	-Rgc	hornblende-biotite granite, granodiorite	Middle Triassic
Round Mountain Leucoadamellite	-Rgrm	biotite leucogranite, hornblende-biotite leucogranite, albite leucogranite dikes	Early to Middle Triassic
Valla Adamellite	-Rgvl	porphyritic microgranite	Early to Middle Triassic
Carrai Granodiorite	-Rgrc	hornblende-biotite granodiorite, monzogranite, leucogranite	Early to Middle Triassic
Fife Adamellite	-Rgfi	hornblende-biotite monzogranite	Early to Middle Triassic
Maryland Granite	-Rgem	hornblende-biotite monzogranite	Early to Middle Triassic
Ruby Creek Granite	-Rgsr	monzogranite, equigranular to porphyritic	Early to Middle Triassic
Mackenzie Monzogranite	-Rgsm	hornblende-biotite leucogranite	Early to Middle Triassic
Nonnington Leucomonzogranite	-Rgsn	granitoids	Early to Middle Triassic
Mole Granite	-Rgom	leucogranite, porphyritic margins	Early to Middle Triassic
Sandy Flat Monzogranite	-Rgsf	hornblende-biotite leucogranite	Early to Middle Triassic
Mount Jonblee Leucomonzogranite	-Rgsj	saccharoidal leucogranite (aplitic)	Early to Middle Triassic
Bolivia Range Leucomonzogranite	-Rgsb	granite, medium-grained to porphyritic	Early to Middle Triassic
Kingsgate Leucogranite	-Rgm7	biotite granite	Early to Middle Triassic
Webbs Consols Leucogranite	-Rgu28	granophyric alkali feldspar granite	Early to Middle Triassic
Dumboy-Gragin Granite	-Rgod	syenogranite	Early to Middle Triassic
Red Range Microleucogranite	-Rgm12	leucogranite	Early to Middle Triassic
Gilgai Granite	-Rgog	biotite-hornblende granite, monzogranite	Early to Middle Triassic
Elsmore Granite	-Rgoe	monzogranite, seriate to porphyritic	Early to Middle Triassic
Ruby Creek Granite	-Rgsr	biotite leucogranite, biotite monzogranite	Early to Middle Triassic
Maryland Granite	-Rgem	hornblende-biotite monzogranite	Early to Middle Triassic
Stanthorpe Granite 3	-Rgst3	granite, porphyritic, and quartz-feldspar porphyry	Early Triassic
Stanthorpe Granite 6	-Rgst6	hornblende-biotite and biotite monzogranite to syenogranite	Early Triassic

Table E2*C*. Map units that define the South sub-tract (009pCu8004c), East Tasmanide tract, Queensland, Australia.—Continued

Map unit	Map symbol	Lithology	Age range
		Intrusive rocks	
Stanthorpe Granite 5	-Rgst5	hornblende-biotite and biotite monzogranite to syenogranite	Early Triassic
Undercliffe Falls Monzogranite	-Rgsu	biotite-hornblende monzogranite	Early Triassic
Stanthorpe Granite 1	-Rgst1	biotite-monzogranite to syenogranite	Early Triassic
Cullens Creek Granite	-Rgcc	granitoids	Early Triassic
Jenny Lind Granite	-Rgcj	hornblende-biotite quartz diorite, tonalite, quartz monzodiorite, granodiorite	Early Triassic
Black Snake Creek Granite	-Rgls	granite, aplitic	Early Triassic
Stanthorpe Granite 3	-Rgst3	leucogranite, microgranite, quartz-feld porphyry	Early Triassic
Bungulla Monzogranite	P-Rgm4	granitoids, porphyritic	Late Permian to Early Triassic
Postmans Creek Granodiorite	-Rgpc	hornblende-biotite granodiorite	Late Permian to Early Triassic
Newton Boyd Granodiorite	P-Rgen	granitoids, equigranular to porphyritic	Late Permian to Early Triassic
Mingimarny Granite	Pgmm	biotite monzogranite	Late Permian to Early Triassic
Bungulla Monzogranite	P-Rgm4	hornblende granodiorite to monzogranite	Late Permian to Early Triassic
Clive Monzogranite	P-Rgsi	leucogranite	Late Permian to Early Triassic
Pyes Creek Leucomonzogranite	P-Rgu30	granitoids	Late Permian to Early Triassic
Wards Mistake Monzogranite	P-Rgu27	hornblende-biotite monzogranite-granodiorite	Late Permian to Early Triassic
Mount Mitchell Monzogranite	P-Rgsm	biotite-hornblende monzogranite and leucogranite	Late Permian to Early Triassic
Wellingrove Granodiorite	P-Rgu10	hornblende-biotite granite and granodiorite	Late Permian to Early Triassic
Oban River Leucomonzogranite	P-Rgm11	leucogranite, biotitic, saccharoidal	Late Permian to Early Triassic
Tingha Monzogranite	P-Rgu9	hornblende-biotite monzogranite	Late Permian to Early Triassic
Glenreach Monzogranite	P-Rgu5	hornblende-biotite monzogranite	Late Permian to Early Triassic
Mount Duval Monzogranite	P-Rgu7	hornblende-biotite monzogranite	Late Permian to Early Triassic
Glenore Monzogranite	P-Rgu4	hornblende-biotite monzogranite	Late Permian to Early Triassic
The Basin Monzogranite	P-Rgu8	granitoid, with minor porphyritic variant	Late Permian to Early Triassic
Parlour Mountain Leucomonzogranite	P-Rgu14	granitoid	Late Permian to Early Triassic
Gwydir River Monzogranite	P-Rgu6	porphyritic granitoids	Late Permian to Early Triassic
Blackfellows Gully Leucomonzogranite	P-Rgu12	biotite-hornblende leucomonzonite	Late Permian to Early Triassic
Yarrowyck Granodiorite	P-Rgu29	hornblende-biotite granodiorite	Late Permian to Early Triassic
Honeysuckle Creek Leucomonzogranite	P-Rgu2	granite, porphyritic leucomonzogranite	Late Permian to Early Triassic
Uralla Granodiorite	P-Rgu23	hornblende-biotite granodiorite	Late Permian to Early Triassic
Wongalee Leucogranite	P-Rgu25	granitoid	Late Permian to Early Triassic
Balala Granodiorite	P-Rgu1	hornblende-biotite granodiorite, minor diorite	Late Permian to Early Triassic
Khatoun Tonalite	Pgu18	granitoid	Late Permian to Early Triassic
Manuka Farm Porphyritic Microtonalite	P-Rgu19	porphyritic granitoid	Late Permian to Early Triassic
Glenburnie Leucomonzogranite	P-Rgu5	hornblende-biotite monzogranite	Late Permian to Early Triassic
Wilhelmshohe Tonalite	P-Rgu24	hornblende-biotite tonalite	Late Permian to Early Triassic
Harnham Grove Porphyritic Microtonalite	P-Rgu16	granitoid	Late Permian to Early Triassic
Terrible Vale Porphyritic Microtonalite	P-Rgu21	porphyritic granitoid	Late Permian to Early Triassic
Standbye Monzogranite	P-Rgsy	hornblende-biotite monzogranite	Late Permian to Early Triassic
Walcha Road Monzogranite	P-Rgm13	hornblende-biotite monzogranite	Late Permian to Early Triassic
Looanga Monzogranite	P-Rgm9	biotite-hornblende monzogranite	Late Permian to Early Triassic
Kentucky Diorite	P-Rgu17	diorite, gabbro	Late Permian to Early Triassic
Campbells Hill Monzogranite	P-Rgsc	granitoids	Late Permian to Early Triassic
Shalimar Tonalite	P-Rgu20	hornblende-biotite tonalite	Late Permian to Early Triassic
Attunga Creek Monzogranite	P-Rgm1	biotite-hornblende monzogranite	Late Permian to Early Triassic
Bendemeer Monzogranite	P-Rgm2	hornblende-biotite monzogranite, minor monzonite	Late Permian to Early Triassic

Table E2*C*. Map units that define the South sub-tract (009pCu8004c), East Tasmanide tract, Queensland, Australia.—Continued

Map unit	Map symbol	Lithology	Age range
		Intrusive rocks	
Congi Creek Monzogranite	P-Rgm5	granitoids	Late Permian to Early Triassic
Moonbi Monzogranite	P-Rgm10	hornblende-biotite monzogranite, minor monzonite	Late Permian to Early Triassic
Inlet Monzonite	P-Rgm6	hornblende-biotite monzonite	Late Permian to Early Triassic
Back Creek Tonalite	P-Rgu15	granitoid	Late Permian to Early Triassic
Felsic intrusives 42189	P-Rg	dioritoids and granitoids	Permian to Triassic
Unnamed granitoids 42188	P-Rgm	biotite-hornblende-clinopyroxene quartz monz and other granitoids	Permian to Triassic
Billygoat Hill Monzonite	Pgm3	monzonite, monzogranite (high-K)	Late Permian
Karikeree Metadolerite	Pdkk	dolerite	Late Permian
Herries Granite	Pgeh	hornblende-biotite monzogranite	Late Permian
Glen Garry Microleucogranite	Pggg	leucogranite	Permian
Felsic intrusives 42187	Pg	granite, granodiorite, tonalite, aplite, microgranite, quartz-feld porphyry	Permian
Mafic intrusives 42185	Pdn	gabbro, dolerite	Permian
Cottesbrook Monzogranite	Pgu26	biotite-hornblende granite	Permian
Moonta Gully Monzogranite	Pgmg	biotite-hornblende monzogranite	Permian
Towgon Grange Granodiorite	Pgct	hornblende-biotite granodiorite, diorite, quartz diorite, equigranular to porphyritic	Permian
Kookabookra Monzogranite	Pgh11	biotite monzogranite with hornblende-rich enclaves	Permian
Dundurrabin Granodiorite	Pged	granitoid	Permian
Boxwell Granodiorite	Pgbx	quartz monzodiorite	Permian
Boxwell Granodiorite	Pgbx	hornblende monzodiorite, quartz monzodiorite	Permian
Highlands Complex	Pgn	granitoids	Permian
Tilbuster Granodiorite	Pgu22	clinopyroxene-hornblende-biotite granodiorite	Permian
Barrington Tops Granodiorite	Pgcb	granitoids, quartz diorite	Early to Middle Permian
Rockisle Granodiorite	Pgnr	granitoids, quartz diorite	Early to Middle Permian
Duncans Creek Trondhjemite	Pgcd	granitoid	Early to Middle Permian
Glenclair Monzogranite	Pgbg	biotite granite	Early Permian
Mornington Diorite	Pgmt	diorite, tonalite, granodiorite	Early Permian
Days Creek Gabbro	Pdh5	gabbro, diorite, granite	Early Permian
Greymare Granodiorite	Pggy	granodiorite	Early Permian
Billys Creek Tonalite	Pgeb	granitoids, porphyritic	Late Carboniferous to Permian
Sheep Station Creek Complex	Cgss	granite, gabbro, granodiorite	Late Carboniferous
Dorrigo Mountain Complex	Cgr	microdiorite, microgranite	Late Carboniferous
		Volcanic rocks	
Werrikimbe Volcanics	-Rfwe	dacite ignimbrite	Late Triassic
Felsic and mafic volcanics 40153	-Rv	rhyolite, andesite, basalt (volcanics)	Triassic
Tent Hill Volcanics	Pfwt	hornblende-biotite andesite to rhyolite ignimbrites and lavas	Middle to Late Permian
Drake Volcanics	Pfwd	porphyritic rhyodacite and andesite flows, tuffs, breccias	Permian
Hianana Volcanics	Pfwh	porphyritic lava and volcaniclastic rocks	Permian

Table E2*D*. Map units that define the North sub-tract (009pCu8004d), East Tasmanide tract, Queensland, Australia.

[Based on Whitaker and others (2007); for additional information about named map units, see Geoscience Australia, Stratigraphic Units Database at http://dbforms.ga.gov.au/www/geodx.strat_units.int/]

Map unit	Map symbol	Lithology	Age range
		Intrusive rocks	
Lizard Island Granite	Pgc18	leucogranite	Late Permian
Trevethan Granodiorite	Pgy5	pyroxene-hornblende-biotite monzogranite	Late Permian
Keating Granodiorite	Pgy3	biotite granodiorite to monzogranite	Late Permian
Talgijah Granodiorite	Pgy2	hornblende-biotite granodiorite	Late Permian
Nulbullulul Granite	Pgp2	hornblende-biotite monzogranite	Permian
Thornton Granite	Pgp3	granite, granophyric	Permian
Mount Hartley Granite	Pgc8	biotite granite	Permian
Mount Poverty Granite	Pgc5	biotite granite, minor greisen	Permian
Mount Leswell Microgranite	Pgc9	biotite monzogranite	Permian
Wolverton Adamellite	Pgwe3	biotite monzogranite, granite, aplite	Permian
Cape Melville Granite	Pgam	hornblende-biotite monzogranite	Permian
Waterfall Granite	Pgc13	biotite granite	Permian
Mount Yates Granodiorite	Pgy4	hornblende-biotite granodiorite with mafic clots	Permian
Spurgeon Granite	Pgw11	biotite monzogranite	Permian
McLeod Granite	Pgw2	biotite monzogranite, granodiorite	Permian
Hope Vale Granite	Pgy7	hornblende-biotite monzogranite	Permian
Weymouth Granite	Pgwe2	hornblende-biotite monzogranite, leucogranite	Permian
Puckley Granite	Pgy9	biotite monzogranite	Permian
Leichhardt Pocket Granite	Pgy10	hornblende-biotite granodiorite, monzogranite	Permian
Mount Pike Granite	Pgw15	biotite monzogranite	Permian
Twin Humps Adamellite	Pgwe4	hornblende-biotite monzogranite, biotite leuco monzogranite	Early Permian
Barrow Point Granite	Pgc19	biotite monzogranite	Early Permian
Howick Island Granite	Pgy8	biotite granodiorite	Early Permian
Wakooka Granite	Pgwk	biotite granite	Early Permian
Dalkum Microgranite	Cgo65	biotite monzogranite	Carboniferous to Late Permian
Felsic intrusives 68931	CPgcy	granite, granodiorite, tonalite, microgranite, rhyolite, dolerite, diorite, gabbro	Carboniferous to Permian
Mafic intrusives 39448	CPd	dolerite, gabbro, diorite, monzonite, meladiorite	Carboniferous to Permian
Intrusive rhyolite 41758	Cgi	rhyolite and dacite intrusives	Carboniferous to Permian
Felsic intrusives 68932	CPggh	granodiorite, monzogranite, hornblende-biotite granite, muscovite-cordierite granite, greisen, dacite	Carboniferous to Permian
Badu Granite	Cgba	biotite leucogranite, monzogranite, hornblende-biotite monzogranite and granodiorite	Late Carboniferous
Horn Island Granite	Cgbh	hornblende microgranite	Carboniferous
		Volcanic rocks	
Mitchell River Volcanics	Pfmi	rhyolite, dacite, andesite, sedimentary rocks	Late Permian
Obree Point Volcanics	Pfob	dacitic to andesitic lava, tuff, breccia, sedimentary rocks	Permian
Cape Grenville Volcanics	Cfcg	rhyolite tuff, welded tuff, breccia	Carboniferous to Permian
Intermediate to felsic extrusives 68930	Ca	rhyolite to andesite, basalt, sedimentary rocks	Carboniferous to Early Permian
Kangaroo River Volcanics	Cfkr	rhyolitic	Late Carboniferous
Janet Ranges Volcanics	Cfjr	rhyolitic	Late Carboniferous
Torres Strait Volcanics	Cfts	rhyolite, rhyodacite, sedimentary rocks	Carboniferous

Table E3. Porphyry copper deposits in the Central sub-tract (009pCu8004b), East Tasmanide tract, Queensland, Australia.

[Ma, million years; Mt, million metric tons; %, percent; t, metric ton; g/t, gram per metric ton; Cu-Mo subtype, deposits that have Au/Mo ratios <3 or average Mo grades >0.03%; NA, not applicable; -, no data. Contained Cu in metric tons is computed as tonnage (Mt × 1,000,000) × Cu grade (%) ÷ 100]

Name	Latitude	Longi-tude	Subtype	Age (Ma)	Tonnage (Mt)	Cu (%)	Mo (%)	Au (g/t)	Ag (g/t)	Contained Cu (t)	Reference
					Carboniferous to Middle Permian						
Ruddygore	-17.129	144.549	NA	275	10	0.4	-	-	-	41,500	Horton (1978), Ewers and others (2002)
Dimbulah	-17.248	145.081	NA	275	20	0.25	-	-	-	50,000	Ewers and others (2002), Geoscience Australia (2010)
					Late Permian to Triassic						
Mount Cannindah	-24.671	151.276	NA	235	17.5	0.65	-	0.16	6.75	120,000	Bedford (1975), Horton (1978), Murray (1990), Singer and others (2008), Planet Metals (2009), Ewers and others (2002), Geoscience Australia (2010), Geological Survey of Queensland (2010)
Limonite Hill	-23.687	150.630	NA	246	100	0.3	-	-	-	300,000	Ford and others (1976), Horton (1978), Lacy (1980), Singer and others (2008), Ewers and others (2002), Geoscience Australia (2010)
Coalstoun	-25.617	151.830	NA	235	80	0.3	-	-	-	240,000	Ashley and others (1978), Horton (1978), Murray (1990), Singer and others (2008), Ewers and others (2002), Geoscience Australia (2010), Geological Survey of Queensland (2010)
Yeppoon	-22.998	150.694	NA	220	50	0.3	0.01	-	-	150,000	Ford and others (1976), Horton (1978), Singer and others (2008), Ewers and others (2002), Geoscience Australia (2010)
Chinaman Creek	-25.230	151.617	NA	250	200	0.2	-	0.33	-	400,000	Horton (1978), Lacy (1980), Murray (1986), Singer and others (2008), Ewers and others (2002), Geoscience Australia (2010), Geological Survey of Queensland (2010)
Struck Oil	-23.605	150.462	NA	244	100	0.2	-	-	-	200,000	Horton (1978), Lacy (1980), Murray (1986), Singer and others (2008), Ewers and others (2002), Geoscience Australia (2010)
Kiwi Carpet	-24.664	150.877	NA	225	200	0.15	0.01	-	-	300,000	Horton (1978), Ewers and others (2002), Singer and others (2008), Aussie Q Resources, Ltd., (2007)
Whitewash	-24.807	150.875	Cu-Mo	237	71.5	0.01	0.04	-	1.19	71,000	Brooks (1976), Horton (1978), Lacy (1980), Singer and others (2008), Aussie Q Resources, Ltd., (2007, 2010), Geoscience Australia (2010), Geological Survey of Queensland (2010)
					Early Cretaceous						
Ben Mohr	-21.266	148.868	NA	123	20	0.2	-	-	-	40,000	Ewers and others (2002), Geoscience Australia (2010)
Mount Leslie	-20.937	148.160	NA	124	20	0.2	-	-	-	40,000	Horton (1978), Lacy (1980), Ewers and others (2002), Geoscience Australia (2010)
Julivon Creek	-20.539	148.299	NA	132	35	0.16	0.01	-	-	54,600	Geological Survey of Queensland (2010), Allen and others (1997)
Mount Abbot	-20.197	147.950	NA	119	200	0.15	-	-	-	300,000	Horton (1978), Lacy (1980), Ewers and others (2002), Geoscience Australia (2010), Allen and others (1997)
total					1,124					2,307,100	
rounded total					1,120					2,300,000	

The Kiwi Carpet porphyry copper and Whitewash porphyry Cu-Mo deposits (Horton's subset L) are in the west-central part of the Permian-Triassic magmatic arc, which is exposed between Rockhampton and Brisbane (fig. E4). These deposits are hosted in a composite quartz monzonitic pluton that is about 50 km long and about 5–10 km wide (Horton, 1978, p. 914; Aussie Q Resources, Ltd., 2007).

The Kiwi Carpet deposit is related to a discrete stock near the eastern margin of the northern part of this composite pluton, and the Whitewash deposit is related to another discrete stock about 9 km to the south. Fracturing is weak to moderate in these deposits. Major hypogene sulfide minerals are pyrite, chalcopyrite, and lesser molybdenite. Minor metallic minerals are magnetite, galena, and sphalerite. The pyrite/chalcopyrite ratio is about 5:1 and the copper/molybdenum ratio is about 10:1. Hydrothermal alteration products include rare inner potassic, medial phyllic, and widespread outer and late propylitic alteration-mineral assemblages. Supergene enrichment is very weak. At Whitewash, a soil geochemical anomaly pattern for copper consists of several narrow, north-trending zones, which coalesce in a broad southern zone. This indicates a swarm of north-striking mineralized fractures, which dip steeply (Aussie Q Resources, Ltd., 2007).

The four highest-grade porphyry copper deposits of Permian-Triassic age are individually described below.

Mount Cannindah

The Mount Cannindah deposit, which was discovered in 1895, is in the south-central part of the Central sub-tract (fig. E1). With past production of about 1,000 t copper and 0.9 t gold, this deposit is currently being explored for porphyry Cu-Au (Planet Metals, Ltd., 2009). A diagrammatic geologic map on the Planet Metals, Ltd., Web site indicates that the Mount Cannindah gold-bearing porphyry copper deposit is hosted in a large body of breccia along the southeastern margin of a stock, identified as the Mount Cannindah intrusive. This stock and the adjacent breccia are about 1.5 km long, and are elongate to the northeast. The width of the stock varies from about 0.2 to 0.5 km, and the breccia body is about 1 km wide. Stockwork veining cuts the mineralized part of the stock, and the adjacent breccia contains hydrothermal minerals between angular fragments. Elsewhere, this large body of breccia contains at least nine widely scattered gold prospects. Another stock, southeast of the breccia, is central to a northeast-trending set of Cu-Mo veins and skarns.

According to Singer and others (2008), igneous rocks associated with the Mount Cannindah deposit include diorite, tonalite, granodiorite, dacite porphyry, and granite. Ore minerals are bornite, chalcopyrite, galena, gold, marcasite, molybdenite, pyrite, arsenopyrite, silver, and sphalerite. Gangue and alteration minerals are quartz, epidote, chlorite, and carbonate minerals. Supergene minerals are limonite, malachite, and azurite in the oxidized zone, and chalcocite and covellite in the reduced zone.

Mineralized breccias and stockwork veining at the Mount Cannindah deposit indicate that compared to most other deposits in the Central sub-tract, relatively high-grade ore at the Mount Cannindah deposit probably formed at relatively shallow depths.

Limonite Hill

The Limonite Hill deposit is in the southern third of the Central sub-tract, southeast of Rockhampton (fig. E1). According to Ford and others (1976), the Limonite Hill deposit is coincident with a breccia pipe near the western margin of a Permian granodiorite intrusion into metasedimentary rocks of Lower Devonian age. The breccia pipe is about 100 m in diameter and is strongly limonitized at the surface. Breccia fragments are strongly sericitized and pyritized. Minor amounts of copper- and molybdenum-bearing minerals are disseminated in breccia fragments and in inter-fragment cement. Ford and others (1976) reported a late-Early Triassic K-Ar age of 246 Ma on sericite from the mineralized breccia pipe. The presence of mineralized breccia at the Limonite Hill deposit probably indicates that the depth of formation of this deposit was shallower than depths of formation of most other deposits of the Central sub-tract.

Coalstoun

The Coalstoun porphyry copper deposit is the southernmost of the Permian-Triassic deposits of southeastern Queensland (fig. E1). The Coalstoun deposit is associated with porphyritic intrusions of microtonalite and microdiorite of Permian age (235±4 Ma) (Ashley and others, 1978). These are hosted in siliciclastic metasedimentary rocks of Devonian to Carboniferous age. Porphyritic textures, metasedimentary inclusions, rafts and screens, and nearby breccia pipes indicate relatively shallow levels of emplacement and exposure. A zone of hydrothermal biotite in the core of the central intrusion contains up to 0.4 percent copper and 0.015 percent molybdenum. Copper grades decrease as pyrite/chalcopyrite ratios increase outward from this biotite zone. The hypogene deposit is partly blanketed by a zone of supergene clay-sericite saprolite containing up to 0.6 percent copper (probably near its base).

Yeppoon

The Yeppoon deposit is near the coast of Queensland, north of Rockhampton (fig. E1). According to Ford and others (1976), the deposit is centered on a small granodioritic stock of Late Triassic age. Three K-Ar age determinations indicate an age of about 220±7 Ma. Dikes of quartz latite porphyry, andesite-dacite and aplite, and breccia pipes also are present. Some dikes cut the stock and some are mineralized. Hydrothermal biotite, pyrite, and low-grade concentrations of chalcopyrite and molybdenite pervade the granodiorite stock. A pyrite halo contains more than 3 volume percent of sulfides.

Early Cretaceous Deposits

Porphyry copper deposits of Early Cretaceous age include the Ben Mohr, Mount Leslie, Julivon Creek, and Mount Abbot deposits (table E3). These deposits are clustered in east-central Queensland (fig. E1). They are related to intrusions of Early Cretaceous age (fig. E4).

The Julivon Creek (or Andromache River) deposit is associated with a granitic intrusion, which yielded a U-Pb zircon age determination of 132 Ma, and K-Ar age determinations of 132–123 Ma on biotite and 130–125 Ma on hornblende (Allen and others, 1997). The age of the Julivon Creek deposit fits within the time range of Early Cretaceous subduction-related magmatism (145–125 Ma) as defined by Allen and others (1997).

The Mount Abbot deposit is associated with the Mount Abbot quartz syenite intrusion, which yielded a U-Pb zircon age determination of 119 Ma (Allen and others, 1997). The age of the Mount Abbot deposit (119 Ma) fits the beginning of an episode of rift-related magmatism from 120 to 98 Ma, as defined by Allen and others (1997). This deposit probably formed during subduction rollback, which initiated post-subduction rifting. Horton (1978) classified the Ben Mohr and Mount Leslie deposits as Early Cretaceous, but we found no isotopic age determinations for these deposits or their associated igneous rocks.

According to Horton (1978), pre-ore host rocks for Julivon Creek and the Mount Abbot deposits are andesites, argillic sedimentary rocks, and calc-alkaline intrusions of Carboniferous-Permian age. Fracturing is locally strong. The major sulfide minerals are pyrite and chalcopyrite. Some deposits also contain minor molybdenite with copper/molybdenum ratios of about 20:1. Phyllic and propylitic alteration products are common, but potassic alteration products are rare. Horton (1978) suggests that the lower-middle parts of these deposits are exposed. There is little or no supergene enrichment.

The Mount Leslie and Ben Mohr deposits are the southeastern deposits of Early Cretaceous age (compare fig. E1 with fig. E4). According to Horton (1978), the Mount Leslie deposit is related to intrusions of granodiorite porphyry or quartz diorite porphyry of Early Cretaceous age. According to Ewers and others (2002), the Ben Mohr deposit is associated with monzosyenite of the Ben Mohr intrusive complex of Early Cretaceous age, emplaced into andesites, argillic sedimentary rocks, and earlier calc-alkaline intrusions of Carboniferous-Permian age.

According to Horton (1978), the Mount Leslie and Ben Mohr deposits are characterized by weak to moderate fracturing. Pyrite and chalcopyrite are the major sulfides, and the minor sulfides are molybdenite, galena, sphalerite, and arsenopyrite. Pyrite/chalcopyrite ratios range from 5:1 to 20:1. Phyllic and propylitic alteration products are common, but potassic alteration products are mostly absent. Horton (1978) suggested that the upper parts of these deposits are exposed. Supergene enrichment is very weak.

Porphyry Copper Prospects, Occurrences, and Related Deposit Types

Significant porphyry copper prospects in the Central sub-tract (009pCu8004b) of the East Tasmanide permissive tract are listed in order of decreasing geologic age in table E4*A*, and are described below.

Late Silurian to Devonian Prospects

The Bank, Barrabas Creek, and Titov porphyry copper prospects are associated with igneous intrusions of a continental magmatic arc of Late Silurian to Devonian age. These prospects and their associated igneous rocks are clustered about 80 km south of Townsville and 90 km inland from the Queensland coast (fig. E1). The Barrabas Creek prospect is grouped with the Claypan and Turkey Gully copper occurrences according to the 2-km rule of Singer and others (2005).

These prospects are associated with intrusions of granodiorite and adamellite porphyry of Silurian-Devonian age (Horton, 1978, table 3, p. 212–213). Fracturing is weak to moderate. Pyrite and chalcopyrite are the major metallic minerals, which are locally accompanied by minor molybdenite, powellite, or galena. Pyrite/chalcopyrite ratios are about 5:1, and copper/molybdenum ratios range from 3:1 to 25:1. Propylitic and phyllic alteration products are common, but potassic alteration products are uncommon. Supergene enrichment is weak. Horton (1978) suggested that these prospects may represent the lower to middle parts of porphyry copper systems.

Carboniferous to Middle Permian Prospects

Porphyry copper prospects at Mount Darcy, Mount Turner, Mountain Maid, and Beaks Mountain are associated with igneous intrusions of a continental magmatic arc of Carboniferous to Middle Permian age. The Mount Darcy, Mount Turner, and Mountain Maid prospects are west and southwest of Cairns, along the northern margin of the Central sub-tract (fig. E1)

According to Horton (1978, table 3, p. 212–213), the Mount Darcy and Mount Turner porphyry copper prospects are associated with granodiorite porphyry intrusions of Carboniferous age (about 310 Ma) in country rocks consisting mostly of Precambrian granodiorite. Fracturing is weak to moderate. Major metallic minerals are pyrite and chalcopyrite, which are locally accompanied by minor molybdenite, galena, or sphalerite, and very minor bornite or pyrrhotite. Potassic, phyllic, and propylitic alteration products are common. Supergene enrichment is weak. Horton (1978) suggests that these prospects may represent upper parts of porphyry copper systems.

The Mountain Maid porphyry copper prospect is 175 km west-southwest of Cairns (fig. E1). It is about 50 km west of the Ruddygore deposit and 100 km west of the Dimbulah deposit. We have no information about the tonnage and grade of copper at the Mountain Maid porphyry copper deposit. However, Axiom Mining, Ltd., (2010a) recently announced a set of preliminary estimates of tonnages and gold grades at a range of cutoff grades for gold at Mountain Maid. These range from 3 Mt averaging 0.67 g/t gold to 72 Mt averaging 0.23 g/t gold.

The Mountain Maid, Ruddygore, and Dimbulah porphyry copper sites are associated with granodiorite and monzonite porphyries of Early Permian age, hosted in metamorphic rocks of Precambrian age and in volcanics and calc-alkaline intrusions of Carboniferous age (Horton, 1978, p. 212–213). Fracturing is moderate to strong. Major metallic minerals are pyrite and chalcopyrite with subordinate bornite, and minor arsenopyrite, pyrrhotite, galena, and molybdenite. Pyrite/chalcopyrite ratios are about 5:1, with copper/molybdenum ratios greater than 100. Phyllic and propylitic alteration products are common, but potassic alteration products are rare. Supergene copper enrichment is generally weak but locally strong. Horton (1978) suggests that these deposits and prospects represent the middle to upper parts of porphyry copper systems.

The Beaks Mountain porphyry copper prospect is about 100 km southeast of Townsville and 25 km inland from the Queensland coast (fig. E1). It is associated with a granodiorite porphyry, emplaced into granite of Precambrian age and volcanic and intrusive rocks of Carboniferous age (Horton, 1978, p. 908–913). Fracturing is weak to moderate. Major metallic minerals are pyrite and chalcopyrite with minor molybdenite, and very minor galena and sphalerite. Pyrite/chalcopyrite ratios are about 5:1 and copper/molybdenum ratios are about 10:1. Phyllic and propylitic alteration products are common, but potassic alteration products are rare. Secondary enrichment is weak. Horton (1978) suggests these sites represent the lower to middle parts of porphyry copper systems.

Late Permian to Triassic Prospects

Porphyry copper prospects of Late Permian to Triassic age are in southeastern Queensland, between Rockhampton and Brisbane (fig. E1). Prospects of this age range include the high-ranked Moonmera and Calgoa prospects, as well as the lower ranked Gibraltar Rock, Mannersley-Riverhead, and Calliope prospects, for which we found no assay data (table E4*A*). The Mannersley and Riverhead prospects are grouped according to the 2-km rule of Singer and others (2005).

The Moonmera, Calgoa, Gibraltar Rock, and Mannersley-Riverhead prospects are related to quartz diorite to granodiorite porphyries of Late Permian to Middle Triassic age (about 250–235 Ma) (Horton, 1978). Host rocks include argillitic metasedimentary rocks and andesitic volcanics of Silurian to Permian age and calc-alkaline intrusions of Permian to Triassic age. Fracturing generally is weak to moderate but is locally strong. Major metallic minerals are pyrite and chalcopyrite, with minor molybdenite, magnetite, gold, and very minor galena and sphalerite. Pyrite/chalcopyrite ratios range from 5:1 to 20:1, and copper/molybdenum ratios range from 10:1 to 50:1. Phyllic, argillic, and propylitic alteration products are common, but potassic alteration products are scarce. Supergene enrichment generally is weak to moderate but locally strong. Horton (1978) suggests that these prospects represent middle to upper parts of porphyry copper systems.

Horton (1978) classified the Calliope prospect as a porphyry Cu-Mo prospect, associated with porphyritic granodiorite to granite of Late Triassic age (220 Ma), emplaced into rocks of Silurian to Permian age. Major sulfides are pyrite and chalcopyrite ± molybdenite ± magnetite ± gold. Alteration assemblages are phyllic and propylitic. Secondary enrichment is weak.

Moonmera Prospect

The Moonmera porphyry copper prospect is located in east-central Queensland, near Rockhampton (fig. E1). It is associated with granitoid intrusions of Late Permian to Early Triassic age (fig. E4). Ford and others (1976) estimated that the exposed half of the Moonmera copper-molybdenum zone has an average copper-equivalent grade of 0.28 percent copper. Their map of the copper-mineralized zone shows it as a semicircular halo that is about 400 m wide and has an inner radius of about 500 m.

The large size and estimated 0.28 percent copper grade of the Moonmera prospect imply intercepts much better than the 20 m of 0.15 percent copper required for rank 3, but lacking an estimation of its tonnage, Moonmera cannot be classified as a known deposit of rank 2. Nevertheless, the Moonmera prospect is the best of the prospects known in the Central sub-tract, and there is a high probability that it would fit the custom grade-tonnage model for porphyry copper deposits in continental magmatic arcs of eastern Australia.

According to Ford and others (1976), the Moonmera prospect is hosted in tonalite, which is intruded by a small stock of monzonite porphyry and breccia. The porphyry and breccia are central to the semicircular zone of copper-mineralized tonalite. Metallic minerals are chalcopyrite, molybdenite, pyrite, minor bornite, and accessory magnetite. Chalcopyrite occurs in fracture-controlled veins and fine disseminations. Secondary biotite and orthoclase occur within and around the monzonite porphyry stock, but the highest copper grades are in a zone of quartz-sericite-kaolinite-altered tonalite around the central stock. However, the rocks are not pervasively altered, except as controlled by fractures. K-Ar age determinations indicate that hydrothermal biotite from the potassic zone formed in Late Permian to Early Triassic time, from 252 to 251 Ma. Breccias formed along with mineralization and alteration.

Dummett (1978) described the igneous rocks and paragenesis of the Moonmera deposit in greater detail. He classified the igneous rocks as pre-ore quartz diorite (rather than tonalite), divided the ore-related stock into older and younger granodiorite porphyries, and divided the breccia into tuffisite, older breccia, and younger breccia. His maps show locations of drill holes, and the data from those holes indicate that zones of mineralized and altered rocks extend beneath cover to form a complete ring-shaped zone of copper-mineralized rock around the central stocks and breccias. A low-grade core is surrounded by an inner ring containing chalcopyrite and molybdenite in fractures. A medial ring contains chalcopyrite, pyrite, and minor molybdenite in fractures. An outer ring contains pyrite, minor chalcopyrite, and minor molybdenite in fractures. These rings resulted from stage 1 mineralization. Stage 2 mineralization produced chalcopyrite, pyrite, and arsenopyrite, which are disseminated in tuffisite that cuts the low-grade core zone of stage 1. Stage 3 mineralization produced chalcopyrite, pyrite, and arsenopyrite, which are disseminated and fill vugs in late breccia. This breccia surrounds a plug of younger granodiorite porphyry, which is within the central low-grade zone of stage 1. No mention of supergene enrichment was found in the articles by Ford and others (1976) or Dummett (1978).

Table E4*A*. Significant porphyry copper prospects and occurrences in the Central sub-tract (009pCu8004b), East Tasmanide tract, Queensland, Australia.

[Ma, million years; %, percent; m, meter; ppm, parts per million; prospect ranking criteria listed in table 2]

Name	Latitude	Longi-tude	Age (Ma)	Comments	Rank	Reference
				Middle Silurian to Devonian		
Bank	-20.138	146.758	395	porphyry-style chalcopyrite, pyrite; minor molybdenite	6	Horton (1978)
Barrabas Creek (in Barrabas Creek group)	-20.110	146.788	395	porphyry-style chalcopyrite, pyrite; minor molybdenite	6	Horton (1978)
Titov	-19.994	146.692	395	porphyry-style chalcopyrite, pyrite; minor molybdenite	6	Horton (1978)
				Carboniferous to Middle Permian		
Mount Darcy	-18.245	143.253	310	porphyry-style chalcopyrite, pyrite; minor molybdenite	6	Horton (1978)
Mount Turner	-18.255	143.405	310	porphyry-style arsenopyrite, bornite, chalcopyrite	6	Baker and Horton (1982), Horton (1978), Lacy (1980), Murray (1986), Solomon and Groves (2000), Singer and others (2008)
Mountain Maid	-17.118	144.122	309	porphyry-style chalcopyrite, pyrite; minor bornite, arsenopyrite, pyrrhotite	6	Horton (1978)
Beaks Mountain	-19.985	147.621	265	porphyry-style chalcopyrite, pyrite; minor molybdenite	6	Horton (1978)
				Late Permian to Triassic		
Moonmera	-23.576	150.393	245	0.28% average Cu-equivalent grade	3	Ayers (1974), Ford and others (1976), Dummet (1978), Horton (1978), Singer and others (2008), Jaireth and Miezitis (2004b), Geoscience Australia (2010)
Calgoa	-25.868	152.229	243	13.4 m at 0.72% Cu, 0.022% Mo, 9.1 ppm Ag	4	Horton (1978), D'Aguilar Gold, Ltd., (2010)
Gibraltar Rock	-26.140	152.404	243	porphyry-style chalcopyrite, pyrite; minor molybdenite	6	Horton (1978)
Mannersley (in Mannersley-Riverhead group)	-24.049	150.815	243	porphyry-style chalcopyrite, molybdenite, pyrite; minor magnetite, gold	6	Horton (1978)
Riverhead (in Mannersley-Riverhead group)	-24.041	150.740	243	porphyry-style chalcopyrite, molybdenite, pyrite; minor magnetite, gold	6	Horton (1978)
Calliope	-24.054	151.254	220	porphyry-style chalcopyrite, pyrite; minor molybdenite	6	Horton (1978)
				Early Cretaceous		
Mount Vista	-20.567	147.880	125	porphyry-style chalcopyrite, pyrite	6	Horton (1978)
Waitara	-21.808	148.815	124	porphyry-style chalcopyrite, pyrite; minor molybdenite	6	Horton (1978)

Calgoa Prospect

The Calgoa porphyry Cu-Mo prospect is about 180 km north-northwest of Brisbane (fig. E1). D'Aguilar Gold, Ltd., (2010) announced a core-drill intercept of 13.4 m with an average grade of 0.72 percent copper, 0.02 percent molybdenum, and 9 g/t silver. Although the average copper grade is quite high, the relatively short intercept may indicate a tabular zone of mineralized fractures rather than a large stockwork of veinlets. This indicates that the Calgoa prospect is a rank 4 prospect. Nevertheless, this prospect is hosted in a dioritic pluton, and it could be a manifestation of a much larger, lower-grade porphyry copper system nearby.

According to a geologic map and description by D'Aguilar Gold, Ltd., (2010), the Calgoa prospect is in an area of many historical copper and gold workings along widely spaced high-grade bornite-chalcopyrite veins. These veins are in and around the western margin of a pluton of Calgoa Diorite of Triassic age. They are within an area of altered diorite, which is known to contain minor chalcopyrite and molybdenite in veinlets and disseminations outside of the high-grade veins. Previously mined bornite-chalcopyrite veins are oriented at high angles to the north-trending contact of the diorite with Carboniferous metasedimentary and volcanic rocks. Dike swarms and mineralized breccias also are associated with the northern and eastern parts of the area of altered diorite, which is within an aeromagnetic low that is 5 km long and 4 km across. The exploration play is for a porphyry copper system in, beneath, or near the area of the high-grade bornite-chalcopyrite veins.

Early Cretaceous Prospects

The Mount Vista porphyry copper and Waitara porphyry Cu-Mo prospects are of Early Cretaceous age. They are in east-central Queensland, in the east-central part of the Central sub-tract (fig. E1).

Mount Vista

According to Horton (1978, p. 912–913), the Mount Vista porphyry copper prospect belongs to a group of porphyry copper sites that are related to intrusions of granodiorite porphyry to quartz diorite porphyry of Early Cretaceous age (about 125 Ma). Country rocks are andesites, argillitic metasedimentary rocks, and calc-alkaline intrusions of Carboniferous to Permian age. Dominant associated structures strike north-south and east-northeast. Fracturing is weak to moderate. Major metallic minerals are pyrite and chalcopyrite with galena, sphalerite, arsenopyrite, and very minor molybdenite. Pyrite/chalcopyrite ratios range from 5:1 to 20:1. Copper/molybdenum ratios are high. Phyllic and propylitic alteration products are common, but potassic alteration products are rare. Secondary enrichment is very weak. Horton (1978) suggests that the upper parts of porphyry copper systems are exposed.

Waitara

The Waitara porphyry Cu-Mo prospect is in the central part of the Central sub-tract (fig. E1). It is related to quartz diorite intrusions of Early Cretaceous age (Horton, 1978, p. 812–813). Country rocks are andesites, argillitic metasedimentary rocks, and calc-alkaline intrusions of Carboniferous to Permian age. Dominant associated structures strike north-south and east-northeast. Fracturing is moderate. Major metallic minerals are pyrite and chalcopyrite with minor molybdenite and magnetite. The pyrite/chalcopyrite ratio is about 5:1, and the copper/molybdenum ratio is about 15:1. Phyllic and propylitic alteration products are common, but potassic alteration products are rare. Supergene enrichment is weak. Horton (1978) suggests such prospects represent the middle to upper parts of porphyry copper systems.

Copper Occurrences and Possible Porphyry-Related Mineral Sites

The Central sub-tract contains at least 24 copper occurrences, as shown on figure E1and listed in appendix F. Possible porphyry-related mineral sites include porphyry Mo-Cu sites, skarn Cu-Au sites, skarn Au-Cu sites, high-sulfidation epithermal sites, medium-sulfidation epithermal sites, intrusive-related breccia pipes with epithermal Au-Ag, low-sulfidation epithermal sites, and many low-F porphyry Mo sites, as listed in table E4*B*, and shown on figure E5.

Whether or not any of these copper occurrences and possible porphyry-related mineral sites is related to a porphyry copper deposit, they are within the area of the East Tasmanide permissive tract for porphyry copper deposits, and their ages are within those of the permissive rocks included in the East Tasmanide permissive tract.

Discussion

According to Blevin and others (1996), copper, gold, and molybdenum tend to concentrate in residual I-type magmas with typically high oxidation states. Gold and copper tend to concentrate in relatively undifferentiated magmas of mafic to intermediate compositions, whereas molybdenum tends to concentrate in relatively differentiated I- and A-type magmas of more felsic compositions.

Some intrusions of dioritic to tonalitic composition are associated with porphyry copper sites in the Central sub-tract of the East Tasmanide permissive tract. For example, the Mount Cannindah porphyry copper deposit, with average grades of 0.65 percent copper and 0.163 g/t gold, is associated with an intrusive complex of diorite, tonalite, granodiorite, dacite porphyry, and relatively minor granite. Similarly, the Coalstoun porphyry copper deposit, with an average grade of 0.3 percent copper and no reported gold, is associated with an intrusive complex of porphyritic microdiorite and microtonalite. Nevertheless, most porphyry copper deposits and prospects in this sub-tract are associated with relatively felsic intrusive complexes, which are predominantly granodioritic to granitic, rather than dioritic to tonalitic. Such deposits commonly contain pyrite + chalcopyrite ± molybdenite, but they lack bornite and gold. Many low-fluorine porphyry molybdenum deposits and prospects in this sub-tract also are associated with granodioritic to granitic intrusions. Thus, many intrusions in this sub-tract appear to be too felsic for preferential concentration of copper and gold, relative to molybdenum.

According to Burnham (1979), porphyry copper deposits form as a result of explosive release of highly saline, copper-bearing magmatic-hydrothermal fluid from apical parts of porphyritic intrusions. Porphyry copper deposits therefore occur within, around, and above the tops of porphyritic intrusions at depths between about 1 and 5 km (as indicated by studies of fluid inclusions in porphyry copper deposits, according to Cox, 1986a; Berger and others, 2008; Singer and others, 2008). At such depths, confining pressures are appropriate for explosive formation of pervasive stockworks of well-mineralized veinlets—low enough to allow explosive release of volatiles from the top of the magma chamber but high enough to confine such volatiles to the zone of explosion-fractured host rocks without explosive escape of volatiles to the atmosphere.

With increasing depths of emplacement, erosion, and exposure, the proportion of preserved volcanic rocks to exposed plutonic rocks decreases, and sizes of exposed plutons increase (Staude and Barton, 2001). Textures of igneous intrusions also tend to coarsen inward and downward. Porphyritic textures with visible phenocrysts in glassy to microcrystalline matrices transition downward to visibly crystalline rocks. Evidence of hydrothermal brecciation and stockwork veining also tends to decrease downward and inward from the tops and sides of intrusions associated with porphyry copper deposits.

In the Central sub-tract of the East Tasmanide permissive tract, the ratio of the area of preserved volcanic rocks to the area of exposed plutonic rocks is fairly low (about 1v/2i). Most intrusions there are predominantly phaneritic (visibly crystalline), as indicated by map-unit names and accompanying lithologic descriptions in source-map attribute tables. However, porphyritic rocks with microcrystalline matrices do occur at many of the known porphyry copper deposits and prospects, in association with stockworks of moderately spaced and weakly to moderately mineralized veinlets.

Alteration products associated with most of the known deposits and prospects in the Central sub-tract indicate the upper to middle parts of porphyry copper systems have been explored. Phyllic and propylitic alteration assemblages, typical of the upper-central and outer parts of porphyry copper systems, are common. However, potassic alteration assemblages, typical of the lower parts of porphyry copper systems, are uncommon to rare. This lack of known potassic alteration assemblages may indicate that the lower parts of many known deposits and prospects in this sub-tract remain to be explored.

Mineralized breccia pipes are spatially and temporally associated with the Mount Cannindah, Limonite Hill, and Coalstoun porphyry copper deposits in this sub-tract. Epithermal deposits also are regionally interspersed with porphyry copper sites in this sub-tract (fig. E5). Examples include epithermal breccia pipes that are mined for precious metals (as at Kidston and Mount Leyshon), as well as other high- to low-sulfidation epithermal precious-metal deposits (table E4*B*). The presence of such epithermal deposits in this sub-tract may indicate that this sub-tract is not so deeply eroded that all of its porphyry copper deposits are either eroded away or exposed at the surface.

Exploration History

Most exploration for porphyry copper deposits in eastern Queensland was done in the 1960s and 1970s. The porphyry copper deposits and prospects that were found were of economically submarginal grade. Since then there has been little porphyry copper exploration in Queensland until recently. As a result of recently rising metal prices, work is in progress in and around known porphyry copper and Cu-Au deposits and prospects.

For example, Planet Metals, Ltd., (2009) recently drilled 42 holes at the Mount Cannindah deposit and has announced an additional drilling program intended to test the deep potential of the deposit. Axiom Mining (2010a) also announced a resource estimate for gold, but not for copper, at the Mountain Maid porphyry copper prospect.

Quality of Information

Principal sources of information used by the assessment team for delineation of the East Tasmanide tract are listed in table E5. Delineation of permissive tracts was accomplished on the basis of data in recently compiled digital geologic maps of high quality at 1:1,000,000 scale. High-quality descriptions of map units are included in attribute tables that accompany these digital source maps. The descriptions provide detailed information about the compositions, textures, and geologic ages of rock types represented by each map unit. The geology and ore deposits of eastern Australia are very well described in English-language journals. An excellent and up-to-date database (Geoscience Australia, 2010) provides estimated tonnages and grades of known deposits. Prospects are well described in published articles, as well as in company reports and conference proceedings, available on the internet.

Grade and Tonnage Model Selection

As shown in Appendix A, tonnages and grades of 14 known porphyry copper deposits in the East Tasmanide tract and 1 known deposit in the Yeoval tract are significantly lower than those of the population of deposits included in the global grade-tonnage model of Singer and others (2008). A custom grade-tonnage model, based on grades and tonnages of these 15 porphyry copper deposits, was developed (appendix A). This model was selected to represent grades and tonnages of undiscovered porphyry copper deposits in the Central sub-tract of the East Tasmanide tract.

Estimate of the Number of Undiscovered Deposits

Only the Central sub-tract was assessed quantitatively. The Central sub-tract contains all known porphyry copper deposits and significant prospects in the East Tasmanide permissive tract (fig. E1). Inasmuch as the Island-arc sub-tract contains no pre-accretionary porphyry copper deposits or significant prospects, the probability that it contains undiscovered pre-accretionary porphyry copper deposits is qualitatively judged to be very low. Similarly, a qualitative assessment of the South and North sub-tracts is that they are unlikely to contain undiscovered porphyry copper prospects. Therefore, these sub-tracts were not quantitatively assessed for undiscovered porphyry copper resources.

Before assessment panel members estimated numbers of undiscovered deposits they reviewed the geology, known deposits, locations, and qualities of significant porphyry prospects and occurrences, as well as the exploration status of the tract, and geophysical evidence for undiscovered deposits in relatively unexplored or underexplored parts of the tract. Then panel members were asked to list and weigh positive factors, which may indicate undiscovered deposits, versus negative factors, which may limit the number of undiscovered porphyry copper deposits in the permissive tract.

Rationale for the Estimate

Rationale for the estimate was that it should be guided by comparing prospects to known deposits, by counting and assigning probabilities to prospects and occurrences, by consideration of spatial constraints, and by weighing positive versus negative factors listed by the panel members.

Table E4*B*. Deposits and prospects of types that may be related to porphyry copper systems in the Central sub-tract (009pCu8004b), East Tasmanide tract, Queensland, Australia.

[Ma, million years; prospect ranking criteria listed in table 2]

Name	Latitude	Longitude	Age (Ma)	Comments	Rank	Reference
Town Creek	-20.434	146.787	300	porphyry molybdenum-copper	5	Horton (1978), Lacy (1980), Murray (1986) Singer and others (2008)
Anduramba	-27.141	152.108	250	porphyry molybdenum-copper	5	Horton (1978), Jaireth and Miezitis (2004b), D'Aguilar Gold, Ltd., (2007), Geoscience Australia (2010)
Eungella	-21.143	148.482	123	porphyry molybdenum-copper	5	Horton (1978), Jaireth and Miezitis (2004b)
Glassford Creek	-24.482	151.340	244	skarn Cu-Au	5	Champion and others (2009)
Many Peaks	-24.527	151.330	244	skarn Cu-Au	5	Ewers and others (2002), Champion and others (2009), Geoscience Australia (2010)
Mungana	-17.107	144.390	298	skarn Au-Cu	5	Geoscience Australia (2010), Geological Survey of Queensland (2010)
Red Dome	-17.119	144.405	314	skarn Au-Cu	5	Horton (1978), Ewers and others (2002), Perkins and Kennedy (1998), Champion and others (2009), Geoscience Australia (2010), Mungana Gold Mines (2010), Geological Survey of Queensland (2010)
Victoria	-17.080	144.428	282	skarn Au-Cu	5	Geological Survey of Queensland (2010)
Shannon-Zillmanton	-17.136	144.477	314	skarn Au-Cu	5	Ewers and others (2002), Geoscience Australia (2010)
Attunga Copper	-30.909	150.929	397	skarn Au-Cu	5	Geoscience Australia (2010), NSW Industry and Investment (2010)
Anastasia	-17.562	144.262	315	epithermal, high sulfidation Au-Ag-Cu vein and replacement	5	Geological Survey of Queensland (2010)
Mount Carlton	-20.279	147.540	315	epithermal, high-sulfidation Cu-Ag-Au vein and replacement	5	Geological Survey of Queensland (2010)
Zelma	-21.360	149.298	344	epithermal, high-sulfidation Au vein and replacement	5	Jacques and others (2002), Geoscience Australia (2010)
Cracow	-25.289	150.270	291	epithermal, medium-sulfidation epithermal Au-Ag	8	Geoscience Australia (2010), Geological Survey of Queensland (2010), Champion and others (2009)
Golden Plateau	-25.285	150.296	288	epithermal, medium-sulfidation epithermal Au	8	Jacques and others (2002), Geoscience Australia (2010), Champion and others (2009)
Mount Leyshon	-20.288	146.272	289	intrusive-related breccia pipe, epithermal Au-Ag-Cu	5	Orr and Orr (2004), Murgulov and others (2008), Scott (1992), Ewers and others (2002), Geoscience Australia (2010)
Kidston	-18.869	144.151	330	intrusive-related breccia pipe, epithermal Au-Ag-Cu	8	Baker and Andrew (1991), Perkins and Kennedy (1998), Ewers and others (2002), Champion and others (2009), Geoscience Australia (2010)
Mount Canton north	-20.278	146.898	302	intrusive-related breccia, epithermal Au-Ag-Cu	8	Geological Survey of Queensland (2010)
Mount Rawdon	-25.271	151.764	230	intrusive-related breccia pipe, epithermal Au-Ag-Cu	8	Geological Survey of Queensland (2010)
Mount Wright	-20.040	146.832	305	intrusive-related breccia pipe, epithermal Au-Ag-Cu	8	Ewers and others (2002), Perkins and Kennedy (1998), Geological Survey of Queensland (2010)
Pajingo	-20.548	146.463	346	epithermal, low-sulfidation epithermal Au veins	8	Geoscience Australia (2010)
Pinevale copper mine	-21.299	148.854	123	intrusion-related Cu-Au veins	8	Axiom Mining, Ltd. (2010b)
Ravenswood	-20.097	146.880	303	intrusion-related Au veins, local stockworks of veinlets	8	Perkins and Kennedy (1998), Champion and others (2009), Geoscience Australia (2010)

Table E4*B*. Deposits and prospects of types that may be related to porphyry copper systems in the Central sub-tract (009pCu8004b), East Tasmanide tract, Queensland, Australia.—Continued

Name	Latitude	Longitude	Age (Ma)	Comments	Rank	Reference
Wirralie	-21.117	147.270	342	epithermal, low-sulfidation epithermal Au veins	8	Geoscience Australia (2010), Geological Survey of Queensland (2010)
Yandan	-21.298	146.971	344	epithermal, low-sulfidation epithermal Au veins	8	Geoscience Australia (2010)
Enoggera	-27.502	152.946	230	low-fluorine porphyry Mo	8	Horton (1978)
Keans	-20.129	146.829	395	low-fluorine porphyry Mo	8	Horton (1978), Jaireth and Miezitis (2004b)
Bald Mtn	-28.902	151.876	250	low-fluorine porphyry Mo	8	Horton (1978)
Biok	-18.210	145.737	300	low-fluorine porphyry Mo	8	Horton (1978)
Carbonate Creek	-17.236	145.056	300	low-fluorine porphyry Mo	8	Horton (1978)
Duingal Creek	-25.118	152.076	250	low-fluorine porphyry Mo	8	Horton (1978)
Funnel Creek	-21.643	149.022	123	low-fluorine porphyry Mo	8	Horton (1978)
Kellys Mountain	-19.665	147.309	300	low-fluorine porphyry Mo	8	Horton (1978)
Knight Island	-21.447	149.713	123	low-fluorine porphyry Mo	8	Horton (1978)
Koombooloomba	-17.846	145.571	300	low-fluorine porphyry Mo	8	Horton (1978)
Native Dog	-24.751	151.916	250	low-fluorine porphyry Mo	8	Horton (1978)
Nitchaga	-17.950	145.556	300	low-fluorine porphyry Mo	8	Horton (1978)
Rocky Creek	-20.468	147.943	300	low-fluorine porphyry Mo	8	Horton (1978)
Roma Peak	-20.303	148.188	123	low-fluorine porphyry Mo	8	Horton (1978), Jaireth and Miezitis (2004b)
Sandy Creek	-20.094	147.711	240	low-fluorine porphyry Mo	8	Ford and others (1976), Horton (1978)
Taronga	-26.709	151.797	250	low-fluorine porphyry Mo	8	Ewers and others (2002)
Wyarra Hills	-21.096	147.517	300	low-fluorine porphyry Mo	8	Horton (1978)
Yamanie	-18.257	145.770	300	low-fluorine porphyry Mo	8	Horton (1978)
Yuccabine	-18.226	145.734	300	low-fluorine porphyry Mo	8	Horton (1978)

Positive Factors

Positive factors that may indicate undiscovered porphyry copper deposits in the Central sub-tract (009pCu8004b) of the East Tasmanide tract include:

1. Moonmera is a well-studied prospect with sufficient grade and likely tonnage to fit the custom grade-tonnage model for porphyry copper deposits in continental magmatic arcs of eastern Australia. Therefore, Moonmera counts as at least one undiscovered deposit at 90 percent probability.
2. At least 12 prospects in this tract have characteristics of porphyry copper deposits, but have not, to our knowledge, been tested by drilling.
3. Until recently, exploration for deposits of the grade and tonnage of the known deposits in this tract has been relatively dormant since the late 1970s.
4. Cu-Au ore of economic grade is present at the Mount Cannindah deposit, and this indicates the possibility of such grades in other prospects that are not yet well tested.
5. Areas of poorly exposed bedrock within the tract may not have been thoroughly explored.

Negative Factors

Negative factors that may limit the probability of the existence of undiscovered porphyry copper deposits in the Central sub-tract (009pCu8004b) of the EastTasmanide tract include the following:

1. The area of mapped intrusive rocks of continental magmatic arcs is about twice that of volcanic rocks of the same magmatic arcs. This indicates that this sub-tract probably is too deeply eroded for preservation of high-grade porphyry copper systems, which typically form above or around high cupolas above larger intrusions at greater depths.
2. Most of the known deposits and prospects consist of relatively sparse stockworks of fairly widely spaced and weakly mineralized fractures.
3. Most of the known deposits and prospects lack zones of abundant potassic alteration products, which commonly accompany stockworks of closely spaced, well-mineralized veinlets in higher grade deposits.
4. The area of this permissive sub-tract was well explored for porphyry copper in the 1960s and 1970s, so the best deposits probably have been found and tested by drilling.

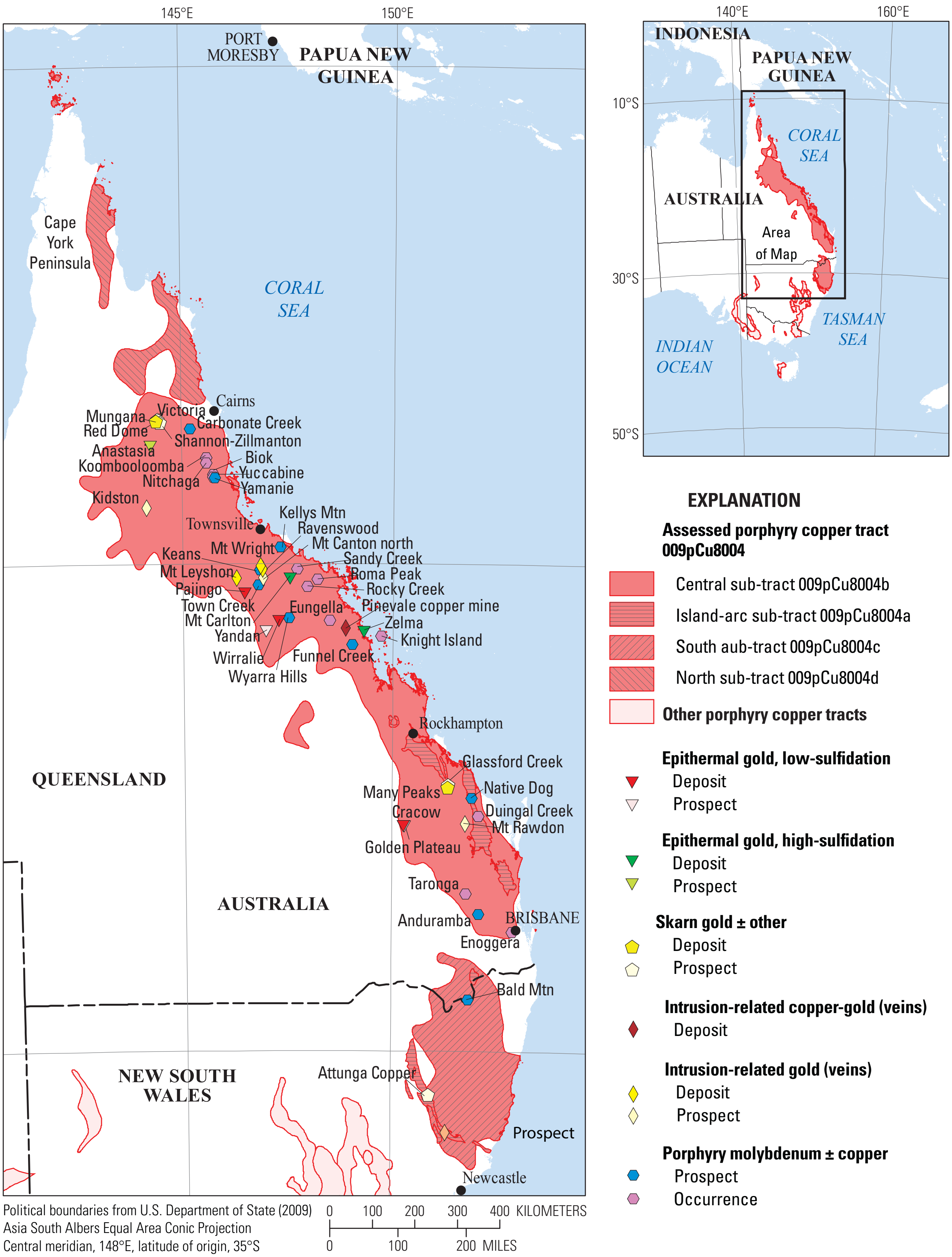

Figure E5. Map showing locations of deposits and prospects of deposit types that may (or may not) be related to porphyry copper systems, East Tasmanide tract (009pCu8004), New South Wales and Queensland, Australia.

Table E5. Principal sources of information used for the East Tasmanide tract (009pCu8004), New South Wales and Queensland, Australia.
[NA, not applicable]

Theme	Name or Title	Scale	Citation
Geology	Surface geology of Australia, New South Wales—2nd edition	1:1,000,000	Raymond and others (2007)
	Surface geology of Australia, Queensland—2nd edition	1:1,000,000	Whitaker and others (2007)
	Geodynamic synthesis of the north Queensland region and implications for metallogeny	NA	Kositcin and others (2009)
	Evolution of the Australian lithosphere	NA	Betts and others (2002)
	The Tasmanides of eastern Australia	NA	Glen (2005)
	Intrusive metallogenic provinces in eastern Australia based on granite source and composition	NA	Blevin and others (1996)
	Geodynamic synthesis of the Phanerozoic of eastern Australia and implications for metallogeny	NA	Champion and others (2009)
Geophysics	Total magnetic anomaly (TMI) grids of Australia, fourth edition	NA	Geoscience Australia (2004)
	Australian National gravity database 0.5 minute offshore-onshore gravity grid	NA	Geoscience Australia (2009)
Mineral occurrences	Porphyry copper deposits of the world: database and grade and tonnage models	NA	Singer and others (2008)
	OZMIN mineral deposits database	NA	Ewers and others (2002)
	OZPOT geoprovince-scale assessment of mineral potential	1:2,500,000	Jaireth and Miezitis (2004b)
	Intierra Resource Intelligence	NA	Intierra (2009)
	Australian mines atlas	NA	Geoscience Australia (2010)
	Mineral occurrence and geological observations	NA	Geological Survey of Queensland (2010)
	Porphyry-type copper-molybdenum mineralization belts in eastern Queensland	NA	Horton (1978)
Exploration	Australian Mineral Exploration	NA	Geoscience Australia (2005–2009)

Consideration of the positive and negative factors listed above guided estimates of numbers of undiscovered deposits. These estimates also were guided by comparisons with the known deposits, counting and assigning probabilities to prospects and occurrences, process constraints implied by a high ratio of intrusive to preserved volcanic rocks and a lack of pervasive stockworks of closely spaced and well-mineralized veinlets in most of the known deposits and prospects. However, strict application of process constraints was tempered by the extent of cover, and the possibility that small intrusions and associated zones of hydrothermally altered and mineralized rocks may not be portrayed on geologic source maps at 1:1,000,000 scale.

Each of four estimators (Bookstrom, Glen, Hammarstrom, and Zientek) gave an independent estimate of the number of undiscovered deposits expected at three levels of subjective probability (90, 50, and 10 percent levels of probability, for example, or if 0 deposits at 90 percent, then at 50, 10, and 5 percent levels of probability). After an anonymous first round of estimation, the high and low estimators explained their reasoning. This led to discussion, negotiation, and settlement on a consensus set of estimates.

Consensus Estimates

Summary statistics, based on the consensus estimates, indicate a mean and standard deviation of 4.8±3.3 undiscovered deposits (table E6). The coefficient of variation (C_v) of 68 percent indicates a moderate degree of uncertainty in the number of undiscovered deposits expected in the Central sub-tract of the East Tasmanide tract. Adding the mean estimate of 4.8 undiscovered deposits to the 14 known deposits indicates a total equivalent to 18.8 porphyry copper deposits expected to occur within 1 km of the surface in this permissive sub-tract. Inasmuch as the area of the Central sub-tract is 290,646 km^2, this indicates an estimated spatial density of 0.000065 porphyry copper deposits/km^2 (or about 6.5 deposits per 100,000 km^2). This value lies within the 90th to 10th percentile range predicted by deposit density models for porphyry copper deposits (Singer and Menzie, 2010; Singer and others, 2005).

Probabilistic Assessment Simulation Results

Undiscovered resources for the tract were estimated (table E7) by combining consensus estimates for numbers of undiscovered porphyry copper deposits with a custom grade-tonnage model for porphyry copper deposits of Australia (appendix A) using the EMINERS program (Root and others, 1992; Duval, 2012; Bawiec and Spanski, 2012). Cumulative probability graphs show expected amounts of the commodities through a range of levels of subjective probabilities (fig. E6).

Table E6. Undiscovered deposit estimates, tract area, and deposit density for the Central sub-tract (009pCu8004b), East Tasmanide tract, Queensland, Australia.

[N_{XX}, estimated number of deposits associated with the xxth percentile; N_{und}, expected number of undiscovered deposits; *s*, standard deviation; C_v%, coefficient of variance; N_{known}, number of known deposits in the tract that are included in the grade and tonnage model; N_{total}, total of expected number of deposits plus known deposits; Tract area, area of permissive tract in square kilometers; Deposit density, total number of deposits per 100,000 km². N_{und}, *s*, and C_v% are calculated using a regression equation (Singer and Menzie, 2005)]

Consensus undiscovered deposit estimates					Summary statistics					Tract area (km²)	Deposit desity (N_{total}/100,000 km²)
N_{90}	N_{50}	N_{10}	N_{05}	N_{01}	N_{und}	*s*	C_v%	N_{known}	N_{total}		
1	4	10	10	10	4.8	3.3	68	14	18.8	290,646	6.5

Table E7. Results of Monte Carlo simulations of undiscovered resources for the Central sub-tract (009pCu8004b), East Tasmanide tract, Queensland, Australia.

[Cu, copper in metric tons (t); Rock, in million metric tons (Mt)]

Material	Probability of at least the indicated amount						Probability of	
	0.95	0.9	0.5	0.1	0.05	Mean	Mean or greater	None
Cu (t)	0	0	190,000	690,000	860,000	280,000	0.39	0.09
Rock (Mt)	0	3	94	250	290	110	0.43	0.06

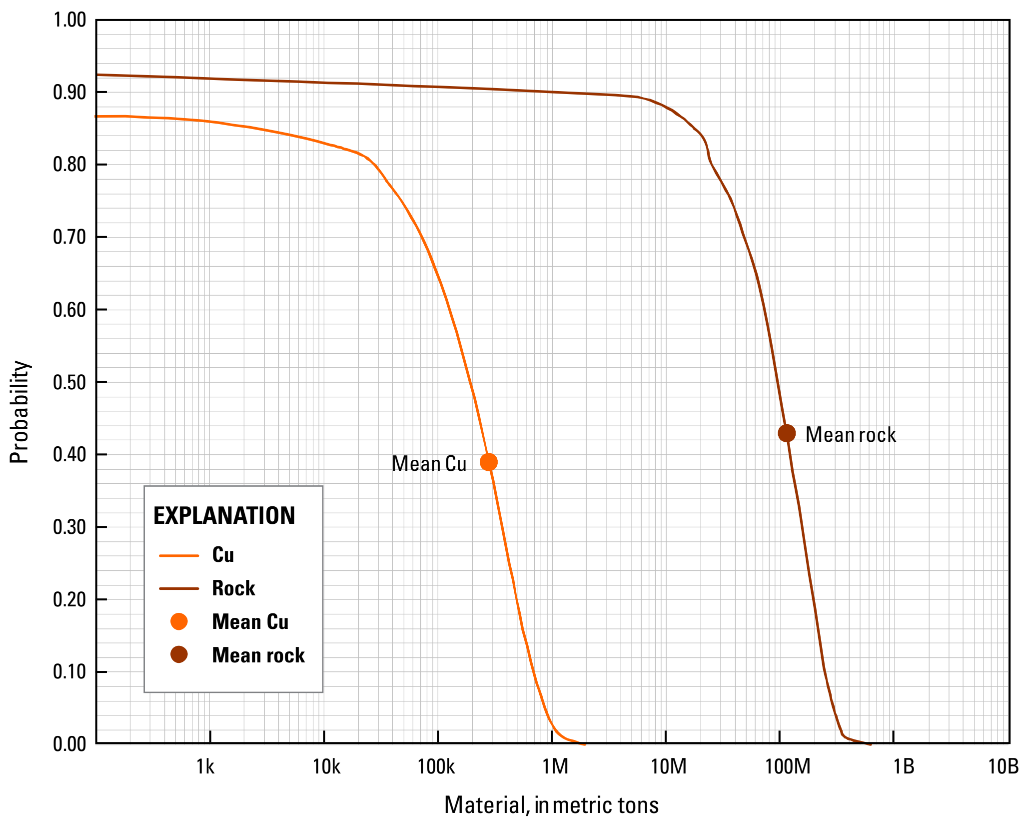

Figure E6. Cumulative frequency plot showing results of Monte Carlo computer simulation of undiscovered resources in the Central sub-tract (009pCu8004b), East Tasmanide tract, Queensland, Australia. k=thousands, M=millions, B=billions.

References Cited

Allen, C.M., Wooden, J.L., and Chappell, B.W., 1997, Late Paleozoic crustal history of central coastal Queensland interpreted from geochemistry of Mesozoic plutons—The effects of continental rifting: Lithos, v. 42, p. 67–88.

Arnold, G.O., and Sillitoe, R.H., 1989, Mount Morgan gold-copper deposit, Queens land, Australia—Evidence for an intrusion-related replacement origin: Economic Geology, v. 84, p. 1805–1816.

Ashley, P.M., Billington, W.G., Graham, R.L., and Neale, R.C., 1978, Geology of the Coalstoun porphyry copper prospect, southeast Queensland, Australia: Economic Geology, v. 73, p. 945–965.

Aussie Q Resources, Ltd., 2007, Prospectus—Information on Whitewash and Kiwi Carpet prospects: Aussie Q Resources, Ltd., Web site, accessed June 9, 2010, at http://www.aussieqresources.com.au/, p. 13–15, 37–44, and 47–56.

Aussie Q Resources, Ltd., 2010, Aussie Q Resources Ltd., ASX: AQR—An emerging molybdenum & copper producer: Aussie Q Resources, Ltd., Web site, accessed May 9, 2011, at http://www.aussieqresources.com.au/.

Axiom Mining, Ltd., 2010a, Initial Mountain Maid JORC resource estimate: Axiom Mining, Ltd., Web site, accessed May 6, 2011, at http://www.axiom-mining.com/.

Axiom Mining, Ltd., 2010b, Pinevale copper-gold project: Axiom Mining, Ltd., Web site, accessed May 6, 2011, at http://www.axiom-mining.com/pinevale.html.

Ayers, D.E., 1974, Relationship of mineralization and hydrothermal alteration at the Moonmera porphyry copper prospect, Queensland: Australasian Institute of Mining and Metallurgy, Southern and Central Queensland Conference, p. 465–477.

Baker, E.M., and Andrew, A.S., 1991, Geologic, fluid inclusion, and stable isotope studies of the gold-bearing breccia pipe at Kidston, Queensland, Australia: Economic Geology, v. 86, p. 810–830.

Baker, E.M., and Horton, D.J., 1982, Geological environment of copper-molybdenum mineralization at Mount Turner, North Queensland: Geological Survey of Queensland Publication 379, p. 30–77.

Bawiec, W.J., and Spanski, G.T., 2012, Quick-start guide for version 3.0 of EMINERS—Economic Mineral Resource Simulator: U.S. Geological Survey Open-File Report 2009–1057, 26 p., available at http://pubs.usgs.gov/of/2009/1057/. (This report supplements USGS OFR 2004–1344.)

Bedford, I.V., 1975, Mount Cannindah copper deposit, *in* Knight, C.L., ed., Economic geology of Australia and New Guinea: Australian Institute of Mining and Metallurgy, Monograph Series, v. 1, no. 5, p. 787–789.

Berger, B.R., Ayuso, R.A., Wynn, J.C., and Seal, R.R., 2008, Preliminary model of porphyry copper deposits: U.S. Geological Survey Open-File Report 2008–1321, 55 p., available at http://pubs.usgs.gov/of/2008/1321/.

Betts, P.G., Giles, D., Lister, G.S., and Frick, L.R., 2002, Evolution of the Australian lithosphere: Australian Journal of Earth Sciences, v. 49, no. 4, p. 661–695.

Blevin, P.L., Chappell, B.W., and Allen, C.M., 1996, Intrusive metallogenic provinces in eastern Australia based on granite source and composition: Transactions of the Royal Society of Edinburgh—Earth Sciences, v. 87, p. 281–290.

Brooks, J.H., 1976, Departmental diamond drilling programme, Whitewash copper-molybdenum prospect, Monto: Queensland Government Mining Journal, v. 77, no. 891, p. 112–120.

Burnham, C.W., 1979, Magmas and hydrothermal fluids, *in* Barnes, H.L., ed., Geochemistry of hydrothermal ore deposits, 2nd ed.: New York, Wiley, p. 71–136.

Champion, D.C., Kositcin, N., Huston, D.L., Mathews, E., and Brown, C., 2009, Geodynamic synthesis of the Phanerozoic of eastern Australia and implications for metallogeny: Geoscience Australia, Record 2009/18, GeoCat#68866, 222 p., digital, accessed October 4, 2010, at http://www.ga.gov.au/products/.

Cooke, D.R., Heithersay, P.S., Wolfe, Rohan, and Calderon, A.L., 1998, Australian and western Pacific porphyry Cu-Au deposits—Exploration model: Australian Geological Survey Organisation Journal of Australian Geology and Geophysics, v. 17, no. 4, p. 97–104.

Cox, D.P., 1986a, Descriptive model of porphyry Cu (model 17), *in* Cox, D.P., and Singer, D.A., eds., Mineral deposit models: U.S. Geological Survey Bulletin 1693, p. 76.

Cox, D.P., 1986b, Descriptive model of porphyry Cu-Mo (model 21a), *in* Cox, D.P., and Singer, D.A., eds., Mineral deposit models: U.S. Geological Survey Bulletin 1693, p. 115.

Cox, D.P., 1986c, Descriptive model of porphyry Cu-Au (model 20c), *in* Cox, D.P., and Singer, D.A., eds., Mineral deposit models: U.S. Geological Survey Bulletin 1693, p. 110.

D'Aguilar Gold, Ltd., 2007, Anduramba molybdenum: D'Aguilar Gold, Ltd., Web site, accessed June 10, 2010, at http://www.daguilar.com.au/anduramba_molybdenum.html/.

D’Aguilar Gold, Ltd., 2010, Encouraging copper molybdenum results in historical drill holes into porphyry at Calgoa: ASX Announcement, D’Aguilar Gold, Ltd., Web site, accessed May 9, 2011, at http://www.daguilar.com.au/.

Dummett, H.T., 1978, Geology of the Moonmera porphyry deposit, Queensland, Australia: Economic Geology, v. 73, p. 922–944.

Duval, J.S., 2012, Version 3.0 of EMINERS—Economic Mineral Resource Simulator: U.S. Geological Survey Open-File Report 2004–1344, available at http://pubs.usgs.gov/of/2004/1344/.

Ewers, G.R., Evans, N., and Hazell, M., (Kilgour, B., compiler), 2002, OZMIN Mineral Deposit Database: Canberra, Geoscience Australia, digital dataset on CD ROM. (Also available at http://www.ga.gov.au/meta/ANZCW0703003393.html.)

Fedikow, M.A.F., and Govett, G.J.S., 1985, Geochemical alteration halos around the Mount Morgan gold-copper deposit, Queensland, Australia: Amsterdam, Elsevier Science Publishers B.V, Journal of Geochemical Exploration, v. 24, p. 247–272.

Ford, J.H., Wood, D.G., and Green, D.C., 1976, Geochronology of porphyry copper-type mineralization near Rockhampton, Eastern Queensland, Australia: Economic Geology, v. 71, p. 526–539.

Geological Survey of Queensland, 2010, Mineral occurrence and geology observations: Queensland Government, Department of Employment, Economic Development and Innovation (digital dataset on DVD).

Geoscience Australia, 2004, Fourth edition total magnetic anomaly (TMI) grids of Australia: Canberra, Geoscience Australia, accessed May 19, 2010, at http://www.geoscience.gov.au/.

Geoscience Australia, 2005–2009, Australian mineral exploration, a review of exploration for the years 2005 to 2009: Canberra, Geoscience Australia, accessed May 25, 2010, at http://www.geoscience.gov.au/.

Geoscience Australia, 2009, Australian national gravity database 0.5 minute offshore-onshore gravity grid: Canberra, Geoscience Australia, accessed May 19, 2010, at http://www.geoscience.gov.au/.

Geoscience Australia, 2010, Australian atlas of mines and mineral deposits: Canberra, Geoscience Australia, accessed October 20, 2010, to December 27, 2010, at http://www.australianminesatlas.gov.au/.

Glen, R.A., 2005, The Tasmanides of eastern Australia: *in* Vaughan, A.P.M., Leat, P.T., and Pankhurst, R.J., eds., Terrane processes at the margins of Gondwana: Geological Society, London, Special Publications, 246, p. 23–96.

Horton, D.J., 1978, Porphyry-type copper-molybdenum mineralization belts in eastern Queensland, Australia: Economic Geology, v. 73, p. 904–921.

Intierra, 2009, Intierra home page: accessed December 10, 2010, at http://www.intierra.com/Homepage.aspx.

Jacques, A.L., Jaireth, S., and Walshe, J.L., 2002, Mineral systems of Australia—An overview of resources, settings and processes: Australian Journal of Earth Sciences, v. 49, no. 4, p. 623–660.

Jaireth, S., and Miezitis, Y., 2004a, Porphyry copper-gold, *in* Jaireth, Subhash, and Miezitis, Yanis, compilers, OZPOT Geoprovince-scale assessment of mineral potential [1:2,500,000 scale GIS]: Canberra, Geoscience Australia, accessed 2010, at http://www.australianminesatlas.gov.au/build/common/minpot.jsp.

Jaireth, S., and Miezitis, Y., 2004b, OZPOT Geoprovince-scale assessment of mineral potential [1:2,500,000 scale GIS]: Canberra, Geoscience Australia, accessed June 21, 2010, to December 27, 2010, at http://www.australianminesatlas.gov.au/build/common/minpot.jsp/.

John, D.A., Ayuso, R.A., Barton, M.D., Blakely, R.J., Bodnar, R.J., Dilles, J.H., Gray, Floyd, Graybeal, F.T., Mars, J.C., McPhee, D.K., Seal, R.R., Taylor, R.D., and Vikre, P.G., 2010, Porphyry copper deposit model, chapter B *of* Mineral deposit models for resource assessment: U.S. Geological Survey Scientific Investigations Report 2010–5070–B, 169 p., accessed January 15, 2011, at http://pubs.usgs.gov/sir/2010/5070/b/.

Kositcin, N., Champion, D.C., and Huston, D.L., 2009, Geodynamic synthesis of the North Queensland region and implications for metallogeny: Canberra, Geoscience Australia, Record 2009/030, GeoCat #69159, 201 p., digital, accessed July 15, 2010, at http://www.ga.gov.au/products/.

Lacy, W.C., 1980, Mineralization along the extension of the New England and Lachlan-Thompson fold belts in North Queensland, *in* Henderson, R.A., and Stephenson, P.J., eds., The Geology and Geophysics of Northeastern Australia: Geological Society of Australia, Queensland Division, Brisbane, p. 269–277.

Lawrence, L.J., 1967, Sulphide neomagmas and highly metamorphosed sulphide deposits: Mineralium Deposita, v. 2, p. 5–10.

Lawrence, L.J., 1972, The thermal metamorphism of a pyritic sulfide ore: Economic Geology, v. 67, p. 487–496.

Mungana Gold Mines, 2010, Red Dome: Mungana Gold Mines Web site, accessed October 12, 2010, at http://www.munganagoldmines.com.au/.

Murgulov, V., O'Reilly, S.Y., Griffin, W.L., and Blevin, P.L., 2008, Magma sources and gold mineralization in the Mount Leyshon and Tuckers igneous complexes, Queensland, Australia—U-Pb and Hf isotope evidence: Lithos, v. 101, p. 281–307.

Murray, C.G., 1986, Metallogeny and tectonic development of the Tasman fold belt system in Queensland: Ore Geology Reviews, v. 1, p. 315–400.

Murray, C.G., 1990, Tasman fold belt in Queensland, *in* Hughes, F.E., ed., Geology of the Mineral Deposits of Australia and New Guinea: Australasian Institute of Mining and Metallurgy, Monograph Series, v. 2, no. 14, p. 1431–1450.

NSW Industry and Investment, 2010, Advanced mineral projects and mineral exploration highlights: New South Wales Department of Primary Industries, geologic map, showing operational mines and active exploration sites, with estimated resources and best intercepts, accessed October 11, 2010, at http://www.industry.nsw.gov.au/.

Orr, T.H., and Orr, L.A., 2004, Mt. Leyshon gold deposit, Charters Towers, Queensland, *in* Butt, C.R.M, Cornelius, M., Scott, K.M., and Robertson, I.D.M., Regolith expression of Australian ore systems—A compilation of geochemical case histories and conceptual models: Cooperative Research Centre for Landscape Environments and Mineral Exploration (CRC LEME), accessed April 17, 2011, at http://crcleme.org.au/RegExpOre/MtLeyshon.pdf.

Panteleyev, A., 1995a, Porphyry Cu±Mo±Au (model L04), *in* Lefebure, D.V., and Ray, G.E., eds., Selected British Columbia mineral deposit profiles, vol. 1—Metallics and coal: British Columbia Ministry of Energy of Employment and Investment, Energy and Minerals Division, Open File 1995–20, p. 87–92, accessed April 5, 2012, at http://www.empr.gov.bc.ca/Mining/Geoscience/MineralDepositProfiles/.

Panteleyev, A., 1995b, Porphyry Cu-Au—Alkalic (model L03), *in* Lefebure, D.V., and Ray, G.E., eds., Selected British Columbia mineral deposit profiles, vol. 1—Metallics and coal: British Columbia Ministry of Employment and Investment, Energy and Minerals Division, Open File 1995–20, p. 83–86, accessed April 5, 2012, at http://www.empr.gov.bc.ca/Mining/Geoscience/MineralDepositProfiles/.

Panteleyev, A., 2005a, Porphyry Cu±Mo±Au L04, *in* Fonseca, A., and Bradshaw, G., compilers, Yukon mineral deposits profiles: Yukon Geological Survey Open File 2005–5, 175 p., accessed July 28, 2009, at http://www.geology.gov.yk.ca/mineral_deposit_profiles.html; http://ygsftp.gov.yk.ca/publications/openfile/2005/of2005_5.pdf; http://www.geology.gov.yk.ca/pdf/l04_porphyry_cu_mo_au.pdf.

Panteleyev, A., 2005b, Porphyry Cu-Au—Alkalic L03, *in* Fonseca, A., and Bradshaw, G., compilers, Yukon Mineral Deposits Profiles: Yukon Geological Survey Open File 2005–5, 175 p., accessed July 28, 2009, at http://www.geology.gov.yk.ca/mineral_deposit_profiles.html; http://ygsftp.gov.yk.ca/publications/openfile/2005/of2005_5.pdf; http://www.geology.gov.yk.ca/pdf/l03_alkalic_porphyry_cu_au.pdf.

Perkins, C., and Kennedy, A.K., 1998, Permo-Carboniferous gold epoch of northeast Queensland: Australian Journal of Earth Sciences, v. 45, no. 2, p. 185–200.

Planet Metals, Ltd., 2009, Mount Cannindah project: accessed August 18, 2010, at http://planetmetals.com.au/.

Raymond, O.L., Liu, S.F., Kilgour, P., Retter, A.J., Stewart, A.J., and Stewart, G., 2007, Surface geology of Australia, 1:1,000,000 scale, New South Wales, 2nd edition [Digital Dataset]: Canberra, Geoscience Australia, accessed May 9, 2010, at http://www.ga.gov.au/.

Root, D.H., Menzie, W.D., and Scott, W.A., 1992, Computer Monte Carlo simulation in quantitative resource estimation: Natural Resources Research, v. 1, no. 2, p. 125–138.

Scott, K.M., 1992, Origin of alunite- and jarosite-group minerals in the Mount Leyshon epithermal gold deposit, northeast Queensland, Australia—Reply: American Mineralogist, v. 77, p. 860–862.

Singer, D.A., Berger, V.I., Menzie, W.D., and Berger, B.R., 2005, Porphyry copper density: Economic Geology, v. 100, no. 3, p. 491–514.

Singer, D.A., Berger, V.I., and Moring, B.C., 2008, Porphyry copper deposits of the world—Database and grade and tonnage models, 2008: U.S. Geological Survey Open-File Report 2008–1155, 45 p., available at http://pubs.usgs.gov/of/2008/1155/.

Singer, D.A., and Menzie, W.D., 2005, Statistical guides to estimating the number of undiscovered mineral deposits: an example with porphyry copper deposits, *in* Cheng, Qiuming, and Bonham-Carter, Graeme, eds., Proceedings of IAMG—The annual conference of the International Association for Mathematical Geology: Toronto, Canada, Geomatics Research Laboratory, York University, p. 1028–1033.

Singer, D.A., and Menzie, W.D., 2010, Quantitative mineral resource assessments—An integrated approach: New York, Oxford University Press, 219 p.

Sivell, W.J., and McCulloch, M.T., 2001, Geochemical and Nd-isotopic systematics of the Permo-Triassic Gympie Group, southeast Queensland: Australian Journal of Earth Sciences, v. 48, p. 377–393.

Solomon, M., and Groves, D.I., 2000, Metallogeny and tectonic development of the Tasman fold belt system in Queensland: Ore Geology Reviews, v. 1, p. 315–400.

Staude, J.G., and Barton, M.D., 2001, Jurassic to Holocene tectonics, magmatism, and metallogeny of northwestern Mexico: GSA Bulletin, v. 113, no. 10, p. 1357–1374.

Stolz, A.J., 1995, Geochemistry of the Mount Windsor Volcanics—Implications for the tectonic setting of Cambro-

Ordovician volcanic-hosted massive sulfide mineralization in northeastern Australia: Economic Geology, v. 90, p. 1060–1097.

U.S. Department of State, 2009, Small-scale digital international land boundaries (SSIB)—Lines, edition 10, and polygons, beta edition 1, *in* Boundaries and sovereignty encyclopedia (B.A.S.E.): U.S. Department of State, Office of the Geographer and Global Issues.

Ulrich, T., Golding, S.D., Kamber, B.S., Khin Zaw, and Taube, A., 2003, Different mineralization styles in a volcanic-hosted ore deposit—The fluid and isotopic signatures of the Mt Morgan Au-Cu deposit, Australia: Ore Geology Reviews, v. 22, p. 61–90.

Whitaker, A.J., Champion, D.C., Sweet, I.P., Kigour, P., and Connolly, D.P., 2007, Surface geology of Australia 1:1,000,000 scale, Queensland [Digital Dataset]: Canberra, Geoscience Australia, accessed May 9, 2010, at http://www.ga.gov.au/.

Appendix F. Attributes of Porphyry Copper Deposits, Prospects, and Occurrences and Other Relevant Deposit Types in Australia

By Arthur A. Bookstrom[1]

Appendix F is a separately available spreadsheet (Australia_SIR_ApdxF_table.xlsx, online at http://pubs.usgs.gov/sir/2010/5090/l/) reporting data for 232 mineral deposits or groups of mineral deposits in Australia. Data presented include:

1. Name, location, age, tonnage and average grade for copper, molybdenum, gold and silver, mineralogy, host rocks and related igneous rocks, along with other descriptive comments and reference citations for sources of information about each of 142 porphyry copper deposits, prospects, and copper-bearing mineral occurrences in permissive tracts for porphyry copper in eastern Australia;
2. Parallel information for deposits that are not porphyry copper deposits but are either:
    - Porphyry-related deposits (such as copper-bearing skarns, epithermal precious-metal deposits, or porphyry molybdenum deposits, which may be closely to distally associated with porphyry copper systems), or
    - Deposits of other types that contain significant copper resources (such as iron-oxide copper-gold deposits, volcanic-hosted massive sulfide deposits, sediment-hosted copper deposits, or metamorphic copper deposits); and
3. Summary data for grouped sites that were combined according to the 2-km rule (Singer and others, 2005).

Full citations for references cited in the table are listed below.

References Cited

Abrams, M., and Gabell, A., 1989, Geologic mapping and mineral exploration in the Coppin Gap greenstone belt, Australia, summary: Proceedings of the Thematic Conference on Geologic Remote Sensing, v. 7, Calgary, Alberta, Canada, p. 361.

Ackerman, B.R., 2003, Frogmore copper deposit, NSW, *in* Butt, C.R.M, Cornelius, M., Scott, K.M., and Robertson, I.D.M., Regolith Expression of Australian Ore Systems—A compilation of geochemical case histories and conceptual models: Cooperative Research Centre for Landscape Environments and Mineral Exploration (CRC LEME), 3 p., accessed April 2, 2013, at http://crcleme.org.au/RegExpOre/Frogmore.pdf.

Alkane Resources, Ltd., 2003, Reconnaissance drilling results from Moorilda: Alkane Resources, Ltd., ASX Announcement—23 June 2003, accessed November 2, 2010, at http://www.alkane.com.au/reports/asx/pdf/20030623.pdf.

Alkane Resources, Ltd., 2004, Prospect acquisitions—New South Wales: Alkane Resources, Ltd., ASX Announcement, 8 January 2004, accessed May 25, 2010, at http://www.alkane.com.au/reports/asx/pdf/20040108.pdf.

Alkane Resources, Ltd., 2006, Peak Hill gold mine: Alkane Resources, Ltd., Web site, accessed November 18, 2010, at http://www.alkane.com.au/projects/nsw/peak-hill/.

Alkane Resources, Ltd., 2008, Core results from the Coloma and Wyoming three gold deposits: Alkane Resources, Ltd., ASX Announcement, 7 August, 2008, accessed November 2, 2010, at http://www.alkane.com.au/reports/asx/pdf/20080807.pdf.

Alkane Resources, Ltd., 2009, Further significant high grade gold results at Caloma: Alkane Resources, Ltd., ASX Announcement, November 2, 2009, accessed November 2, 2010, at http://www.alkane.com.au/reports/asx/pdf/20091102.pdf.

Alkane Resources, Ltd., 2010, McPhillamys first resource estimate—2.96 million oz. gold: Alkane Resources, Ltd., ASX Announcement, 5 July, 2010, accessed November 2, 2010 at http://www.alkane.com.au/reports/asx/pdf/20100705.pdf.

Alkane Resources, Ltd., 2011a, Discovery of porphyry style gold-copper mineralization at Bodangora: Alkane Resources, Ltd., ASX Announcement, accessed 19 April, 2011, at http://www.alkane.com.au/reports/asx/pdf/20110419.pdf.

Alkane Resources, Ltd., 2011b, Tomingley gold project, environmental assessment, public exhibition: Alkane Resources, Ltd., Web site accessed January 26, 2012, at http://www.alkane.com.au/.

Allen, C.M., Wooden, J.L., and Chappell, B.W., 1997, Late Paleozoic crustal history of central coastal Queensland interpreted from geochemistry of Mesozoic plutons—The

[1]U.S. Geological Survey, Spokane, Washington, United States.

effects of continental rifting: Lithos, v. 42, p. 67–88.

Allibone, A., 1997, Gold mineralization and advanced argillic alteration at the Dobroyde prospect, central New South Wales: Australian Journal of Earth Sciences, v. 44, no. 6, p. 727–742.

Allibone, A., 1998, Synchronous deformation and hydrothermal activity in the shear zone hosted high-sulphidation Au-Cu deposit at Peak Hill, NSW, Australia: Mineralium Deposita, v. 33, p. 495–512.

Allibone, A.H., Cordery, G.R., Morrison, G.W, Jaireth, S., and Lindhorst, J.W., 1995, Synchronous advanced argillic alteration and deformation in a shear zone-hosted magmatic hydrothermal Au-Ag deposit at the Temora (Gidginbung) mine, NSW, Australia: Economic Geology, v. 90, p. 1570–1603.

Ambler, E.P., and Facer, R.A., 1975, A Silurian porphyry copper prospect near Yeoval, New South Wales: Australian Journal of Earth Sciences, v. 22, no. 2, p. 229–241.

Arnold, G.O., and Sillitoe, R.H., 1989, Mount Morgan gold-copper deposit, Queensland, Australia—Evidence for an intrusion-related replacement origin: Economic Geology, v. 84, p. 1805–1816.

Arundell, M.C., 2004, Northparkes Cu-Au mines, central NSW, *in* Butt, C.R.M, Cornelius, M., Scott, K.M., and Robertson, I.D.M., Regolith expression of Australian ore systems—A compilation of geochemical case histories and conceptual models: Cooperative Research Centre for Landscape Environments and Mineral Exploration (CRC LEME), 3 p., accessed May 18, 2011, at http://crcleme.org.au/RegExpOre/Northparkes.pdf.

Ashley, P.M., Billington, W.G., Graham, R.L., and Neale, R.C., 1978, Geology of the Coalstoun porphyry copper prospect, southeast Queensland, Australia: Economic Geology, v. 73, p. 945–965.

Augur Resources, Ltd., 2009, Maiden JORC resource estimate, Yeoval copper-gold-molybdenum-silver deposit: Augur Resources, Ltd., Web site, accessed April 18, 2010, at http://augur.com.au/Maiden%20Resource%Yeoval.

Aussie Q Resources, Ltd., 2007, Prospectus—Information on Whitewash and Kiwi Carpet prospects: Aussie Q Resources, Ltd., Web site, accessed June 9, 2010, at http://www.aussieqresources.com.au/, p. 13–15, 37–44, and 47–56.

Aussie Q Resources, Ltd., 2010, Aussie Q Resources Ltd., ASX:AQR—An emerging molybdenum & copper producer: Aussie Q Resources, Ltd., Web site, accessed May 9, 2011, at http://www.aussieqresources.com.au/.

Axiom Mining, Ltd., 2010a, Initial Mountain Maid JORC resource estimate: Axiom Mining, Ltd., Web site, accessed May 6, 2011, at http://www.axiom-mining.com/.

Axiom Mining, Ltd., 2010b, Pinevale copper-gold project: Axiom Mining, Ltd., Web site, accessed May 6, 2011, at http://www.axiom-mining.com/pinevale.html.

Ayers, D.E., 1974, Relationship of mineralization and hydrothermal alteration at the Moonmera porphyry copper prospect, Queensland: Australasian Institute of Mining and Metallurgy, Southern and Central Queensland Conference, p. 465–477.

Baker, E.M., and Andrew, A.S., 1991, Geologic, fluid inclusion, and stable isotope studies of the gold-bearing breccia pipe at Kidston, Queensland, Australia: Economic Geology, v. 86, p. 810–830.

Baker, E.M., and Horton, D.J., 1982, Geological environment of copper-molybdenum mineralization at Mount Turner, North Queensland: Geological Survey of Queensland Publication 379, p. 30–77.

Barley, M.E., 1982, Porphyry-style mineralization associated with Early Archean calc-alkaline igneous activity, eastern Pilbara, Western Australia: Economic Geology, v. 62, p. 1230–1236.

Bedford, I.V., 1975, Mount Cannindah copper deposit, *in* Knight, C.L., ed., Economic Geology of Australia and New Guinea: Australian Institute of Mining and Metallurgy, Monograph Series, v. 1, no. 5, p. 787–789.

Bird, Damon, 1999, The Ferndale copper-gold project—A case study on exploring for Ordovician porphyry systems beneath Tertiary cover: accessed November 29, 2010, at http://www.smedg.org.au/Sym99bird.htm.

Blevin, P.L., 2002, The petrographic and compositional character of variably K-enriched magmatic suites associated with Ordovician porphyry Cu-Au mineralization in the Lachlan fold belt, Australia: Mineralium Deposita, v. 37, p. 87–99.

Bonzle, 2010, Digital atlas of Australia—what's mined where—Australia: accessed May 6, 2011, at http://www.bonzle.com/.

Bowman, H.N., Hobbs, J.J., and Barron, L.M., 1983, Goonumbla copper district northwest of Parkes: New South Wales Geological Survey Records, v. 21, no. 2, p. M11–M28.

Bowman, H.N., and Richardson, S.J., 1983, Alteration zoning at the Peak Hill disseminated copper-gold deposit: New South Wales Geological Survey Records, v. 21, no. 2, p. M75–M83.

Brooks, J.H., 1976, Departmental diamond drilling programme, Whitewash copper-molybdenum prospect, Monto: Queensland Government Mining Journal, v. 77, no. 891, p. 112–120.

Burraga Copper, Ltd., 2012, Burraga Copper corporate background, 3 p., Burraga Copper, Ltd., Web site, accessed June 26, 2012, at http://www.burragacopper.com.au/about/company/.

Carr, G.R., Dean, J.A., Suppel, D.W., and Heithersay, P.S., 1995, Precise lead isotope fingerprinting of hydrothermal activity associated with Ordovician to Carboniferous metallogenic events in the Lachlan fold belt of New South Wales: Economic Geology, v. 90, p. 1467–1505.

Catalyst Metals, Ltd., 2008, Catalyst earns into significant molybdenum project: Catalyst Metals, Ltd., ASX Release, February 18, 2008, Catalyst Metals, Ltd., Web site accessed June, 2011, at http://www.catalystmetals.com/.

Chalmers, D.I., Ransted, T.W., Kairaitis, R.A., and Meates, D.G., 2007, The Wyoming gold deposits—Volcanic-hosted lode-type gold mineralisation in the eastern Lachlan Orogen, Australia: Mineralium Deposita, v. 42, p. 505–513.

Champion, D.C., Kositcin, N., Huston, D.L., Mathews, E., and Brown, C., 2009, Geodynamic synthesis of the Phanerozoic of eastern Australia and implications for metallogeny: Geoscience Australia, Record 2009/18, GeoCat#68866, 222 p., digital, accessed October 4, 2010, at http://www.ga.gov.au/products/.

Chapman, J.R., 2003, Peak Hill Au deposit, Peak Hill, NSW, *in* Butt, C.R.M, Cornelius, M., Scott, K.M., and Robertson, I.D.M., Regolith Expression of Australian Ore Systems—A compilation of geochemical case histories and conceptual models: Cooperative Research Centre for Landscape Environments and Mineral Exploration (CRC LEME), 3 p., accessed April 2, 2013, at http://crcleme.org.au/RegExpOre/PeakHill.pdf.

Chivas, A.R., and Nutter, A.H., 1975, Copper Hill porphyry copper prospect, *in* Knight, C.L., ed., Economic Geology of Australia and Papua New Guinea, I, Metals: Australasian Institute of Mining and Metallurgy Monograph 5, p. 716–720.

Clancy Exploration, Ltd., 2009, Myall Exploration Lease 6913 (Kingswood prospect), *in* Quarterly activities report for the period ending 30 June 2009: Clancy Exploration, Ltd., accessed August 11, 2010, at http://www.clancyexploration.com/Shared/Sites/clancy/Assets/Your%20Files/News/press_releases/June%202009%20Qly%20activities.pdf.

Clancy Exploration, Ltd., 2010, Annual report 2010: Clancy Exploration, Ltd., accessed May 19, 2011, at http://www.clancyexploration.com/Shared/Sites/clancy/Assets/Your%20Files/Clancy%20Exploration%202010%20Annual%20Report%20LowResNew.pdf.

Coianiz, Glenn, and Burrell, Paul, 2007, Update on the Copper Hill Cu-Au porphyry project [abs.]: Orange, New South Wales, Mines and Wines Symposium 2007, Mineral exploration in the Tasmanides, Australian Institute of Geoscientists, AIG Bulletin 46, p. 27–28. (Also available at http://www.smedg.org.au/M&W2007Abs.pdf, and presentation available at http://smedg.org.au/M&W07/.)

Collett, D.K., 2007, The Cadia East deposit—ensuring at least 30 more years of mining at Cadia Valley—Newcrest Mining [abs.]: Orange, New South Wales, Mines and Wines Symposium 2007, Mineral exploration in the Tasmanides, Australian Institute of Geoscientists, AIG Bulletin 46, p. 31 (Also available at http://www.smedg.org.au/M&W2007Abs.pdf, and presentation available at http://smedg.org.au/M&W07/.)

Cooke, D.R., Wilson, A.J., House, M.J., Wolfe, R.C., Walshe, J.L., Lickfold, Vanessa., and Crawford, A.J., 2007, Alkalic porphyry Au-Cu and associated mineral deposits of the Ordovician to Early Silurian Macquarie Arc, New South Wales: Australian Journal of Earth Sciences, v. 54, p. 445–463.

Crawford, A.J., Cooke, D.R., and Fanning, C.M., 2007, Geochemistry and age of magmatic rocks in the unexposed Narromine, Cowal and Fairholme igneous complexes in the Ordovician Macquarie Arc, New South Wales: Australian Journal of Earth Sciences, v. 54, no. 2, p. 243–271.

Cube Consulting, Pty. Ltd., 2006a, Discovery Ridge gold project NSW, Australia: Perth, Western Australia, NI-43–101 compliant Independent Technical Report for Goldminco Corporation, March, 2006, 68 p., Cube Consulting, Pty. Ltd., Web site accessed May 24, 2011, at http://www.sedar.com/.

Cube Consulting Pty Ltd., 2006b, Brown's Creek gold mine, NSW, Australia: Perth, Western Australia, NI-43–101 compliant Independent Technical Report for Straits Gold Pty Ltd., 84 p., Cube Consulting, Pty. Ltd., Web site accessed May 24, 2011, at http://www.sedar.com/.

D'Aguilar Gold, Ltd., 2007, Anduramba molybdenum: D'Aguilar Gold, Ltd., Web site, accessed June 10, 2010, at http://www.daguilar.com.au/anduramba_molybdenum.html/.

D'Aguilar Gold, Ltd., 2010, Encouraging copper molybdenum results in historical drill holes into porphyry at Calgoa: D'Aguilar Gold, Ltd., ASX Announcement, accessed May 9, 2011, at http://www.daguilar.com.au/.

De Laeter, J.R., and Martyn, J.E., 1986, Age of molybdenum-copper mineralization at Coppin Gap, Western Australia: Australian Journal of Earth Sciences, v. 33, p. 65–71.

Dummett, H.T., 1978, Geology of the Moonmera porphyry deposit, Queensland, Australia: Economic Geology, v. 73, p. 922–944.

Ewers, G.R., Evans, N., and Hazell, M., (Kilgour, B., compiler), 2002, OZMIN mineral deposits database [Digital Datasets]: Canberra, Geoscience Australia, scale 1:1,000,000 on CD ROM. (Also available at http://www.ga.gov.au/meta/ANZCW0703003393.html.)

Fedikow, M.A.F., and Govett, G.J.S., 1985, Geochemical alteration halos around the Mount Morgan gold-copper deposit, Queensland, Australia: Journal of Geochemical Exploration, v. 24, p. 247–272.

Ford, J.H., Wood, D.G., and Green, D.C., 1976, Geochronology of porphyry copper-type mineralization near Rockhampton, Eastern Queensland, Australia: Economic Geology, v. 71, p. 526–539.

Forster, D.B., Seccombe, P.K., and Phillips, David, 2004, Controls on skarn mineralization and alteration at the Cadia deposits, New South Wales, Australia: Economic Geology, v. 99, p. 761–788.

Fredricksen, D., 2006, Sustainable gold and copper production, Cadia Valley operations: Orange, New South Wales, Mines and Wines Symposium 2006, Mineral exploration in the Tasmanides, Speaker Program, Abstracts and Presentations, accessed July, 22, 2010, at http://www.smedg.org.au/M&WProg.htm.

Geological Survey of Queensland, 2010, Mineral occurrence and geology observations: Department of Employment, Economic Development and Innovation, digital data released on DVD. (Building of Access database and annual extraction of data by Withnall, I.W., and von Gnmielinski, F.E.)

Geoscience Australia, 2010, Australian atlas of mines and mineral deposits: Canberra, Geoscience Australia, accessed October 20, 2010, to December 27, 2010, at http://www.australianminesatlas.gov.au/.

Gilmore, P., Greenfield, J., Reid, W., and Kingsley, M., 2007, Metallogenesis of the Koonenberry belt [abs.]: Orange, New South Wales, Mines and Wines Symposium 2007, Mineral exploration in the Tasmanides, Australian Institute of Geoscientists, AIG Bulletin 46, p. 49–63. (Also available at http://www.smedg.org.au/M&W2007Abs.pdf, and presentation available at http://smedg.org.au/M&W07/.)

Glen, R.A., 1992, Thrust, extensional and strike-slip tectonics of an evolving Palaeozoic orogen—A structural synthesis of the Lachlan Orogen of southeastern Australia: Tectonophysics, v. 214, p. 341–380.

Glen, R.A, Crawford, A.J., and Cooke, D.R., 2007, Tectonic setting of porphyry Cu-Au mineralization in the Ordovician-Early Silurian Macquarie arc, eastern Lachlan orogen, New South Wales: Australian Journal of Earth Sciences, v. 54, p. 465–479.

Glen, R.A., Meffre, S., and Scott, R.J., 2007, Benambran orogeny in the eastern Lachlan orogen, Australia: Australian Journal of Earth Sciences, v. 54, no. 2, p. 385–415.

Golden Cross Resources, Ltd., 2009, Cargo: Golden Cross Resources, Ltd., Web site, accessed August 18, 2010, at http://www.goldencross.com.au/projects/cargo/default.html.

Golden Cross Resources, Ltd., 2011, Copper Hill: Golden Cross Resources, Ltd., Web site, accessed January 26, 2012, at http://www.goldencross.com.au/projects/australian-projects/copper-hill/.

Golding, S.D., Huston, D.L., Dean, J.A., Messenger, P.R., Jones I.W.O., Taube, A., and White, A.H., 1993, Mount Morgan gold-copper deposit—The 1992 perspective: Proceedings Australasian Institute of Mining and Metallurgy Centenary Conference, 30 March to 4 April, Adelaide, p. 95–111.

Goldminco Corp., 2008, Goldminco acquires ground along strike from the Dam porphyry copper-gold deposit, at its 100% owned Temora Project: Goldminco Corp., accessed October 2010, at http://www.goldminco.com/images/stories/newsrelease/2008/Goldminco_acquires_ground_along_strike_from_the%20_DAM_Porphyry_Coopper-Gold_Deposit,_at_its_100_owned_Temora_Project_%2120080229.pdf.

Goldminco Corp., 2010, Additional strong copper and gold intersection recorded at Culingerai: Goldminco Corp., accessed October 2010, at http://www.goldminco.com/media/files/new_releases/2010/Additional_Strong_Copper_and_Gold_Intersection_Recorded_at_Culingerai_!20100726.pdf.

Gray, D.R., and Foster, D.A., 2004, Tectonic evolution of the Lachlan orogen, southeast Australia—Historical review, data synthesis and modern perspectives: Australian Journal of Earth Sciences, v. 51, no. 6, p. 773–817.

Gray, N., Mandyczewsky, A., and Hine, R., 1995, Geology of the zoned gold skarn system at Junction Reefs, New South Wales: Economic Geology, v. 90, p. 1533–1552.

Harris, A.C., Cooke, D.R., Fox, Nathan, Cuison, Ana Lisa, Tosdal, Richard, Groome, Melissa, Percival, Ian, Dunham, Paul, Collett, Dean, Holliday, John, and Allen, C.M., 2010, Architectural controls on Palaeozoic porphyry Au-Cu mineralization in the Cadia Valley, NSW: Mudgee, New South Wales, Mines and Wines Symposium 2010, accessed October 12, 2010, at http://www.smedg.org.au/M&W2010program.html.

Heithersay, P.S., O'Neill, W.J., van der Helder, P., Moore, C.R., and Harbon, P.G., 1990, Goonumbla porphyry copper district —Endeavour 26 North, Endeavour 22 and Endeavour 27 copper-gold deposits: Australasian Institute of Mining and Metallurgy Monograph 14, p. 1385–1398.

Heithersay, P.S., and Walshe, J.L., 1995, Endeavour 26 North: a porphyry copper-gold deposit in the Late Ordovician, shoshonitic Goonumbla volcanic complex, New South Wales, Australia: Economic Geology, v. 90, p. 1506–1552.

Holliday, J., McMillan, C., and Tedder, I., 2001, Discovery of the Cadia Ridgeway gold-copper porphyry deposit: accessed April 2, 2013, at http://www.smedg.org.au/Sym99cadia.htm, 7 p.

Holliday, J.R., Wilson, A.J., Blevin, P.L., Tedder, I.J., Dunham, P.D., and Pfitzner, Michael, 2002, Porphyry gold-copper mineralization in the Cadia district, eastern Lachlan Fold Belt, New South Wales, and its relationship to shoshonitic magmatism: Mineralium Deposita, v. 37, p. 100–116.

Hooper, B., Heithersay, P.S., Mills, M.B., Lindhorst, J.W, and Freyberg, J., 1996, Shoshonite-hosted Endeavour 48 porphyry copper-gold deposit, Northparkes, central New

South Wales: Australian Journal of Earth Sciences, v. 43, p. 279–288.

Horton, D.J., 1978, Porphyry-type copper-molybdenum mineralization belts in eastern Queensland, Australia: Economic Geology v. 73, p. 904–921.

Hough, M.A., Bierlein, F.P., and Wilde, A.R., 2007, A review of the metallogeny and tectonics of the Lachlan Orogen: Mineralium Deposita, v. 42, p. 435–448.

Hutton, L., and Withnall, I., 2007, Depositional systems, crustal structure and mineralization in the Thalanga province, north Queensland [abs.]: Orange, New South Wales, Mines and Wines Symposium 2007, Mineral exploration in the Tasmanides: Australian Institute of Geoscientists, AIG Bulletin 46, p. 79–86. (Also available at http://www.smedg.org.au/M&W2007Abs.pdf.)

Industry and Investment NSW, 2010, Advanced mineral projects and mineral exploration highlights: New South Wales Department of Primary Industries, geologic map, showing operational mines and active exploration sites, with estimated resources and best intercepts: accessed October 11, 2010, at http://www.industry.nsw.gov.au/.

Jaireth, S., and Miezitis, Y., 2004, OZPOT Geoprovince-scale assessment of mineral potential [1:2,500,000 scale GIS]: Canberra, Geoscience Australia, accessed June 21, 2010, to December 27, 2010, at http://www.australianminesatlas.gov.au/build/common/minpot.html.

Jaques, A.L., Jaireth, S., and Walshe, J.L., 2002, Mineral systems of Australia—An overview of resources, settings and processes: Australian Journal of Earth Sciences, v. 49, no. 4, p. 623–660.

Jones, G.J., 1985, The Goonumbla porphyry copper deposits, New South Wales: Economic Geology, v. 80, p. 591–613.

Kargara, Ltd., 2010, Kargara Mining—Growing more than our business: Kargara, Ltd., Web site, accessed November 15, 2012, at http://www.kargara.com.au/.

Lachlan Star, 2007, Bushranger project, Racecourse prospect: Lachlan Star, Ltd., Web site, accessed September 30, 2010, at http://www.Lachlanstar.com.au/.

Lacy, W.C., 1980, Mineralisation along the extension of the New England and Lachlan-Thompson fold belts in North Queensland, *in* Henderson, R.A., and Stephenson, P.J., eds., The geology and geophysics of northeastern Australia: Geological Society of Australia, Queensland Division, Brisbane, p. 269–277.

Lawrie, K.C., Mernagh, T.P., Ryan, C.G., van Achterbergh, E., and Black, L.P., 2007, Chemical fingerprinting of hydrothermal zircons—An example from the Gidginbung high sulphidation Au-Ag-(Cu) deposit, New South Wales, Australia: Proceedings of the Geologists' Association, v. 118, p. 37–46.

Lehany, T., 2007, Marsden Project—Presentation to Diggers and Dealers, 2007: accessed 2010, at http://www.newcrest.com/au/.

Lewis, P., and Downes, P.M., 2008, Mineral systems and processes in New South Wales—A project to enhance understanding and assist exploration: Geological Survey of New South Wales, Quarterly Notes, no. 128, 13 p., accessed February 2, 2012, at http://www.dpi.nsw.gov.au/__data/assets/pdf_file/0009/229914/00128-Quarterly-Notes-April-2008.pdf.

Lickfold, V., Cooke, D.R., Smith, S.G., and Ullrich, T.D., 2003, Endeavour copper-gold porphyry deposits, Northparkes, New South Wales—Intrusive history and fluid evolution: Economic Geology, v. 98, p. 1607–1636.

Lickfold, V., Cooke, D.R., Crawford, A.F., and Fanning, C.M., 2007, Shoshonitic magmatism and the formation of the Northparkes porphyry Cu-Au deposits, New South Wales: Australian Journal of Earth Sciences, v. 54, p. 417–444.

Lorrigan, A., 2010, Exploration techniques at Henty gold mine: Mudgee, New South Wales, Mines and Wines Symposium 2010, Presentation accessed October 12, 2010, at http://www.smedg.org.au/M&W2010program.html.

Lye, A., 2010, Northparkes—Still prospective almost 40 years later: Mudgee, New South Wales, Mines and Wines Symposium 2010, Presentation accessed October 12, 2010, at http://www.smedg.org.au/M&W2010program.html.

Lye, A., Crook, G., and van Oosterwijk, L.K., 2006, The discovery history of the Northparkes deposits: Cessnock, New South Wales, Mines and Wines Symposium 2006, Speaker Programme, Abstracts and Presentations accessed September 29, 2010, at http://smedg.org.au/M&WProg.htm.

MacCorquodale, F., 1997, The Mandamah porphyry Cu-Au prospect—Abstracts: Geological Society of Australia, v. 51, p. 51.

Maher, S., 2003, Dogwood porphyry Cu-Mo prospect, Benambra terrane, Victoria, *in* Butt, C.R.M, Cornelius, M., Scott, K.M., and Robertson, I.D.M., Regolith expression of Australian ore systems—A compilation of geochemical case histories and conceptual models: Cooperative Research Centre for Landscape Environments and Mineral Exploration (CRC LEME), 3 p., accessed April 2, 2013, at http://crcleme.org.au/RegExpOre/Dogwood.pdf.

Masterman, G.J., White, N.C., and Wilson, C.J.L., 2002, High sulfidation gold-copper mineralization at Peak Hill, NSW, Australia—Deformation of an unusual epithermal deposit [abs.]: Geological Society of America, Abstracts with Programs, v. 34, no. 6, p. 186.

Marston, R.J., 1979, Copper mineralization in Western Australia: Western Australia Geological Survey, Mineral Resources Bulletin 13, 208 p.

Maynard, A.J., 2003, Blayney porphyry gold-copper project, New South Wales, Australia, exploration license 5922 (including the Discovery Ridge and Ferndale prospects): Independent Geologist's Report for Goldminco Corp., 29 p., accessed May 24, 2011, at http://www.sedar.com/.

McInnes, B., 2006, Exploration reviews, Australasia, New South Wales: Society of Economic Geologists Newsletter, no. 67, p. 35.

McInnes, P., and Freer, L., 2007, The Cowal gold corridor—Opening other doors [abs.]: Orange, New South Wales, Mines and Wines Symposium 2007, Mineral exploration in the Tasmanides, AIG Bulletin 46, p. 107–112. (Also available at http://smedg.org.au/M&W2007Abs.pdf, and presentation available at http://smedg.org.au/M&W07/.)

McQuaig, T.C., Behn, M., Stein, H., Hagemann, S.G., McNaughton, N.J., Cassidy, K.F., Champion, D., and Wyborn, L., 2001, The Boddington gold mine—A new style of Archaean Au-Cu deposit: AGSO—Geoscience Australia, p. 453–455.

Miles, I.N., and Brooker, M.R., 1998, Endeavour 42 deposit, Lake Cowal, New South Wales—A structurally controlled gold deposit: Australian Journal of Earth Sciences, v. 45, p. 837–847.

Morris, B.J., 1979, Porphyry style copper /molybdenum mineralization at Anabama Hill: Mineral Resources Review, South Australia, no. 150, p. 5–24.

Mowat, B., 2007, Characteristics of porphyry copper-gold mineralization in the Gidginbung Volcanics [abs.]: Orange, New South Wales, Mines and Wines Symposium 2007, Mineral exploration in the Tasmanides, AIG Bulletin 46, p. 107–112. (Also available at http://www.smedg.org.au/M&W2007Abs.pdf, and presentation available at http://smedg.org.au/M&W07/.)

Mowat, B., and Smith, S., 2006, Characteristics of porphyry Au-Cu systems in the Ordovician Macquarie arc of NSW: Cesnock, New South Wales, Mines and Wines Symposium 2006, Speaker Programme, Abstracts and Presentations, accessed September 29, 2010, at http://smedg.org.au/M&WProg.htm.

Mungana Gold Mines, Ltd., 2010, Red Dome: Mungana Gold Mines, Ltd., Web site, accessed October 12, 2010, at http://www.munganagoldmines.com.au/.

Munro, S., 2010, Developments at Goldminco's Temora exploration project: Mudgee, New South Wales, Mines and Wines Symposium 2010, accessed October 12, 2010, at http://www.smedg.org.au/M&W2010program.html.

Murgulov, V., O'Reilly, S.Y., Griffin, W.L., and Blevin, P.L., 2008, Magma sources and gold mineralization in the Mount Leyshon and Tuckers igneous complexes, Queensland, Australia—U-Pb and Hf isotope evidence: Lithos, v. 101, p. 281–307.

Murray, C.G., 1986, Metallogeny and tectonic development of the Tasman fold belt system in Queensland: Ore Geology Reviews, v. 1, p. 315–400.

Murray, C.G., 1990, Tasman fold belt in Queensland, *in* Hughes, F.E., ed., Geology of the Mineral Deposits of Australia and New Guinea: Melbourne, Australasian Institute of Mining and Metallurgy, Monograph Series, v. 2, no. 14, p. 1431–1450.

Newcrest Mining Staff, 1998, Cadia gold-copper deposit, *in* Berkman, D.A., and Mackenzie, D.H., eds., Geology of Australian and Papua New Guinea mineral deposits: Melbourne, Australasian Institute of Mining and Metallurgy Monograph 22, p. 641–646.

NSW New Frontiers, 2010, New Frontiers Minerals Program: accessed November 15, 2012, at http://www.resources.nsw.gov.au/geological/initiatives/new-frontiers/.

Orr, T.H., and Orr, L.A., 2004, Mt. Leyshon gold deposit, Charters Towers, Queensland, *in* Butt, C.R.M, Cornelius, M., Scott, K.M., and Robertson, I.D.M., Regolith expression of Australian ore systems—A compilation of geochemical case histories and conceptual models: Cooperative Research Centre for Landscape Environments and Mineral Exploration (CRC LEME), accessed April 17, 2011, at http://crcleme.org.au/RegExpOre/MtLeyshon.pdf.

Paradigm Metals, Ltd., 2008, Frogmore—High-grade copper intersections in RC drilling including 6m @ 3.1% Cu from 80m depth: Paradigm Metals, Ltd., ASX Release, 10 June 2008: Paradigm Metals, Ltd., Web site, accessed 2011, at http://www.paradigmgold.com.au/.

Paradigm Metals, 2011, Projects, Base Metals—Frogmore: Paradigm Metals, Ltd., Web site accessed March 23, 2011, at http://www.paradigmgold.com.au/.

Park, C.F., and MacDiarmid, R.A., 1970, Ore Deposits, second edition: San Francisco, W.H. Freeman and Company, 522 p.

Paterson, I.B.L., Bowman, H.N., and Hobbs, J.J., 1983, Yeoval copper-gold-molybdenum district: Geological Survey of New South Wales Records, v. 21, no. 2, p. M53–M73.

Peel Exploration, 2009, Attunga copper mine: Peel Exploration Web site, accessed April 27, 2011, at http://www.peelex.com.au/Projects/attunga.aspx.

Perkins, C., Hinman, M.C., and Walshe, J.L., 1994, Timing of mineralization and deformation, Peak Au mine, Cobar, New South Wales: Australian Journal of Earth Sciences, v. 41, p. 509–522.

Perkins, C., and Kennedy, A.K., 1998, Permo-Carboniferous gold epoch of northeast Queensland: Australian Journal of Earth Sciences, v. 45, no. 2, p. 185–200.

Perkins, C., McDougall, I., Claoue-Long, J., and Heithersay, P.S., 1990, $^{40}Ar/^{39}Ar$ and U-Pb geochronology of the

Goonumbla porphyry Cu-Au deposits, New South Wales, Australia: Economic Geology, v. 85, p. 1808–1824.

Perkins, C., McDougall, I., and Walshe, J.L., 1992, Timing of shoshonitic magmatism and gold mineralization, Sheahan-Grants and Glendale, New South Wales: Australian Journal of Earth Sciences, v. 39, p. 99–110.

Perkins, C., Walshe, J.L., and Morrison, G., 1995, Metallogenic episodes of the Tasman fold belt system, eastern Australia: Economic Geology, v. 90, p. 1443–1466.

Planet Metals, Ltd., 2010, Mount Cannindah project: Planet Metals, Ltd., Web site, accessed August 18, 2010, at http://planetmetals.com.au/.

Primary Industries and Resources South Australia (PIRSA), 2010, SA Geodata [digital database]—Mineral deposit information: Primary Industries and Resources South Australia Web site, accessed October 18, 2010, at https://egate.pir.sa.gov.au/minerals/.

Porter, T.M., and Glen, R.A., 2005, The porphyry Cu-Au deposits and related shoshonitic magmatism of the Palaeozoic Macquarie volcanic arc, eastern Lachlan orogen in New South Wales, Australia—A review, *in* Porter, T.M., ed., Super porphyry copper and gold deposits—A global perspective, v. 2: Adelaide, PGC Publishing, p. 287–312.

Preiss, W.V., 2000, The Adelaide geosyncline of South Australia and its significance in Neoproterozoic continental reconstruction: Precambrian Research, v. 100, p. 21–63.

Radojkovic, A. 2003, Thursdays gossan porphyry copper prospect, western Victoria, *in* Butt, C.R.M, Cornelius, M., Scott, K.M., and Robertson, I.D.M., Regolith expression of Australian ore systems—A compilation of geochemical case histories and conceptual models: Cooperative Research Centre for Landscape Environments and Mineral Exploration (CRC LEME), 3 p., accessed February 16, 2011, at http://crcleme.org.au/RegExpOre/ThursdaysGossan.pdf.

Rajagopalan, S., 1999a, Thursdays gossan project, *in* Willcocks, A.J., Haydon, S.J., Asten, M.W., and Moore, D.H., eds., Geophysical signatures of base metal deposits in Victoria: Geological Survey of Victoria Report 119, p. 129–136.

Rajagopalan, S., 1999b, Porphyry-type copper deposits, eastern Victoria, *in* Willcocks, A.J., Haydon, S.J., Asten, M.W., and Moore, D.H., eds., Geophysical signatures of base metal deposits in Victoria: Geological Survey of Victoria Report 119, p. 113–127.

Raymond, O.L., Liu, S.F., Kilgour, P., Retter, A.J., Stewart, A.J., and Stewart, G., 2007, Surface geology of Australia, 1:1,000,000 scale, New South Wales, 2nd edition [Digital Dataset]: Canberra, Geoscience Australia, accessed June 7, 2010, at http://www.ga.gov.au/.

Republic Gold, Ltd., 2010, Burraga copper project presents significant development potential—New drilling programme planned: Republic Gold, Ltd., ASX Announcement, accessed October 6, 2010, at http://www.republicgold.com.au/projects/nsw/.

Richardson, S.J., Bowman, H.N., Paterson, I.B.L., and Hobbs, J.J., 1983, Disseminated copper-gold mineralization at Cargo: Geological Survey of New South Wales Records, v. 21, no. 2, p. M29–M52.

Scott, K.M., 1978, Geochemical aspects of the alteration-mineralization at Copper Hill, New South Wales, Australia: Economic Geology, v. 73, p. 966–976.

Scott, K.M., 1992, Origin of alunite- and jarosite-group minerals in the Mount Leyshon epithermal gold deposit, northeast Queensland, Australia—Reply: American Mineralogist, v. 77, p. 860–862.

Scott, K.M., Chalmers, D.I., Ransted, T., and Kairaitis, R., 2003, Wyoming gold deposit, central western NSW, *in* Butt, C.R.M, Cornelius, M., Scott, K.M., and Robertson, I.D.M., Regolith expression of Australian ore systems—A compilation of geochemical case histories and conceptual models: Cooperative Research Centre for Landscape Environments and Mineral Exploration (CRC LEME), 3 p., accessed January 26, 2012, at http://crcleme.org.au/Pubs/Monographs/RegExpOre.html.

Scott, K.M., and Torrey, C.E., 2003, Copper Hill porphyry Cu-Au prospect, central NSW, *in* Butt, C.R.M, Cornelius, M., Scott, K.M., and Robertson, I.D.M., Regolith expression of Australian ore systems—A compilation of geochemical case histories and conceptual models: Cooperative Research Centre for Landscape Environments and Mineral Exploration (CRC LEME), 3 p., accessed May 18, 2011, at http://crcleme.org.au/RegExpOre/CopperHill.pdf.

Seccombe, P.K., Spry, P.G., Both, R.A., Jones, M.T., and Schiller, J.C., 1985, Base metal mineralization in the Kanmantoo Group, South Australia—A regional sulfur isotope study: Economic Geology, v. 80, p. 1824–1841.

Singer, D.A., Berger, V.I., Menzie, W.D., and Berger, B.R., 2005, Porphyry copper density: Economic Geology, v. 100, no. 3, p. 491–514.

Singer, D.A., Berger, V.I., and Moring, B.C., 2008, Porphyry copper deposits of the world—Database and grade and tonnage models, 2008: U.S. Geological Survey Open-File Report 2008–1155, 45 p., available at http://pubs.usgs.gov/of/2008/1155/.

Smith, S., Mowat, B., and Sharry, M., 2004, Macquarie Arc porphyry Au-Cu systems—A review of the critical exploration features, *in* Bierlien, F.P. and Hough, M.A., eds., Tectonics to mineral discovery—Deconstructing the Lachlan Orogen: Geological Society of Australia, Abstracts 74, p. 51–62.

Solomon, M., and Groves, D.I., 2000, Metallogeny and tectonic development of the Tasman fold belt system in Queensland: Ore Geology Reviews, v. 1, p. 315–400.

Squire, R.J., and Crawford, A.J., 2007, Magmatic characteristics and geochronology of Ordovician igneous rocks from the Cadia-Neville region, New South Wales—Implications for tectonic evolution: Australian Journal of Earth Sciences, v. 54, p. 293–314.

Stanton, R.L., 1953, The Lloyd copper mine, Burraga, *in* Edwards, A.B., ed., Geology of Australian Ore Deposits: Melbourne, Australasian Institute of Mining and Metallurgy, p. 906–909.

Stanton-Cook, K., 2011, Golden Cross Resources Copper Hill porphyry Cu-Au deposits: accessed January 26, 2012, at http://smedg.org.au/Kim_Stanton-Cook_Copper_Hill.pdf.

Taube, A., 1990, Mount Morgan gold-copper deposit, Queensland, Australia—evidence for an intrusion-related replacement origin—A discussion: Economic Geology, v. 85, p. 1947–1955.

Taylor, G.R., 1983, Copper and gold in skarn at Brown's Creek, Blayney, N.S.W.: Australian Journal of Earth Sciences, v. 30, no. 3, p. 431–442.

Tonui, E., Jones, R., and Scott, K., 2002, Regolith mineralogy and geochemical dispersion at the Northparkes Cu-Au deposits, New South Wales, Australia: Geological Society, London, Geochemistry—Exploration, Environment, Analysis, v. 2, p. 345–360.

Torrey, C., and Burrell, P., 2006, Geology and mineralization of the Copper Hill area: Orange, New South Wales, Mines and Wines Symposium 2006, Mineral exploration in the Tasmanides, Speaker Program, Abstracts and Presentations, accessed July, 22, 2010, at http://www.smedg.org.au/M&WProg.htm.

Torrey, C.E., and White, P.D., 1998, Porphyry copper and gold mineralization at Cargo, NSW: Townsville, Geological Society of Australia, 14th Australian Geological Convention, July 1998, abstracts, no. 49, p. 442.

Tri Origin Minerals, Ltd., 2006, Annual Report 2006: Tri Origin Minerals, Ltd., Web site accessed November 15, 2012, at http://www.triausmin.com/.

Wels, C., Findlater, L., and McCombe, C., 2009, Contaminant load balance study for Mount Morgan mine, QLD, Australia: Skelleftea, Sweden, Paper presented at Securing the Future and 8th ICARD, 8 p.

Wilson, A.J., Cooke, D.R., and Harper, B.L., 2003, The Ridgeway gold-copper deposit—A high-grade alkalic porphyry deposit in the Lachlan fold belt, New South Wales, Australia: Economic Geology, v. 98, p. 1637–1666.

Wilson, A.J., Cooke, D.R., Harper, B.J., and Deyell, C.L., 2007, Sulfur isotopic zonation in the Cadia district, southeastern Australia—Exploration significance and implications for the genesis of alkalic porphyry gold-copper deposits: Mineralium Deposita, v. 42, p. 465–487.

Wilson, A.J., Cooke, D.R., Stein, H.J., Fanning, M.C., Holliday, J.R., and Tedder, I.J., 2007, U-Pb and Re-Os geochronologic evidence for two alkalic porphyry ore-forming events in the Cadia district, New South Wales, Australia: Economic Geology, v. 102, p. 3–26.

Wyborn, D., Turner, B.S., and Chappell, B.W., 1987, The Boggy Plain Supersuite—A distinctive belt of I-type igneous rocks of potential economic significance in the Lachlan Fold Belt: Australian Journal of Earth Sciences, v. 34, no. 1, p. 21–43.

Appendix G. Description of GIS files

By Pamela M. Cossette[1] and John C. Wallis[1]

Two ESRI feature classes contained within a file geodatabase (.gdb) are included with this report. The GIS package may be downloaded from the USGS Web site as zipped file **sir2010-5090-l_gis.zip**.

The geodatabase is: **Australia_Porphyry_Copper_Assessment.gdb** and the feature classes are as follows:

Tracts_Sub_tracts is a polygon feature class that describes eleven permissive tracts and sub-tracts for porphyry copper deposits. Four of these permissive tracts and sub-tracts (the Delamerian-Adelaide sub-tract, the Macquarie tract, the Yeoval tract, and the East Tasmanide-Central sub-tract) were quantitatively assessed for resources contained in undiscovered deposits. Feature class attributes of permissive tracts include the tract identifiers, tract name, a brief description of the basis for tract delineation, and assessment results. Attributes are defined in metadata that accompany each feature class. Metadata are provided in .xml format.

Sites is a point feature class of locations for known porphyry copper deposits (sites of identified porphyry copper resources that have well-defined tonnage and copper grade) and prospects (sites explored for potential porphyry copper resources). Also included are copper occurrences, which may or may not be of porphyry copper type, and other types of deposits and prospects, which may or may not be directly or indirectly related to porphyry copper systems. All mineral locations are listed in both the feature class attribute table and in appendix F of this report. Feature class attributes of mineral sites include the assigned tract, alternate site names, information on grades and tonnages, age, deposit-type classification, mineralogy, site status, comments, data sources, and references. Attributes are defined in the metadata that accompany the feature class. Metadata are provided in .xml format.

Appendix H. Assessment Team

Arthur A. Bookstrom, USGS Western Mineral and Environmental Resources Science Center, Spokane, Washington, United States. Economic geologist with expertise in porphyry copper and mineral resource assessment.

Richard A. Glen, Geological Survey of New South Wales, Industry and Investment NSW, Maitland, New South Wales, Australia. Regional expert on the geology and tectonic and metallogenic history of eastern Australia.

Jane M. Hammarstrom, USGS Eastern Mineral and Environmental Resources Science Center, Reston, Virginia, United States. Co-chief, USGS Global Mineral Resource Assessment Project since 2007. Task leader, porphyry copper assessment.

Gilpin R. Robinson, Jr., USGS Eastern Mineral and Environmental Resources Science Center, Reston, Virginia, United States. Geologist, geochemist and mineral resources specialist, working on mineral resource assessment and other projects, including geologic mapping, studies of the origin and genesis of metal and industrial mineral-deposits, and geochemical modeling.

Michael L. Zientek, USGS Western Mineral and Environmental Resources Center, Spokane, Washington, United States. Co-chief, USGS Global Mineral Resource Assessment Project since 2007.

[1]U.S. Geological Survey, Spokane, Washington, United States.

Menlo Park Publishing Service Center
Manuscript approved for publication June 4, 2013
Layout by Judy Weathers, Jeanne S. DiLeo, and Vivan Nguyen

USGS

Bookstrom and others—**Porphyry Copper Assessment of Eastern Australia**—Scientific Investigations Report 2010–5090–L

ISSN 2328-0328 (online)

http://dx.doi.org/10.3133/sir20105090L